

**SYNTHESIS, CHARACTERIZATION, AND
MOLECULAR DOCKING OF NOVEL 4-
AMINOQUINOLINES AND SALICYLALDIMINE
COMPLEXES: EVALUATION AS ANTIMALARIAL
AND ANTITUMOR AGENTS**

Asanda V. Busa

*A thesis submitted in partial fulfilment of the requirements for the
award of the Philosophiae Doctor in the Department of Chemistry,*

University of the Western Cape, South Africa.

UNIVERSITY of the
WESTERN CAPE

Supervisor: Prof. Martin O. Onani

2016



UNIVERSITY *of the*
WESTERN CAPE

I, Asanda Vincent Busa, declare that **“SYNTHESIS, CHARACTERIZATION, AND MOLECULAR DOCKING OF NOVEL 4-AMINOQUINOLINES AND SALICYLALDIMINE COMPLEXES: EVALUATION AS ANTIMALARIAL AND ANTITUMOR AGENTS.”** is my own work and that all sources I have used or quoted have been acknowledged by means of complete referencing at the end of each chapter. By submitting this thesis/dissertation, I declare that the entirety of the work contained therein is my own, original work, that I am the sole author thereof (save to the extent explicitly otherwise stated), that reproduction and publication thereof by University of the Western Cape will not infringe any third party rights and that I have not previously in its entirety or in part submitted it for obtaining any qualification.



.....

Asanda Vincent Busa

.....

Date

To my mother Lulama Busa and my whole family, thank you for believing in me. This is as much as of an achievement for you as it is for me.

To the ones that left us too soon, you prayed for me without ceasing! The next world will hear about this achievement and your contributions. Till we meet again, be at peace.



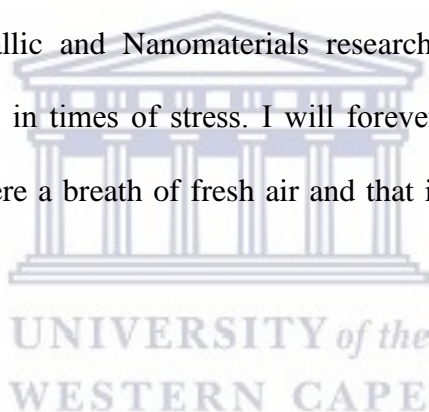
UNIVERSITY *of the*
WESTERN CAPE

Sincere gratitude to the person that was there till the end of this of endeavor, Prof. Marin O. Onani, besides being a supervisor, you were a father and your wise words and encouragement made yet another milestone possible. I will always be grateful for the opportunity to learn but most importantly your willingness to teach! Asante

Professor Ebbe Nordlander, twice as much can only be a charm! Thanks you once more. Your valuable insight strengthened and contribution this work. Thank you for allowing me to learn from and interact with young researchers like myself in your lab. Tack så mycket!

For financial support I would like to thank CSIR and EUROSA

To the Organic, Organometallic and Nanomaterials research groups: Thank you all for providing a space for venting in times of stress. I will forever treasure the “great Gatsby” times we had. The outings were a breath of fresh air and that is etched across my heart. To the future, cheers to us!



Malaria remains a major global health problem and to date, hundreds of thousands of people die as a result of this disease every year. Malaria has been able to adapt and rebound despite various efforts made to combat the disease. The decrease in efficacy of many front-line drugs against malaria, due to increased resistance, prompts investigation into obtaining effective compounds that are able to overcome this resistance. This study investigated the synthesis, characterisation and biological evaluation of new quinoline (as antimalarial agents) as well as non-quinoline (as antitumor agents) based compounds.

Three new ligands based on a 4-amino-7-chloroquinoline moiety with a pendant symmetric pyrazole arm, N-(2-(2-(3,5-dimethyl-1H-pyrazol-1-yl)ethylamino)ethyl)-7-chloroquinolin-4-amine (**L**¹), N-(2-(2-(3,5-diphenyl-1H-pyrazol-1-yl)ethylamino)ethyl)-7-chloroquinolin-4-amine (**L**²) and N-(2-(bis(2-(3,5-dimethyl-1H-pyrazol-1-yl)ethyl)amino)ethyl)-7-chloroquinolin-4-amine (**L**³) were successfully synthesized. The ligands **L**¹, **L**² and **L**³ were then subsequently reacted with Pd²⁺, Pt²⁺, Ir³⁺ and Rh³⁺ metal precursors to afford the corresponding metal complexes [Cp*⁺Rh^{III}Cl(**L**¹)]⁺PF₆⁻ (**C1**), [Cp*⁺Ir^{III}Cl(**L**¹)]⁺PF₆⁻ (**C2**) (Cp* = pentamethylcyclopentadienyl), [Pd^{II}Cl₂(**L**¹)] (**C3**), [Pt^{II}Cl₂(**L**²)] (**C4**), [Pd^{II}Cl(**L**²-H)] (**C5**) and [Pt^{II}Cl(**L**²-H)] (**C6**). Characterization of the ligands and complexes were carried out by using the FT-IR, ¹H/¹³C NMR, UV-Vis, ESI and elemental analysis. This study focused on the preliminary investigation of the antimalarial activity of the designed chloroquine analogous ligands **L**¹-**L**³ as well as the corresponding metal complexes **C1**-**C6** against **NF54**, a chloroquine sensitive (CQS) strain of *P. falciparum*. **L**¹ and **L**³ exhibited the highest activity of the ligands tested and the complexes **C1** and **C2** exhibited the highest activity of the metal complexes with the IC₅₀ values below 20 nM. The chloroquine analogues **L**¹, **L**² and **L**³ were subjected to molecular docking studies in order to gain insight into the interaction of the ligands with the dimeric enzyme, *Plasmodium falciparum* dihydrofolate

reductase-thymidylate synthase (*Pf*DHFR-TS), in the binding site of the enzyme. **L**³ exhibited the highest interaction with protein residues inside the binding site of the enzyme.

In addition to the quinoline analogues, three new non-quinoline based salicylaldimine ligands, 2-((E)-((thiophen-2-yl)methylimino)methyl)-4-tert-butylphenol (**SL**¹), 2-((E)-(2-(thiophen-2-yl)ethylimino)methyl)-4-tert-butylphenol (**SL**²), 2-((E)-((thiophen-2-yl)methylimino)methyl)-4,6-di-tert-butylphenol (**SL**³) appended with a thiophene arm and two new hydrazinic 1,2-bis(1-(5-methylthiophen-2-yl)ethylidene)hydrazine (**SL**⁴), 1,2-bis(1-(5-bromothiophen-2-yl)ethylidene)hydrazine (**SL**⁵) ligands have been synthesized and fully characterized. Generic novel salicylaldiminato complexes [Cp*Rh^{III}Cl(**SL**¹)] (**C7**), [Cp*Ir^{III}Cl(**SL**¹)] (**C8**), [Cp*Ru^{II}Cl(**SL**³)] (**C9**), [(dmsO)Pt^{II}(**SL**¹)] (**C10**) and [(HCO₂)Pt^{II}(**SL**³)] (**C11**) have also been successfully synthesized and characterized using a range of aforementioned spectroscopic and analytical techniques. The molecular structures of the salicylaldiminato **SL**¹ and **SL**³, azine **SL**⁴ and **SL**⁵ ligands with the salicylaldiminato-Rh (**C7**), Ir(**C8**), Pt(**C10**) and Pt(**C11**) complexes have been confirmed by single crystal X-ray diffraction studies. The salicylaldimine ligands and corresponding metal complexes were screened for their cytotoxicity against five different cancer cell lines such as a breast adenocarcinoma (MCF-7), Human hepatocellular liver carcinoma (HepG2), non-cancer human fibroblast (KMST-6), non-tumorigenic epithelial cell line (MCF-12). The best IC₅₀ values obtained for all the compounds were for **SL**¹ and **C10** on all tested cancer cell lines.

Journal article and manuscripts**1. *Towards Discovery of New Organometallic Complexes: Synthesis, Characterization and Antimalarial Activity***

Asanda V. Busa, Erik Ekengard, Ebbe Nordlander, Martin O. Onani (submitted, Journal Of Organometallic Chemistry)

2. *Synthesis, Characterization and molecular structure of N,O-salicylaldiminePt^{II}, Ru^{III}, Rh^{III} and Ir^{III} complexes: Evaluation as anticancer agents*

Asanda V. Busa, M. Meyer, M. Saibu, Martin O. Onani (manuscript)

3. *Crystal structure of the novel ligands N,N'-Bis-[1-(5-methyl-thiophen-2-yl)-ethylidene]-hydrazine and N,N'-Bis-[1-(5-bromo-thiophen-2-yl)-ethylidene]-hydrazine*

Asanda V. Busa, Martin O. Onani (manuscript)

4. *Synthesis, Characterization and Molecular Structure of the unprecedented salicylaldimine complex of platinum and its use as an antitumor agent.*

Asanda V. Busa, Martin O. Onani (manuscript)

Conferences and symposia: Oral presentations:

A. Busa, E. Ekengard, E. Nordlander and M. Onani

Development of novel 4-aminoquinolines as antimalarial agents

PACN, University of Nairobi, Nairobi, Kenya, 17-21/11/2015.

Development of organometallic complexes based on a novel of 4-aminoquinolines scaffold: Molecular docking and evaluation as antimalarial agents.

Cape Organometallic Symposium, University of Cape Town, Cape Town, South Africa, 26-10-2014

Synthesis, Characterization, and crystal structure of salicylaldimine complexes of Pd^{II}, Pt^{II}, Ru^{II}, Rh^{III} and Ir^{III}: Evaluation as anticancer agents

NACOSTI, Kenyatta University, Nairobi, Kenya, 14-22/12/2014.



UNIVERSITY *of the*
WESTERN CAPE

δ	chemical shift
2D	two-dimensional
ACT	artemisinin combination therapy
ATR	attenuated total reflectance
Br	broad
Bu	butyl
<i>ca.</i>	approximately
COD	1,5-cyclooctadiene
COSY	correlation spectroscopy
Cp	cyclopentadiene
Cp*	1,2,3,4,5-pentamethylcyclopentadiene
CQ	chloroquine
CQDP	chloroquine diphosphate
CQR	chloroquine-resistant
CQS	chloroquine-sensitive
d	doublet
DCM	dichloromethane
dd	doublet of doublets
DMSO	dimethylsulfoxide
DMSO-<i>d</i>6	deuterated dimethylsulfoxide
EI	electron impact
eq	equivalents
ESI-MS	electrospray ionisation mass spectrometry
Et	ethyl

Fc	ferrocene
FQ	ferroquine
Hb	haemoglobin
HR	high resolution
HSQC	heteronuclear single quantum coherence
IC₅₀	50% inhibitory concentration
IR	infrared
J	coupling constant
m	multiplet
Me	methyl
MTT	3-(4,5-dimethylthiazol-2-yl)-2,5-diphenyltetrazolium bromide
m/z	mass to charge ratio
nd	not determined
NMR	nuclear magnetic resonance
PfCRT	<i>Plasmodium falciparum</i> chloroquine-resistant transporter
ppm	parts per million
RI	resistance index
r.t.	room temperature
s	singlet
SD	standard deviation
SI	selectivity index
sub	substituted
t	triplet
td	triplet of doublets
unsub	unsubstituted

Declaration	ii
Dedication	iii
Acknowledgements	iv
Abstract	v
Conference contributions	vii
Abbreviations	ix
Table of contents	xi
List of Figures	xx
List of Schemes	xxvi
List of Tables	xxvii
CHAPTER 1: Malaria causing parasite and the constant battle to find a cure	1
1. Introduction: Malaria.....	1
1.2. Life cycle of the malaria causing Plasmodium parasite.....	3
1.3 Antimalarial drugs.....	5
1.3.1 Quinolines as antimalarial agents.....	5
1.3.1.1 <i>Quinolinemethanols</i>	6
1.3.1.2 <i>4-aminoquinolines</i>	7
1.3.1.3 <i>8-aminoquinolines</i>	11
1.3.2 <i>Artemisin and its derivatives</i>	12
1.3.3 <i>Mode of action of quinoline compounds</i>	13
1.3.3.1 <i>Structure-Activity Relationships for CQ</i>	18
1.3.4 <i>Emergence and Spread of drug resistance in malaria parasites</i>	21
1.4 Organometallic complexes as antimalarials.....	24
1.4.1 <i>Platinum complexes</i>	24

1.4.2 Ruthenium and Gold complexes.....	28
1.4.3 Rhodium and Iridium complexes.....	32
1.4.4 Ferroquine and derivatives.....	34
1.5. Scope of the thesis.....	41
1.6. Aims and Objectives.....	42
1.6.1. General Aims.....	42
1.6.2. Specific Objectives.....	42
1.7. References.....	45
CHAPTER 2: Synthesis and characterisation of N,N'- and C,N,N'-Pd^{II}, Pt^{II}, Rh^{III} and Ir^{III} complexes	69
2.1. Introduction.....	69
2.2. Results and Discussion.....	71
2.2.1 Synthesis and characterisation of CQ-analogues, L ¹ -L ³	71
2.2.1.1. Infrared Spectroscopy	72
2.2.1.2. ¹ H and ¹³ C { ¹ H} NMR Spectroscopy.....	75
2.2.1.3 Mass Spectroscopy.....	76
2.2.2 Synthesis and Characterization of metal complexes, C1-C6.....	76
2.2.2.1 Infrared Spectroscopy.....	78
2.2.2.2 ¹ H and ¹³ C { ¹ H} NMR Spectroscopy.....	79
2.2.2.3 Elemental Analysis and Mass Spectroscopy.....	82
2.3 Summary and Conclusions.....	84
2.4 Experimental.....	84
2.4.1 Chemistry.....	84

2.4.1.1 <i>Materials and Methods</i>	84
2.5. Synthesis.....	84
2.5.1 Synthesis of <i>N</i> -(2-(2-(3,5-dimethyl-1 <i>H</i> -pyrazol-1-yl)ethylamino)ethyl)-7-chloroquinolin-4-amine, L¹	85
2.5.2 Synthesis of <i>N</i> -(2-(2-(3,5-diphenyl-1 <i>H</i> -pyrazol-1-yl)ethylamino)ethyl)-7-chloroquinolin-4-amine, L²	86
2.5.3 Synthesis of <i>N</i> -(2-(bis(2-(3,5-dimethyl-1 <i>H</i> -pyrazol-1-yl)ethyl)amino)ethyl)-7-chloroquinolin-4-amine, L³	87
2.5.4. Preparation of (η^5 -Cp*) <i>N</i> -(2-(2-(3,5-diphenyl-1 <i>H</i> -pyrazol-1-yl)ethylamino)ethyl)-7-chloroquinolin-4-amine)chlororhodium/iridium (III), [RhClCp*(L¹)], (C1), and [IrClCp*(L¹)], (C2).....	88
2.5.5 Preparation of (<i>N</i> -(2-(2-(3,5-diphenyl-1 <i>H</i> -pyrazol-1-yl)ethylamino)ethyl)-7-chloroquinolin-4-amine)dichloropalladium/platinum (II), [PdCl ₂ (L¹)], (C3), and [PtCl ₂ (L²)], (C4).....	89
2.5.6 Preparation of cyclometallated Pd(II) (C5) and Pt(II) (C6) complexes.....	91
2.5.6.1 [Pd{ κ^2 -C,N,N'-{[1-(CH ₂) ₂ NH(CH ₂) ₂ NH-4-CQ]-3-(C ₅ H ₄)-5-Ph-pzol}}]C L² (C5).....	92
2.5.6.2 [Pt{ κ^2 -C,N,N'-{[1-(CH ₂) ₂ NH(CH ₂) ₂ NH-4-CQ]-3-(C ₅ H ₄)-5-Ph-pzol}}]C L² (C6).....	92
2.6 References.....	93

CHAPTER 3: Synthesis and characterisation of N,N'- and C,N,N'-Pd^{II}, Pt^{II}, Rh^{III} and Ir^{III} complexes.....101

3.1 Introduction.....101

3.2 Results and Discussion.....104

3.2.1 Synthesis and Characterization of N,O-salicylaldimine ligands, **SL¹-SL³**.....104

3.2.1.1 *Infrared Spectroscopy of the N,O-salicylaldimine ligands, SL¹-SL³*.....106

3.2.1.2 *¹H and ¹³C {H} NMR, SL¹-SL³*108

3.2.1.3 *Elemental Analysis and Mass Spectroscopy, SL¹-SL³*.....111

3.2.1.4 Synthesis and Characterization of hydrazinic/ketimine ligands, **SL⁴-SL⁵**.....112

3.2.1.5. *Infrared Spectroscopy of ligands of SL⁴ and SL⁵*113

3.2.1.6 *¹H and ¹³C {H} NMR, SL⁴ and SL⁵*.....114

3.3 Single X-ray crystallography.....115

3.3.1 *Crystal and Molecular structure of salicylaldimines, SL¹ and SL³*.....115

3.3.2 *Crystal and Molecular structure of hydrazinicketimine ligands, SL⁴ and SL⁵*.....118

3.4 Synthesis and Characterization of N,O-salicylaldimine complexes, **C7-C11**.....121

3.4.1 *Infrared Spectroscopy, C7-C11*.....124

3.4.2 *¹H and ¹³C {H} NMR, C7-C11*.....125

3.4.3 *Elemental Analysis and Mass Spectroscopy, C7-C11*.....129

3.5 Single crystal X-ray diffraction.....129

3.5.1 Crystal and molecular structures of complex C7 and C8	129
3.5.2 Crystal and molecular structures of complex C10 and C11	132
3.6 Summary and Conclusions.....	135
3.7 Experimental.....	136
3.7.1 Chemistry.....	136
3.7.1.1 Materials and Methods.....	136
3.8 Synthesis	137
3.8.1 General Synthesis of salicylaldimine ligands, SL ¹ - SL ³	137
3.8.1.1 2-((<i>E</i>)-((thiophen-2-yl)methylimino)methyl)-4- <i>tert</i> -butylphenol, SL ¹	137
3.8.1.2 2-((<i>E</i>)-(2-(thiophen-2-yl)ethylimino)methyl)-4- <i>tert</i> -butylphenol, SL ²	138
3.8.1.3 2-((<i>E</i>)-((thiophen-2-yl)methylimino)methyl)-4,6- <i>di-tert</i> -butylphenol, SL ³	138
3.8.2 General synthesis of hydrazinic/ketimines, SL ⁴ and SL ⁵	139
3.8.2.1 1,2-bis(1-(5-methylthiophen-2-yl)ethylidene)hydrazine, SL ⁴	139
3.8.2.2 1,2-bis(1-(5-bromothiophen-2-yl)ethylidene)hydrazine, SL ⁵	139
3.8.3 General synthesis of [Cp*Rh ^{III} Cl(SL ¹)] (C7), [Cp*Ir ^{III} Cl(SL ¹)] (C8) and [Cp*Ru ^{II} Cl(SL ²)] (C9) complexes.....	139
3.8.3.1 Synthesis of platinumacycle, C10	141
3.8.3.2 Synthesis of [Pt ^{II} SL ³ (<i>H</i> COD)] (C11).....	141
3.9 References.....	142

CHAPTER 4: Antimalarial activity and molecular docking of Pd^{II}, Pt^{II}, Rh^{III} and Ir^{III} chloroquine analogous complexes.....158

4.1 Introduction.....158

4.2 *In vitro* antiplasmodial activity of chloroquine analogues and corresponding complexes.....160

4.2.1 *Antiplasmodial activity of ligand L¹-L³ against the chloroquine sensitive strain of plasmodium falciparum.....160*

4.2.2 *Antiplasmodial activity of complex C1-C6 against the chloroquine sensitive strain of plasmodium falciparum, NF54.....162*

4.2.3 *Heme Aggregation Inhibition Assays.....164*

4.2.3.1 *Heme Aggregation Inhibition Assays of the ligands, L¹-L³.....165*

4.2.3.2 *Heme Aggregation Inhibition Assays of the metal complexes, C1-C6.....167*

4.3 Computational studies.....170

4.3.1 Molecular docking of ligands, L¹-L³.....170

4.4 Summary and Conclusions.....173

4.5 Experimental.....174

4.5.1 *Determination of in vitro antiplasmodial activity.....174*

4.5.2 *Heme Aggregation Inhibition Assay.....175*

4.6 Computational Studies.....176

4.6.1 Molecular Docking.....	176
4.7 Reference.....	177
Chapter 5: Anticancer activity of N,O-salicylaldimine Pt^{II}, Ru^{II}, Rh^{III} complexes against selected cancer cell lines.....	188
5.1 Introduction.....	188
5.1.1 Biochemical mechanism of cis-platin action.....	189
5.1.2 Binding modes of bioinorganics to DNA structure.....	190
5.1.2.1 Covalent binding.....	191
5.2 Other bioinorganic compounds as anticancer agents.....	193
5.2.1 Ruthenium.....	193
5.2.2 Rhodium and Iridium.....	196
5.3 Results and Discussion.....	198
5.3.1 <i>In vitro</i> screening of N,O-salicylaldimine ligands and corresponding complexes.....	198
5.3.1.1 <i>In vitro</i> anticancer activity of N,O-salicylaldimine ligands, SL¹-SL³	198
5.3.1.2 <i>In vitro</i> anticancer activity of N,O-salicylaldimine complexes, C1-C4	200
5.4 Summary and Conclusions.....	203
5.5 Experimental.....	204

5.5.1 Materials.....	204
5.5.2 Commercial kits/Molecular probes.....	204
5.5.3 General solutions and buffer.....	204
5.5.4 Tissue culture.....	204
5.5.5 Thawing of cells.....	205
5.5.6 Trypsinization of cells.....	206
5.5.7 Cell count.....	206
5.5.8 Seeding of cells.....	206
5.5.9 Freezing of cells.....	207
5.6. Bioassay.....	207
5.6.1 Evaluation of cytotoxicity using MTT assay.....	207
5.7 References.....	209
Chapter 6: Conclusions, Recommendations and Future outlooks.....	222
6.1 Conclusions.....	222
6.1.1 Synthesis.....	222
6.1.2 <i>In vitro</i> antiplasmodial activity.....	223
6.1.3 Molecular docking.....	224
6.1.4 <i>In vitro</i> antitumor activity.....	224

6.2 Recommendations and future outlooks.....225



UNIVERSITY *of the*
WESTERN CAPE

Chapter 1

Figure 1.1: Countries around the world where malaria was known to occur in 2015. The different colour shades denotes malaria prevalence in countries from around the world. Picture taken from World Health Organization [19].....	2
Figure 1.2: Countries and territories that are recently affected by Zika virus. Picture taken from ref [23].....	3
Figure 1.23 Life cycle of the malaria-causing <i>Plasmodium</i> parasite. Image taken from [24].....	5
Figure 1.4: Quinoline based antimalarials.....	8
Figure 1.5: Potent chloroquine analogues that exhibit enhanced activity compared to CQ....	9
Figure 1.6: Bridged alkyl bisquinoline compounds active against malaria and exhibiting cytotoxicity.....	10
Figure 1.7: Synthetic antimalarial bisquinoline compounds bridged by the heterocyclic piperazinyl moiety.....	11
Figure 1.8: Artemisinin and its synthetic derivatives.....	13
Figure 1.9: Digestive vacuole of the plasmodium parasite. Picture taken and modified from [74,75].....	14
Figure 1.10: Evolution of understanding chemical structure of hemazoin: (a) linear polymer [81]; (b) antiparallel polymer chains linked by hydrogen bonds [82]; (c) centrosymmetric dimers linked by hydrogen bonds [83]. Picture taken from ref [84].....	16
Figure 1.11: Structure-activity relationships (SAR) for chloroquine (CQ).....	18

Figure 1.12: Structure-activity relationships of carbon isoesters.....	19
Figure 1.13: Chloroquine (CQ) derivatives with different position of the chloro group.....	20
Figure 1.14: Predicted protein structure of PfCRT postulated to possess 10 transmembrane. Picture taken from ref [108].....	23
Figure 1.15: Mixed-ligand platinum (II) complexes with pronounced tendency to undergo self-aggregation in solution.....	25
Figure 1.16: Cationic platinum (II) complexes possessing antimalarial activity.....	26
Figure 1.17: Chemical structures of palladium/platinum chloroquine [<i>trans</i> -Pt(II)X ₂ (CQ) ₂] and chloroquine diphosphate [<i>trans</i> -Pt(II)X ₂ (CQDP) ₂] (X = Cl ⁻ and I ⁻) complexes.....	27
Figure 1.18: Ruthenium-chloroquine complexes possessing antimalarial activity.....	29
Figure 1.19: Proposed structure of gold-quinoline complexes.....	30
Figure 1.20: Half-sandwich Ru(II)-CQ p-cymene complexes.....	31
Figure 1.21: Ruthenocene 4-amino-7-chloroquinolines complexes with known antimalarial activity [136].....	32
Figure 1.22: Rhodium- and Iridium-CQ complexes possessing antimalarial activity.....	33
Figure 1.23: Organosilicon Ru(II) (1.58), Rh(III) (1.59) and Rh(I) (1.60) quinolines.....	34
Figure 1.24: Ferrocene derivatives that possess antimalarial activity.....	35
Figure 1.25: A potent antimalarial agents that has entered phase-II clinical trials, Ferroquine (FQ).....	36
Figure 1.26: Ferroquine derivatives that are actively comparable to Ferroquine.....	38
Figure 1.27: Ferroquine-chloroquine conjugates.....	40

Chapter 2:

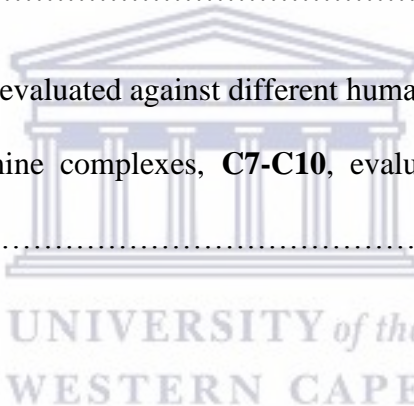
Figure 2.1: Selected pyrazole derivatives evaluated for their pharmacological activity, chemical structures reported from references [13–21].....	70
Figure 2.2: Chloroquine analogue ligands L¹-L³ , with insert for ¹ H and ¹³ C NMR numbering system.....	74
Figure 2.3: ¹ H NMR spectrum of ligand L¹ , with numbering inserts.....	75
Figure 2.4: ¹ H NMR spectrum of ligand L² , with numbering inserts.....	76
Figure 2.5: ¹ H NMR spectrum of complex C5 , with ¹ H numbering insert.....	82
Figure 2.6: ¹³ C NMR spectrum of complex C6 , with ¹ H numbering insert.....	82

Chapter 3:

Figure 3.1: Different subclass of Schiff base ligands.....	101
Fig. 3.2: ¹ H NMR of <i>N,O</i> -salicyladimine ligand SL¹ with insert for ¹ H NMR numbering scheme.....	109
Figure. 3.3: ¹ H NMR of <i>N,O</i> -salicyladimine ligand SL³ with insert for ¹ H NMR numbering scheme.....	110
Figure 3.4: ¹ H NMR spectra of ligand SL⁵ recorded in CDCl ₃	114
Figure 3.5: ORTEP representations of molecular structures of salicyaldimine ligands SL¹ (<i>left</i>) with hydrogen atoms included, and SL³ (<i>right</i>) shown with 50% probability ellipsoids.....	116
Figure 3.6: ORTEP representations of mononuclear ketamine ligands SL⁴ (<i>left</i>)and SL⁵ (<i>right</i>). Thermal ellipsoids are drawn at the 50 % probability level. Hydrogen atoms have been included.....	119

Figure 3.7: ^1H NMR spectrum of the salicylaldiminato-rhodium(III) complex C7 , recorded in CDCl_3	126
Figure 3.8: ^1H NMR spectrum of the salicylaldiminato-iridium(III) complex C8 , recorded in CDCl_3	127
Figure 3.9: ^1H NMR spectrum of the salicylaldiminato-ruthenium(II) complex C9 , recorded in CDCl_3	127
Figure 3.10: ORTEP representations of mononuclear ligand C7 (<i>left</i>) and C8 (<i>right</i>). Thermal ellipsoids are drawn at the 50 % probability level. Hydrogen atoms have been omitted for clarity.....	130
Figure 3.11: ORTEP representations of mononuclear ligand C10 (<i>left</i>) and C11 (<i>right</i>). Thermal ellipsoids are drawn at the 50 % probability level. Hydrogen atoms have been omitted for clarity.....	133
Chapter 4:	
Figure 4.1: Ligands evaluated for their antiparasmodial activity against the CQS NF54 of <i>plasmodium falciparum</i>	160
Figure 4.2: Complexes evaluated for their antiparasmodial activity against the CQS NF54 of <i>plasmodium falciparum</i>	162
Figure 4.3: Process of haemoglobin degradation and heme detoxification by intraerythrocytic malaria parasite, picture taken from ref [6].....	167
Figure 4.4: Graphical representation of the IC_{50} values for the ligands L¹-L³ and corresponding complexes C1-C6	169

- Figure 4.5: Correlation of drug inhibition of β -haematin inhibition induced by haemozoin at pH 4.7 and inhibition of parasite growth using the CQ-sensitive *P. falciparum* strain **NF54**. Values are given for ligands (**L¹-L³**), metal complexes (**C1-C6**), amodiaquine (AQ), chloroquine (CQ).....169
- Figure 4.6: Docked conformation of **L¹** with *P. falciparum* dihydrofolate reductase-thymidylate synthase (The dotted line shows the hydrogen bonds between the **L¹** and protein residues).....172
- Figure 4.7: **L²** bound into the *P. falciparum* dihydrofolate reductase-thymidylate synthase. The dotted lines show the hydrogen bonds.....172
- Figure 4.8: Docked conformation of dihydrofolate reductase-thymidylate synthase with **L³**.....173
- Chapter 5:**
- Figure 5.1: Structure of the prominent anticancer platinum derivatives, cis-platin (**i**), carboplatin (**ii**), and oxaliplatin (**iii**).....189
- Figure 5.2: Different components of platinum anticancer agents. Additional factors that can be varied are the stereochemistry and the respective number of non-leaving group and leaving group ligands, picture modified from ref [27].....191
- Figure 5.3(a): Representation of the *cis*-Pt-DNA adduct formed with the N-7 of the guanine base, picture take from ref [28].....192
- Figure 5.4(b): Reaction of *cis*-PtCl₂(NH₃)₂ with DNA to form *cis*-Pt-DNA adduct, picture taken from ref [42].....193

Figure 5.5: The first reported half-sandwich Ru ^{II} -based antitumor agent [43].....	194
Figure 5.6: Chemical structures of the Ru ^{II} -based drug candidates in clinical trial: NAMI-A and KP1019.....	195
Figure 5.7: A general representation of Ru ^{II} , Os ^{II} -, Rh ^{III} - and Ir ^{III} -based 1 half-sandwich ‘piano-stool’ complexes.....	196
Figure 5.8: General structure of half-sandwich Ir ^{III} cyclopentadienyl complexes. The ligands tune the chemical and biological activity, picture taken and modified from ref [74].....	197
Figure 5.9: Ligands, SL¹-SL³ , evaluated against different human cancer cell lines.....	199
Figure 5.10: <i>N,O</i> -salicylaldimine complexes, C7-C10 , evaluated against different human cancer cell lines.....	200
	
Chapter 6:	
Figure 6.1: Proposed structural modifications for a new series of ferroquine analogues as antimalarial agents.....	226

Chapter 2:

Scheme 2.1: Synthesis of ligand L^1 , L^2 and L^3	72
Scheme 2.2: Synthesis of half-sandwich complexes C1 and C2 , coordination compounds C3 and C4 , and metallacycles C5 and C6	78

Chapter 3:

Scheme 3.1: Synthesis of <i>N,O</i> -salicylaldimine ligands, SL^1 - SL^3	104
Scheme 3.2: Mechanistic outline of a general Schiff-base condensation reaction.....	105
Scheme 3.3: Possible tautomerism of the hydroxyimine (SL^1 , <i>left</i>) to the keto-amine (<i>right</i>).....	107
Scheme 3.4: General synthetic route for the hydrazinic/ketimines, SL^4 and SL^5	112
Scheme 3.5: General synthesis of half-sandwich/arenesalicylaldimine complexes, C7 - C9	122
Scheme 3.6: Synthesis of the unexpected platinacycle C10	122
Scheme 3.7: Synthesis of salicylaldiminePt ^{II} - H (COD) complex, C11	123
Scheme 3.8: Deprotonation mechanism of the phenolic proton for the salicylaldimine ligands, SL^1 - SL^3	128

Chapter 2:

Table 2.1: Selected Infrared spectroscopy (KBr) data for ligands, L¹-L³	74
Table 2.2: ESI-MS data for the title ligands L¹-L³	76
Table 2.3: Selected FT-IR data for the complexes C1-C6	78
Table 2.4: Selected ¹ H and ¹³ C{ ¹ H} NMR data for complexes C1-C6	81

Chapter 3:

Table 3.1: Infrared data of the N,O-salicylaldimine ligands, SL¹-SL³	107
Table 3.2: ¹ H NMR spectral data (δ in ppm)in CDCl ₃ (unless noted otherwise).....	110
Table 3.3: ¹³ C{ ¹ H} NMR spectral data (δ in ppm)in CDCl ₃ (unless noted otherwise).....	111
Table 3.4: Infrared data of the N,O-salicylaldimine ligands, SL⁴ and SL⁵	113
Table 3.5: ¹ H and ¹³ C{ ¹ H} NMR data for ligands, SL⁴-SL⁵	115
Table 3.6: Crystal data and structure refinement of ligand SL¹ and SL³	117
Table 3.7: Selected bond lengths [\AA] and angles [$^{\circ}$] for salicylaldimine ligands SL³ and SL¹	118
Table 3.8: Crystal data and structure refinement of ligand SL⁴ and SL⁵	120
Table 3.9: Selected bond lengths [\AA] and angles [$^{\circ}$] for ketamine ligand SL¹ and SL³	121
Table 3.10: Infrared data of the N,O-salicylaldimine ligands, C7-C11	125
Table 3.11: Data collection and selected parameters for the salicylaldimine complexes C7 and C8	131
Table 3.12: Selected bond lengths [\AA] and angles [$^{\circ}$] for salicylaldimine complexes C7 and C8	132
Table 3.13: Data collection and selected parameters for the salicylaldimine complexes C10 and C11	134

Table 3.14: Selected bond lengths [\AA] and angles [$^\circ$] for salicylaldimine complexes C10 and C11	135
--	-----

Chapter 4:

Table 4.1: <i>In vitro</i> anti-plasmodial activities of L¹-L³ and C1-C6 , against NF54	161
Table 4.2: <i>In vitro</i> anti-plasmodial activities of C1-C6 , against CQ-susceptible strain NF54	164
Table 4.3: β -haematin inhibition activity of ligands L¹-L³	166
Table 4.4: β -haematin inhibition activity of complexes C1-C6	168
Table 4.5: List parameters generated from molecular docking showing the interaction behaviours of protein and ligands.....	173

Chapter 5:

Table 5.1: IC_{50} (μm) values of the salicylaldimine ligands SL¹-SL³ and the reference drug <i>cis</i> -platin against the different human tumor cell lines ^b	199
Table 5.2: IC_{50} (μm) values of the complexes C1-C4 against the different human tumor cell lines ^b	201
Table 5.3: Tissue culture media used in the study and the suppliers.....	204
Table 5.4: Cell lines used in this study.....	205

1. Introduction

Malaria is a deadly disease that has been known to cause strife in humans from as early as the days of Neolithic dwellers, early Chinese and Greeks, princes and paupers [1]. It still continues to afflict human beings to this day and age, accounting for 150 to 300 million deaths in the 20th century alone [2]. The World Health Organisation (WHO), in 2015, compiled 220 million cases of malarial infections globally with 800 000 reported deaths (Figure 1.1) [3]. This infectious disease is transmitted by a bite from a female *Anopheles* mosquito that carries the protozoan parasite. Five species of the infectious protozoan parasite that belong to the genus *Plasmodium* are known i.e. *P. falciparum*, *P. vivax*, *P. malariae*, *P. ovale* and *P. knowlesi* [4,5]. The two common species are *P. falciparum* and *P. vivax*, the former being the most lethal of them all. The fifth species, *P. knowlesi*, was reported to infect human in Malaysian Borneo 10 years ago [7]. Countries that bear the most burden nowadays are those located in the sub-Saharan region of Africa as malaria weighs heavy on the economies of the poverty stricken countries [8–10]. The fight against malaria has only intensified after the emergence of the resistance for the advocated first line drug artemisinin [11,12]. Resistance against artemisinin and derivatives has since spread with cases of emergence being documented in Thailand and bordering countries [13–17].

Although malaria has been “known”, it was not until the 1800’s that the dawn into the parasites “life journey” began when Alphonse Laveran discovered the parasite in the blood stream of an infected patient [18].

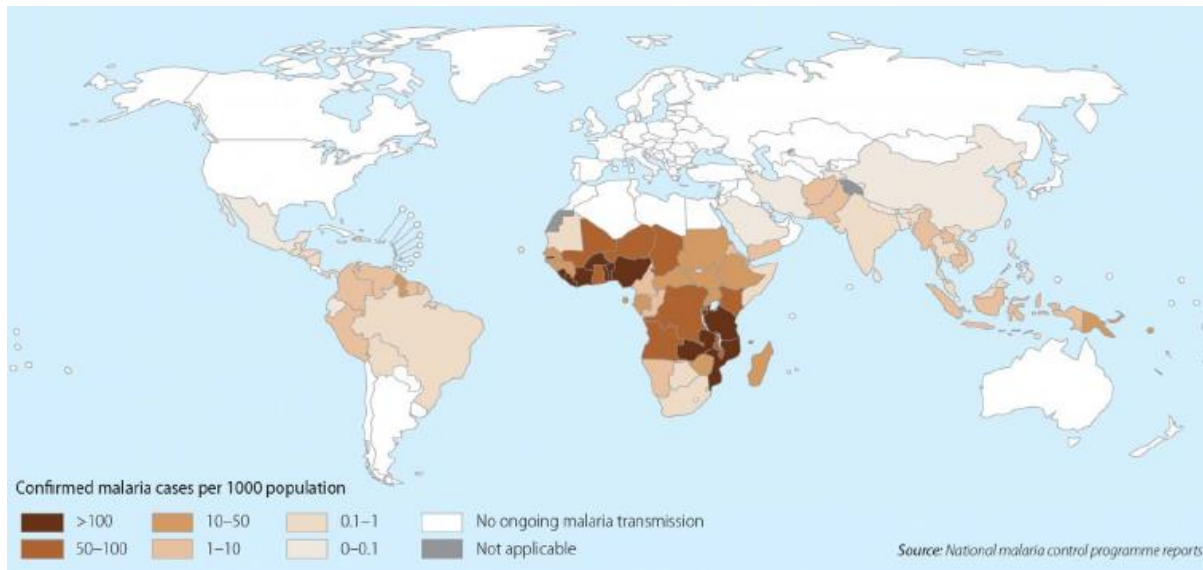


Figure 1.1: Countries around the world where malaria was known to occur in 2015. The different colour shades denotes malaria prevalence in countries from around the world. Picture taken from World Health Organization [19].

The other deadly disease that is spread by the bite of a mosquito is Zika virus that is carried by the mosquitoes from the *Aedes* genus. This family of mosquitoes have been associated with the transmission of the deadly known tropical diseases such as dengue, chikungunya and yellow fever. This is a fairly new virus that was isolated in 1947 in the Zika forest of Uganda from infected monkeys [20,21]. It was not until 1952 that its first human related case was reported. Since then, its cases were only recorded mostly in Africa with occasional cases recorded in Asia [20,21]. In 2014, Chile reported its first Zika virus encounter with other South American countries such as Brazil, Barbados, Bolivia, Colombia, Ecuador, El Salvador, French Guiana, Guadeloupe, Guatemala, Guyana, Haiti, Honduras, Martinique, Mexico, Panama, Paraguay, Puerto Rico, Saint Martin, Suriname, and Venezuela reporting their first cases since May 2015 [20–22]. Figure 1.2 depicts countries that are affected by the emergence of the Zika virus. The emergence of this virus has attracted international attention as Brazil has reported on babies born with microcephaly, a medical condition that causes shrinkage in the head of babies that result in incomplete brain development. There is no

available medication for the treatment of Zika virus and the only recommended option is avoiding mosquito bites with the use of mosquito nets and mosquito skin repellents [20–23].

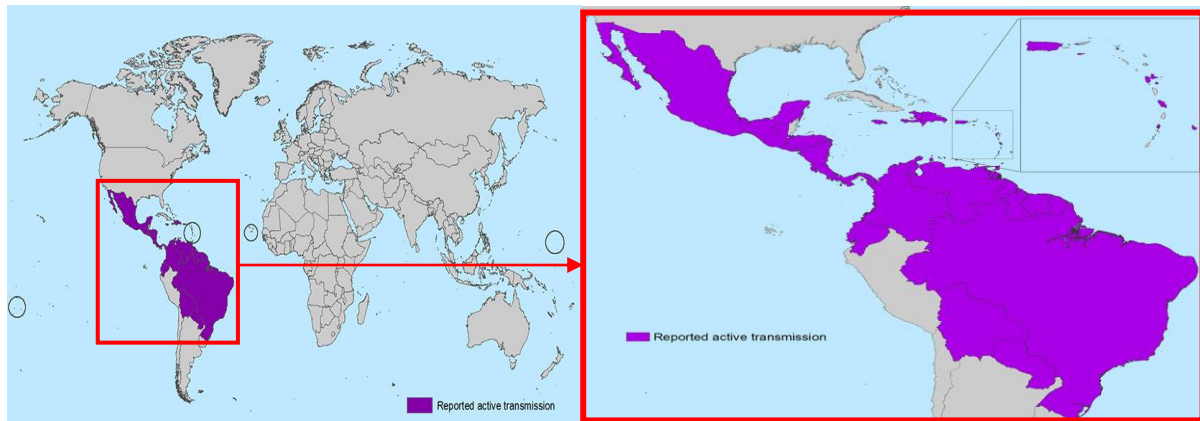


Figure 1.2: Countries and territories that are recently affected by Zika virus. Picture taken from ref [23].

It is within this perspective that there is high demand to develop low cost antiparasitic drug candidates that offer diverse modes of action so as to avert resistance while restoring activity in order to combat the some of the deadliest parasitic diseases such as malaria.

1.2 Life cycle of the malaria-causing *Plasmodium* parasite

The malaria parasite can be viewed to co-exist in two types of habitats: human beings and female *Anopheles* mosquito and its lifecycle revolves around these two innkeepers. The malaria-causing parasite is transmitted to human beings by the female *Anopheles* mosquito (Figure 1.3). The bite from the mosquito thus injects the parasite as threadlike sporozoites into the bloodstream of the human host. The sporozoites are carried from the bloodstream into liver cells where they infest liver cells (liver stage infection). Depending on the malaria parasite, sporozoites (per liver cell) can take more or less than 16 days to mature, divide, and

produce merozoites [24]. The occupancy of the liver cells as merozoites multiply, ruptures the liver cell releasing merozoites into the bloodstream to begin what is known as the erythrocytic stage, where they prey and replicate on the red blood cells (RBCs). In the RBCs the parasite is at its peak, degrading an enormous percentage of hemoglobin (*vide infra*, **section 1.3.3**). The merozoites mature and transmute into trophozoites that through asexual replication form a schizont. The cycle is accelerated when inside the infected erythrocyte the schizont mature and rupture, damaging the host cells and releasing a “new” batch of merozoites that in turn invade RBC, maintain the erythrocytic phase. In the erythrocytic cycle, asexual blood parasites differentiate into gametocytes i.e. male and female sexual forms, which maintain the existence of the parasite through ingestion by the mosquito vector. As the mosquito feeds on the infected human, it ingests gametocytes that burst upon reaching the gut of the mosquito. The transformations inside the gut of the vector results in sporozoites being formed that eventually migrate and invade the salivary glands of the mosquito, therefore completing the life cycle [24–26].

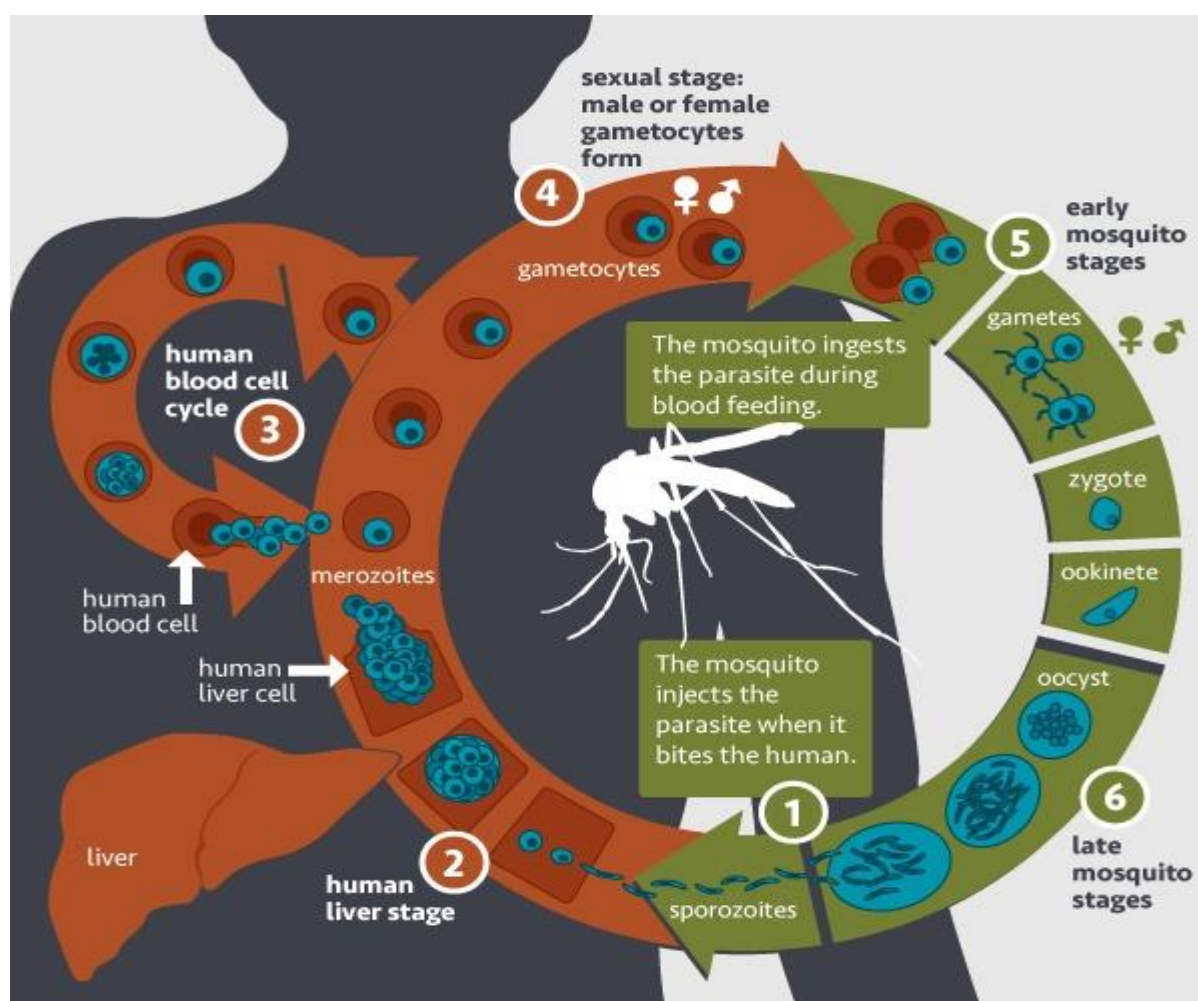


Figure 1.3 Life cycle of the malaria-causing *Plasmodium* parasite. Image taken from ref [24].

WESTERN CAPE

1.3 Antimalarial drugs

1.3.1 Quinolines as antimalarial agents

A variety of the aromatic heterocyclic quinoline compounds have been used as antimalarial drugs and are available for the prophylaxis of the malaria causing parasite. These aromatic heterocyclic quinoline compounds can be grouped according to subcategories with similar structural features. These different structural features permit each subcategory class of compounds to target the parasite differently as they possess peculiar mechanism that is

characteristic to each class. This family of aromatic heterocyclic compounds can be grouped into three subcategories [27]:

(i) Quinoline methanols that include;

— quinine (QN), quinidine (QD), and mefloquine (MQ)

(ii) 4-aminoquinolines that include;

— chloroquine (CQ), amodiaquine (AQ), and piperaquine (PQ), and

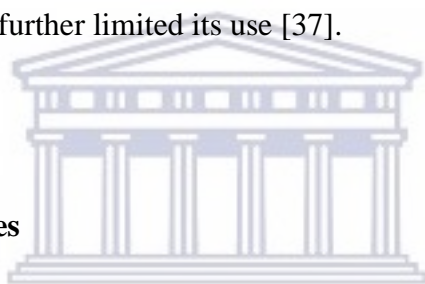
(iii) 8-aminoquinolines that include;

— primaquine (PQ), pamaquine (PQ'), and tafenoquine (TQ)

1.3.1.1 Quinoline methanols

First antimalaria agents that became known to men were the cinchona alkaloids that were extracted from the bark of different species of cinchona trees. Although the therapeutic effects of these cinchona alkaloids were known, it was not until the early 1700s when they were approved in the European market as antimalarial drugs [28]. The active compound of this class of cinchona alkaloids; a quinoline methanol, quinine (**1.4**, QN, Figure 1.3), was only successfully isolated in 1820 by Pelletier and Caventou and the first total synthetic pathway of the active quinine was reported in 1944 by Woodward and Doering [29], since then, several more efficient total synthetic pathways have been reported [30]. Quinine is a basic aryl amino alcohol that is mostly achieved as a salt [31]. Various forms of the quinine salts have been prepared, and these include hydrochloride, dihydrochloride, sulphate, bisulphate, and gluconate salts. Dihydrochloride salt is the mostly used derivative of them all

[28]. As antimalarial properties of quinine were identified, for nearly two centuries it was used as the only chemotherapeutic agents [32]. The role of quinine and congeners as an active antimalarial is still evident, as recent publications have reported on its effective use for treatment of multidrug-resistant malaria parasite [27,33], but its use is still hampered by severe side effects that include cinchonism, with mild forms including tinnitus, slight impairment of hearing, headache and nausea [34–36]. Resistance has also been documented for quinine although it has been observed to build over a span of time with the first case reported in 1908. Amongst the limitations of quinine that include poor tolerability, poor compliance with complex dosing regimens, accessibility to more efficacious quinolines such as chloroquine as antimalarial further limited its use [37].



1.3.1.2 4-aminoquinolines

Chloroquine (1.1, CQ, Figure 1.4) is one of the successfully used heterocyclic aromatic groups against malaria in the quinoline family. Quinolines have been shown to form a pool of the most commonly used heterocyclic aromatics as antimalarial agents. Figure 1.4 depicts some of the prominent organic quinoline-based antimalarials that are either on the commercial market or clinically approved.

In this family of quinolines, chloroquine (CQ), since its synthesis in 1934 [32], has been the chief drug in this family of antimalarials. CQ's activity can be attributed to a delineate nature of its pharmaceutical properties that renders its use crucial in prophylaxis due to better effectiveness, low cost of production and reduced toxicity compared to its forerunner QN that had deleterious side effects. Studies into the physicochemical nature of CQ, AQ, and Pyronaridine (PD) revealed that at neutral pH, these compounds are diprotonated and

lipophilic [38] assisting with accumulation to therapeutic concentrations inside the digestive vacuole of the parasite before the build-up of resistance.. Although resistance has hindered the activity of this widely used and effective antimalarial in most parts of the world, mostly in Sub-Saharan Africa, it still retains its efficacy against *P. ovale*, *P. malariae* and most cases of *P. vivax* malaria [27,33]. Alternatives based on 4-aminoquinolines and amodiaquine derivatives that would restore activity were developed and reported [39].

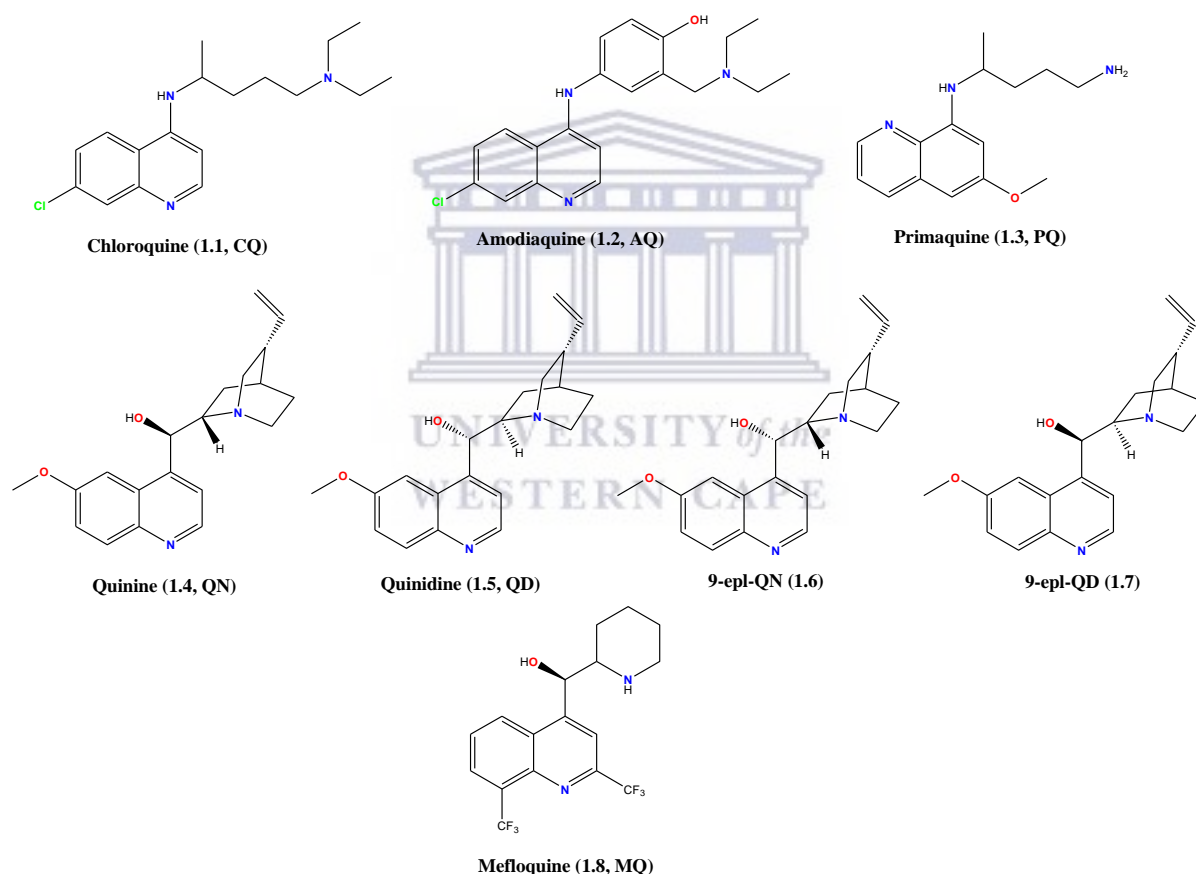


Figure 1.4: Quinoline based antimalarials.

Restoration of the activity of the know parent quinoline-based antimalarials became the subject of intense investigation for many chemists. These modifications realized the

importance of the quinoline moiety in the search for new antimalarial that might offer different modes of action. These efforts, amongst many, led to the synthesis of chloroquine N-oxide (**1.9**, Figure 1.5) and 5-azachloroquine (**1.10**, Figure 1.5) that were reported to be more potent antimalarials *in vivo* compared to chloroquine [40].

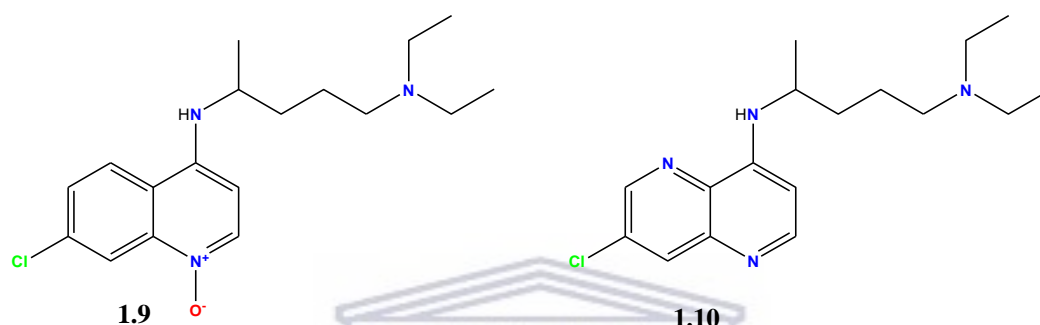
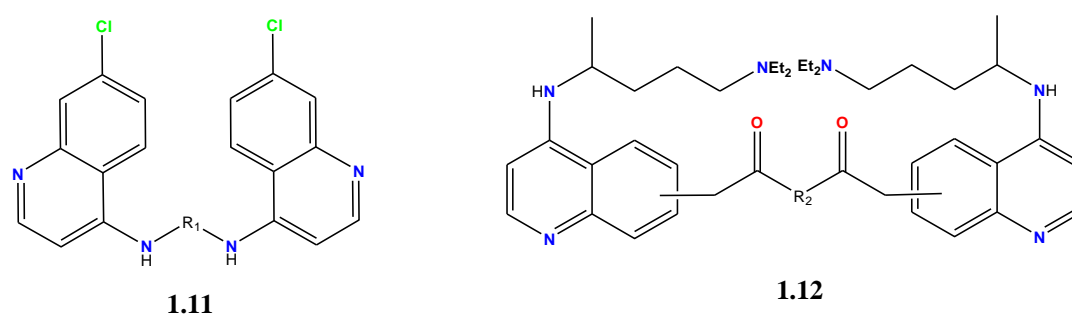


Figure 1.5: Potent chloroquine analogues that exhibit enhanced activity compared to CQ.

Other endeavors aimed at modifying the quinoline moiety by the introduction of electron withdrawing (NO_2 and CF_3) and electron donating groups such as NH_2 , OH , OCH_3 , H and CH_3 on the quinoline scaffold (Figure 1.6). These modifications, like many others, were observed to bring about a decrease in the potency of these CQ analogues [41,42]. Modification of the aminoquinoline moiety that proved favourable as far as the antimalarial activity is concerned were the shortening or lengthening of the appended alkyl side chain that resulted in improved antimalarial activity against CQ-resistant strain of *P. falciparum* [43,44].



R₁ = (CH₂)_n; *trans*-1,2-cyclohexyl; (CH₂)₃CH(CH₃)₃CH₂; (CH₂)₂O(CH₂)₂; (CH₂)₂NH(CH₂)₂
R₂ = (CH₂)_n, where n = 0, 2, 4, , 8.

Figure 1.6: Bridged alkyl bisquinoline compounds active against malaria and exhibiting cytotoxicity.

Other ventures included the synthesis of bis-aminoquinolines (Figure 1.7) that were designed based on the principle that they might be efficaciously retained by the CQ-resistant strain thus inhibiting the emergence of resistance. This class of CQ-analogues proved effective as they exhibited activity against CQ-sensitive and CQ-resistant strains while also being cytotoxic [45–48]. As an expansion to the scope of bis-aminoquinolines, bis-aminoquinolines endowed with a piperazine moiety were also synthesized and evaluated as antiplasmodial agents. These included piperazine (1.13, Figure 1.7), hydroxypiperazine (1.14, Figure 1.7), dichloroquinazine (1.15, Figure 1.7), 12,494RP (1.16, Figure 1.7) and 1,4-bis(7-chloro-4-quinolylamino)piperazine (1.17, Figure 1.7) which were found to exhibit antiplasmodial activity via a similar mechanism to CQ as they possess the quinoline moiety [49–51].

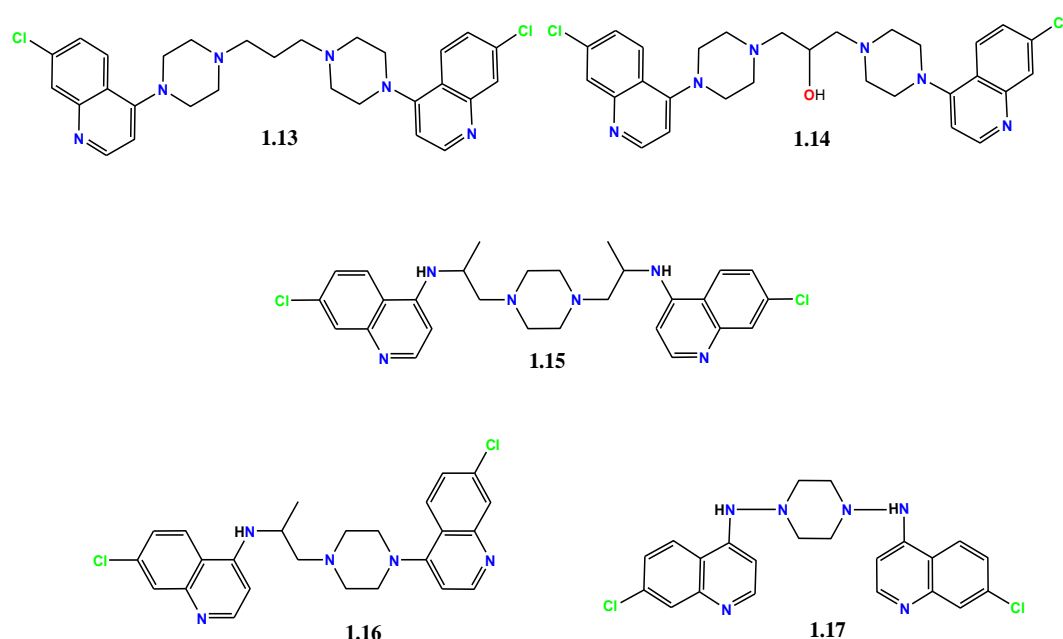


Figure 1.7: Synthetic antimalarial bisquinoline compounds bridged by the heterocyclic piperazinyl moiety.

1.3.1.3 8-aminoquinolines

The observation that methyl blue possesses chemotherapeutic effects against the malaria causing parasite led to analogues of methyl blue where one methyl group was substituted by a basic side chain that resulted in improved antiplasmodium activity. The notion that a basic side chain was essential was immediately adopted and the first 8-aminoquinoline compound plasmoquine (later termed pamaquine) was synthesized in the 1920s by the German research workers in the Bayer laboratories. The therapeutic effect of pamaquine (**1.3**, PQ', Figure 1.4) was soon realized and it was employed as antimalarial agent in 1926 but severe side effects namely, toxicity steered researchers into the syntheses of its derivative primaquine (PQ') that was used to eliminate refractory hypnozoites (liver reservoirs) of *P. vivax* and *P. ovale* [39,52,53].

1.3.2 Artemisinin and its derivatives

Artemisia annua (sweet wormwood) has been known to be an antimalarial medicine for centuries by Chinese herbalists, hence the quote “take a handful of sweet wormwood, soak it in a sheng of water, squeeze out the juice and drink it all.” Ge Hang, AD 340 and in 1971, the Chinese chemists isolated from the leafy part of the plant its phytoconstituent derivative artemisinin that was responsible for the remedial antimalarial action [54]. It was not until 1975 that the chemical structure of artemisinin was unequivocally elucidated to be a sesquiterpene lactone bearing an endoperoxy group [55].

This class of endoperoxides have been shown to be effective in the intervention of cerebral malaria and CQ- resistant falciparum malaria [56-57]. This remedial activity was attributed to the effectiveness, nonresistant characteristics, and minimal side effects of artemisinin and its synthetic derivatives that the WHO has regarded this class of compounds as the “best hope for the treatment of malaria” [56-57]. Although artemisinin has exhibited antimalarial activity, this prototype drug has been shown to possess pharmacokinetic limitations *viz* low solubility in water or oil, poor bioavailability, and a short half-life *in vivo* (~2.5 h) [55,58]. To overcome these shortfalls, three generations of artemisinin-like endoperoxides were synthesized and it was discovered that active metabolite of artemisinin is dihydroartemisinin (DHA, **1.21**, Figure 1.8) [59–61]. Derivatives of the parent artemisinin drug that have entered clinical trials are DHA, artemether (**1.19**), artesunate (**1.20**), and arteether. The antimalarial activity of artemisinin and its derivatives have been linked to the endoperoxo bridge that is inherent to all these compounds (Figure 1.8) as compounds without the endoperoxo bridge lack the activity that is comparable to artemisinin and derivatives, such as deoxyartemisinin [62–66]. The general consensus for the antimalarial activity is the reductive split of the peroxy bridge by reduced heme iron inside the acidic compartment (DV) of the parasite. It is

also suggested that this class of compounds might exert activity through the splitting of the peroxo bridge by intracellular iron-sulfur redox cluster, thus activating them to kill the parasite [67,68].

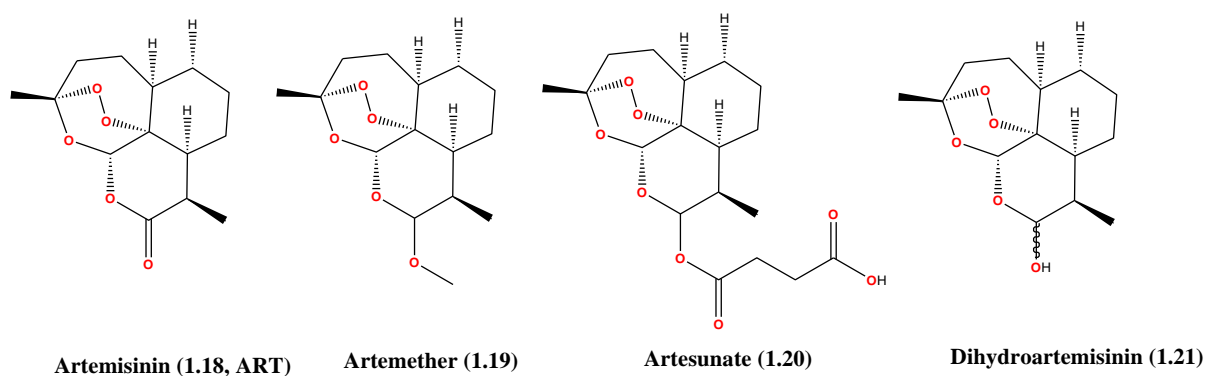


Figure 1.8: Artemisinin and its synthetic derivatives.

1.3.3 Mode of action of quinoline compounds

As the plasmodium parasite invades the red blood cells (RBCs), it does so at a cost of depleting 60-80% of the host heameglobin as the source of nourishment. They degrade hemoglobin into small amino acids and peptides which aresubsequently transported to the cytoplasm of the parasite. The degradation of hemoglobin occurs inside the digestive vacuole (DV) of the parasite (Figure 1.9) [69–71]. The DV of the parasite is located inside cytoplasm and is the most “unique and sophisticated” proteolytic organelle (Figure 1.9) [72]. The DV is an acidic compartment (pH 5.0-5.4) and has been demonstrated to be equipped for hemoglobin degradation [73].

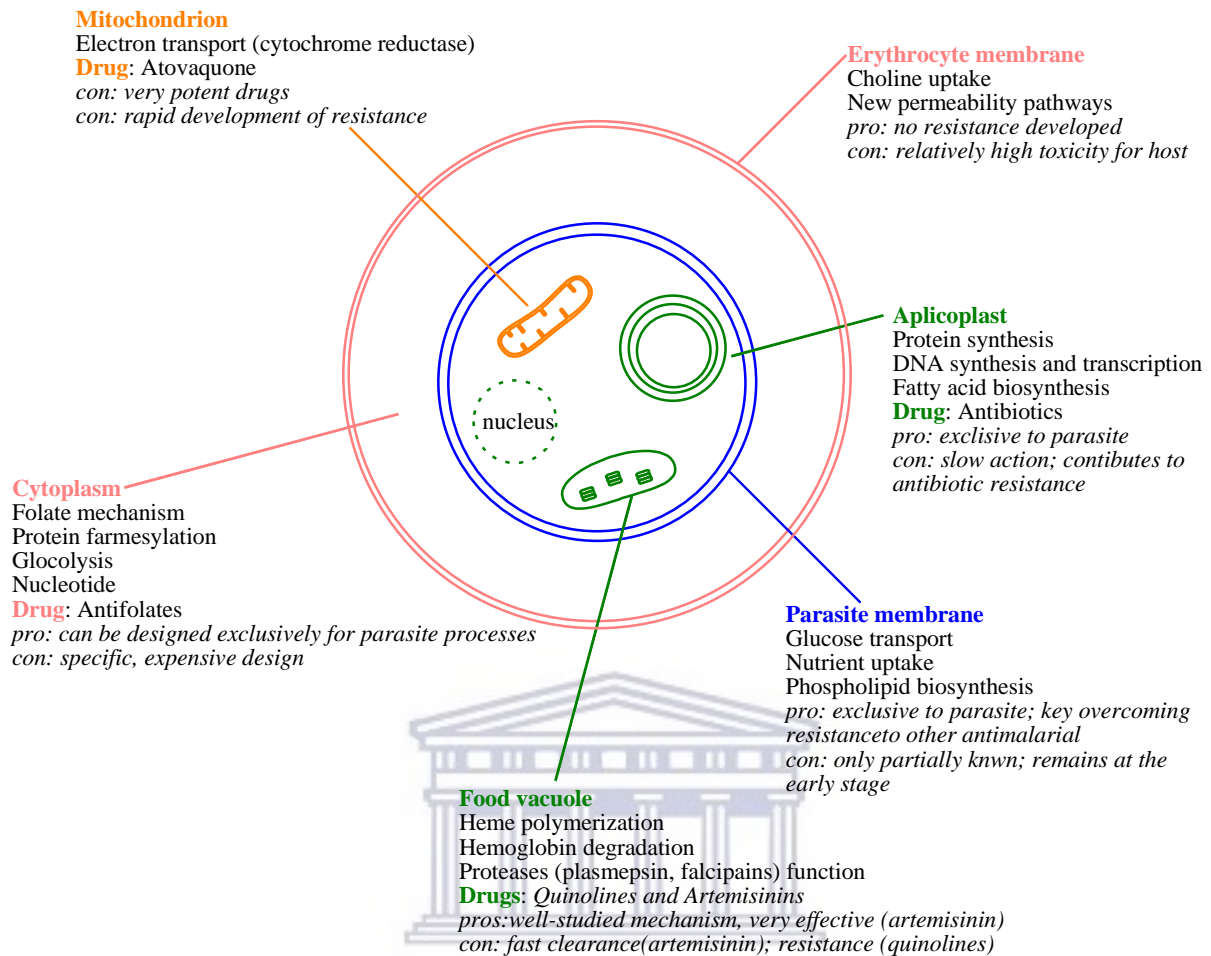


Figure 1.9: Digestive vacuole of the plasmodium parasite. Picture taken and modified from ref [74] and [75].

For decades the mechanism of action of the quinoline-based drugs was not fully understood as conflicting theories suggested different modes of action. The general consensus nowadays is that quinoline-based drugs exert activity through the interruption of hemozoin formation [76,77]. The drug activity of CQ and related derivatives as antimalarial agents is thus associated with the ability to accumulate inside the DV of the parasite via a mechanism known as ion-trapping in the intraerythrocytic stage of the malaria parasite [38,76,77]. The complexity of the mechanism of action has not been disregarded as an array of factors that govern the accumulation in the DV and influence its potency, but binding to heme or ferriprotoporphyrin IX (FPIX) as the drug target has been manifested [78-79]. Heme or

ferriprotoporphyrin IX (FPIX) is the toxic byproduct produced as a result of hemoglobin degradation by the parasite. Accumulation of this cytotoxic byproduct inside the DV is not favoured by the parasite and as such, the plasmodium parasite has evolved and developed an in situ detoxification mechanisms of sequestering heme into a non-cytotoxic chemically inert crystalline malaria pigment, hemazoin, inside the DV [80].



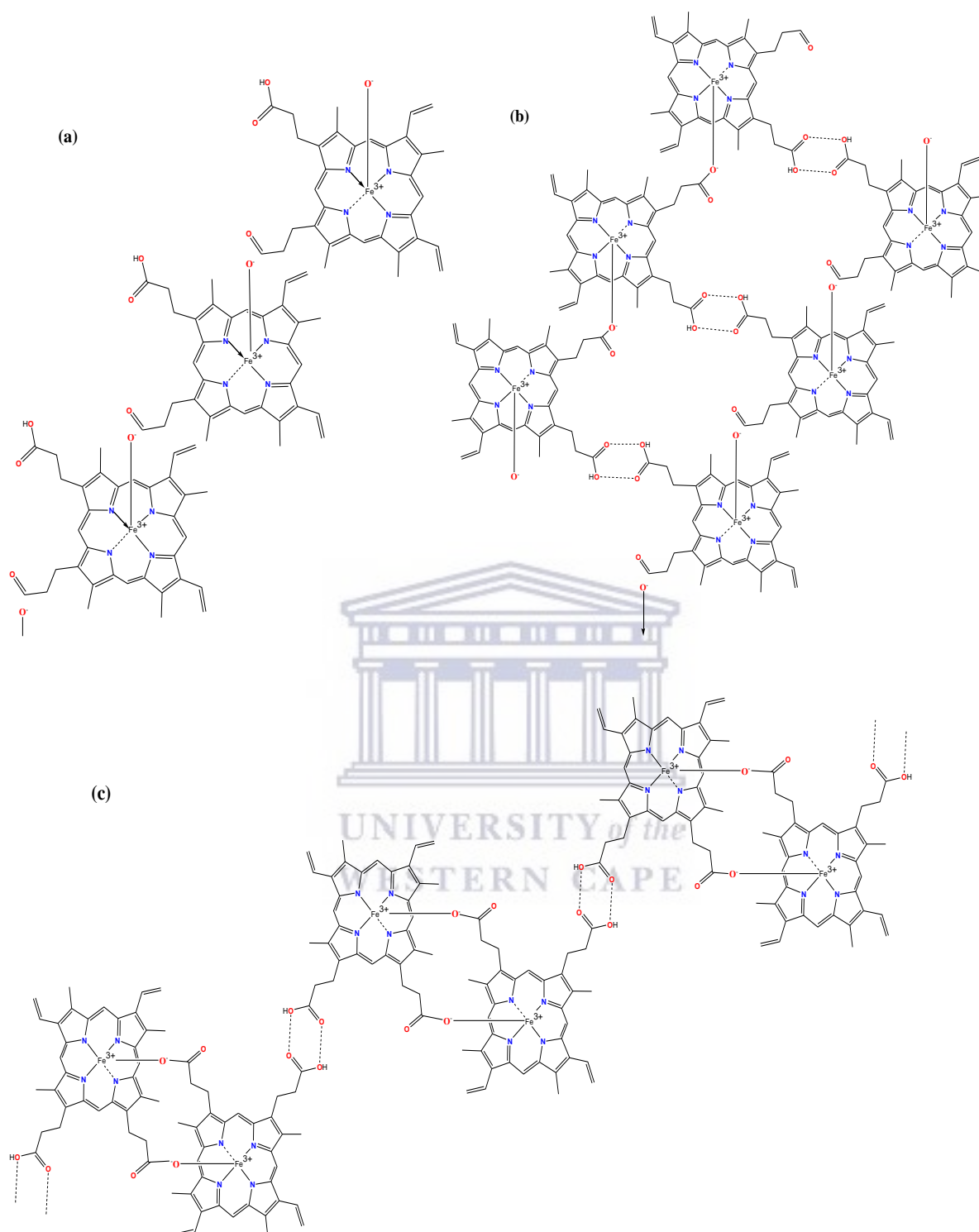


Figure 1.10: Evolution of understanding chemical structure of hemazoin: (a) linear polymer [81]; (b) antiparallel polymer chains linked by hydrogen bonds [82]; (c) centrosymmetric dimers linked by hydrogen bonds [83]. Picture taken from ref [84].

Earlier studies into the composition and chemical structure of hemazoin were reported in 1987 by Fitch and Kanjananggulpan. They reported on the purification of hemazoin and showed that it consisted of ferriprotoporphyrin IX (Fe(III)PPIX) residue [85]. They also linked the chemical structure of hemazoin to synthetic β -haematin. It was not until 1991, Slater *et. al.* reported for the first time the elemental analysis data and x-ray diffraction studies that hemazoin was indeed indistinguishable to the chemical structure of the synthetic β -haematin [81]. The study proved that the Fe(III)PPIX molecules are linked through coordination of the haem propionate group of one molecule to the Fe(III) center of its neighbor. They proposed the polymer arrangement/linkage of hemazoin as depicted in Figure 1.10 (a). Bohle *et. al.* reported on the *in situ* arrangement of hemazoin and confirmed the identical nature to β -haematin [82]. The breakthrough into the structure of haematin was reported by Pogola *et. al.*, in 2000, when for the first time they confirmed the crystal structure of β -haematin and proved that it was in fact not a polymer but rather a dimer linked through hydrogen bonding of the propionic acid groups [83].

DNA interaction studies of quinoline-containing drugs, particularly CQ, have shown that these heterocyclic aromatic groups intercalate into DNA to bring about biological and physical changes [86–91]. Although it was subsequently concluded that the dominating mode of action is through the intercalation mechanism, it was later reported that metal congeners of CQ such as CQ-Ru exerted their activity and interact with DNA through DNA-intercalation [92].

1.3.3.1 Structure-Activity relationships for CQ

The activity of the aminoquinoline compounds has been shown to be highly governed and dependent on the structure of the molecule [41]. The study suggested that in order for the aminoquinolines and related compounds to act as effective antimalarials they should meet these requirements:

- (i) To form strong complexes with heamatin (Fe(III)PPIX)
- (ii) the ability to inhibit the formation of β -hemin/hemozoin
- (iii) and the ability to accumulate to toxic concentrations in the *Plasmodium* that is assisted by the presence of the basic side chain

The chemical structure of CQ moiety has been shown to meet all of the above requirements and the following structure-activity relationships for CQ were proposed by Egan *et. al.* [41].

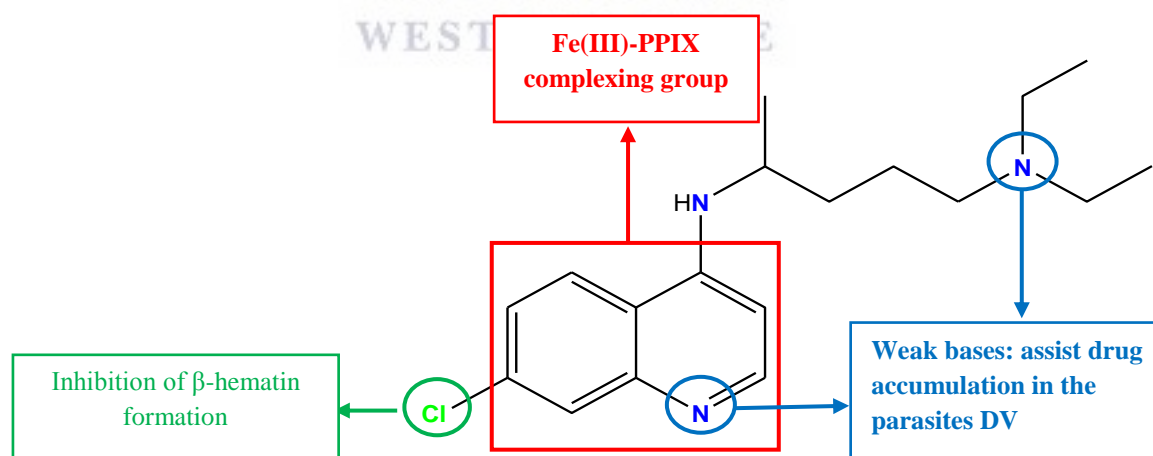


Figure 1.11: Structure-activity relationships (SAR) for chloroquine (CQ).

The 4-aminoquinoline pharmacophore has been shown to be essential for the π - π stacking with hemozoin (Fe(III)PPIX) to occur [74,75,84]. Cheruku *et al.* reported on the carbon isosteres of CQ (Figure 1.12). The carbon isosteres (**1.22** and **1.23**) are CQ analogues where the quinolone and the aniline (4-amino) nitrogen atoms have been replaced by a carbon atom. These were found to be inactive as antimalarials as no binding to Fe(III)PPIX and no β -hemozoin inhibitory activity was observed. They also observed that replacing the aniline (4-amino) nitrogen atom resulted in weak binding affinity to Fe(III)PPIX and weak β -hemozoin inhibitory activity compared to CQ.

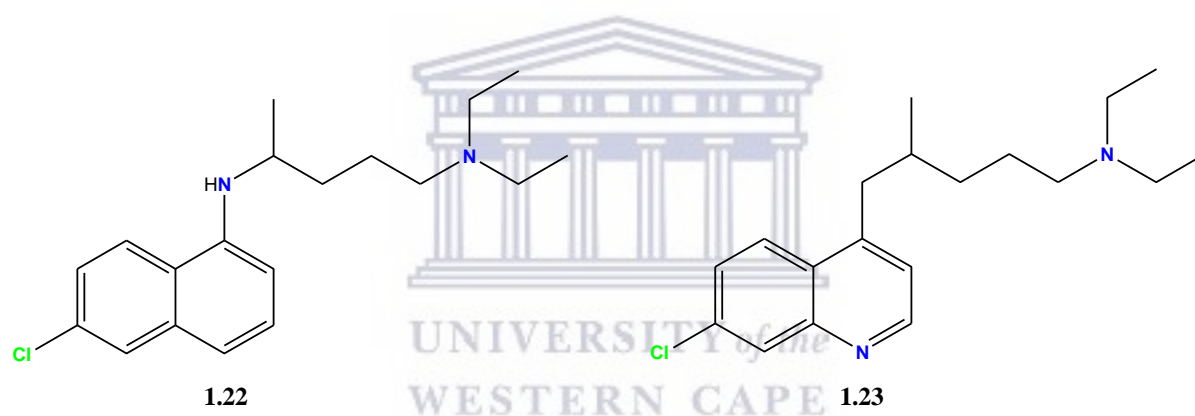


Figure 1.12: Structure-activity relationships of carbon isoesters.

Although it has been shown that the positional change of the amino nitrogen atom, to 2- and 4-aminoquinolines, results in the formation of strong complexes with Fe(III)PPIX, other positional changes of the amino nitrogen atom, 3-, 5-, 6- or 8-, are not favored and do not form a strong complex with Fe(III)PPIX [41].

The other crucial feature that is necessary for β -hematin inhibition is the chloro substituent at 7-position of CQ. It has been shown that chloro substituent at 7-position is a minimum requirement for anti-plasmodial activity. Replacing the chloro with the hydrogen (compound **1.24**) retains the binding affinity to Fe(III)PPIX but there was no β -hematin inhibition that was observed. CQ analogues that possess a bromo-(**1.25**) or an iodo-(**1.26**) substituent at 7-position, respectively, were shown to exhibit comparable activity to CQ against the CQ-sensitive strains with improved activity against CQ-resistant strains compared to CQ. On the other hand, the removal of the chloro group to 6-(**1.27**) and 8-position (**1.28**), respectively, resulted in decrease of activity or total loss of antimalarial activity. The antimalarial activity of chloroquine analogues has been associated with lipophilic and moderately electron-withdrawing groups at 7-position [41,42,44], [93-94].

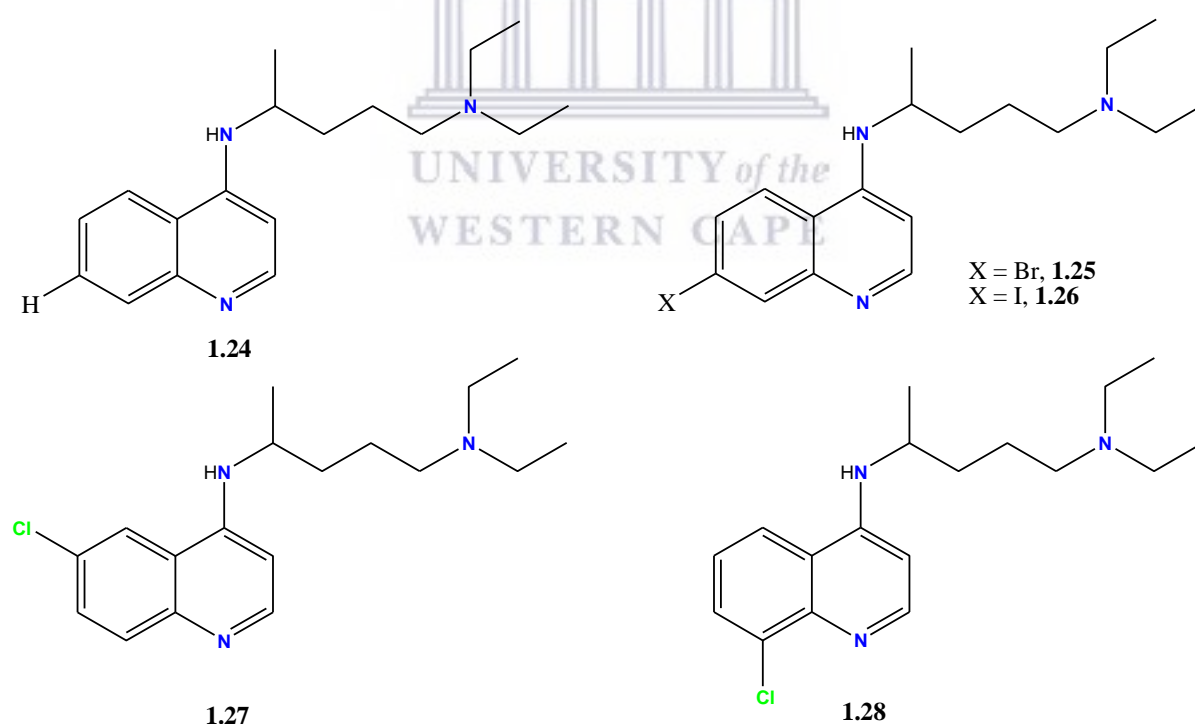


Figure 1.13: Chloroquine (CQ) derivatives with different position of the chloro group.

The correlation between the extent of accumulation in the plasmodium DV and the antimalarial activity has been studied and established [95]. The drug accumulation inside the DV of the parasite has been shown to be dependent on the basic terminal nitrogen atom. Although the drug accumulation has been shown to be slightly dependent on the drug-Fe(III)PPIX association [78], evidence that supports pH trapping of CQ has been shown to be crucial for activity and necessitate equilibrium to be reached [42,96]. The pendant side chain has been shown not to be essential for β -hematin inhibition activity but it has been shown to be essential for 7-chloro-4-aminoquinoline compounds as the lack of the basic side chain, or compounds that have an appendant alkyl chain that terminates with a hydroxyl group to have been shown to exhibit poor antimalarial activity [41]. It was also shown that varying the length of the side chain, from short (2-3 carbons) and longer (10-12 carbons) of the CQ diaminoalkyl spacer resulted in increased activity that overcame CQ-resistance while compounds with (4 – 8 carbons) alkyl spacer exhibited limited activity against CQ-sensitive malaria strains [43,94,97]. The results and the observations about the relationship between structure and activity of CQ vividly indicate the importance of the 7-chloro-4-aminoquinoline pharmacophore as structural modifications might yield compounds that are able to circumvent resistance.

1.3.4 Emergence and Spread of drug resistance in malaria parasites

The emergence of resistance was first observed when one of the “old” quinoline-based antimalarial drug, quinine, was exhibiting signs of ineffectiveness in Brazil in 1908 and the emergence was documented again in 1938 in German [98]. It was not until 1957 that the

emergence of resistance against chloroquine was observed in Thailand and later, in 1959, in the border of Colombia-Venezuela. The rapid spread of resistances against anti-malarial drugs was observed to surface in Sub-Saharan Africa in 1988. Nowadays, the effectiveness of chloroquine is limited to a small portion of the world populace as resistance rendered it useless [99-101]. Multiple factors contribute to the emergence and spread of resistance in *Plasmodium* parasites, including (i) the mutation rate of the parasite, (ii) the fitness costs associated with the resistance mutations, (iii) the overall parasite load, (iv) the strength of drug selection, and (v) the treatment compliance [102]. The emergence of drug resistance in malaria parasites is indirectly related to the gene mutation rate of the parasite. The emergence of *P. falciparum* resistance against chloroquine has been shown to involve the chloroquine-resistance transporter (*CRT*) gene [103]. The resistance has been linked to poor accumulation of the chloroquine drug inside the digestive vacuole of the resistant parasite compared to CQ-sensitive strain although the reason is unclear and has not been unequivocally substantiated [104]. A probe into the genetic cross between CQ-resistant and CQ-sensitive strains identified the *P. falciparum* chloroquine-resistant transporter (*PfCRT*) protein as the principal target for the CQ resistance which is encoded by the *PfCRT* gene. The *PfCRT* gene is the one responsible for encoding a 48.6-kDa protein (*PfCRT*) consisting of 424 amino acids and this has been shown to be located on chromosome 7 [105,106]. In all the amino acids of *PfCRT* protein, one amino acid mutation Lys76 → Thr (K76T, Figure 1.14) has been associated with the changes that are observed in CQ-resistant parasites and it is located at position 76. It is responsible for the observed changes from lysine to threonine (K76T). This was shown to be found on the first of ten transmembrane domain [105,107]. It was also reported that three other amino acids namely; Arg²²⁰ → Ser, Ala¹⁴⁴ → Thr and Leu¹⁶⁰ → Tyr that also experience the accompanied mutational changes [108]. The assumptions are that the mutated

K76T is orientated inwards, where it faces the vascular side of the membrane. This mutation has been suggested to act as an effective efflux pump, where it expels chloroquine effectively from the DV of the parasite by altering the selectivity [100,109,110]. The effective mechanism of the efflux-pump by the mutants from the DV is mediated by the PfCRT and is associated with the reduction of CQ concentration in resistant *P. falciparum* isolates [111]. Two routes have been suggested that the parasite employs in order to pump out CQ in the CQ-resistant strains. Warhurst *et. al.* [112] suggested the first route, where the diprotonated CQ passively diffuses through the DV assisted by the mutated *PfCRT* down along an electrochemical gradient. The second route suggested energy-dependant transport model, where it was assumed that the PfCRT is responsible for effectively pumping out CQ from the DV of the parasite [113,114].

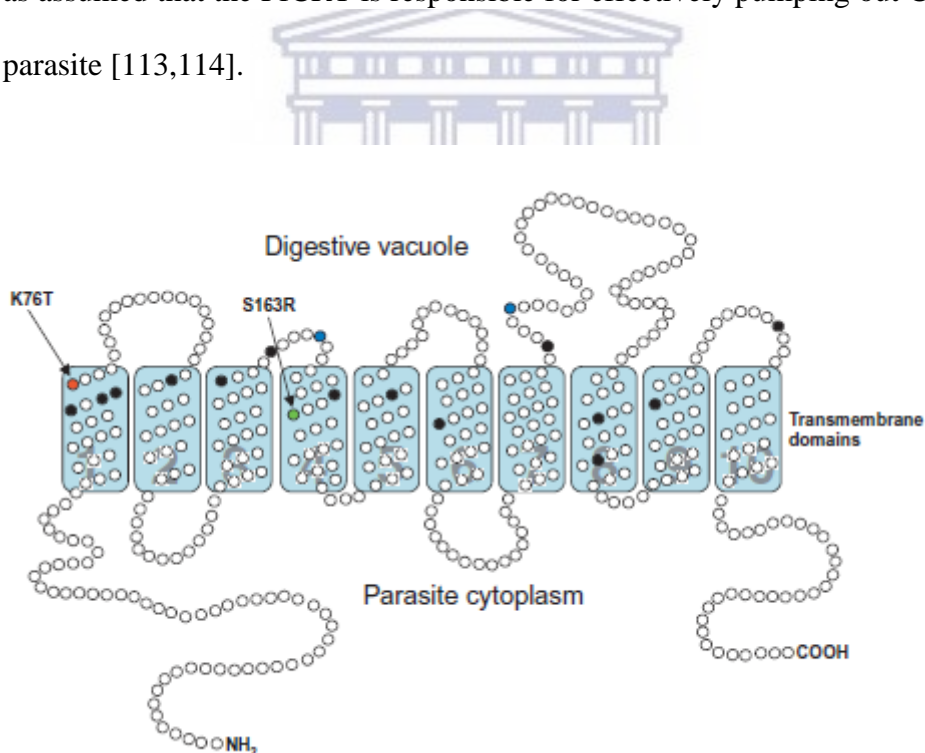


Figure 1.14: Predicted protein structure of PfCRT postulated to possess 10 transmembrane. Picture taken from ref [108].

1.4 Organometallic complexes as antimalarials

One of the strategies devised as an alternative to the “failing” CQ and relative derivatives as far as efficacy is concerned when evaluated against CQR strain of the parasite as resistance built was the modification of the organic moiety of the CQ family. An intergration or grafting of transition metals was incorporated into the molecular structures of these known organic frameworks with antimalarial activity. This venture proved to be beneficial due to the inherent binding capabilities and reactivity of the transition metals that are governed by the donor/acceptor abilities of the d-orbitals [115]. These structural modifications brought about by covalently or coordinatively introduction of a metal centre have yielded a range of metalloantimalarials [116–119]. The rationale aimed at restoring potency of the “primitive” organic antimalarials through incorporation of a metal-framework was reported to augment the activity [120,121]. This growing field of designing metal-containing CQ analogues has produced a library of metal complexes with promising antiplasmodial activity [120,122–125]. Organometallic-CQ complexes have been shown to affect biologically relevant properties such as solubility, lipophilicity and haematin formation [120,126,127].

Some of the metal complexes worth mentioning are discussed in the following subsections.

1.4.1 Platinum complexes

The first cationic platinum based non-quinoline complexes ligated by sterically demanding aromatic bipyridyl or phenanthroline ligands with dialkyl thioureate were reported by Koch *et. al.* (**1.29** and **1.30**, Figure 1.15) where they showed the propensity of these complexes to self-aggregate into dimers in a acetonitrile solution, exhibiting a behaviour that has been observed for porphyrins. They suggested that the dimers aggregated as a result of non-

covalent $\pi - \pi$ stacking interactions between the planar aromatic rings and the cationic- π interactions induced by the charged complex and aromatic ligands [128]. These observations were correlated to the possible π -stacking with haematin that is observed with known aromatic antimalarials such as CQ and the likelihood of these platinum complexes to exert activity in a similar fashion.

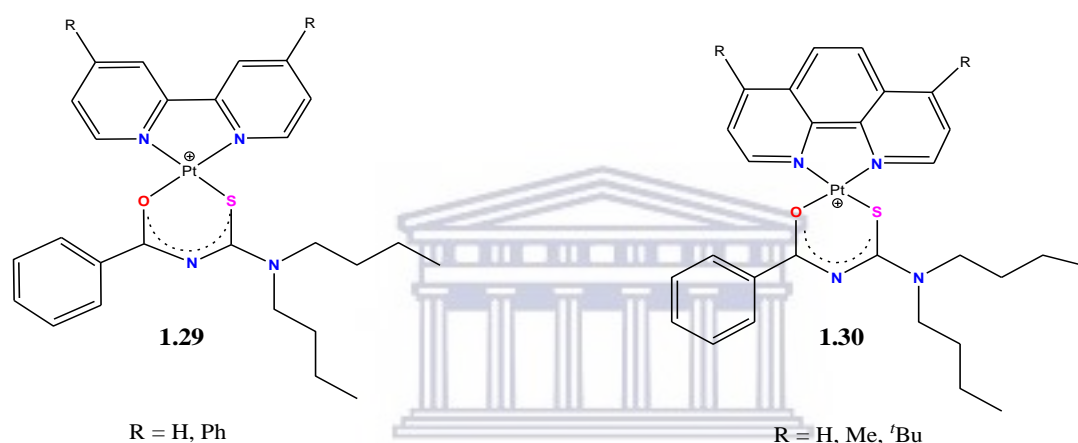


Figure 1.15: Mixed-ligand platinum (II) complexes with pronounced tendency to undergo self-aggregation in solution

Motivated by the above mentioned observations, a series of similar cationic complexes were synthesized and evaluated for their efficacy as antimalarial agents against CQ-sensitive (*D10*) and CQ-resistant (*K1*) parasite strain as well as their β -haematin inhibition ability. These cationic square planar platinum (II) complexes (**1.31-1.37**, Figure 1.16), endowed with *N,N'*-bipyridyl and phenanthroline ligands were reported by Egan *et. al.* [129] and were found to exhibit antiplasmodial activity that is more than the standard drug CQ under the same conditions.

Although they were conceived to exert their activity through the inhibitory mechanism of β -hematin in the acetate solution, they were disregarded as potential antimalaria agents.

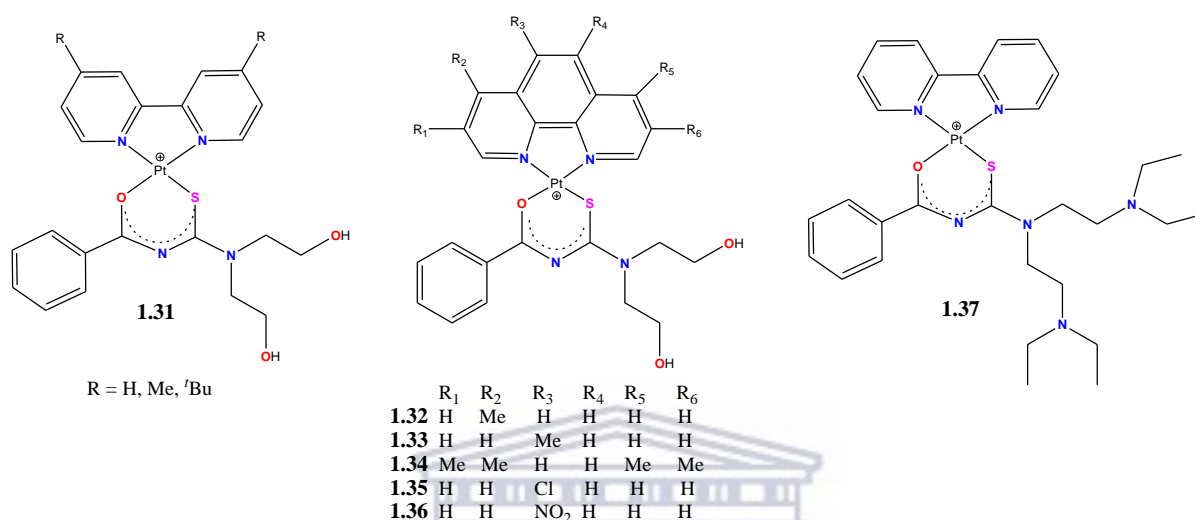


Figure 1.16: Cationic platinum (II) complexes possessing antimalarial activity.

Coordinative platinum-chloroquine, *trans*-[PtCl₂(CQ)₂], complexes (1.38, Figure 1.17) were also prepared and evaluated for their antiprotozoan activity against the CQ-resistant (*KI*) of *P. falciparum* [117]. The *trans*-Pt(II)-CQ complexes exhibited enhanced activity against the CQ-resistant strain compared to the reference drug CQ.

To further expand on the scope of the platinum-chloroquine complexes, two research groups have been tirelessly working to synthesize new *trans*-[PtCl₂(CQ)₂], *trans*-[PtCl₂(CQDP)₂] (1.39, Figure 1.17) and *trans*-[Pd/Pt₂(CQDP)₂] (1.40, Figure 1.17) [117,130,131]. The *trans*-[PtCl₂(CQDP)₂] and *trans*-[Pd/Pt₂(CQDP)₂] complexes were tested for their antiplasmodial activity against the CQ-sensitive strain (Dd7) and CQ-resistant strain (W2).

The CQDP was also evaluated as the reference drug against the same strains of *Plasmodium falciparum*. The two platinum, (*trans*-[PtCl₂/I₂(CQDP)₂], **1.39** and **1.40**, Figure 1.17) complexes exhibited better activity against the CQ-sensitive strain compared to CQDP with the exception of the palladium, (*trans*-[PdI₂(CQDP)₂], **1.41**, Figure 1.17) complexes which exhibited lesser activity. When the complexes were evaluated against the CQ-resistant strain (W2), it was again observed that the *trans*-[PtCl₂/I₂(CQDP)₂] complexes were active that the palladium counterpart although complexes were observed to be more active than the reference drug CQDP [131]. It was thus extrapolated that platinum and gold complexes possess a tendency to augment antiplasmodial activity. These metal-CQ complexes exhibited heightened activity against CQ-sensitive strain compared to CQ-resistant [131].

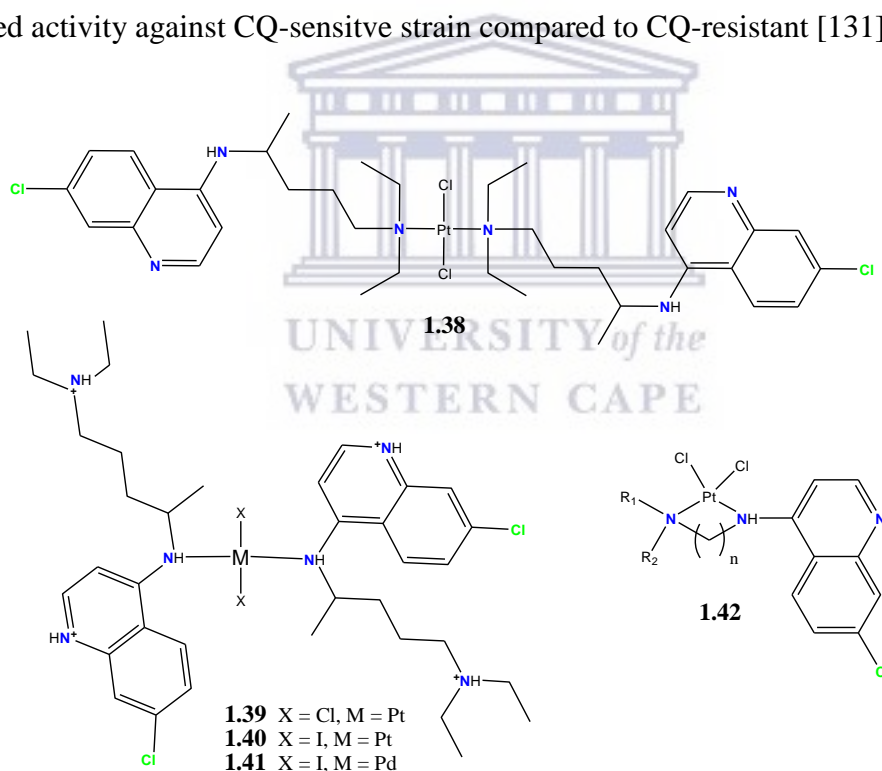


Figure 1.17: Chemical structures of palladium/platinum chloroquine [*trans*-Pt(II)X₂(CQ)₂] and chloroquine diphosphate [*trans*-Pt(II)X₂(CQDP)₂] (X = Cl⁻ and I⁻) complexes.

1.4.2 Ruthenium and Gold complexes

Ruthenium is amongst the metal-CQ containing fragments that possess increased activity. The Ru^{II}-CQ ([RuCl₂(CQ)]₂, **1.43**, Figure 1.18) analogue as well as the Au^I-CQ ([Au(CQ)(PPh₃)]PF₆, **1.47**, Figure 1.19) analogue have been reported to have remarkable inhibitory index when evaluated against different CQR strains of *P. falciparum*. Interactive studies to gain an insight into the mechanism of action of these chloroquine congeners was undertaken against two crucial targets, Fe(III)PPIX and DNA, and the study revealed the inhibitory effect of the metal complexes against the formation of β-haematin [126,132]. This inhibitory effect of the Ru^{II}-CQ analogues (**1.43-1.46**, Figure 1.18) was reported to be effective at acidic medium (≤-pH 5) and the extent that the Ru^{II}-CQ metal complex inhibited heme superseded the standard drug CQ. The observation led to conclusions that heme, at the water/lipid interface, was the primary target of these Ru^{II}-CQ analogues which can act as a template for the mechanism of resistance for CQ [133,134]. Physicochemical properties, solubility, high lipophilicity and basicity, of these metal-containing complexes were attributed to be the contributing factor for the improved potency and the intrinsic character of these congeners to decrease resistance.

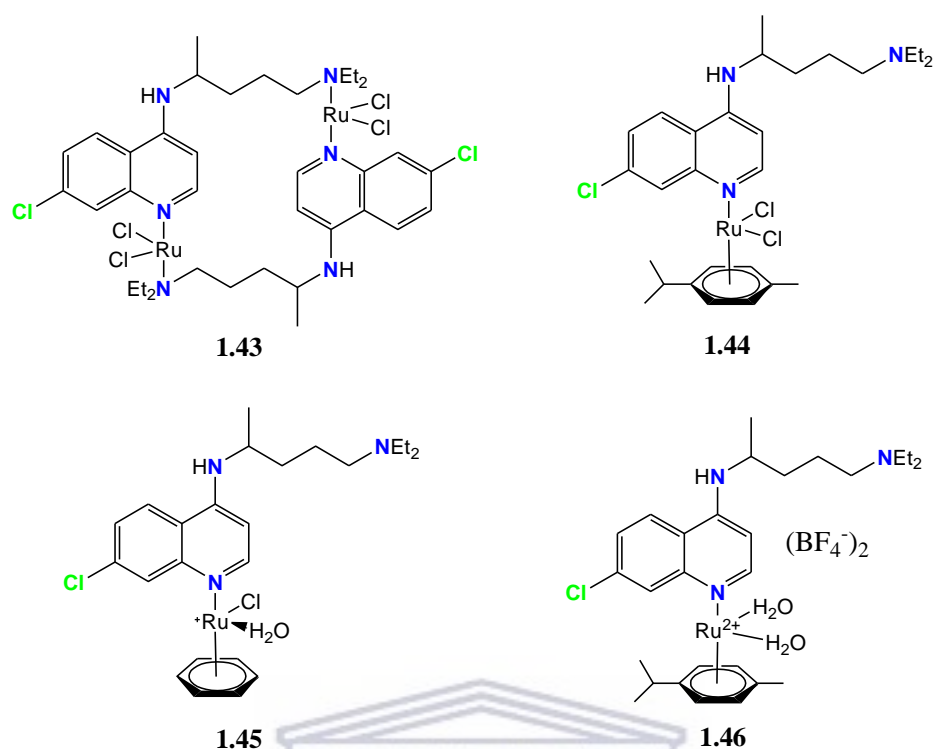


Figure 1.18: Ruthenium-chloroquine complexes possessing antimalarial activity.

Derivatives of Au^I-CQ ([Au(CQ)(PPh₃)]PF₆, Figure 1.19) were prepared so as to effectively compare activity [135]. The Au(III) chloroquine complexes were evaluated *in vitro* against a variety of CQ-sensitive and CQ-resistant strains of *P. falciparum*. The gold derivatives exhibited antimalarial activity that was comparable to the parent standard drug, CQ, when evaluated against CQ-sensitive strain and the activity was better for CQ-resistant strains as compared to CQ. The derivatization of the complexes from Au(I) to Au(III) and the modification of the complexes via the change of the counterion and phosphine ligand did not yield significant activity.

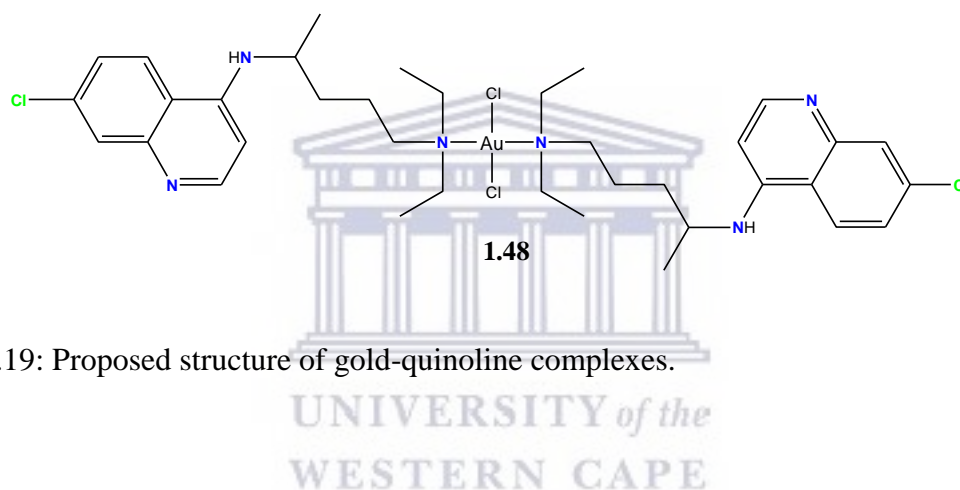
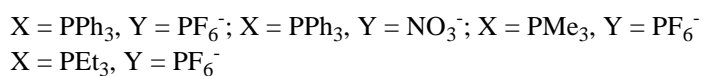
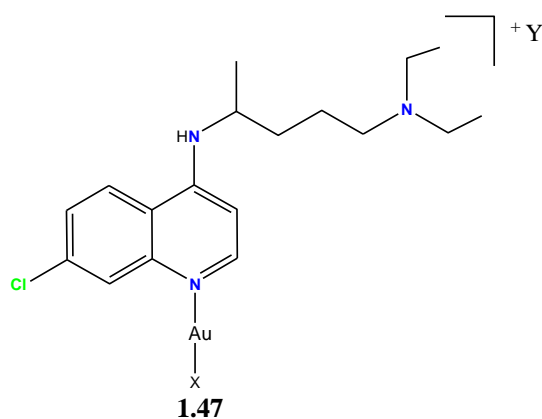


Figure 1.19: Proposed structure of gold-quinoline complexes.

Recently half-sandwich-CQ complexes (**1.49-1.51**, Figure 1.20) were synthesized and evaluated against the CQ-sensitive (*D10*) and CQ-resistant (*Dd2*) strains of *P. Falciparum* [125]. These coordination compounds were shown to be less potent *in vitro* compared to their uncoordinated ligands and a reasonable potency was only exhibited by the arene *N,O*-Ru complex.

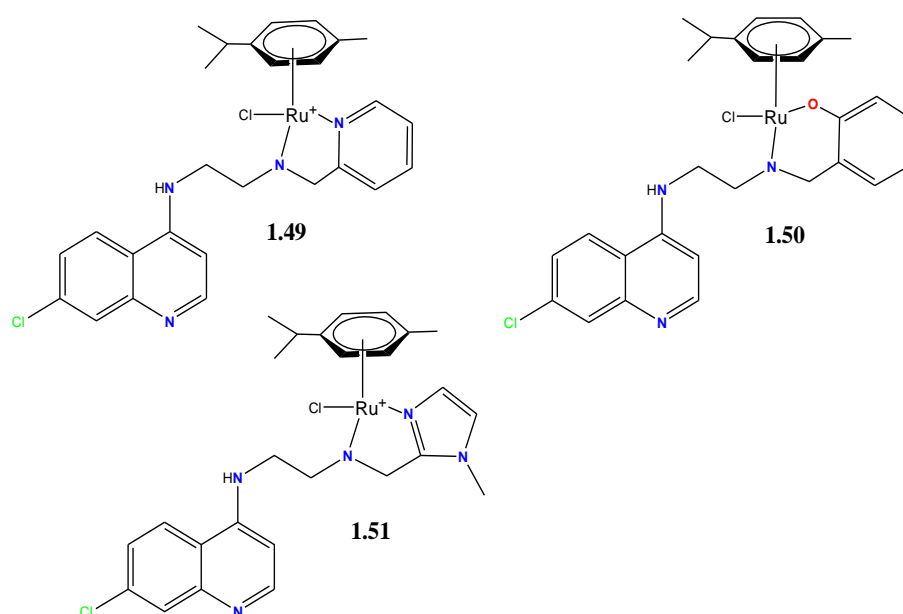


Figure 1.20: Half-sandwich Ru(II)-CQ p-cymene complexes

Ruthenocene-chloroquine (**1.52** and **1.53**, Figure 1.21) analogues were also prepared in order to draw comparison with ferrocene. The prepared Ru-CQ complexes were evaluated *in vitro* against CQ-resistant (*K1*) and CQ-sensitive (*D10*) strains of *P. falciparum*. These complexes proved to be equally active against both parasitic strain of *P. falciparum*. The observed improved activity of the Ru-CQ complexes against CQ-resistant strain indicated the imparted superiority of these complexes, with the incorporation of the ruthenocene sandwich, to overcome resistance that has been encountered by the standard parent drug CQ. The activity exhibited by these complexes was thus observed to be comparable to the ferroquine complex [136].

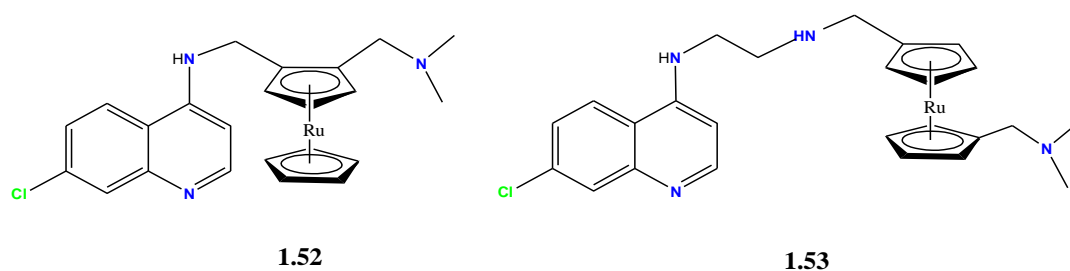


Figure 1.21: Ruthenocene 4-amino-7-chloroquinolines complexes with known antimalarial activity [136].

1.4.3 Rhodium and Iridium complexes

Rhodium-CQ and Iridium-CQ coordination complexes are amongst a series of metalloantimalarial synthesized and evaluated against different *Plasmodium falciparum* strains. The first metal-CQ complex synthesized between these two was the [RhCl(COD)] (COD = cyclooctadiene) (**1.54**, Figure 1.22) [137]. The coordinative mode of the metal ion was discovered not to substantially augment the antiplasmodial activity. The Iridium complexes were synthesized and reported by Navarro *et. al.* [123]. As observed with the Rh^I-CQ coordination complex, no substantial activity was attributed to the coordination of the iridium (**1.55**) metal ion compared to the standard drug CQ when evaluated *in vitro* against *P. berghei* [123].

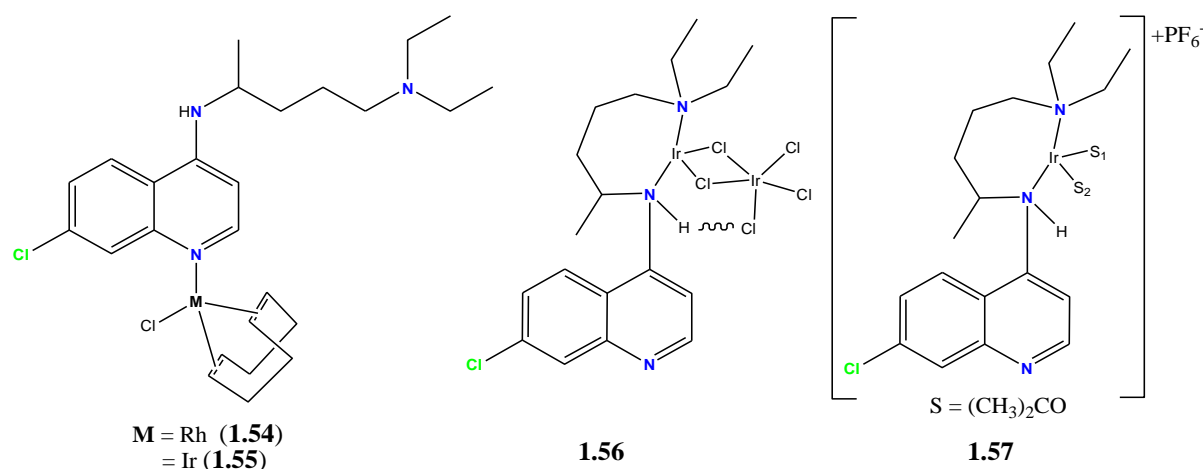
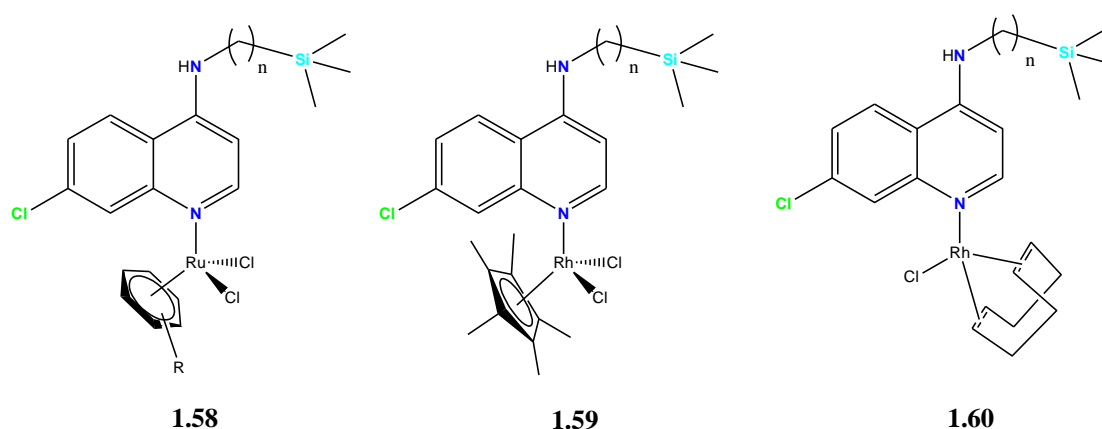


Figure 1.22: Rhodium- and Iridium-CQ complexes possessing antimalarial activity.

A series of quinoline derivatives with appended silicon functionality and their generic Ru^{II} (**1.58**), Rh^I (**1.59**) and Rh^{III} (**1.60**) complexes have been recently reported (Figure 1.23) [138]. This new class of quinoline ligands and corresponding complexes was evaluated against CQ-sensitive (*NF54*) and CQ-resistant (*Dd2*) *P. falciparum* strains and were reported to be more potent *in vitro* than the parent ligands although the complexes were less active against the CQ-resistant compared to CQ-sensitive strain. The differences in activities against the two strains of *P. falciparum* were attributed to the immunity (cross-resistance) experienced by CQ against *P. falciparum*.



$n = 1$ or 3 ; arene = *p*-cymene, benzene, $n^6\text{-C}_6\text{H}_5\text{OCH}_2\text{CH}_2\text{OH}$

Figure 1.23: Organosilicon Ru(II) (**1.58**), Rh(III) (**1.59**) and Rh(I) (**1.60**) quinolines.

1.4.4 Ferroquine and derivatives

Although ferrocene was discovered in 1951 [139,140], it was only later that its chemical structure was elucidated by two independent researcher teams, Wilkinson *et. al.* and Fischer and Pfab [141,142]. The scientific and technical community immediately realized the chemical potential that can be manipulated from the ferrocenyl moiety and as a result, the chemistry of ferrocene-chloroquine (FQ-CQ) analogues was explored and new organometallic FQ-CQ complexes, where the ferrocenyl fragment was covalently bound to the 4-amino-quinoline moiety including ferroquine (**1.65**, FQ, Figure 1.25, *vide infra*), were evaluated against CQ-sensitive, CQ-intermediate, and CQ-resistant clones of *P. falciparum* and one of these 7-chloro-4{[2-(N,N-dimethylaminomethyl)]-N-methylferrocenylamino}quinoline derivatives, a tartaric acid with better solubility than its counterparts, exhibited the ability to cooperatively assist to restore activity against CQ-

resistant clone of *P. falciparum* [143,144]. Amongst other properties discovered to be inherent to compounds that possess the ferrocenyl moiety, stability of ferrocenyl moiety in aqueous and aerobic media, the accessibility to a large variety of derivatives, and its favorable electrochemical properties that promote its use as a suitable candidates for biological applications [145–151].

With the rationale indicated above, ferrocenyl derivatives were synthesized and evaluated for their efficacy as antimalarials. Different classes of antimalarials were thus synthesized by covalently incorporating the ferrocenyl fragment into the scaffold of known antimalarials such as artemisinin (**1.61**, Figure 1.24) [152,153], atovaquone (**1.62**, Figure 1.24) [154], mefloquine (**1.63**, Figure 1.24) and quinine (**1.64**, Figure 1.24) [155]. The resulting modifications were not observed to augment the activity of these standard antimalarial drugs, instead the parent drugs exhibited better activity compared to the ferrocenyl derivatives.

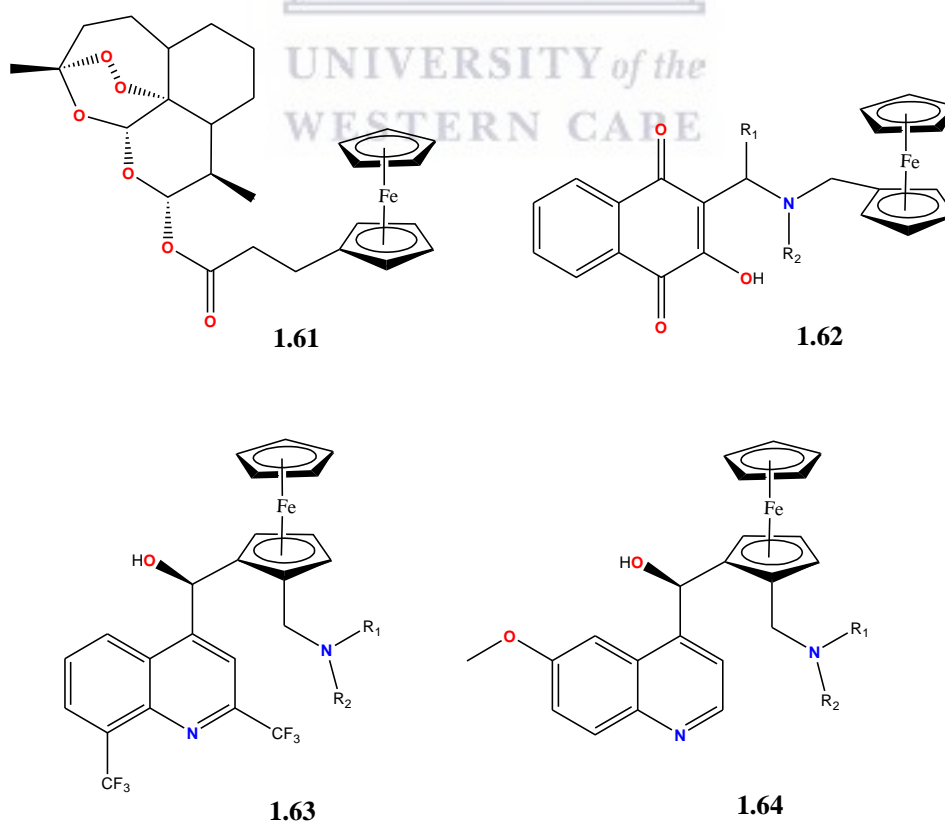
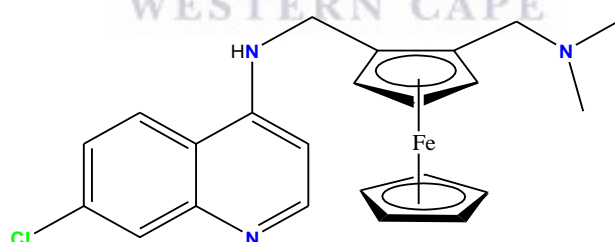


Figure 1.24: Ferrocene derivatives that possess antimalarial activity.

The greatest achievement in the fight against malaria was observed with the advent of the ferroquine complex (FQ, **1.65**, Figure 1.25), which is a result of the introduction of the ferrocenyl moiety covalently in the lateral side chain of the CQ standard drug [156,157]. This complex, also known as 7-chloro-4-[[[2-[(*N,N*-dimethylamino)methyl]-*N*-ferrocenyl]methyl]amino]quinolone, gained prominence as it exhibited superior antimalarial activity against CQ-sensitive and CQ-resistant clones that superseded the CQ standard drug when evaluated against 19 laboratory *P. falciparum* clones, exhibiting 22- folds of activity against schizontocides than chloroquine *in vitro* against a drug-resistant strain of *P. falciparum* [156,158]. It was also indicated that the activity is highly dependent on the position of the ferrocenyl moiety within the lateral side chain of CQ [159] and the activity was not hampered by the different structural formulations of ferroquine: base, ditartrate or dihydrochloride salts as the organometallic complex endowed with tartaric acid exhibited improved solubility and was highly effective [160].



Ferroquine (FQ, 1.65)

Figure 1.25: A potent antimalarial agents that has entered phase-II clinical trials, Ferroquine (FQ).

Structural modifications of FQ have been undertaken to assess whether derivatives of FQ might possess enhanced activity compared to already active FQ complex. Thus the basic tertiary amino group of FQ was varied by covalently introducing different alkyl substituents such as H, C₂H₅, CH₃ and FcCH₂ aimed at augmenting the activity of FQ (**1.66**, Figure 1.26). These FQ derivatives were found to exhibit comparable activity to FQ when evaluated against CQ-resistant strains (*Dd2* and *W2*) of *P. falciparum*. It was also shown that the introduction of a secondary ferrocenyl unit was detrimental to the efficacy of the derivatives as it resulted in decrease activity [161]. Modification of the basic tertiary amino group by introduction of a secondary amine was seen not to alter the activity much but rather essential when evaluated against the CQ-sensitive strain, as enhanced activity was observed compared to CQ [162]. Introduction of the hydroxyl moiety on the terminal nitrogen atom gave the FQ derivative hydroxylferroquine (**1.67**, Figure 1.26) and this derivative was shown to exhibit decrease activity compared to FQ, leading to conclusion that the modification was not favourable. The positive aspect of these structural modifications was the enhanced activity displayed by these derivatives *in vitro* when evaluated against the parasitic *P. falciparum* compared to CQ [163].

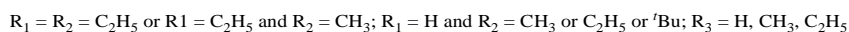
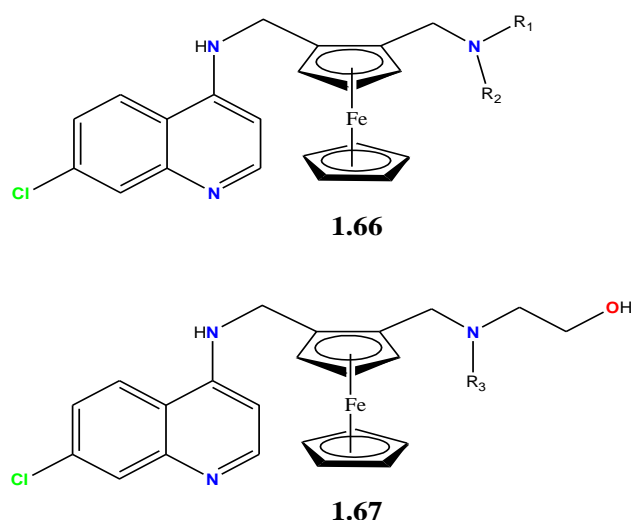


Figure 1.26: Ferroquine derivatives that are actively comparable to Ferroquine.

Ferroquine-chloroquine (FQ-CQ) conjugates were also synthesized and evaluated against CQ-sensitive strain (*BH3*) and CQ-resistant strain (*Dd2*) of *Plasmodium falciparum*. These conjugates were synthesized in order to gauge the activity and correlate it to different substitution positions of the ferrocenyl moiety. The salt bridge complex (**1.68**, Figure 1.27) was synthesized by direct condensation of the ferrocenecarboxylic acid with CQ [160]. This conjugate exhibited antimalarial activity although antagonistic effect was observed for the two fragments. A decrease in activity was reported for the quaternary ammonium cationic complex (**1.69**, Figure 1.27) that was achieved as a direct condensation of the ferrocenylmethyl moiety. This is a consequence of charged species not being able to cross through the membrane of the parasite, hence the observed decrease in activity for both CQ-sensitive and CQ-resistant strains of *P. falciparum* [164]. Substitution of the ferrocenyl moiety at position C-3 of the quinoline moiety (**1.70**, Figure 1.27) also resulted in decrease activity and this was attributed to the bulkiness of the ferrocenyl moiety that hinders the vital

π -stacking between the quinoline moiety and heme. Covalently attaching a ferrocenyl moiety in the pendant basic side chain of CQ (**1.71-1.74**, Figure 1.27) produced an observed decrease in the activity of these complexes as this basic site has been shown to be crucial for β -heamatin inhibition. The bisquinoline complex (**1.75**, Figure 1.27) exhibited better activity when evaluated against the CQ-resistant (*Dd2*) compare to the CQ-sensitive strain (*BH3*).



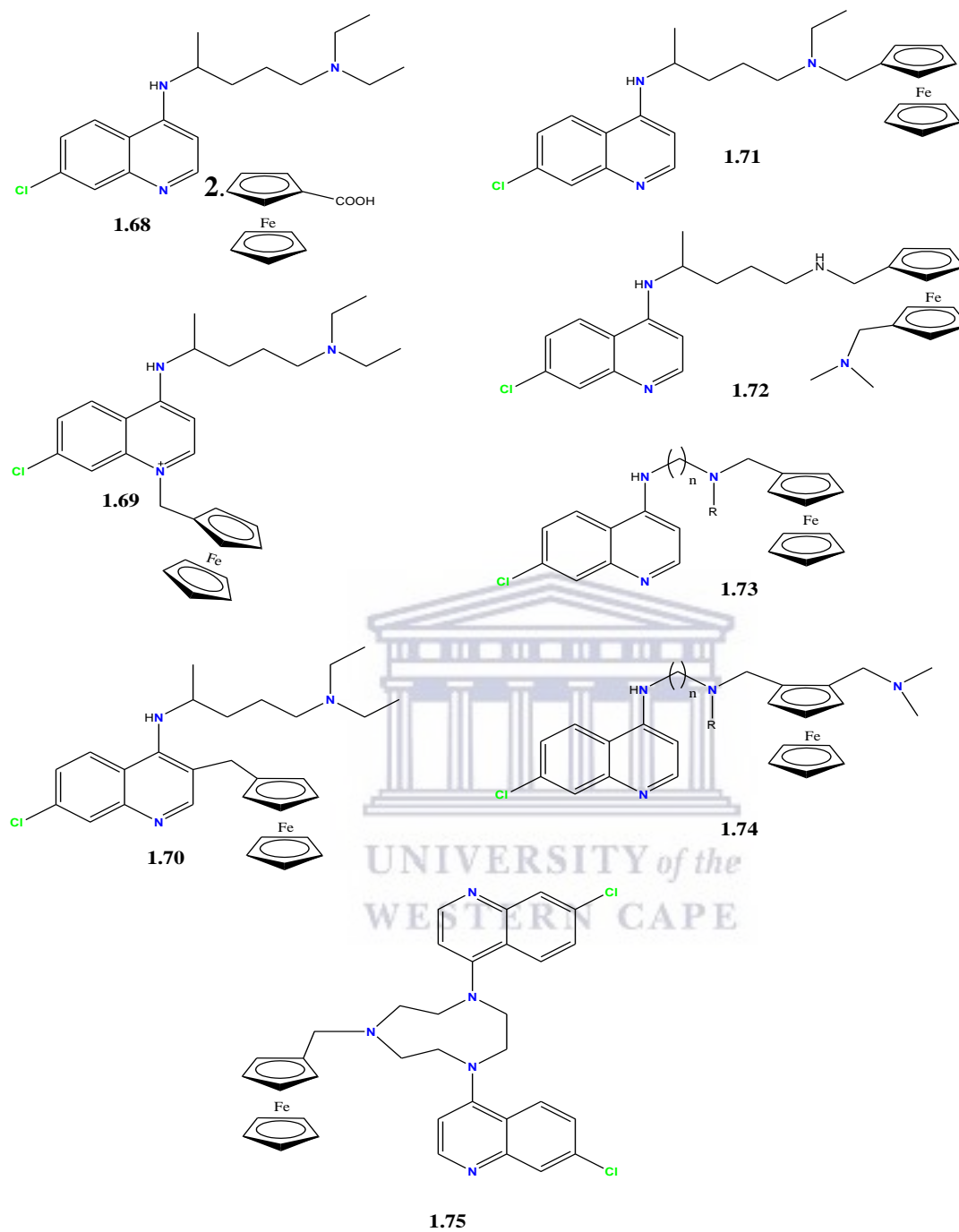


Figure 1.27: Ferroquine-chloroquine conjugates.

1.5 Scope of the thesis

Combining two biologically active motifs (pharmacophores) has been shown to possess the ability to enhance activity due to the synergistic effect. This strategy has been extensively explored into the synthesis of new quinoline-based antimalarials. Quinoline has been investigated in order to devise new potent antimalarial agents that might circumvent the emergence of resistance and restore activity to the failing drugs and offer an avenue to antimalarial discovery.

This study was aimed at synthesizing 4-aminoquinolines that possess a pendant pyrazole arm. The rationale to retain the known biologically active 4-aminoquinoline moiety and endow it with the pharmacologically active pyrazole is envisioned to accentuate key structural features in the fight against malaria. As highlighted in this chapter, organometallic complexes have played a pivotal role in the fight against malaria with the discovery of ferroquine exhibiting the greatest success with biological properties that overcome cross-resistance in the CQ-resistant strains of *P. falciparum*. The advances made by ferroquine, ferroquine derivatives and other organometallic complexes have led to intense search for organometallic complexes as only a few metal-complexes that are able to act as effective antimalarials are known. In that light, we aimed at expanding the search for active organometallic and coordination compounds that might be effective against known disease, such as malaria and cancer, that bothers human health.

1.6 Aims and Objectives

1.6.1 General Aims

The studies of chloroquine analogues/salicylaldimine ligands and corresponding metal complexes have paved an avenue into the search of new lead compounds in the study of malaria and cancer. With that in mind, the primary aims of the present study were thus:

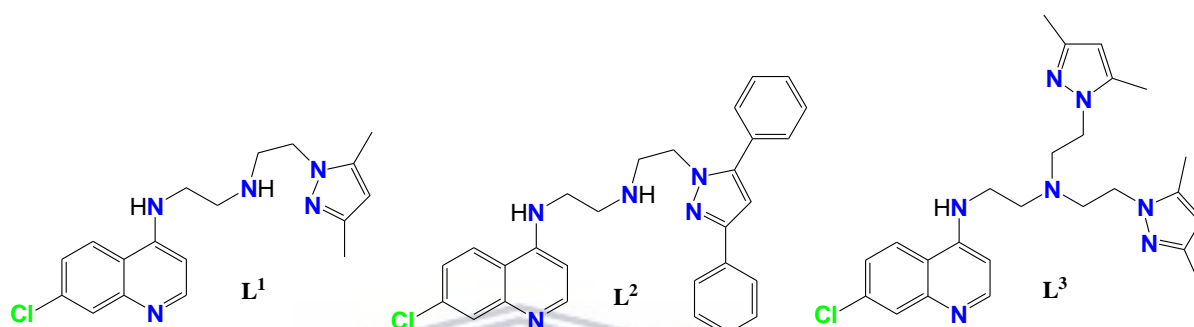
1. The synthesis of new chloroquine analogue ligands with a pendant pyrazole arm
2. The chelation of the chloroquine analogue ligands to Pd(II), Pt(II), Rh(III) and Ir(III) metal ions
3. The synthesis of new salicylaldimine and azine ligands appended with a thiophene moiety
4. The synthesis of salicylaldiminato-Pt(II), Ru(II), Rh(III) and Ir(III) complexes
5. The evaluation of new coordination/organometallic complexes as anti-malarial and,
6. The evaluation of the salicylaldiminato complexes *in vitro* as anticancer agents



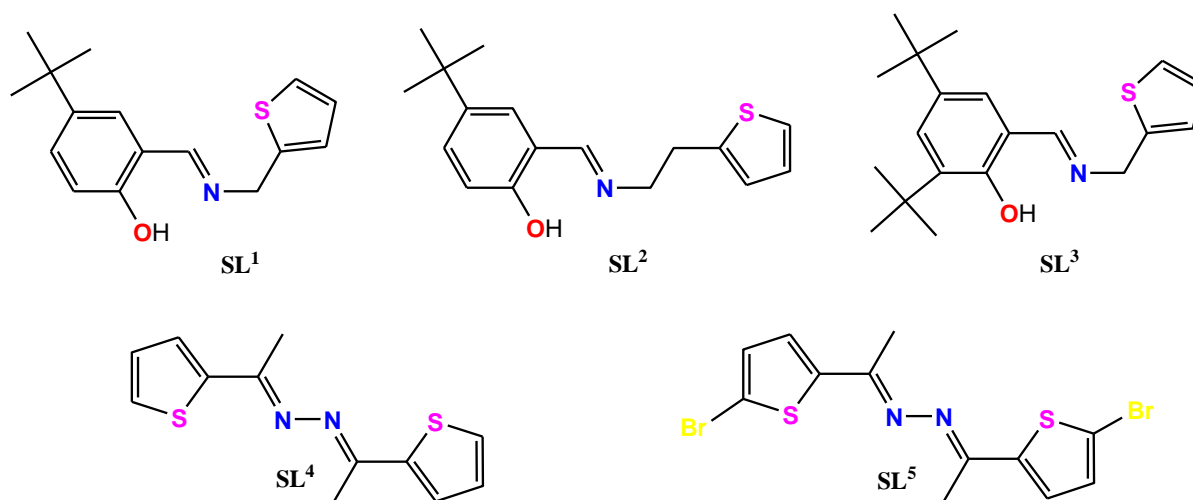
1.6.2 Specific Objectives

The specific objectives of the study were:

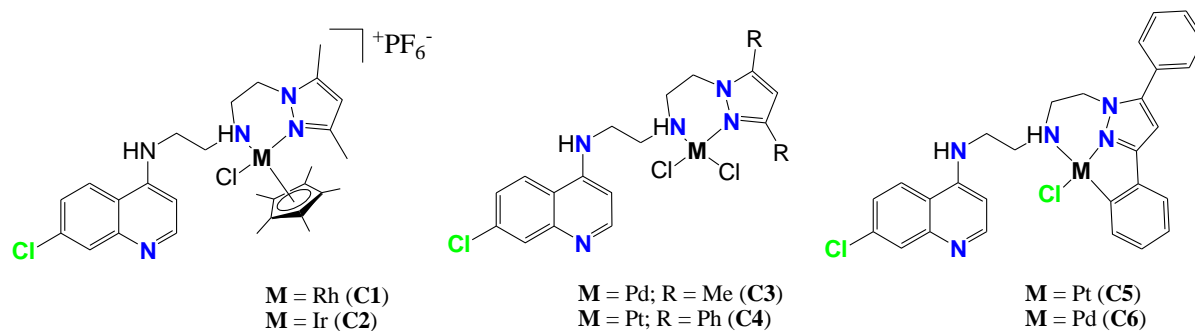
- 1) To design, synthesize and characterize novel 4-aminoquinolines with pendant pyrazole arms, L^1 , L^2 and L^3



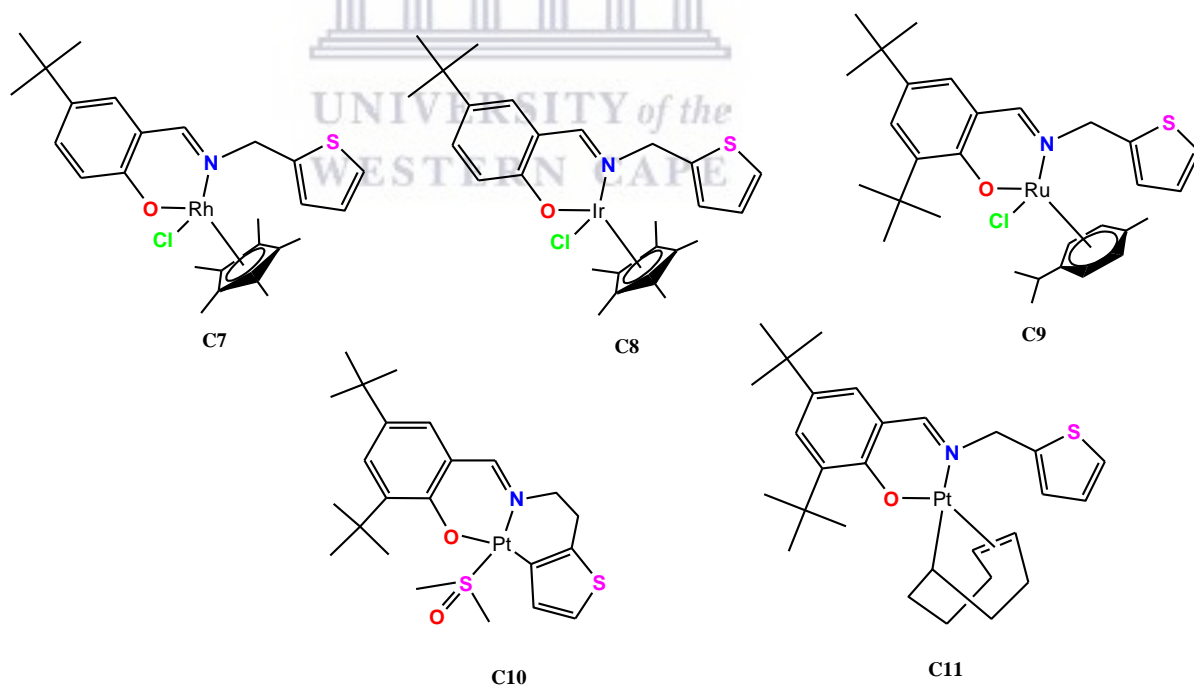
- 2) To design, synthesize and characterize new salicylaldehyde ligands with a pendant thiophenyl moiety, SL^1 - SL^3 and hydrazine derivatives with a thiophenyl moiety SL^4 - SL^5



- 3) To chelate L^1 and L^2 with different metal precursors (Pd^{II} , Pt^{II} , Rh^{III} and Ir^{III}) to afford cationic N,N' -(**C1** and **C2**), neutral N,N' -(**C3** and **C4**), and C,N,N' -(**C5** and **C6**) metal complexes.



- 4) To chelate the salicylaldehyde ligands SL^1 - SL^3 with different metal precursors (Pd^{II} , Pt^{II} , Ru^{II} , Rh^{III} and Ir^{III}) in order to achieve corresponding salicylaldimato metal complexes, **C7-C11**



- 5) To evaluate the antimalarial activity of three novel 4-aminoquinoline derivatives **L¹**-**L³** and their corresponding complexes **C1-C6**
- 6) To study the protein-ligand interaction of **L¹**, **L²** and **L³** with dihydrofolate reductase-thymidylate synthase with molecular docking
- 7) To evaluate the cytotoxic activity of three new salicylaldimine ligands **SL¹**-**SL³** and generic metal complexes **C7-C11** on different cancer cell lines



1.7 References:

- [1] K. J Arrow, C. Panosian, and H. Gelband, "Saving Lives, Buying Time: Economics of Malaria Drugs in an Age of Resistance." National Academies Press (US), 2004.
- [2] R. Carter and K. N. Mendis, "Evolutionary and historical aspects of the burden of malaria.," *Clin. Microbiol. Rev.*, vol. 15, no. 4, pp. 564–594, Oct. 2002.
- [3] "WHO | World Malaria Report 2015."
- [4] J. Cox-Singh, T. M. E. Davis, K.-S. Lee, S. S. G. Shamsul, A. Matusop, S. Ratnam, H. A. Rahman, D. J. Conway, and B. Singh, "Plasmodium knowlesi malaria in humans is widely distributed and potentially life threatening.," *Clin. Infect. Dis.*, vol. 46, no. 2, pp. 165–171, Jan. 2008.
- [5] N. J. White, "Plasmodium knowlesi: the fifth human malaria parasite.," *Clin. Infect. Dis.*, vol. 46, no. 2, pp. 172–173, Jan. 2008.
- [6] P. C. C. Garnham, "Malaria Parasites and other Haemosporidia.," 1966.
- [7] I. Vythilingam, C. H. Tan, M. Asmad, S. T. Chan, K. S. Lee, and B. Singh, "Natural transmission of Plasmodium knowlesi to humans by Anopheles latens in Sarawak, Malaysia.," *Trans. R. Soc. Trop. Med. Hyg.*, vol. 100, no. 11, pp. 1087–108, Nov. 2006.
- [8] A. Teklehaimanot and P. Mejjia, "Malaria and poverty.," *Ann. N. Y. Acad. Sci.*, vol. 1136, pp. 32–37, Jan. 2008.
- [9] R. I. Chima, C. A. Goodman, and A. Mills, "The economic impact of malaria in Africa: a critical review of the evidence.," *Health Policy*, vol. 63, no. 1, pp. 17–36,

- Jan. 2003.
- [10] A. Teklehaimanot and A. Bosman, “Opportunities, problems and perspectives for malaria control in sub-Saharan Africa.,” *Parassitologia*, vol. 41, no. 1–3, pp. 335–8, Sep. 1999.
- [11] A. M. Dondorp, F. Nosten, P. Yi, D. Das, A. P. Phy, J. Tarning, K. M. Lwin, F. Ariey, W. Hanpithakpong, S. J. Lee, P. Ringwald, K. Silamut, M. Imwong, K. Chotivanich, P. Lim, T. Herdman, S. S. An, S. Yeung, P. Singhasivanon, N. P. J. Day, N. Lindegardh, D. Socheat, and N. J. White, “Artemisinin resistance in Plasmodium falciparum malaria.,” *N. Engl. J. Med.*, vol. 361, no. 5, pp. 455–467, Jul. 2009.
- [12] A. M. Dondorp, S. Yeung, L. White, C. Nguon, N. P. J. Day, D. Socheat, and L. von Seidlein, “Artemisinin resistance: current status and scenarios for containment.,” *Nat. Rev. Microbiol.*, vol. 8, no. 4, pp. 272–280, Apr. 2010.
- [13] R. J. Maude, W. Pontavornpinyo, S. Saralamba, R. Aguas, S. Yeung, A. M. Dondorp, N. P. J. Day, N. J. White, and L. J. White, “The last man standing is the most resistant: eliminating artemisinin-resistant malaria in Cambodia.,” *Malar. J.*, vol. 8, p. 31, Jan. 2009.
- [14] W. O. Rogers, R. Sem, T. Tero, P. Chim, P. Lim, S. Muth, D. Socheat, F. Ariey, and C. Wongsrichanalai, “Failure of artesunate-mefloquine combination therapy for uncomplicated Plasmodium falciparum malaria in southern Cambodia.,” *Malar. J.*, vol. 8, p. 10, Jan. 2009.
- [15] A. Khamsiriwatchara, P. Sudathip, S. Sawang, S. Vijakadge, T. Potithavoranan, A. Sangvichean, W. Satimai, C. Delacollette, P. Singhasivanon, S. Lawpoolsri, and J.

- Kaewkungwal, “Artemisinin resistance containment project in Thailand. (I): Implementation of electronic-based malaria information system for early case detection and individual case management in provinces along the Thai-Cambodian border.” *Malar. J.*, vol. 11, p. 247, Jan. 2012.
- [16] W. Satimai, P. Sudathip, S. Vijaykadga, A. Khamsiriwatchara, S. Sawang, T. Potithavoranan, A. Sangvichean, C. Delacollette, P. Singhasivanon, J. Kaewkungwal, and S. Lawpoolsri, “Artemisinin resistance containment project in Thailand. II: Responses to mefloquine-artesunate combination therapy among falciparum malaria patients in provinces bordering Cambodia.” *Malar. J.*, vol. 11, p. 300, Jan. 2012.
- [17] K. Na-Bangchang, P. Muhamad, R. Ruaengweerayut, W. Chaijaroenkul, and J. Karbwang, “Identification of resistance of Plasmodium falciparum to artesunate-mefloquine combination in an area along the Thai-Myanmar border: integration of clinico-parasitological response, systemic drug exposure, and in vitro parasite sensitivity.” *Malar. J.*, vol. 12, p. 263, Jan. 2013.
- [18] C. L. Laveran, “Classics in infectious diseases: A newly discovered parasite in the blood of patients suffering from malaria. Parasitic etiology of attacks of malaria: Charles Louis Alphonse Laveran (1845-1922).” *Rev. Infect. Dis.*, vol. 4, no. 4, pp. 908–11, Jan. .
- [19] “WHO | World Malaria Report 2014.”
- [20] “Zika Virus Is Spreading, Here’s Everything You Need To Know About The Mosquito-Borne Illness.” [Online]. Available: <http://www.medicaldaily.com/zika-virus-united-states-mosquito-borne-illness-what-you-should-know-370604>. [Accessed: 17-Mar-2016].

- [21] “WHO | Zika virus.”
- [22] “CDC Confirms Zika Virus Case In Texas; Person Traveled To Latin America.” [Online]. Available: <http://www.medicaldaily.com/cdc-confirms-zika-virus-case-texas-person-traveled-latin-america-369042>. [Accessed: 17-Mar-2016].
- [23] “About Zika Virus Disease | Zika virus | CDC.” [Online]. Available: <http://www.cdc.gov/zika/about/index.html>. [Accessed: 17-Mar-2016].
- [24] “Life Cycle of the Malaria Parasite.” [Online]. Available: <https://www.niaid.nih.gov/topics/Malaria/Pages/lifecycle.aspx>. [Accessed: 26-Feb-2016].
- [25] B. M. Greenwood, D. A. Fidock, D. E. Kyle, S. H. I. Kappe, P. L. Alonso, F. H. Collins, and P. E. Duffy, “Malaria: progress, perils, and prospects for eradication.,” *J. Clin. Invest.*, vol. 118, no. 4, pp. 1266–1276, Apr. 2008.
- [26] C.-C. for D. C. and Prevention, “CDC - Malaria - About Malaria - Biology.”
- [27] T. J. Egan, “Quinoline antimalarials,” *Expert Opin. Ther. Pat.*, vol. 11, no. 2, pp. 185–209, Feb. 2005.
- [28] D. J. Wallace, “The use of chloroquine and hydroxychloroquine for non-infectious conditions other than rheumatoid arthritis or lupus: a critical review.,” *Lupus*, vol. 5 Suppl 1, pp. S59–64, Jun. 1996.
- [29] R. B. Woodward and W. E. Doering, “The total synthesis of quinine 1,” *J. Am. Chem. Soc.*, vol. 66, no. 5, pp. 849–849, May 1944.
- [30] T. S. Kaufman and E. A. Rúveda, “Die Jagd auf Chinin: Etappenerfolge und

- Gesamtsiege,” *Angew. Chemie*, vol. 117, no. 6, pp. 876–907, Jan. 2005.
- [31] L. L. G. Urban Hellgren, Orjan Ericsson, Yakoub AdenAbdi, *Handbook of Drugs for Tropical Parasitic Infections - CRC Press Book*. 1995.
- [32] P. J. Rosenthal, “Antimalarial Chemotherapy. Mechanisms of Action, Resistance and New Directions in Drug Discovery,” *J. Antimicrob. Chemother.*, vol. 51, no. 4, pp. 1053–1053, Apr. 2003.
- [33] P. Winstanley and S. Ward, “Malaria chemotherapy,” *Adv. Parasitol.*, vol. 61, pp. 47–76, Jan. 2006.
- [34] D. N. Bateman and E. H. Dyson, “Quinine toxicity,” *Adverse Drug React. Acute Poisoning Rev.*, vol. 5, no. 4, pp. 215–233, Jan. 1986.
- [35] K. K. Karlsson, U. Hellgren, G. Alván, and L. Rombo, “Audiometry as a possible indicator of quinine plasma concentration during treatment of malaria,” *Trans. R. Soc. Trop. Med. Hyg.*, vol. 84, no. 6, pp. 765–767, Jan. 1990.
- [36] “Severe falciparum malaria. World Health Organization, Communicable Diseases Cluster,” *Trans. R. Soc. Trop. Med. Hyg.*, vol. 94 Suppl 1, pp. S1–90, Apr. 2000.
- [37] J. Achan, A. O. Talisuna, A. Erhart, A. Yeka, J. K. Tibenderana, F. N. Baliraine, P. J. Rosenthal, and U. D’Alessandro, “Quinine, an old anti-malarial drug in a modern world: role in the treatment of malaria,” *Malar. J.*, vol. 10, p. 144, Jan. 2011.
- [38] P. Olliaro, “Mode of action and mechanisms of resistance for antimalarial drugs,” *Pharmacol. Ther.*, vol. 89, no. 2, pp. 207–219, Feb. 2001.
- [39] M. Foley and L. Tilley, “Quinoline Antimalarials: Mechanisms of Action and

- Resistance and Prospects for New Agents =,” *Pharmacol. Ther.*, vol. 79, no. 1, pp. 55–87, 1998.
- [40] E. F. Elslager, E. H. Gold, F. H. Tendick, L. M. Werbel, and D. F. Worth, “Amodiaquine N-oxides and other 7-chloro-4-aminoquinoline n-oxides,” *J. Heterocycl. Chem.*, vol. 1, no. 1, pp. 6–12, Feb. 1964.
- [41] T. J. Egan, R. Hunter, C. H. Kaschula, H. M. Marques, A. Mispion, and J. Walden, “Structure-function relationships in aminoquinolines: effect of amino and chloro groups on quinoline-hematin complex formation, inhibition of beta-hematin formation, and antiplasmodial activity.,” *J. Med. Chem.*, vol. 43, no. 2, pp. 283–291, Jan. 2000.
- [42] C. H. Kaschula, T. J. Egan, R. Hunter, N. Basilico, S. Parapini, D. Taramelli, E. Pasini, and D. Monti, “Structure–Activity Relationships in 4-Aminoquinoline Antiplasmodials. The Role of the Group at the 7-Position,” *J. Med. Chem.*, vol. 45, no. 16, pp. 3531–3539, Aug. 2002.
- [43] R. Ridley, W. Hofheinz, H. Matile, C. Jaquet, A. Dorn, R. Masciadri, S. Jolidon, W. Richter, A. Guenzi, M. Girometta, H. Urwyler, W. Huber, S. Thaithong, and W. Peters, “4-aminoquinoline analogs of chloroquine with shortened side chains retain activity against chloroquine-resistant Plasmodium falciparum,” *Antimicrob. Agents Chemother.*, vol. 40, no. 8, pp. 1846–1854, Aug. 1996.
- [44] D. De, F. M. Krogstad, L. D. Byers, and D. J. Krogstad, “Structure-activity relationships for antiplasmodial activity among 7-substituted 4-aminoquinolines.,” *J. Med. Chem.*, vol. 41, no. 25, pp. 4918–4926, Dec. 1998.
- [45] S. Srivastava, S. Tewari, P. M. S. Chauhan, S. K. Puri, A. P. Bhaduri, and V. C.

- Pandey, "Synthesis of bisquinolines and their in vitro ability to produce methemoglobin in canine hemolysate," *Bioorg. Med. Chem. Lett.*, vol. 9, no. 5, pp. 653–658, Mar. 1999.
- [46] J. L. Vennerstrom, A. L. Ager, A. Dorn, S. L. Andersen, L. Gerena, R. G. Ridley, and W. K. Milhous, "Bisquinolines. 2. Antimalarial N,N-bis(7-chloroquinolin-4-yl)heteroalkanediamines," *J. Med. Chem.*, vol. 41, no. 22, pp. 4360–4364, Oct. 1998.
- [47] J. L. Vennerstrom, W. Y. Ellis, A. L. Ager, S. L. Andersen, L. Gerena, and W. K. Milhous, "Bisquinolines. 1. N,N-bis(7-chloroquinolin-4-yl)alkanediamines with potential against chloroquine-resistant malaria," *J. Med. Chem.*, vol. 35, no. 11, pp. 2129–2134, May 1992.
- [48] K. Raynes, D. Galatis, A. F. Cowman, L. Tilley, and L. W. Deady, "Synthesis and activity of some antimalarial bisquinolines," *J. Med. Chem.*, vol. 38, no. 1, pp. 204–206, Jan. 1995.
- [49] Y. Q. and Y. G. Y. Lin, Y. Qin, "Hydroxypiperaquine phosphate interacting with chloroquine resistant falciparum malaria," *Chin. Med. J.*, vol. 94, p. 303, 1981.
- [50] J. Le Bras, P. Deloron, and G. Charmot, "Dichlorquinazine (alpha 4-aminoquinoline) effective in vitro against chloroquine-resistant Plasmodium falciparum," *Lancet (London, England)*, vol. 1, no. 8314–5, pp. 73–74, Jan. 1983.
- [51] Y. Zhang and E. Hempelmann, "Lysis of malarial parasites and erythrocytes by ferriprotoporphyrin IX-chloroquine and the inhibition of this effect by proteins," *Biochem. Pharmacol.*, vol. 36, no. 8, pp. 1267–1273, Apr. 1987.
- [52] D. Greenwood, "Conflicts of interest: the genesis of synthetic antimalarial agents in

- peace and war.," *J. Antimicrob. Chemother.*, vol. 36, no. 5, pp. 857–872, Nov. 1995.
- [53] M. Foley and L. Tilley, "Quinoline antimalarials: Mechanisms of action and resistance," *Int. J. Parasitol.*, vol. 27, no. 2, pp. 231–240, Feb. 1997.
- [54] D. L. Klayman, "Qinghaosu (artemisinin): an antimalarial drug from China.," *Science*, vol. 228, no. 4703, pp. 1049–1055, May 1985.
- [55] Q. Li, P. Weina, and W. Milhous, "Pharmacokinetic and pharmacodynamic profiles of rapid-acting artemisinins in the antimalarial therapy," *Curr. Drug ther.*, 2007.
- [56] N. J. White, "Qinghaosu (artemisinin): the price of success.," *Science*, vol. 320, no. 5874, pp. 330–334, Apr. 2008.
- [57] M. B. van Hensbroek, E. Onyiorah, S. Jaffar, G. Schneider, A. Palmer, J. Frenkel, G. Enwere, S. Forck, A. Nusmeijer, S. Bennett, B. Greenwood, and D. Kwiatkowski, "A trial of artemether or quinine in children with cerebral malaria.," *N. Engl. J. Med.*, vol. 335, no. 2, pp. 69–75, Jul. 1996.
- [58] M. Ashton, D. S. Nguyen, V. H. Nguyen, T. Gordi, N. H. Trinh, X. H. Dinh, T. N. Nguyen, and D. C. Le, "Artemisinin kinetics and dynamics during oral and rectal treatment of uncomplicated malaria.," *Clin. Pharmacol. Ther.*, vol. 63, no. 4, pp. 482–493, Apr. 1998.
- [59] R. K. Haynes, H. W. Chan, M. K. Cheung, W. L. Lam, M. K. Soo, H. W. Tsang, A. Voerste, and I. D. Williams, "C-10 ester and ether derivatives of dihydroartemisinin - 10- α artesunate, preparation of authentic 10- β artesunate, and of other ester and ether derivatives bearing potential aromatic intercalating groups at C-10," *European J. Org. Chem.*, no. 1, pp. 113–132, 2002.

- [60] D. L. Klayman, "Qinghaosu (Artemisinin): An antimalarial drug from China," *Science*, vol. 228, no. 4703, pp. 1049–1055, 1985.
- [61] "Artemisinin and Derivatives Pathway, Pharmacokinetics." [Online]. Available: <https://www.pharmgkb.org/pathway/PA165378192>. [Accessed: 01-Mar-2016].
- [62] China Cooperative Research Group, "Metabolism and pharmacokinetics of qinghaosu and its derivatives. China Cooperative Research Group on qinghaosu and its derivatives as antimalarials.," *J. Tradit. Chin. Med.*, vol. 2, no. 1, pp. 25–30, Mar. 1982.
- [63] C. C. R. Group, "The chemistry and synthesis of qinghaosu derivatives. China Cooperative Research Group on qinghaosu and its derivatives as antimalarials.," *J. Tradit. Chin. Med.*, vol. 2, no. 1, pp. 9–16, Mar. 1982.
- [64] C. C. R. Group, "Clinical studies on the treatment of malaria with qinghaosu and its derivatives. China Cooperative Research Group on qinghaosu and its derivatives as antimalarials.," *J. Tradit. Chin. Med.*, vol. 2, no. 1, pp. 45–50, Mar. 1982.
- [65] C. C. R. Group, "Chemical studies on qinghaosu (artemisinine). China Cooperative Research Group on qinghaosu and its derivatives as antimalarials.," *J. Tradit. Chin. Med.*, vol. 2, no. 1, pp. 3–8, Mar. 1982.
- [66] China Cooperative Research Group, "Antimalarial efficacy and mode of action of qinghaosu and its derivatives in experimental models. China Cooperative Research Group on qinghaosu and its derivatives as antimalarials.," *J. Tradit. Chin. Med.*, vol. 2, no. 1, pp. 17–24, Mar. 1982.
- [67] R. T. Eastman and D. A. Fidock, "Artemisinin-based combination therapies: a vital

- tool in efforts to eliminate malaria,” *Nat. Rev. Microbiol.*, vol. 7, no. 12, pp. 864–874, Dec. 2009.
- [68] J. Golenser, J. H. Waknine, M. Krugliak, N. H. Hunt, and G. E. Grau, “Current perspectives on the mechanism of action of artemisinins,” *Int. J. Parasitol.*, vol. 36, no. 14, pp. 1427–1441, Dec. 2006.
- [69] S. Zarchin, M. Krugliak, and H. Ginsburg, “Digestion of the host erythrocyte by malaria parasites is the primary target for quinolinecontaining antimalarials,” *Biochem. Pharmacol.*, vol. 35, no. 14, pp. 2435–2442, Jul. 1986.
- [70] M. Krugliak, J. Zhang, and H. Ginsburg, “Intraerythrocytic *Plasmodium falciparum* utilizes only a fraction of the amino acids derived from the digestion of host cell cytosol for the biosynthesis of its proteins,” *Mol. Biochem. Parasitol.*, vol. 119, no. 2, pp. 249–256, Feb. 2002.
- [71] V. L. Lew, L. Macdonald, H. Ginsburg, M. Krugliak, and T. Tiffert, “Excess haemoglobin digestion by malaria parasites: a strategy to prevent premature host cell lysis,” *Blood Cells. Mol. Dis.*, vol. 32, no. 3, pp. 353–359, Jan. 2004.
- [72] P. L. Olliaro and D. E. Goldberg, “The *Plasmodium* digestive Vacuole: Metabolic Headquarters and Choice Drug Target,” *Parasitol. Today*, vol. 11, no. 8, pp. 294–297, Aug. 1995.
- [73] D. E. Goldberg, A. F. Slater, A. Cerami, and G. B. Henderson, “Hemoglobin degradation in the malaria parasite *Plasmodium falciparum*: an ordered process in a unique organelle,” *Proc. Natl. Acad. Sci. U. S. A.*, vol. 87, no. 8, pp. 2931–2935, Apr. 1990.

- [74] T. J. Egan, "Haemozoin formation.," *Mol. Biochem. Parasitol.*, vol. 157, no. 2, pp. 127–136, Feb. 2008.
- [75] T. J. Egan, J. Y.-J. Chen, K. A. de Villiers, T. E. Mabothe, K. J. Naidoo, K. K. Ncokazi, S. J. Langford, D. McNaughton, S. Pandiancherri, and B. R. Wood, "Haemozoin (beta-haematin) biomineralization occurs by self-assembly near the lipid/water interface.," *FEBS Lett.*, vol. 580, no. 21, pp. 5105–5110, Sep. 2006.
- [76] L. Tilley, P. Loria, and M. Foley, "Chloroquine and Other Quinoline Antimalarials," pp. 87–121, 2001.
- [77] G. Padmanaban and P. N. Rangarajan, "Emerging targets for antimalarial drugs.," *Expert Opin. Ther. Targets*, vol. 5, no. 4, pp. 423–441, Aug. 2001.
- [78] P. G. Bray, M. Mungthin, R. G. Ridley, and S. A. Ward, "Access to hemozoin: The basis of chloroquine resistance.," *Mol. Pharmacol.*, vol. 54, no. 1, pp. 170–179, 1998.
- [79] P. G. Bray, O. Janneh, K. J. Raynes, M. Mungthin, H. Ginsburg, and S. A. Ward, "Cellular Uptake of Chloroquine Is Dependent on Binding to Ferriprotoporphyrin IX and Is Independent of NHE Activity in Plasmodium falciparum.," *J. Cell Biol.*, vol. 145, no. 2, pp. 363–376, Apr. 1999.
- [80] S. E. Francis, D. J. Sullivan, and D. E. Goldberg, "Hemoglobin metabolism in the malaria parasite plasmodium falciparum.," *Annu. Rev. Microbiol.*, vol. 51, no. 1, pp. 97–123, Oct. 1997.
- [81] A. F. G. Slater, W. J. Swiggard, B. R. Orton, W. D. Flitter, D. E. Goldberg, A. Cerami, and G. B. Henderson, "An iron-carboxylate bond links the heme units of malaria pigment.," *Proc. Natl. Acad. Sci. U. S. A.*, vol. 88, no. 2, pp. 325–329, 1991.

- [82] D. S. Bohle, R. E. Dinnebier, S. K. Madsen, and P. W. Stephens, "Characterization of the Products of the Heme Detoxification Pathway in Malarial Late Trophozoites by X-ray Diffraction," *J. Biol. Chem.*, vol. 272, no. 2, pp. 713–716, Jan. 1997.
- [83] S. Pagola, P. W. Stephens, D. S. Bohle, A. D. Kosar, and S. K. Madsen, "The structure of malaria pigment beta-haematin.," *Nature*, vol. 404, no. 6775, pp. 307–310, Mar. 2000.
- [84] T. J. Egan, "Haemozoin formation.," *Mol. Biochem. Parasitol.*, vol. 157, no. 2, pp. 127–136, Feb. 2008.
- [85] C. D. Fitch and P. Kanjanangulpan, "The state of ferriprotoporphyrin IX in malaria pigment.," *J. Biol. Chem.*, vol. 262, no. 32, pp. 15552–15555, 1987.
- [86] J. L. Irvin, E. M. Irvin, and F. S. Parker, "The Interaction of Antimalarials with Nucleic Acids.," *Science*, vol. 110, no. 2860, pp. 426–428, Oct. 1949.
- [87] F. S. Parker and J. L. Irvin, "The interreaction of chloroquine with the albumin of bovine plasma.," *J. Biol. Chem.*, vol. 199, no. 2, pp. 889–895, Dec. 1952.
- [88] R. G. Allison and F. E. Hahn, "Changes in Superhelical Density of Closed Circular Deoxyribonucleic Acid by Intercalation of Anti-R-Plasmid Drugs and Primaquine," *Antimicrob. Agents Chemother.*, vol. 11, no. 2, pp. 251–257, Feb. 1977.
- [89] D. Stollar and L. Levine, "Antibodies to denatured deoxyribonucleic acid in lupus erythematosus serum. V. Mechanism of DNA-anti-DNA inhibition by chloroquine.," *Arch. Biochem. Biophys.*, vol. 101, pp. 335–341, May 1963.
- [90] S. N. Cohen and K. L. Yielding, "Spectrophotometric studies of the interaction with deoxyribonucleic acid.," *J. Biol. Chem.*, vol. 240, pp. 3123–3131, Jul. 1965.

- [91] S. N. Cohen and K. L. Yielding, "Inhibition of DNA and RNA polymerase reactions by chloroquine.," *Proc. Natl. Acad. Sci. U. S. A.*, vol. 54, no. 2, pp. 521–527, Aug. 1965.
- [92] A. Martínez, C. S. K. Rajapakse, R. A. Sánchez-Delgado, A. Varela-Ramirez, C. Lema, and R. J. Aguilera, "Arene-Ru(II)-chloroquine complexes interact with DNA, induce apoptosis on human lymphoid cell lines and display low toxicity to normal mammalian cells.," *J. Inorg. Biochem.*, vol. 104, no. 9, pp. 967–977, Sep. 2010.
- [93] S. R. Cheruku, S. Maiti, A. Dorn, B. Scorneaux, A. K. Bhattacharjee, W. Y. Ellis, and J. L. Vennerstrom, "Carbon isosteres of the 4-aminopyridine substructure of chloroquine: effects on pK(a), hemozoin binding, inhibition of hemozoin formation, and parasite growth.," *J. Med. Chem.*, vol. 46, no. 14, pp. 3166–3169, Jul. 2003.
- [94] D. De, F. M. Krogstad, F. B. Cogswell, and D. J. Krogstad, "Aminoquinolines that circumvent resistance in *Plasmodium falciparum* in vitro.," *Am. J. Trop. Med. Hyg.*, vol. 55, no. 6, pp. 579–583, Dec. 1996.
- [95] S. R. Hawley, P. G. Bray, P. M. O'Neill, B. K. Park, and S. A. Ward, "The role of drug accumulation in 4-aminoquinoline antimalarial potency," *Biochem. Pharmacol.*, vol. 52, no. 5, pp. 723–733, Sep. 1996.
- [96] S. Parapini, N. Basilico, E. Pasini, T. J. Egan, P. Olliaro, D. Taramelli, and D. Monti, "Standardization of the physicochemical parameters to assess in vitro the beta-hematin inhibitory activity of antimalarial drugs.," *Exp. Parasitol.*, vol. 96, no. 4, pp. 249–256, Dec. 2000.
- [97] D. De, F. M. Krogstad, L. D. Byers, and D. J. Krogstad, "Structure-activity

- relationships for antiplasmodial activity among 7-substituted 4-aminoquinolines.,” *J. Med. Chem.*, vol. 41, no. 25, pp. 4918–4926, Dec. 1998.
- [98] D. F. Clyde, “Antimalarial effect of diaphenylsulfone and three sulfonamides among semi-immune Africans.,” *Am. J. Trop. Med. Hyg.*, vol. 16, no. 1, pp. 7–10, Jan. 1967.
- [99] J. E. Hyde, “Mechanisms of resistance of Plasmodium falciparum to antimalarial drugs.,” *Microbes Infect.*, vol. 4, no. 2, pp. 165–174, Feb. 2002.
- [100] J. E. Hyde, “Drug-resistant malaria - an insight.,” *FEBS J.*, vol. 274, no. 18, pp. 4688–4698, Sep. 2007.
- [101] I. B. Müller and J. E. Hyde, “Antimalarial drugs: modes of action and mechanisms of parasite resistance.,” *Future Microbiol.*, vol. 5, no. 12, pp. 1857–1873, Dec. 2010.
- [102] I. Petersen, R. Eastman, and M. Lanzer, “Drug-resistant malaria: molecular mechanisms and implications for public health.,” *FEBS Lett.*, vol. 585, no. 11, pp. 1551–1562, Jun. 2011.
- [103] T. E. Wellems and C. V Plowe, “Chloroquine-Resistant Malaria,” pp. 770–776.
- [104] D. J. Krogstad, I. Y. Gluzman, D. E. Kyle, A. M. Oduola, S. K. Martin, W. K. Milhous, and P. H. Schlesinger, “Efflux of chloroquine from Plasmodium falciparum: mechanism of chloroquine resistance.,” *Science*, vol. 238, no. 4831, pp. 1283–1285, Nov. 1987.
- [105] D. A. Fidock, T. Nomura, A. K. Talley, R. A. Cooper, S. M. Dzekunov, M. T. Ferdig, L. M. B. Ursos, A. bir Singh Sidhu, B. Naudé, K. W. Deitsch, X. Su, J. C. Wootton, P. D. Roepe, and T. E. Wellems, “Mutations in the P. falciparum Digestive Vacuole Transmembrane Protein PfCRT and Evidence for Their Role in Chloroquine

- Resistance,” *Mol. Cell*, vol. 6, no. 4, pp. 861–871, Oct. 2000.
- [106] T. Mita, K. Tanabe, and K. Kita, “Spread and evolution of *Plasmodium falciparum* drug resistance.,” *Parasitol. Int.*, vol. 58, no. 3, pp. 201–209, Sep. 2009.
- [107] J. C. Wootton, X. Feng, M. T. Ferdig, R. A. Cooper, J. Mu, D. I. Baruch, A. J. Magill, and X.-Z. Su, “Genetic diversity and chloroquine selective sweeps in *Plasmodium falciparum*.,” *Nature*, vol. 418, no. 6895, pp. 320–323, Jul. 2002.
- [108] P. G. Bray, R. E. Martin, L. Tilley, S. A. Ward, K. Kirk, and D. A. Fidock, “Defining the role of PfCRT in *Plasmodium falciparum* chloroquine resistance.,” *Mol. Microbiol.*, vol. 56, no. 2, pp. 323–333, Apr. 2005.
- [109] V. Lakshmanan, P. G. Bray, D. Verdier-Pinard, D. J. Johnson, P. Horrocks, R. A. Muhle, G. E. Alakpa, R. H. Hughes, S. A. Ward, D. J. Krogstad, A. B. S. Sidhu, and D. A. Fidock, “A critical role for PfCRT K76T in *Plasmodium falciparum* verapamil-reversible chloroquine resistance.,” *EMBO J.*, vol. 24, no. 13, pp. 2294–2305, Jul. 2005.
- [110] G. A. Biagini, D. A. Fidock, P. G. Bray, and S. A. Ward, “Mutations conferring drug resistance in malaria parasite drug transporters Pgh1 and PfCRT do not affect steady-state vacuolar Ca^{2+} .,” *Antimicrob. Agents Chemother.*, vol. 49, no. 11, pp. 4807–4808, Nov. 2005.
- [111] C. P. Sanchez, J. E. McLean, P. Rohrbach, D. A. Fidock, W. D. Stein, and M. Lanzer, “Evidence for a pfert-associated chloroquine efflux system in the human malarial parasite *Plasmodium falciparum*.,” *Biochemistry*, vol. 44, no. 29, pp. 9862–9870, Jul. 2005.

- [112] D. C. Warhurst, J. C. Craig, and I. S. Adagu, "Lysosomes and drug resistance in malaria.," *Lancet (London, England)*, vol. 360, no. 9345, pp. 1527–1529, Nov. 2002.
- [113] D. J. Krogstad, I. Y. Gluzman, B. L. Herwaldt, P. H. Schlesinger, and T. E. Wellems, "Energy dependence of chloroquine accumulation and chloroquine efflux in *Plasmodium falciparum*," *Biochem. Pharmacol.*, vol. 43, no. 1, pp. 57–62, Jan. 1992.
- [114] C. P. Sanchez, P. Rohrbach, J. E. McLean, D. A. Fidock, W. D. Stein, and M. Lanzer, "Differences in trans-stimulated chloroquine efflux kinetics are linked to PfCRT in *Plasmodium falciparum*," *Mol. Microbiol.*, vol. 64, no. 2, pp. 407–420, Apr. 2007.
- [115] N. P. Farrell, Ed., *Uses of Inorganic Chemistry in Medicine*. Cambridge: Royal Society of Chemistry, 1999.
- [116] C. Biot, W. Castro, C. Y. Botté, and M. Navarro, "The therapeutic potential of metal-based antimalarial agents: implications for the mechanism of action.," *Dalton Trans.*, vol. 41, no. 21, pp. 6335–6349, Jun. 2012.
- [117] P. A. Ajibade and G. A. Kolawole, "Synthesis, characterization and antiprotozoal studies of some metal complexes of antimalarial drugs," *Transit. Met. Chem.*, vol. 33, no. 4, pp. 493–497, Mar. 2008.
- [118] A. C. Pena, N. Penacho, L. Mancio-Silva, R. Neres, J. D. Seixas, A. C. Fernandes, C. C. Romão, M. M. Mota, G. J. L. Bernardes, and A. Pamplona, "A novel carbon monoxide-releasing molecule fully protects mice from severe malaria.," *Antimicrob. Agents Chemother.*, vol. 56, no. 3, pp. 1281–1290, Mar. 2012.
- [119] P. F. Salas, C. Herrmann, and C. Orvig, "Metalloantimalarials.," *Chem. Rev.*, vol. 113, no. 5, pp. 3450–3492, May 2013.

- [120] M. Navarro, H. Pérez, and R. A. Sánchez-Delgado, "Toward a novel metal-based chemotherapy against tropical diseases. 3. Synthesis and antimalarial activity in vitro and in vivo of the new gold-chloroquine complex $[\text{AuPPh}_3(\text{CQ})]\text{PF}_6$," *J. Med. Chem.*, vol. 40, no. 12, pp. 1937–1939, Jun. 1997.
- [121] R. A. Sánchez-Delgado, M. Navarro, H. Pérez, and J. A. Urbina, "Toward a novel metal-based chemotherapy against tropical diseases. 2. Synthesis and antimalarial activity in vitro and in vivo of new ruthenium- and rhodium-chloroquine complexes," *J. Med. Chem.*, vol. 39, no. 5, pp. 1095–1099, Mar. 1996.
- [122] C. S. K. Rajapakse, A. Martínez, B. Naoulou, A. A. Jarzecki, L. Suárez, C. Deregnacourt, V. Sinou, J. Schrével, E. Musi, G. Ambrosini, G. K. Schwartz, and R. A. Sánchez-Delgado, "Synthesis, characterization, and in vitro antimalarial and antitumor activity of new ruthenium(II) complexes of chloroquine," *Inorg. Chem.*, vol. 48, no. 3, pp. 1122–31, Feb. 2009.
- [123] M. Navarro, S. Pekarar, and H. A. Pérez, "Synthesis, characterization and antimalarial activity of new iridium–chloroquine complexes," *Polyhedron*, vol. 26, no. 12, pp. 2420–2424, Jul. 2007.
- [124] M. Navarro, "Gold complexes as potential anti-parasitic agents," *Coord. Chem. Rev.*, vol. 253, no. 11–12, pp. 1619–1626, Jun. 2009.
- [125] L. Glans, A. Ehnbohm, C. de Kock, A. Martínez, J. Estrada, P. J. Smith, M. Haukka, R. a. Sánchez-Delgado, and E. Nordlander, "Ruthenium(ii) arene complexes with chelating chloroquine analogue ligands: Synthesis, characterization and in vitro antimalarial activity," *Dalt. Trans.*, vol. 41, no. 9, p. 2764, 2012.

- [126] M. Navarro, W. Castro, A. Martínez, and R. A. Sánchez Delgado, “The mechanism of antimalarial action of $[\text{Au}(\text{CQ})\text{PPh}_3]\text{PF}_6$: structural effects and increased drug lipophilicity enhance heme aggregation inhibition at lipid/water interfaces.,” *J. Inorg. Biochem.*, vol. 105, no. 2, pp. 276–82, Feb. 2011.
- [127] A. Martínez, C. S. K. Rajapakse, B. Naoulou, Y. Kopkalli, L. Davenport, and R. a. Sánchez-Delgado, “The mechanism of antimalarial action of the ruthenium(II)-chloroquine complex $[\text{RuCl}_2(\text{CQ})_2]$,” *J. Biol. Inorg. Chem.*, vol. 13, no. 5, pp. 703–712, 2008.
- [128] K. R. Koch, C. Sacht, and C. Lawrence, “Self-association of new mixed-ligand diimine–N-acyl–N',N'-dialkyl thiourea complexes of platinum(II) in acetonitrile solution†,” *J. Chem. Soc. Dalt. Trans.*, vol. 4, no. 4, pp. 689–696, Feb. 1998.
- [129] T. J. Egan, K. R. Koch, P. L. Swan, C. Clarkson, D. A. Van Schalkwyk, and P. J. Smith, “In vitro antimalarial activity of a series of cationic 2,2'-bipyridyl- and 1,10-phenanthrolineplatinum(II) benzoylthiourea complexes,” *J. Med. Chem.*, vol. 47, no. 11, pp. 2926–2934, May 2004.
- [130] M. Navarro, W. Castro, A. R. Higuera-Padilla, A. Sierraalta, M. J. Abad, P. Taylor, and R. A. Sánchez-Delgado, “Synthesis, characterization and biological activity of trans-platinum(II) complexes with chloroquine,” *J. Inorg. Biochem.*, vol. 105, no. 12, pp. 1684–1691, Dec. 2011.
- [131] M. Navarro, W. Castro, M. Madamet, R. Amalvict, N. Benoit, and B. Pradines, “Metal-chloroquine derivatives as possible anti-malarial drugs: evaluation of anti-malarial activity and mode of action,” *Malar. J.*, vol. 13, no. 1, p. 471, 2014.

- [132] C. S. K. Rajapakse, a. Martinez, B. Naoulou, a. a. Jarzecki, L. Suárez, C. Deregnacourt, V. Sinou, J. Schrével, E. Musi, G. Ambrosini, G. K. Schwartz, and R. a. Sanchez-Delgado, "Synthesis, Characterization and in vitro Antimalarial and Antitumor Activity of New Ruthenium(II) Complexes of Chloroquine," *Inorg. Chem.*, vol. 48, no. 3, pp. 1122–1131, 2009.
- [133] A. Martínez, C. S. K. Rajapakse, B. Naoulou, Y. Kopkalli, L. Davenport, and R. A. Sánchez-Delgado, "The mechanism of antimalarial action of the ruthenium(II)-chloroquine complex $[\text{RuCl}_2(\text{CQ})]_2$," *J. Biol. Inorg. Chem.*, vol. 13, no. 5, pp. 703–712, Jun. 2008.
- [134] A. Martínez, C. S. K. Rajapakse, D. Jalloh, C. Dautriche, and R. A. Sánchez-Delgado, "The antimalarial activity of Ru-chloroquine complexes against resistant *Plasmodium falciparum* is related to lipophilicity, basicity, and heme aggregation inhibition ability near water/n-octanol interfaces.," *J. Biol. Inorg. Chem.*, vol. 14, no. 6, pp. 863–871, Aug. 2009.
- [135] M. Navarro, F. Vásquez, R. A. Sánchez-Delgado, H. Pérez, V. Sinou, and J. Schrével, "Toward a novel metal-based chemotherapy against tropical diseases. 7. Synthesis and in vitro antimalarial activity of new gold-chloroquine complexes.," *J. Med. Chem.*, vol. 47, no. 21, pp. 5204–5209, Oct. 2004.
- [136] P. Beagley, M. A. L. Blackie, K. Chibale, C. Clarkson, J. R. Moss, and P. J. Smith, "Synthesis and antimalarial activity in vitro of new ruthenocene–chloroquine analogues," *J. Chem. Soc., Dalton Trans.*, no. 23, pp. 4426–4433, Nov. 2002.
- [137] R. a Sánchez-Delgado, M. Navarro, H. Pérez, and J. a Urbina, "Toward a novel metal-based chemotherapy against tropical diseases. 2. Synthesis and antimalarial activity in

- vitro and in vivo of new ruthenium- and rhodium-chloroquine complexes.," *J. Med. Chem.*, vol. 39, no. 5, pp. 1095–1099, 1996.
- [138] L. Li, K. Du, Y. Wang, H. Jia, X. Hou, H. Chao, and L. Ji, "Self-activating nuclease and anticancer activities of copper(II) complexes with aryl-modified 2,6-di(thiazol-2-yl)pyridine.," *Dalton Trans.*, vol. 42, no. 32, pp. 11576–11588, 2013.
- [139] T. J. KEALY and P. L. PAUSON, "A New Type of Organo-Iron Compound," *Nature*, vol. 168, no. 4285, pp. 1039–1040, Dec. 1951.
- [140] S. A. Miller, J. A. Tebboth, and J. F. Tremaine, "114. Dicyclopentadienyliron," *J. Chem. Soc.*, p. 632, Jan. 1952.
- [141] E. O. Fischer and W. Pfab, "Cyclopentadiene-metallic complex, a new type of organo-metallic compound.," *Zeitschrift fuer Naturforschung. B, Anorg. Org. und Biol. Chemie, Bot. Zool. und verwandte Gebiete*, vol. 7b, no. 7, pp. 377–379, 1952.
- [142] G. Wilkinson, M. Rosenblum, M. C. Whiting, and R. B. Woodward, "The structure of iron bis-cyclopentadienyl," *J. Am. Chem. Soc.*, vol. 74, no. 8, pp. 2125–2126, Apr. 1952.
- [143] J. M. Harkin, "Chemistry of the Iron Group Metallocenes: Ferrocene, Ruthenocene, Osmocene. Teil I. Von M. Rosenblum. Interscience Publishers, New York-London-Sydney 1965. 1. Aufl. XV, 241 S., mehrere Abb., geh. £ 4.15.-," *Angew. Chemie*, vol. 78, no. 16, pp. 786–787, Aug. 1966.
- [144] A. Togni and T. Hayashi, Eds., *Ferrocenes*. Weinheim, Germany: Wiley-VCH Verlag GmbH, 1994.
- [145] G. Gasser and N. Metzler-Nolte, "The potential of organometallic complexes in

- medicinal chemistry,” *Curr. Opin. Chem. Biol.*, vol. 16, no. 1–2, pp. 84–91, 2012.
- [146] J. C. Swarts, E. W. Neuse, and G. J. Lamprecht, “Synthesis and characterization of water-soluble polyaspartamide-ferrocene conjugates for biomedical applications,” *J. Inorg. Organomet. Polym.*, vol. 4, no. 2, pp. 143–153, Jun. 1994.
- [147] D. R. van Staveren and N. Metzler-Nolte, “Bioorganometallic chemistry of ferrocene,” *Chem. Rev.*, vol. 104, no. 12, pp. 5931–5985, Dec. 2004.
- [148] C. S. Allardyce, A. Dorcier, C. Scolaro, and P. J. Dyson, “Development of organometallic (organo-transition metal) pharmaceuticals,” *Appl. Organomet. Chem.*, vol. 19, no. 1, pp. 1–10, Jan. 2005.
- [149] E. W. Neuse, “Macromolecular Ferrocene Compounds as Cancer Drug Models,” *J. Inorg. Organomet. Polym. Mater.*, vol. 15, no. 1, pp. 3–31, Mar. 2005.
- [150] M. F. R. Fouda, M. M. Abd-Elzaher, R. A. Abdelsamaia, and A. A. Labib, “On the medicinal chemistry of ferrocene,” *Appl. Organomet. Chem.*, vol. 21, no. 8, pp. 613–625, Aug. 2007.
- [151] A. Nguyen, A. Vessières, E. A. Hillard, S. Top, P. Pigeon, and G. Jaouen, “Ferrocifens and Ferrocifenols as New Potential Weapons against Breast Cancer,” *Chim. Int. J. Chem.*, vol. 61, no. 11, pp. 716–724, Nov. 2007.
- [152] L. Delhaes, C. Biot, L. Berry, L. Maciejewski, D. Camus, J. Brocard, and D. Dive, “Novel ferrocenic artemisinin derivatives: synthesis, in vitro antimalarial activity and affinity of binding with ferroprotoporphyrin IX,” *Bioorg. Med. Chem.*, vol. 8, no. 12, pp. 2739–2745, Dec. 2000.
- [153] S. Paitayatat, B. Tarnchompoo, Y. Thebtaranonth, and Y. Yuthavong, “Correlation of

- antimalarial activity of artemisinin derivatives with binding affinity with ferroprotoporphyrin IX.," *J. Med. Chem.*, vol. 40, no. 5, pp. 633–638, Feb. 1997.
- [154] A. Baramée, A. Coppin, M. Mortuaire, L. Pelinski, S. Tomavo, and J. Brocard, "Synthesis and in vitro activities of ferrocenic aminohydroxynaphthoquinones against *Toxoplasma gondii* and *Plasmodium falciparum*," *Bioorg. Med. Chem.*, vol. 14, no. 5, pp. 1294–1302, Mar. 2006.
- [155] C. Biot, L. Delhaes, L. A. Maciejewski, M. Mortuaire, D. Camus, D. Dive, and J. S. Brocard, "Synthetic ferrocenic mefloquine and quinine analogues as potential antimalarial agents," *Eur. J. Med. Chem.*, vol. 35, no. 7–8, pp. 707–714, Aug. 2000.
- [156] C. Biot, G. Glorian, L. A. Maciejewski, and J. S. Brocard, "Synthesis and antimalarial activity in vitro and in vivo of a new ferrocene-chloroquine analogue," *J. Med. Chem.*, vol. 40, no. 23, pp. 3715–3718, Nov. 1997.
- [157] M. Henry, S. Briolant, A. Fontaine, J. Mosnier, E. Baret, R. Amalvict, T. Fusaï, L. Fraisse, C. Rogier, and B. Pradines, "In vitro activity of ferroquine is independent of polymorphisms in transport protein genes implicated in quinoline resistance in *Plasmodium falciparum*," *Antimicrob. Agents Chemother.*, vol. 52, no. 8, pp. 2755–2759, Aug. 2008.
- [158] C. Biot, F. Nosten, L. Fraisse, D. Ter-Minassian, J. Khalife, and D. Dive, "The antimalarial ferroquine: from bench to clinic," *Parasite*, vol. 18, no. 3, pp. 207–214, 2011.
- [159] C. Biot, W. Daher, C. M. Ndiaye, P. Melnyk, B. Pradines, N. Chavain, A. Pellet, L. Fraisse, L. Pelinski, C. Jarry, J. Brocard, J. Khalife, I. Forfar-Bares, and D. Dive,

- “Probing the role of the covalent linkage of ferrocene into a chloroquine template,” *J. Med. Chem.*, vol. 49, no. 15, pp. 4707–4714, 2006.
- [160] O. Domarle, G. Blampain, H. Agnani, T. Nzadiyabi, J. Lebibi, J. Brocard, L. Maciejewski, C. Biot, A. J. Georges, and P. Millet, “In Vitro Antimalarial Activity of a New Organometallic Analog, Ferrocene-Chloroquine,” *Antimicrob. Agents Chemother.*, vol. 42, no. 3, pp. 540–544, Mar. 1998.
- [161] C. Biot, W. Daher, C. M. Ndiaye, P. Melnyk, B. Pradines, N. Chavain, A. Pellet, L. Fraisse, L. Pelinski, C. Jarry, J. Brocard, J. Khalife, I. Forfar-Bares, and D. Dive, “Probing the role of the covalent linkage of ferrocene into a chloroquine template,” *J. Med. Chem.*, vol. 49, no. 15, pp. 4707–4714, Jul. 2006.
- [162] C. Biot, L. Delhaes, C. M. N’Diaye, L. A. Maciejewski, D. Camus, D. Dive, and J. S. Brocard, “Synthesis and antimalarial activity in vitro of potential metabolites of ferrochloroquine and related compounds,” *Bioorg. Med. Chem.*, vol. 7, no. 12, pp. 2843–2847, Dec. 1999.
- [163] C. Biot, W. Daher, N. Chavain, T. Fandeur, J. Khalife, D. Dive, and E. De Clercq, “Design and Synthesis of Hydroxyferroquine Derivatives with Antimalarial and Antiviral Activities,” *J. Med. Chem.*, vol. 49, no. 9, pp. 2845–2849, May 2006.
- [164] C. Biot, L. Delhaes, H. Abessolo, O. Domarle, L. . Maciejewski, M. Mortuaire, P. Delcourt, P. Deloron, D. Camus, D. Dive, and J. . Brocard, “Novel metallocenic compounds as antimalarial agents. Study of the position of ferrocene in chloroquine,” *J. Organomet. Chem.*, vol. 589, no. 1, pp. 59–65, Oct. 1999.

2.1 Introduction

Pyrazole compounds and derivatives (Figure 2.1) have attracted considerable attention from medicinal chemists recently. The ease of synthesis of many differently substituted pyrazoles, permitting the tuning of their steric and metal complexes, is an important reason for the popularity of this structural motif. Pyrazoles have relatively poor π -acceptor abilities but are good π -donors. Their donor properties may be characterized as “hard” which affect the electronic properties of metal complexes accordingly [1]. This class of compounds has been investigated for a range of biological activities, such as anti-inflammatory [2,3], antimicrobial [4-6], antiviral [7] and antitumor activity [8,9].

There has been a great need to synthesize compounds (organic and inorganic) based on the classical (artemisinin and its derivatives) and the non-classical (4-aminoquinolines e.g. chloroquine, primaquine) antimalarial agents that can restore activity and offer different modes. Glans *et. al.* [10] and recently Ekengard *et. al.* [11,12] have reported the bidentate 7-chloroamino-quinoline containing ligands with salicylaldimine, amino pyridyl, and amino imidazole moieties as the chelating binding site, and ruthenium and osmium complexes of these ligands.

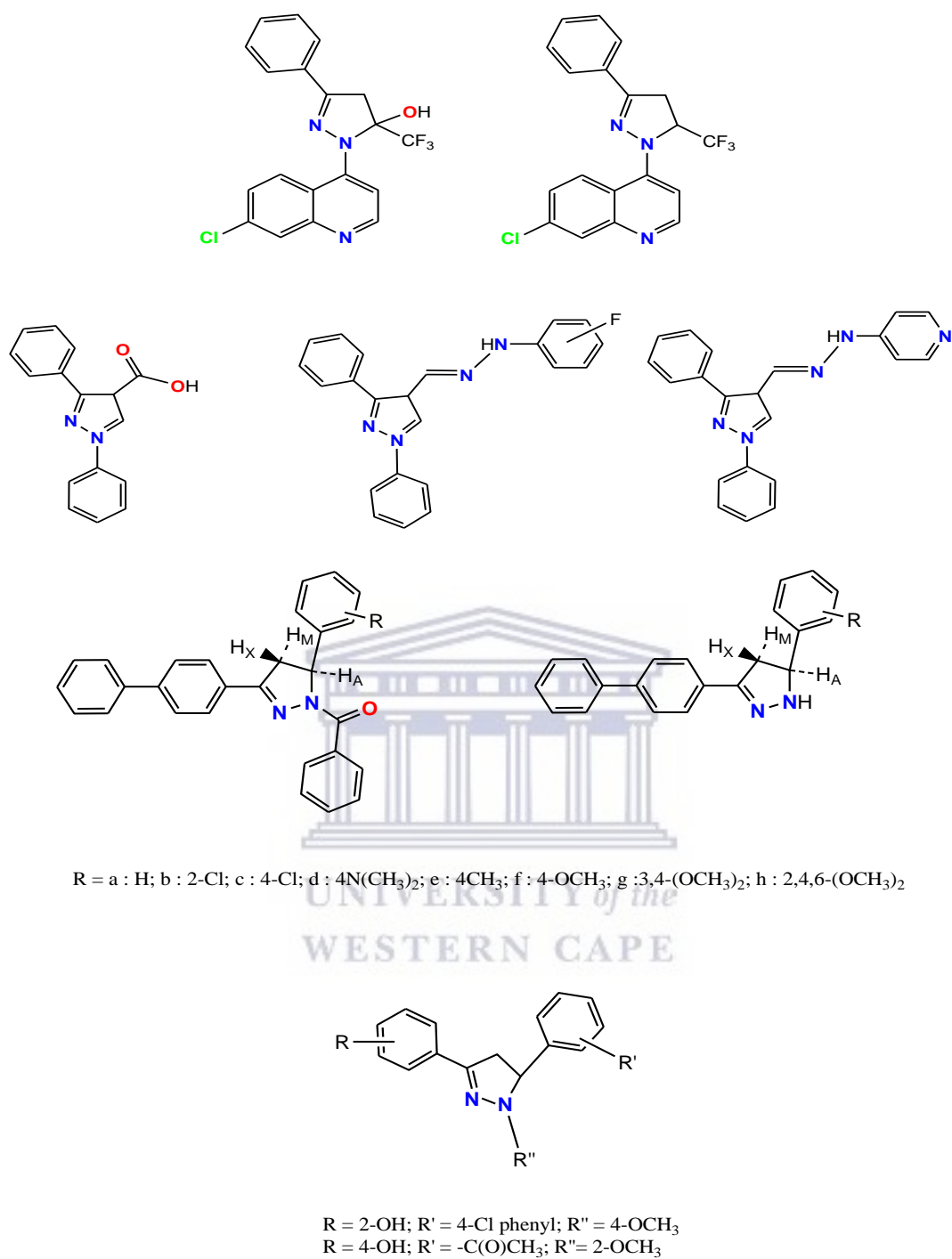


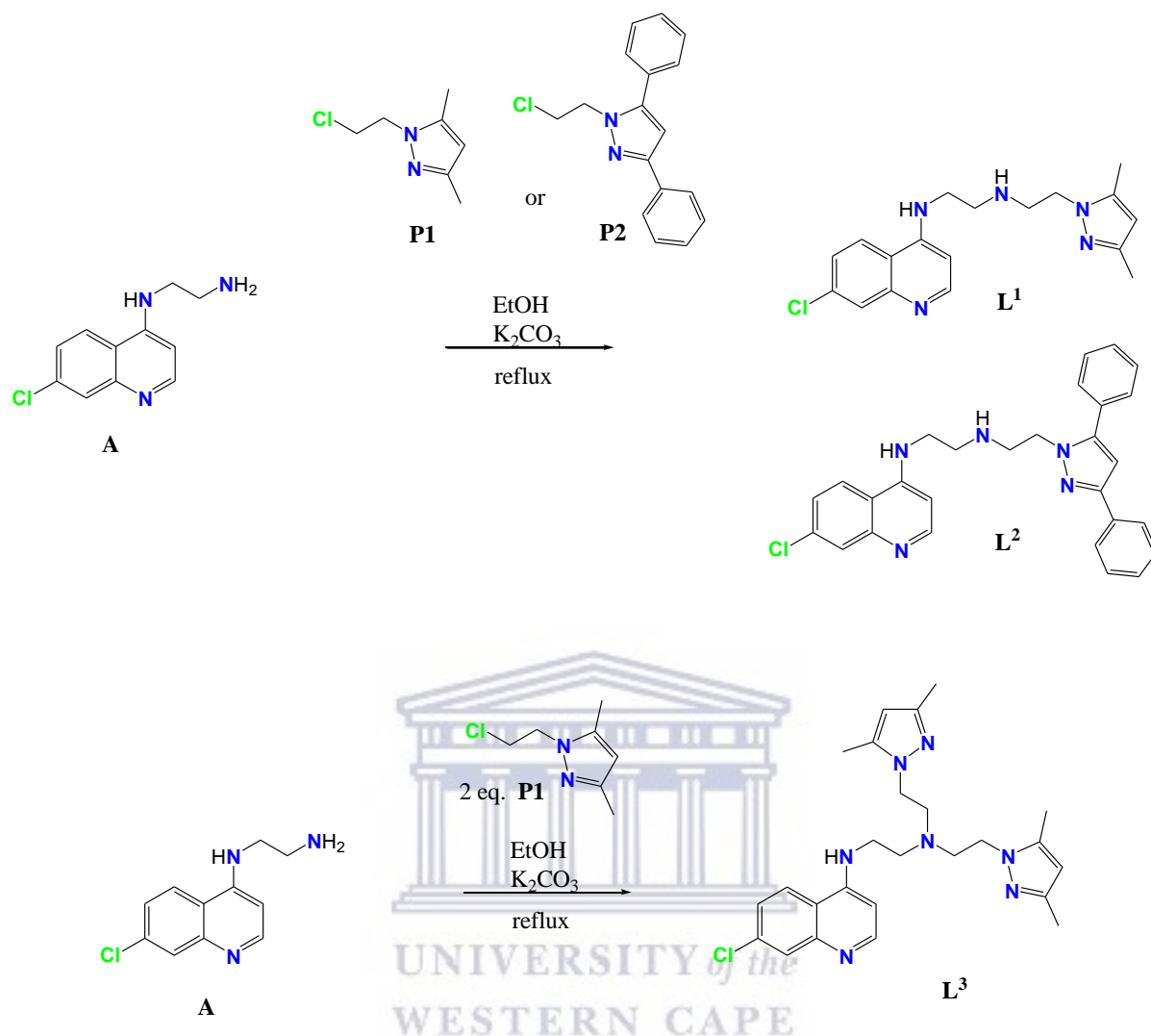
Figure 2.1: Selected pyrazole derivatives evaluated for their pharmacological activity, chemical structures reported from references [13-21].

In this study, we set out to expand the scope of this family of metal-containing chloroquine derivatives by designing a set of ligands with pyrazole-containing side chains which may coordinate to suitable transition metals. Here, we report the syntheses and characterization of *N*-(2-(2-(3,5-dimethyl-1*H*-pyrazol-1-yl)ethylamino)ethyl)-7-chloroquinolin-4-amine (**L**¹), *N*-(2-(2-(3,5-diphenyl-1*H*-pyrazol-1-yl)ethylamino)ethyl)-7-chloroquinolin-4-amine (**L**²) and *N*-(2-(bis(2-(3,5-dimethyl-1*H*-pyrazol-1-yl)ethyl)amino)ethyl)-7-chloroquinolin-4-amine (**L**³) as well as the metal complexes [(**L**¹)*Rh*(Cp*)Cl], **C1**, [(**L**¹)*Ir*(Cp*)Cl], **C2**, [(**L**¹)*Pd*Cl₂], **C3**, [(**L**²)*Pt*Cl₂], **C4**, and the cyclometallated complexes [(**L**²-**H**)*Pt*Cl], **C5**, and [(**L**²-**H**)*Pd*Cl], **C6**.

2.2 Results and Discussion

2.2.1 Synthesis and Characterization of *CQ*-analogues, **L**¹-**L**³

The ligands **L**¹ and **L**², bearing a sterically different pendant pyrazole arm, and ligand **L**³, that is structurally similar to **L**¹ except that **L**³ is endowed with two sterically similar pendant pyrazole arms, were synthesized by reaction of the appropriate chloro-alkyl pyrazole (**P1** and **P2**) with the primary amine *N*-(7-chloroquinolin-4-yl)ethane-1,2-diamine (**A**). The general synthesis of the new 4-aminoquinoline derivative is shown Scheme 2.1. The ligands were isolated in good yields as light-brown solids.



Scheme 2.1: Synthesis of ligand L^1 , L^2 and L^3 .

2.2.1.1 Infrared Spectroscopy

Infrared spectroscopy was used to investigate the stretching frequencies of the key functional group that are informative and indicative of a successful elimination reaction between the chloro-alkyls and the primary amine. Potassium bromide (KBr) pellet was thus used to record the stretching frequencies of the ligands L^1 - L^3 . Formation of the new secondary amine (NH) bonds for the ligands L^1 - L^3 was confirmed by the appearance of the stretching frequencies in

the region $3230 - 3262 \text{ cm}^{-1}$ attributed to the successful amination reaction. The 4-amino, NH moiety, stretching frequencies were observed in the region $3259-3253 \text{ cm}^{-1}$ and the stretching frequencies characteristic to the $C=N$ quinoline moiety were observed within the range $1616-1649 \text{ cm}^{-1}$, respectively. Infrared spectroscopic data for the ligands is summarized in Table 2.1. The observed stretching frequencies were within reported limits for similar ligands, confirming the success of the amination reactions [11,12,22].

Table 2.1: Selected Infrared spectroscopy (KBr) data for ligands, L^1-L^3 .

Ligands	Stretching frequencies (cm^{-1})		
	$\nu (N-H)_{4\text{-amino}}$	$\nu (N-H)$	$\nu (7-CQ)$
L^1	3253	3230	$1616m^a, 1581s^a, 1550m^a$
L^2	3255	3259	$1615s^a, 1582s, 1549m^a$
L^3	3259	-	$1616m^a, 1578s^a, 1550m^a$

^a: m = medium; s = strong; w = weak

2.2.1.2 1H and $^{13}C \{^1H\}$ NMR Spectroscopy

The 1H NMR spectra of all the ligands L^1-L^3 (Figure 2.2, with an insert showing 1H and $^{13}C \{^1H\}$ NMR numbering scheme) were recorded using CD_3OD . Analysis of the 1H NMR spectra of the ligands L^1-L^3 confirmed that the proposed compounds were obtained and were all in agreement with all the proposed structural formulations.

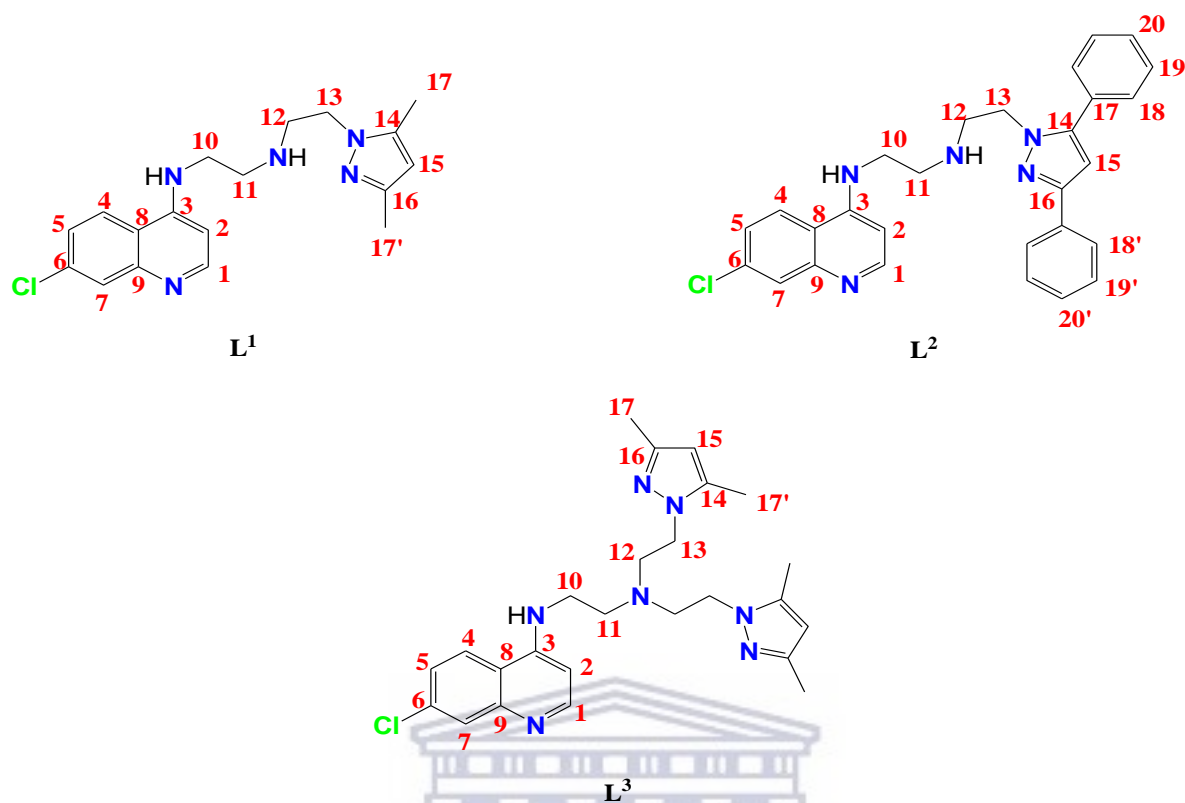


Figure 2.2: Chloroquine analogue ligands L^1 - L^3 , with insert for 1H and ^{13}C NMR numbering system.

The integration of all the proton resonances in the spectrum of L^1 was consistent with the mono-alkylated chloroquine analogue when compared with the L^3 , with two parallel alkylated pyrazole arms (Figure 2.2). Similar results were observed with bis-alkylated chloroquine analogues derived from 2-pyridinecarboxaldehyde [10]. The spectrum of L^1 (Figure 2.3) and L^3 (Figure 2.4) showed two distinct singlets resonating close to each other that are attributed to the $-CH_3$ substituents at position C-14 and C-16 of the pyrazole. Alkylating the parent pyrazole removes the tautomeric nature of the pyrazole, in relation to the equivalence of position C-14 and C-16 of the pyrazole, resulting in resonances observed at 2.16 ppm (H -17) and 2.27 ppm (H -17'), respectively. The resonances, for both the ethyl linkers, appeared at 2.97 (H -11), 3.44 (H -12), 3.85 (H -10), 4.27 (H -13) ppm, respectively. Successful synthesis of L^2 was confirmed by the appearance of additional multiplet in the

region 7.28 – 7.53 ppm, ascribed by the presence of the phenyl rings on position C-14 and C-16 of the heterocyclic pendant arm [23]. Further confirmation of the ligands was done using $^{13}C\{^1H\}$, 2-dimensional homo COSY, 2-dimensional heteronuclear HSQC and HMBC NMR.

The two dimensional heteronuclear $\{^1H-^{13}C\}$ -HSQC and HMBC experiments helped to unambiguously assign 1H and ^{13}C nuclei chemical shifts that arose from the presence of an extra aromatic system in the pyrazole moiety for ligand L^2 . The $\{^1H-^{13}C\}$ -HMBC spectra of L^2 exhibited cross-peaks that were assigned to the coupling of $H-18$, $H-19$ and $H-20$ and further confirmed the existence of quaternary $C-14$, $C-16$ and $C-17$ carbon atoms. The doublet observed for $H-18$ showed two interactions with 2 ($C-17$) and three ($C-16$) bond distance quaternary carbons.

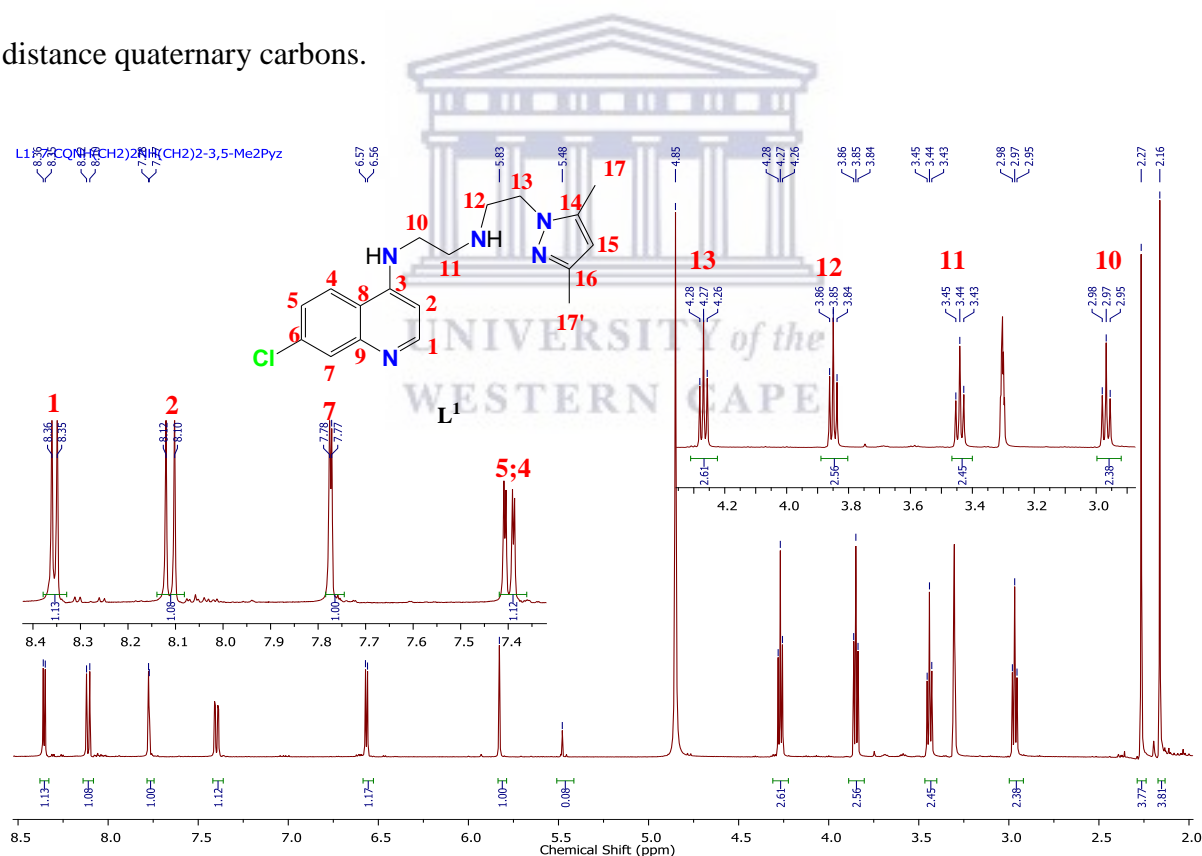


Figure 2.3: 1H NMR spectrum of ligand L^1 , with numbering inserts

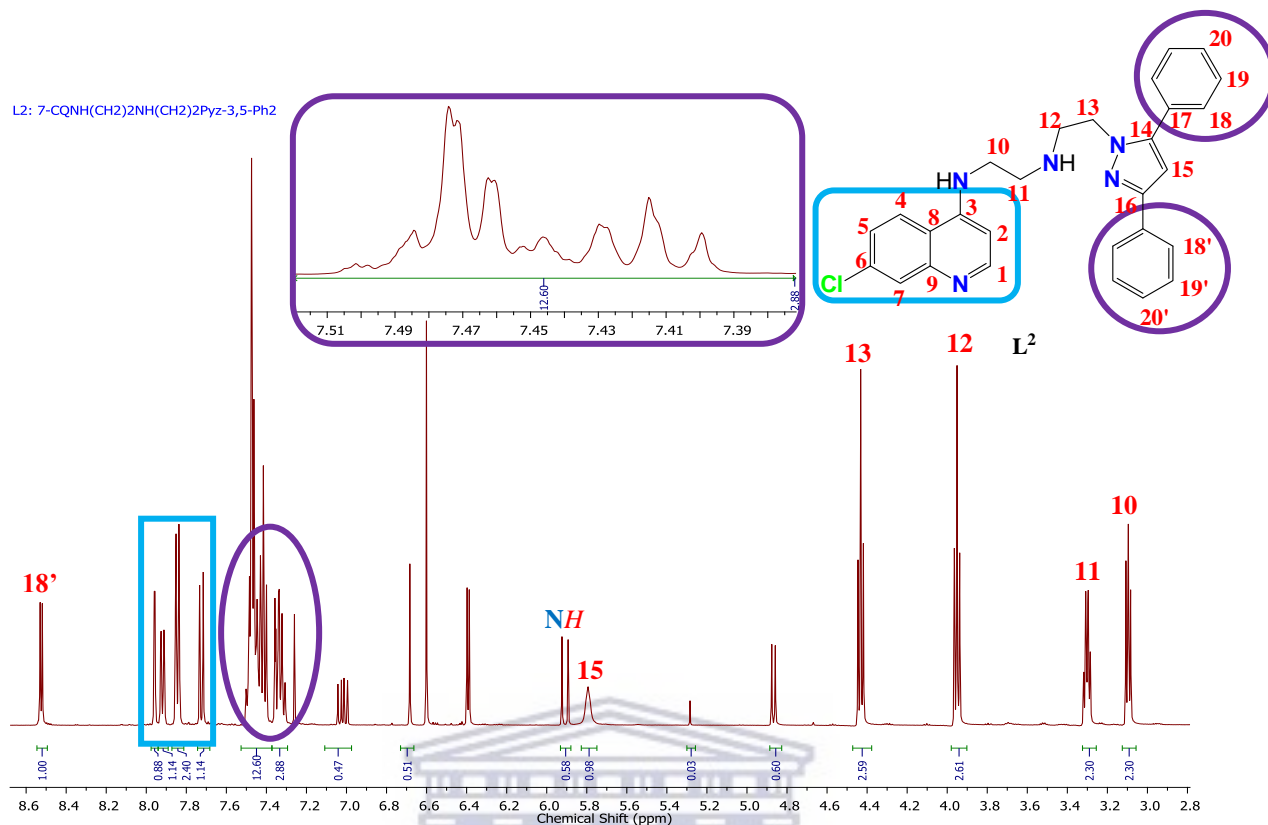


Figure 2.4: ^1H NMR spectrum of ligand L^2 , with numbering inserts.

UNIVERSITY of the
WESTERN CAPE

2.2.1.3 Mass Spectroscopy

The parent molecular peaks for all the ligands were confirmed using Electron Spray Ionization Mass Spectrometry (ESI-MS)⁺ in the positive mode. The data obtained was in agreement with the proposed structural formulations. The ESI-MS molecular ion, $\{[M] + H\}^+$, for all the ligands was observed to be protonated analogues of the free ligands [11, 12, 22]. Summary of the ESI-MS data is given in Table 2.2. The microanalysis data for the ligands was also within accepted limits for the synthesized ligands further confirming the successful synthesis of the targeted ligands.

Table 2.2: ESI-MS data for the title ligands **L¹**-**L³**.

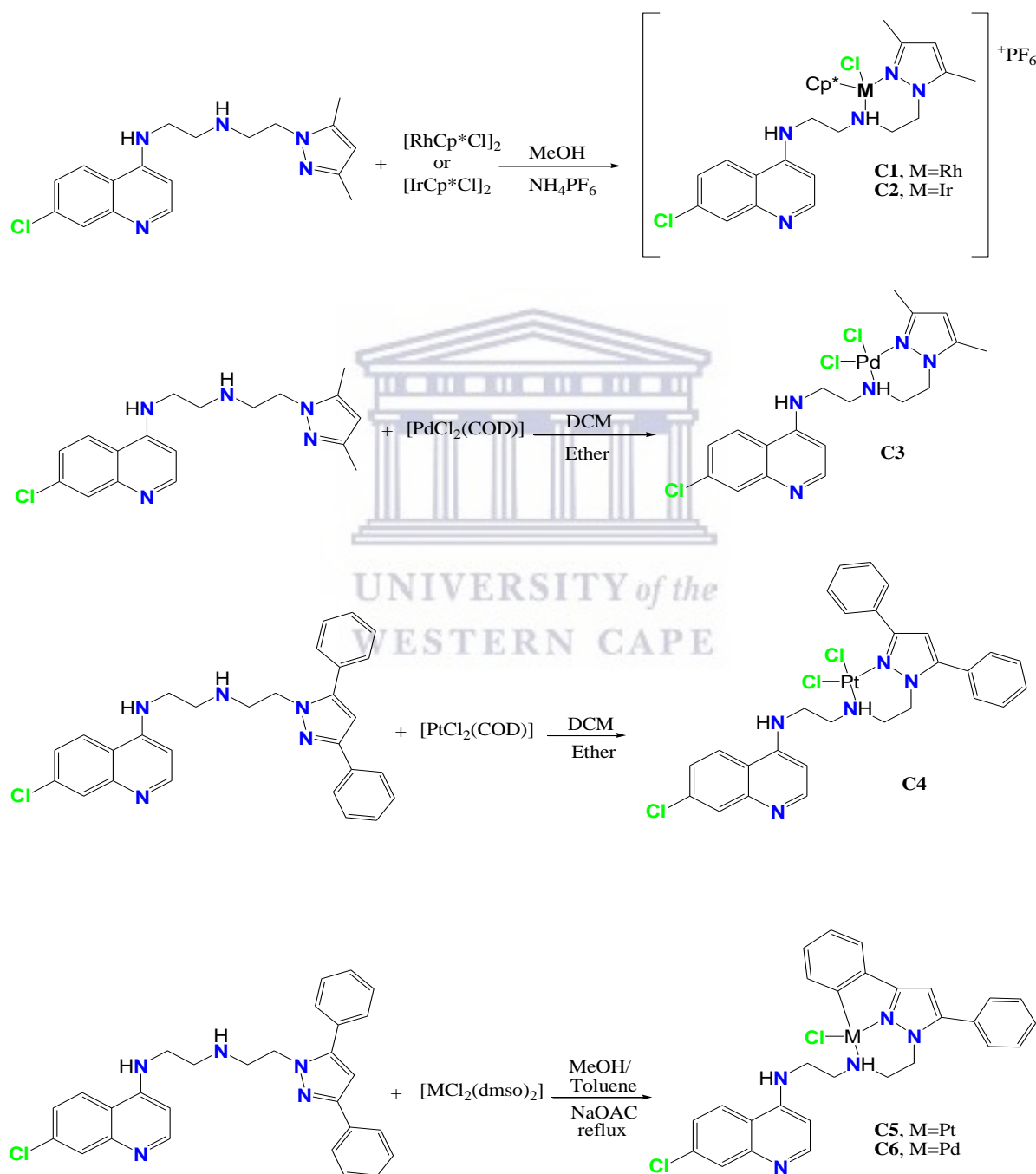
Ligand	Molecular Formula	MS ^a (assignment, fragment) [<i>m/z</i>]
L¹	C ₁₈ H ₂₂ ClN ₅	{[M] + H} ⁺ 343.16
L²	C ₂₅ H ₃₂ ClN ₇	{[M] + H} ⁺ 465.25
L³	C ₂₈ H ₂₇ ClN ₅	{[M] + H} ⁺ 468.19

^a = Electron Spray Ionization Mass Spectroscopy.

2.2.2 Synthesis and Characterization of metal complexes, **C1-C6**.

The half-sandwich complexes [(**L¹**)Rh(Cp*)Cl] (**C1**) and [(**L¹**)Ir(Cp*)Cl] (**C2**) were synthesized by reacting **L¹** with [Rh(Cp*)Cl₂]₂ and [Ir(Cp*)Cl₂]₂, respectively, in methanol at room temperature in the presence of one equivalent of NH₄PF₆. The palladium complex [(**L¹**)PdCl₂] (**C3**) was obtained from reacting **L¹** with [PdCl₂(COD)] in a mixture of dichloromethane and diethyl ether in the absence of base. The platinum complex [(**L²**)PtCl₂] (**C4**) was synthesized from **L²** and PtCl₂(COD) following the same reaction conditions as for the synthesis of [(**L¹**)PdCl₂] (**C3**). The cyclometallated platinum complex [(**L²**-H)PtCl] (**C5**) was the product of the reaction between **L²** and [PtCl₂(DMSO)₂] in a refluxing mixture of methanol and toluene with the addition of NaOAc as a base. Under the same reaction conditions the palladacycle [(**L²**-H)PdCl] (**C6**) was produced from the reaction between **L²** and [PdCl₂(DMSO)₂], (Scheme 2.2).

The complexes were stable both on exposure to air and in solution – important characteristics for any potential biological usage. Thorough characterization of the complexes was done using various spectroscopic (IR, 1H -, $^{13}C\{^1H\}$ -, COSY- and HSQC-NMR, ESI-MS) techniques in combination with elemental (C, H, N) analysis.



Scheme 2.2: Synthesis of half-sandwich complexes **C1** and **C2**, coordination compounds **C3** and **C4**, and metallacycles **C5** and **C6**.

2.2.2.1 Infrared Spectroscopy

Crucial structural information about the functionalities taking part in the chelation of the synthesized complexes **C1-C6** was elucidated by use of infrared spectroscopy. The bidentate capability of the ligands **L¹** and **L²** was confirmed by the blue-shift that was observed in the *NH* stretching frequency of the free ligand from 3258 cm^{-1} to 3444 cm^{-1} the complexes **C1-C6** as the amine participated in the chelation via the lone pairs of the nitrogen [11,12,22]. There was also an observed blue-shift for the stretching frequencies of the $N_{\text{pyz}}=C$ participating in the metal chelation. A similar behaviour has been reported for similar N,N' -bidentate chelating ligands [23,26]. There were no observable vibrations associated with coordination of the N-atom of the 7-chloroquine's moiety [12,22]. The Infrared spectroscopy results are summarized in Table 2.3.

Table 2.3: Selected FT-IR data for the complexes **C1-C6**.

Ligands	Stretching frequencies (cm^{-1})		
	$\nu (N-H)_{4\text{-amino}}$	$\nu (N-H)$	$\nu (7-CQ)$
C1	3240	3439	1610 ^m ^a , 1580 ^s ^a , 1538 ^m ^a
C2	3241	3435	1609, 1582 ^s ^a , 1541 ^m ^a
C3	3237	3423	1615 ^s ^a , 1581 ^s ^a , 15390 ^m ^a
C4	3239	3438	1613 ^m ^a , 1581 ^s ^a , 1542 ^w ^a
C5	3240	3442	1614 ^m ^a , 1578 ^s ^a , 1530 ^m ^a
C6	3241	3444	1613 ^m ^a , 1579 ^s ^a , 1550 ^m ^a

^a: m = medium; s = strong; w = weak

2.2.2.2 ¹H and ¹³C {¹H} NMR Spectroscopy of chloroquine analogues metal complexes, **C1-C6**

In the ¹H NMR spectra of **C1**, **C2** and **C3**, the only chemical shifts observed were the ones that correspond to the coordination of the ligand **L**¹ to the metal ion via one nitrogen donor of the pyrazole, *N*_{pyz} and the alkyl amine, *N*_{amine}. This was confirmed by the absence of a significant chemical shift of the *H*-1 proton, suggesting coordination only at the chelating site *N*_{amine}, *N*_{pyz} [11,12,22]. Coordination of **L**¹ to the metal centres (Rh(III) = **C1**, Ir(III) = **C1** and Pd(II) = **C3**) resulted in an upfield chemical shift of the protons adjacent to the alkyl amine, *N*_{amine}, for the complexes compared to the free ligand. A diastereotopic splitting for the methylene (CH₂) protons adjacent to the *N*_{amine} was observed for the complexes attributed to the bidentate coordination fashion of the ligand **L**¹, resulting in a stereogenic metal centre. A similar pattern where the chemical shifts of the protons adjacent to the coordinating *NH* moiety experiencing diastereotopic splitting has been reported for *N,N*- and *N,O*-Ru(II), Os(II) Rh(III) and Ir(III) complexes [12,22,27-31]. In the ¹H NMR spectrum of **C4**, no evidence of the *C-H* activation was observed in the absence of the activating base (NaOAc). The presence of a base, especially NaOAc, has been deemed crucial in the isolation of metallacycles as reported in the literature [43]. In the synthesis of the metallacycles **C5** and **C6**, a slight excess of NaOAc was used to ensure successful isolation of the intended metallacycles. The success of the intended metallacycles **C5** and **C6** was confirmed by the downfield chemical shifts in the ¹H NMR spectra of these complexes, attributed to the removal of the electron density on *Pd/Pt-C* bond [32,33], that confirms the presence of σ (M-C) bond and the presence of five-membered ring metallacycles (Figure 2.5 and 2.6). In addition, success of the formation of the *Pd/Pt-C* was confirmed by the disappearance of the *H*-18' chemical shift of the free ligand in the ¹H and the observed low-field shift of *C*-18' in the ¹³C{¹H} NMR

spectra of the cyclometallated complexes **C5** and **C6**. Absence of a cross-peak interaction in the [1H - ^{13}C]-HSQC spectra of cyclometallated compounds **C5** and **C6** between H-18' and C-18', observed in the free ligand, further cemented the successful isolation of the metallacycles. The metallacycles **C5** (Figure 2.5) and **C6** (Figure 2.5) were successfully prepared using the *cis*- $MCl_2(dmsO)_4$ ($M = Pd(\mathbf{C5})$ and $Pt(\mathbf{C6})$) metal (II) precursors as compared to the synthesis of complexes **C4** employing $PtCl_2(COD)$. The choice of using *cis*- $PtCl_2(dmsO)_4$ as the capable electrophilic cyclometallating agent [34-38] was motivated by the ease of synthesis of the *cis*- $Pd/PtCl_2(dmsO)_4$ metal precursors as well as their high stability. The alternative *cis*- $PtCl_2(COD)$ was chosen for synthesis of the *N,N'*- complex **C4** because the *N,N'*- compounds from this platinum source can be isolated as prior steps to the cyclometallating process thus increasing the overall reaction yields. The *N,N'*- coordination compounds synthesized from *cis*- $PtCl_2(COD)$ thus can subsequently be converted to platinacycles in a donor solvent such as methanol, under reflux, in the presence of sodium acetate base (NaOAc) [37,38].

In the $^{13}C\{^1H\}$ NMR spectrum of the complexes, 9 distinct peaks that are characteristic to the aromatic quinoline moiety within the region 151-121 ppm. The methylenic (CH_2) chemical shifts were observed as four signals in the region 68-22 ppm (Figure 2.6).

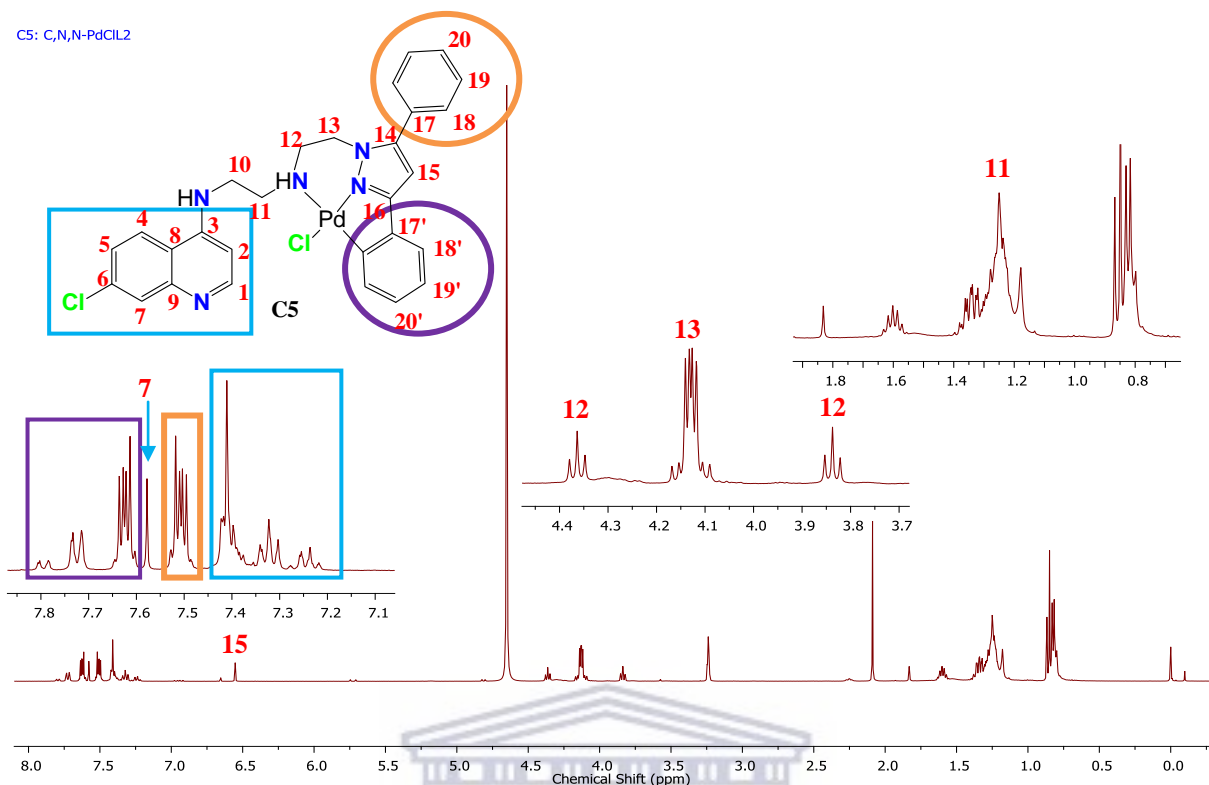


Figure 2.5: 1H NMR spectrum of complex C5, with 1H numbering insert.

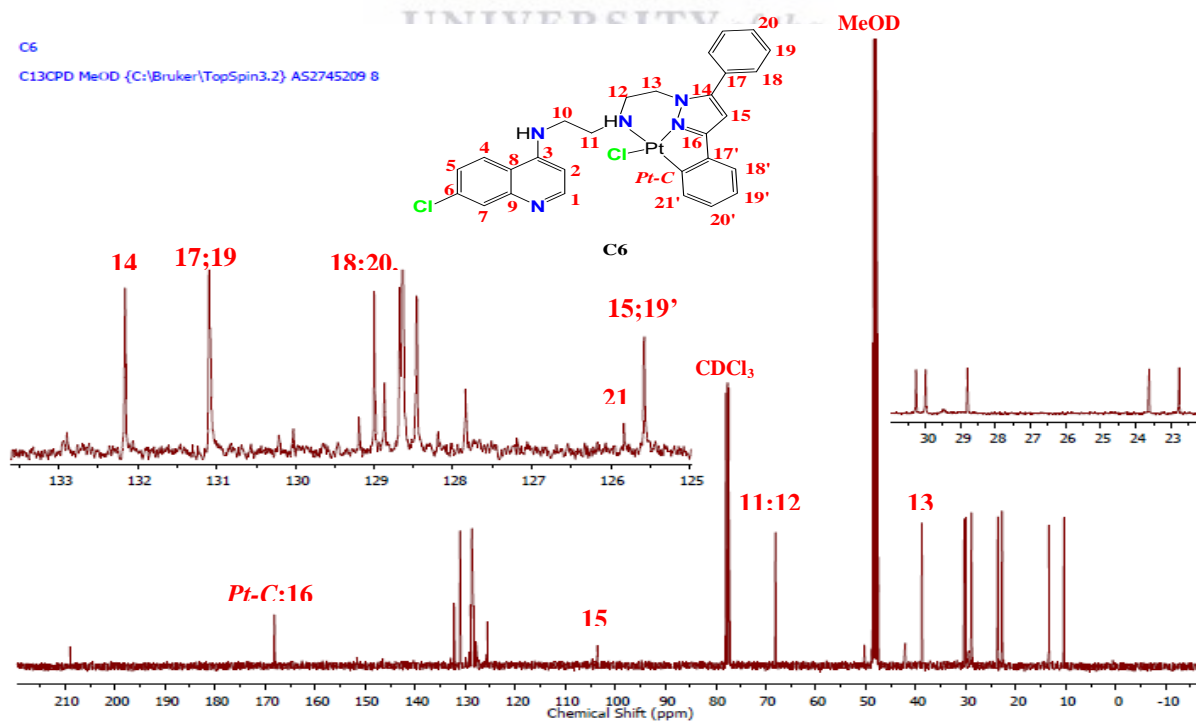


Figure 2.6: $^{13}C\{^1H\}$ NMR spectrum of complex C6, with 1H numbering insert.

Table 2.4: Selected 1H and $^{13}C\{^1H\}$ NMR data for complexes **C1-C6**.

complexes	δ (C=N) _{quin} 1H ($^{13}C\{^1H\}$) ppm	δ (C ¹¹ & C ¹²) 1H ($^{13}C\{^1H\}$) ppm	δ (3,5-di-Me) 1H ($^{13}C\{^1H\}$) ppm	δ (3,5-diPh) 1H ($^{13}C\{^1H\}$) ppm
C1	8.02(151.42)	2.58;2.62 (59.59, 53.12)	2.37;2.45(11.8;14.7)	-
C2	8.11(150.92)	2.53;2.57 (59.59, 53.12)	2.38;2.44(12.4;14.9)	-
C3	8.21(150.78)	2.54;2.59 (53.56;65.21)	2.33;2.40(12.1;15.2)	-
C4	8.12(151.02)	2.55;4.43 (54.45;69.26)	-	
C5	7.98(151.32)	3.83;4.71 (51.22;67.88)	-	-(167)
C6	7.82(151.11)	3.91;4.82 (53.11;69.23)	-	-(169)

2.2.2.3 Elemental Analysis and Mass Spectroscopy of **C1-C6**.

The ESI mass for complex **C1** and **C2** exhibited the most abundant peaks at m/z 617.44 and 706.75, respectively, which are assigned to the the $\{[M] - PF_6\}^+$ fragment ($[M] = Rh$ and Ir) for each complex stabilized as hexafluorophosphate salt. The palladium **C3** and platinum **C4** complexes synthesized from ligand **L¹** and **L²**, respectively, showed the protonated $\{[M] + H\}^+$ ($[M] = Pd$ and Pt) as the abundant peak with m/z values at 521.17 and 733.97, respectively. The metallacycles **C5** and **C6** had m/z values at 473.40 and 660.66, respectively, as the prominent peaks corresponding to the $\{[M]-Cl\}^+$ fragment ($[M] = Pd$ and Pt).

2.3 Summary and Conclusions:

In the present work, three new 4-aminoquinoline-pyrazole ligands have been synthesized and complexes of the generic structures [(L)M(Cp*)] (M=Rh, Ir), [(L)MCl₂] and [(L-H)MCl] (M=Pd, Pt; L=general pyrazole ligand) have been prepared and fully characterized using spectroscopic (IR, ¹H, ¹³C{¹H}), 2-dimensional homo COSY, 2-dimensional heteronuclear HSQC and HMBC NMR and ESI-MS) techniques in combination with elemental (C, H, N) analysis. The prepared ligands **L¹-L³** and corresponding complexes **C1-C6** will be evaluated as antimalarial agents against the chloroquine susceptible strain **NF54**.

2.4 Experimental

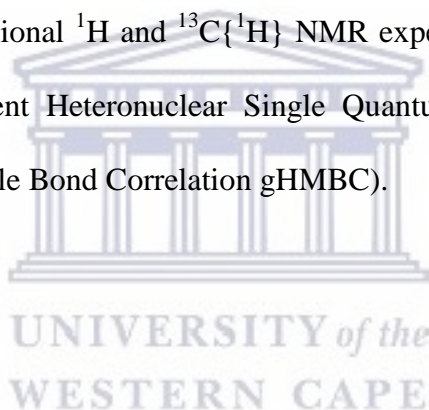
2.4.1 Chemistry

2.4.1.1 Materials and methods

All reactions were carried out under nitrogen atmosphere using a dual vacuum/nitrogen line and standard Schlenk line techniques unless stated otherwise. All commercial chemicals, used herein, were purchased from Sigma Aldrich and used as received. The palladium and platinum metal precursors, MCl₂(COD) and *cis*-[M(II)Cl₂(DMSO)₂] (M = Pd or Pt) [39-41], [M(III)(η⁵-C₁₀H₁₅)(μ-Cl)₂Cl]₂, (M = Rh and Ir) [42] were prepared according to the established protocols reported in the literature. The Solvents were dried and purified by heating at reflux under nitrogen in the presence of a suitable drying agent. Dichloromethane was dried over phosphorus pentoxide while hexane was refluxed and distilled from calcium hydride (CaH). Diethyl ether was dried over sodium wire and benzophenone under nitrogen



while methanol and ethanol were dried by magnesium wire. Reaction progress and product mixtures were monitored by IR spectroscopy. Anhydrous magnesium sulphate (MgSO₄) was used for drying the organic layer of organic:water extraction. NMR spectra were recorded on a Varian Inova 500 MHz (Lund University, Sweden) and Bruker 500 MHz (University of the Western Cape, South Africa) spectrometer using the solvent resonances as an internal standard for ¹H NMR and ¹³C NMR shifts. Infrared spectra were recorded on a Nicolet Avatar 360 FT-IR spectrometer (Lund University, Sweden). ¹H and ¹³C chemical shifts (δ) are reported in ppm. The deuterated solvents used are CDCl₃, CD₃OD-*d*₄ and DMSO-*d*₆ respectively and coupling constants (*J*) are given in Hz. All NMR assignments were made based on one and two dimensional ¹H and ¹³C{¹H} NMR experiments (gradient correlation spectroscopy gCOSY, Gradient Heteronuclear Single Quantum Correlation gHSQC, and gradient Heteronuclear Multiple Bond Correlation gHMBC).



2.5 Synthesis

2.5.1 Synthesis of *N*-(2-(2-(3,5-dimethyl-1*H*-pyrazol-1-yl)ethylamino)ethyl)-7-chloroquinolin-4-amine, **L**¹.

N-(7-chloro-4-quinolinyl)-1,2-diaminoethane **A** (0.200 g, 1.1 mmol) and 1-(2-chloroethyl)-3,5-dimethyl-pyrazole **P1** (0.185 g, 1.0 mmol) were dissolved in ethanol (16 mL) and stirred for two minutes at room temperature. Potassium carbonate (0.215 g, 1.5 mmol) was added and the mixture was refluxed for 19 h at 80 °C. The solvent was removed under reduced pressure before the residue was extracted with dichloromethane and washed with water. The organic phase was dried over sodium sulfate and evaporated under reduced pressure to yield the product as a yellow powdery solid. ¹H NMR (500 MHz, CD₃OD) δ 8.35 (d, *J* = 5.6 Hz,

1H), 8.11 (d, *J* = 9.0 Hz, 1H), 7.77 (t, *J* = 4.3 Hz, 3H), 7.40 (dd, *J* = 9.0, 2.1 Hz, 1H), 6.58 (dd, *J* = 17.8, 5.6 Hz, 2H), 5.83 (s, 1H), 5.48 (s, 1H), 4.85 (s, 1H), 4.27 (t, *J* = 6.0 Hz, 2H), 3.85 (t, *J* = 6.0 Hz, 2H), 3.44 (t, *J* = 6.4 Hz, 2H), 3.30 (dt, *J* = 3.2, 1.6 Hz, 3H), 2.97 (t, *J* = 6.4 Hz, 2H), 2.27 (s, H-10'), 2.16 (s, H-10). ¹³C NMR (101 MHz, CD₃OD) δ 154.5, 151.4, 149.4, 148.2, 140.9, 134.9, 129.4, 127.3, 122.5, 119.7, 113.0, 105.4, 49.9, 48.7, 48.1, 49.0, 18.0, 11.5. MS (ESI) *m/z* calc. for C₁₈H₂₃ClN₅ 344.16420, found 344.16420. MS (ESI⁺) *m/z* calc. for C₁₈H₂₂ClN₅ 343.16, found {[M] + H}⁺ 343.16

2.5.2 Synthesis of *N*-(2-(2-(3,5-diphenyl-1*H*-pyrazol-1-yl)ethylamino)ethyl)-7-chloroquinolin-4-amine, **L²**.

L² was synthesized by the same procedure as **L¹** from *N*-(7-chloro-4-quinolinyl)-1,2-diaminoethane **A** (0.7169 g, 3.23 mmol) and 1-(2-chloroethyl)-3,5-diphenyl-pyrazole **P2** (0.8862 g, 3.13 mmol) to yield the product as a tan solid (80%). ¹H NMR (500 MHz, CD₃OD) δ 8.35 (d, *J* = 5.6 Hz, 3H), 8.11 (d, *J* = 9.0 Hz, 3H), 7.77 (t, *J* = 4.3 Hz, 2H), 7.40 (dd, *J* = 9.0, 2.1 Hz, 2H), 6.58 (dd, *J* = 17.8, 5.6 Hz, 2H), 5.83 (s, 1H), 5.48 (s, 1H), 4.85 (s, 1H), 4.27 (t, *J* = 6.0 Hz, 101H), 3.85 (t, *J* = 6.0 Hz, 97H), 3.44 (t, *J* = 6.4 Hz, 2H), 3.30 (dt, *J* = 3.2, 1.6 Hz, 3H), 2.97 (t, *J* = 6.4 Hz, 3H), 2.27 (s, 10H), 2.16 (s, 10H). ¹³C NMR (101 MHz, CD₃OD) δ 152.18, 151.50, 151.41, 151.02, 148.19, 146.49, 145.07, 135.05, 133.01, 132.64, 130.15, 129.99, 129.51, 129.07, 128.97, 128.91, 128.85, 128.69, 128.58, 128.55, 128.52, 128.43, 128.35, 128.32, 128.03, 127.85, 127.65, 127.52, 126.19, 125.63, 125.38, 125.36, 125.31, 124.76, 122.97, 117.43, 104.46, 103.31, 103.12, 100.90, 99.50, 98.37, 60.55, 51.04, 50.23, 48.27, 48.06, 47.85, 47.63, 47.42, 47.21, 46.99, 44.19, 42.18, 39.18. MS (ESI⁺) *m/z* calc. for C₂₅H₃₂ClN₇ 465.24, found {[M] + H}⁺ 465.25

^{13}C DEPT 135 NMR (101 MHz, CD_3OD) δ 151.02, 130.17, 129.07, 128.98, 128.91, 128.85, 128.69, 128.58, 128.55, 128.52, 128.43, 128.35, 128.32, 128.03, 127.85, 127.65, 127.52, 126.19, 125.63, 125.38, 125.36, 125.31, 124.76, 122.97, 104.46, 103.31, 103.12, 100.90, 99.50, 98.37, 60.55, 51.05, 50.24, 47.92, 44.19, 42.18, 39.18.

2.5.3 Synthesis of *N*-(2-(bis(2-(3,5-dimethyl-1*H*-pyrazol-1-yl)ethyl)amino)ethyl)-7-chloroquinolin-4-amine, **L**³.

L³ was synthesized by the same procedure as **L**¹ except that two equivalents of **P1** was used from *N*-(7-chloro-4-quinoliny)-1,2-diaminoethane **A** (0.200 g, 1.1 mmol) and 2 mol. equiv. of 1-(2-chloroethyl)-3,5-dimethyl-pyrazole **P1** (0.370 g, 2.0 mmol) to yield the product as a orange solid (80%). 1H NMR (500 MHz, CD_3OD) δ 8.35 (d, $J = 5.6$ Hz, 1H), 8.11 (d, $J = 9.0$ Hz, 1H), 7.77 (t, $J = 4.3$ Hz, 4H), 7.40 (dd, $J = 9.0, 2.1$ Hz, 1H), 6.58 (dd, $J = 17.8, 5.6$ Hz, 2H), 5.83 (s, 1H), 5.48 (s, 1H), 4.85 (s, 1H), 4.27 (t, $J = 6.0$ Hz, 2H), 3.85 (t, $J = 6.0$ Hz, 2H), 3.44 (t, $J = 6.4$ Hz, 4H), 3.30 (dt, $J = 3.2, 1.6$ Hz, H), 2.97 (t, $J = 6.4$ Hz, 4H), 2.27 (s, H-10', 6H), 2.16 (s, H-10, 6H). ^{13}C NMR (101 MHz, CD_3OD) δ 154.5, 151.4, 149.4, 148.2, 140.9, 134.9, 129.4, 127.3, 122.5, 119.7, 113.0, 105.4, 49.9, 48.7, 48.1, 49.0, 18.0, 11.5. MS (ESI⁺) m/z calc. for $C_{28}H_{27}ClN_5$ 467.1855, found $\{[M] + H\}^+$ 468.19.

2.5.4. Preparation of (η^5 -Cp*)*N*-(2-(2-(3,5-diphenyl-1*H*-pyrazol-1-yl)ethylamino)ethyl)-7-chloroquinolin-4-amine)chlororhodium/iridium (III) , [*RhClCp*(L*¹)] (C1), and [*IrClCp*(L*¹)] (C2).

A mixture of the appropriate metal dimer (Rh, 89.78 mg, 0.145265 mmol; Ir, 97.42 mg, 0.12229 mmol) and the ligand **L**¹ (99.9 mg, 0.29053 mmol for Rh; 84.1 mg, 0.24458 mmol for Ir) and one equivalent of NH₄PF₆ was stirred in dry MeOH (25 mL) overnight at room temperature. The precipitate formed was filtered, washed with EtOH, Et₂O and dried under reduced pressure. The product was obtained as an orange-solid for Rh (III) and yellow solids for Ir (III).

[*RhClCp*(L*¹)] (C1): ¹H NMR (500 MHz, dms_o-*d*₆) δ 9.20 (s, 1H), 8.56 (d, *J* = 2.0 Hz, 1H), 8.48 (d, *J* = 9.1 Hz, 1H), 8.51 – 8.32 (m, 8H), 8.23 (d, *J* = 8.9 Hz, 1H), 8.09 (d, *J* = 9.2 Hz, 1H), 7.67 (s, 1H), 7.58 (s, 1H), 7.49 – 7.33 (m, 3H), 7.21 (s, 1H), 6.57 (dd, *J* = 11.1, 5.4 Hz, 2H), 5.59 – 5.46 (m, 1H), 5.35 (s, 1H), 4.31 (d, *J* = 19.3 Hz, 3H), 4.04 (s, 7H), 3.52 (t, *J* = 6.2 Hz, 1H), 3.42 (dd, *J* = 13.8, 7.0 Hz, 1H), 3.38 – 3.24 (m, 4H), 3.07 (t, *J* = 6.3 Hz, 1H), 2.52 – 2.45 (m, 4H), 2.32 (d, *J* = 12.1 Hz, 3H), 1.76 – 1.70 (m, 1H), 1.71 – 1.65 (m, 1H), 1.64 – 1.56 (m, 3H), 1.55 – 1.45 (m, 3H), 1.11 – 0.99 (m, 3H). ¹³C NMR (101 MHz, dms_o-*d*₆) δ 179.92, 155.67, 152.42, 147.09, 135.72, 128.58, 126.83, 125.41, 123.23, 118.94, 116.45, 100.39, 95.44, 49.81, 42.28, 39.48, 7.72. MS (ESI⁺) *m/z* calc. for C₂₈H₃₆C L²F₆N₅PRh 762.40, found {[M] - PF₆}⁺ 617.44

[*IrClCp*(L*¹)] (C2): ¹H NMR (500 MHz, dms_o-*d*₆) δ 9.20 (s, 1H), 8.56 (d, *J* = 2.0 Hz, 1H), 8.48 (d, *J* = 9.1 Hz, 1H), 8.51 – 8.32 (m, 8H), 8.23 (d, *J* = 8.9 Hz, 1H), 8.09 (d, *J* = 9.2 Hz, 1H), 7.67 (s, 1H), 7.58 (s, 1H), 7.49 – 7.33 (m, 3H), 7.21 (s, 1H), 6.57 (dd, *J* = 11.1, 5.4 Hz, 2H), 5.59 – 5.46 (m, 1H), 5.35 (s, 1H), 4.31 (d, *J* = 19.3 Hz, 23H), 4.04 (s, 1H), 3.52 (t, *J* = 6.2 Hz, 1H), 3.42 (dd, *J* = 13.8, 7.0 Hz, 1H), 3.38 – 3.24 (m, 4H), 3.07 (t, *J* = 6.3 Hz, 1H),

2.52 – 2.45 (m, 4H), 2.32 (d, $J = 12.1$ Hz, 3H), 1.76 – 1.70 (m, 1H), 1.71 – 1.65 (m, 1H), 1.64 – 1.56 (m, 3H), 1.55 – 1.45 (m, 15H), 1.11 – 0.99 (m, 3H). ^{13}C NMR (101 MHz, $\text{dms}\text{-}d_6$) δ 179.94, 167.13, 155.00, 152.42, 147.10, 136.09, 128.56, 126.83, 125.41, 123.23, 118.93, 100.42, 95.06, 61.17, 50.18, 42.28, 39.78, 11.63, 8.09, 7.34. MS (ESI⁺) m/z calc. for $\text{C}_{28}\text{H}_{36}\text{C}$ $\text{L}^2\text{F}_6\text{N}_5\text{PIr}$ 851.71, found $\{[\text{M}] - \text{PF}_6\}^+$ 706.75.

$[\text{IrClCp}^*(\text{L}^1)]$ (C2), stability test: after 24 hours in DMSO stock solution.

^1H NMR (500 MHz, $\text{dms}\text{-}d_6$) δ 9.20 (s, 1H), 8.56 (s, 1H), 8.49 – 8.39 (m, 17H), 8.34 (t, $J = 9.7$ Hz, 10H), 8.08 (d, $J = 9.4$ Hz, 2H), 7.78 (d, $J = 5.7$ Hz, 12H), 7.64 (s, 7H), 7.54 (s, 1H), 7.44 (dd, $J = 19.1, 9.1$ Hz, 23H), 7.22 (s, 3H), 7.10 – 7.07 (m, 1H), 3.51 (t, $J = 5.9$ Hz, 2H), 3.07 (t, $J = 6.1$ Hz, 2H), 2.98 (s, 9H), 2.42 – 2.28 (m, 7H), 1.65 – 1.56 (m, 15H), 1.51 (d, $J = 12.9$ Hz, 3H).

2.5.5 Preparation of (*N*-(2-(2-(3,5-diphenyl-1*H*-pyrazol-1-yl)ethylamino)ethyl)-7-chloroquinolin-4-amine)dichloropalladium/platinum (II), $[\text{PdCl}_2(\text{L}^1)]$, (C3), and $[\text{PtCl}_2(\text{L}^2)]$, (C4).

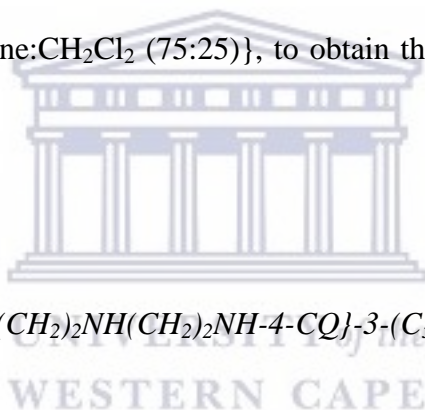
To a suspension of *cis*- $[\text{Pt/PdCl}_2(\text{COD})]$ (65.6 mg, 0.15534 mmol for Pd; 70.1 mg, 0.1658 mmol for Pt) in a DCM solution (10 mL), L^1 (72.7 mg, 0.15534 mmol for Pd) and L^2 0.1658 mmol for Pt) was added to a solvent mixture of MeOH: toluene (25 mL, 1: 12) and the reaction mixture was refluxed for 12 h while being monitored by TLC. When it was deemed complete, the reaction mixture was concentrated to dryness. The precipitate formed was subsequently dissolved in dry DCM and filtered through celite. The resulting filtrate was then evaporated to yield a residue that was purified by column chromatography $\{\text{Al}_2\text{O}_3$, hexane: CH_2Cl_2 (75:25) $\}$, to obtain the respective metal complexes as yellow solids.

[PdCl₂(L¹)] (C3): ¹H NMR (500 MHz, DMSO) δ 10.18 (s, 1H), 8.46 (dd, *J* = 11.4, 6.5 Hz, 2H), 8.31 (s, 1H), 7.84 (s, 1H), 7.65 (s, 1H), 7.53 (s, 1H), 6.80 – 6.56 (m, 3H), 5.66 (d, *J* = 7.6 Hz, 1H), 5.48 (s, 4H), 3.63 (t, *J* = 8.3 Hz, 3H), 3.10 (d, *J* = 5.9 Hz, 4H), 2.48 (s, 1H), 2.28 (s, 1H), 1.97 (s, 1H). ¹³C NMR (101 MHz, CD₃OD) δ 167.43, 131.58, 130.48, 128.59, 128.38, 128.27, 128.13, 128.11, 127.89, 127.34, 125.25, 125.01, 103.07, 67.50, 48.66, 42.99, 39.24, 17.88, 10.77. MS (ESI⁺) *m/z* calc. for C₂₈H₂₆C L³N₃Pd 521.17, found {[M] + H}⁺ 521.17.

[PtCl₂(L²)] (C4): ¹H NMR (500 MHz, pyridine) δ 8.07 (d, *J* = 8.9 Hz, 1H), 7.48 (d, *J* = 5.5 Hz, 1H), 7.44 (d, *J* = 5.3 Hz, 1H), 7.11 (s, 1H), 7.05 (s, 1H), 6.37 (s, 4H), 6.24 (d, *J* = 7.0 Hz, 1H), 6.00 (s, 1H), 5.35 (dt, *J* = 17.0, 8.4 Hz, 1H), 4.65 (s, 1H), 4.51 (s, 1H), 4.48 (s, 1H), 4.36 (s, 3H), 3.18 (s, 1H), 3.05 (t, *J* = 6.0 Hz, 1H), 2.84 – 2.73 (m, 2H), 2.65 – 2.58 (m, 2H), 2.43 (d, *J* = 32.2 Hz, 1H), 2.29 (s, 1H), 2.19 (s, 1H), 2.10 (d, *J* = 6.6 Hz, 1H), 1.93 (d, *J* = 6.7 Hz, 1H), 1.05 (d, *J* = 7.0 Hz, 3H). ¹³C NMR (101 MHz, CD₃OD) δ 167.59, 131.58, 130.48, 128.60, 128.40, 128.29, 128.09, 128.05, 127.87, 127.26, 125.25, 125.01, 103.07, 67.49, 49.72, 41.54, 38.14, 29.74, 29.48, 28.91, 28.27, 28.27, 23.05, 22.17, 12.89, 9.88. MS (ESI⁺) *m/z* calc. for C₂₈H₂₆C L³N₅Pt 733.97, found {[M] + H}⁺ 733.97.

2.5.6 Preparation of cyclometallated Pd (II)(C5) and Pt (II)(C6) complexes

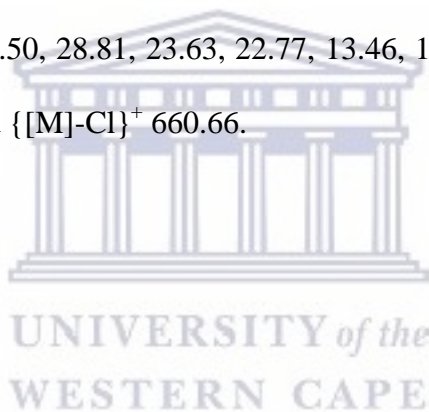
The complexes were synthesized using a modified literature procedure [43]. Briefly, a suspension of cis-[Pt/PdCl₂(DMSO)₂] (65.6 mg, 0.15534 mmol for Pd; 70.1 mg, 0.1658 mmol for Pt) in a DCM solution (10 mL), **L²** (72.7 mg, 0.15534 mmol for Pd; 0.1658 mmol for Pt) was added to a solvent mixture of MeOH: toluene (25 mL, 1:12) and 1 mL solution of NaOAc (16.4 mg, 0.2 mmol) and the reaction mixture was refluxed for 12 h while monitored with TLC. After deemed complete, the reaction mixture was concentrated to dryness. The precipitate formed was subsequently dissolved in dry DCM and filtered through celite. The resulting filtrate was then evaporated to yield a residue that was purified by column chromatography {Al₂O₃, hexane:CH₂Cl₂ (75:25)}, to obtain the respective metal complexes as yellow solids.

2.5.6 [Pd{κ²-*C,N,N'*-[1-(CH₂)₂NH(CH₂)₂NH-4-CQ]-3-(C₅H₄)-5-Ph-pzol]}C(L²)] (C5)

¹H NMR (500 MHz, CDCl₃) δ 7.85 (d, *J* = 7.3 Hz, 1H), 7.77 (d, *J* = 7.4 Hz, 1H), 7.64 (dd, *J* = 5.5, 3.3 Hz, 2H), 7.46 (dd, *J* = 5.6, 3.3 Hz, 2H), 7.41 (t, *J* = 5.3 Hz, 2H), 7.35 (dd, *J* = 14.2, 7.1 Hz, 2H), 7.30 – 7.22 (m, 3H), 6.99 – 6.91 (m, 1H), 6.61 (d, *J* = 7.9 Hz, 1H), 6.53 (s, 1H), 5.23 (s, 2H), 4.79 (t, *J* = 7.5 Hz, 1H), 4.41 – 4.34 (m, 3H), 4.15 (qd, *J* = 10.9, 6.0 Hz, 3H), 3.89 (t, *J* = 6.6 Hz, 3H), 2.10 (s, 1H), 1.40 – 1.32 (m, 4H), 1.26 (dt, *J* = 47.1, 20.5 Hz, 3H), 0.84 (dd, *J* = 13.8, 6.4 Hz, 2H). ¹³C NMR (101 MHz, CD₃OD) δ 167.60, 131.59, 130.49, 128.41, 128.29, 128.10, 128.06, 127.88, 127.27, 125.02, 103.08, 77.32, 77.00, 76.67, 67.50, 49.73, 48.22, 48.01, 47.79, 47.58, 47.37, 47.16, 46.94, 41.55, 38.15, 29.70, 29.46, 28.91, 28.23, 23.06, 22.18, 12.89, 9.89. MS (ESI⁺) *m/z* calc. for C₂₈H₂₅C L²N₅Pd 608.85, found {[M]-Cl}⁺ 573.40.

2.5.7 [*Pt*{ κ^2 -*C,N,N'*-{[1-(*CH*₂)₂*NH*(*CH*₂)₂*NH*-4-*CQ*]-3-(*C*₅*H*₄)-5-*Ph*-*pzol*]})*C*(**L**²)] (**C6**)

¹H NMR (500 MHz, *CDCl*₃) δ 7.85 (d, *J* = 7.3 Hz, 1H), 7.77 (d, *J* = 7.4 Hz, 1H), 7.64 (dd, *J* = 5.5, 3.3 Hz, 2H), 7.46 (dd, *J* = 5.6, 3.3 Hz, 2H), 7.41 (t, *J* = 5.3 Hz, 10H), 7.35 (dd, *J* = 14.2, 7.1 Hz, 2H), 7.30 – 7.22 (m, 3H), 6.99 – 6.91 (m, 1H), 6.61 (d, *J* = 7.9 Hz, 1H), 6.53 (s, 1H), 5.23 (s, 2H), 4.79 (t, *J* = 7.5 Hz, 1H), 4.41 – 4.34 (m, 3H), 4.15 (qd, *J* = 10.9, 6.0 Hz, 3H), 3.89 (t, *J* = 6.6 Hz, 3H), 2.10 (s, 1H), 1.40 – 1.32 (m, 3H), 1.26 (dt, *J* = 47.1, 20.5 Hz, 2H), 0.84 (dd, *J* = 13.8, 6.4 Hz, 48H). ¹³C NMR (101 MHz, *CD*₃*OD*) δ 168.19, 132.16, 131.08, 129.19, 129.00, 128.87, 128.68, 128.64, 128.46, 127.84, 125.83, 125.57, 103.63, 77.93, 77.80, 77.61, 77.29, 68.05, 50.29, 48.77, 48.56, 48.35, 48.13, 47.92, 47.71, 47.50, 42.14, 38.73, 30.28, 30.01, 29.50, 28.81, 23.63, 22.77, 13.46, 10.45. MS (ESI⁺) *m/z* calc. for *C*₂₈*H*₂₅*CL*²*N*₃*Pt* 696.11, found {[*M*]-*Cl*}⁺ 660.66.



2.6 References:

- [1] R. Mukherjee, "Coordination chemistry with pyrazole-based chelating ligands: molecular structural aspects," *Coord. Chem. Rev.*, vol. 203, no. 1, pp. 151–218, 2000.
- [2] A. A. Bekhit and T. Abdel-Aziem, "Design, synthesis and biological evaluation of some pyrazole derivatives as anti-inflammatory-antimicrobial agents.," *Bioorg. Med. Chem.*, vol. 12, no. 8, pp. 1935–45, Apr. 2004.
- [3] J. Milano, M. F. Rossato, S. M. Oliveira, C. Drewes, P. Machado, P. Beck, N. Zanatta, M. A. P. Martins, C. F. Mello, M. A. Rubin, J. Ferreira, and H. G. Bonacorso, "Antinociceptive action of 4-methyl-5-trifluoromethyl-5-hydroxy-4, 5-dihydro-1H-pyrazole methyl ester in models of inflammatory pain in mice.," *Life Sci.*, vol. 83, no. 21–22, pp. 739–46, Nov. 2008.
- [4] B. F. Abdel-Wahab, H. A. Abdel-Aziz, and E. M. Ahmed, "Convenient synthesis and antimicrobial activity of new 3-substituted 5-(benzofuran-2-yl)-pyrazole derivatives.," *Arch. Pharm. (Weinheim)*, vol. 341, no. 11, pp. 734–9, Nov. 2008.
- [5] H. A. Abdel-Aziz, T. S. Saleh, and H. S. A. El-Zahabi, "Facile synthesis and in-vitro antitumor activity of some pyrazolo[3,4-b]pyridines and pyrazolo[1,5-a]pyrimidines linked to a thiazolo[3,2-a]benzimidazole moiety.," *Arch. Pharm. (Weinheim)*, vol. 343, no. 1, pp. 24–30, Jan. 2010.
- [6] B. F. Abdel-Wahab, H. A. Abdel-Aziz, and E. M. Ahmed, "Synthesis and antimicrobial evaluation of 1-(benzofuran-2-yl)-4-nitro-3-arylbutan-1-ones and 3-(benzofuran-2-yl)-4,5-dihydro-5-aryl-1-[4-(aryl)-1,3-thiazol-2-yl]-1H-pyrazoles.," *Eur. J. Med. Chem.*, vol. 44, no. 6, pp. 2632–5, Jun. 2009.

- [7] R. Aggarwal, V. Kumar, P. Tyagi, and S. P. Singh, "Synthesis and antibacterial activity of some new 1-heteroaryl-5-amino-3H/methyl-4-phenylpyrazoles.," *Bioorg. Med. Chem.*, vol. 14, no. 6, pp. 1785–91, Mar. 2006.
- [8] I. Akritopoulou-Zanze, D. H. Albert, P. F. Bousquet, G. A. Cunha, C. M. Harris, M. Moskey, J. Dinges, K. D. Stewart, and T. J. Sowin, "Synthesis and biological evaluation of 5-substituted 1,4-dihydroindeno[1,2-c]pyrazoles as multitargeted receptor tyrosine kinase inhibitors.," *Bioorg. Med. Chem. Lett.*, vol. 17, no. 11, pp. 3136–40, Jun. 2007.
- [9] P. Diana, A. Carbone, P. Barraja, A. Martorana, O. Gia, L. DallaVia, and G. Cirrincione, "3,5-bis(3'-indolyl)pyrazoles, analogues of marine alkaloid nortopsentin: synthesis and antitumor properties.," *Bioorg. Med. Chem. Lett.*, vol. 17, no. 22, pp. 6134–7, Nov. 2007.
- [10] L. Glans, A. Ehnbohm, C. de Kock, A. Martínez, J. Estrada, P. J. Smith, M. Haukka, R. A. Sánchez-Delgado, and E. Nordlander, "Ruthenium(II) arene complexes with chelating chloroquine analogue ligands: synthesis, characterization and in vitro antimalarial activity.," *Dalton Trans.*, vol. 41, no. 9, pp. 2764–73, Mar. 2012.
- [11] E. Ekengard, L. Glans, I. Cassells, T. Fogeron, P. Govender, T. Stringer, P. Chellan, G. C. Lisensky, W. H. Hersh, I. Doverbratt, S. Lidin, C. de Kock, P. J. Smith, G. S. Smith, and E. Nordlander, "Antimalarial activity of ruthenium(II) and osmium(II) arene complexes with mono- and bidentate chloroquine analogue ligands.," *Dalton Trans.*, vol. 44, no. 44, pp. 19314–29, Nov. 2015.
- [12] E. Ekengard, K. Kumar, T. Fogeron, C. de Kock, P. J. Smith, M. Haukka, M. Monari, and E. Nordlander, "Pentamethylcyclopentadienyl-rhodium and iridium complexes

- containing (N[^]N and N[^]O) bound chloroquine analogue ligands: synthesis, characterization and antimalarial properties.,” *Dalton Trans.*, Feb. 2016.
- [13] A. Gürsoy, “Synthesis and preliminary evaluation of new 5-pyrazolinone derivatives as analgesic agents,” *Eur. J. Med. Chem.*, vol. 35, no. 3, pp. 359–364, Mar. 2000.
- [14] M. Amir, H. Kumar, and S. A. Khan, “Synthesis and pharmacological evaluation of pyrazoline derivatives as new anti-inflammatory and analgesic agents.,” *Bioorg. Med. Chem. Lett.*, vol. 18, no. 3, pp. 918–22, Feb. 2008.
- [15] F. Chimenti, B. Bizzarri, F. Manna, A. Bolasco, D. Secci, P. Chimenti, A. Granese, D. Rivanera, D. Lilli, M. M. Scaltrito, and M. I. Brenciaglia, “Synthesis and in vitro selective anti-Helicobacter pylori activity of pyrazoline derivatives.,” *Bioorg. Med. Chem. Lett.*, vol. 15, no. 3, pp. 603–7, Feb. 2005.
- [16] F. Manna, F. Chimenti, A. Bolasco, D. Secci, B. Bizzarri, O. Befani, P. Turini, B. Mondovì, S. Alcaro, and A. Tafi, “Inhibition of amine oxidases activity by 1-acetyl-3,5-diphenyl-4,5-dihydro-(1H)-pyrazole derivatives,” *Bioorg. Med. Chem. Lett.*, vol. 12, no. 24, pp. 3629–3633, Dec. 2002.
- [17] N. P. Pereira, T. M. Monteiro, A. C. Freitas, E. J. Barreiro, and A. L. Miranda, “Synthesis and analgesic properties of new 5-thioaryl pyrazole derivatives.,” *Boll. Chim. Farm.*, vol. 137, no. 3, pp. 82–6, Mar. 1998.
- [18] E.-S. A. M. Badawey and I. M. El-Ashmawey, “Nonsteroidal antiinflammatory agents - Part 1: Antiinflammatory, analgesic and antipyretic activity of some new 1-(pyrimidin-2-yl)-3-pyrazolin-5-ones and 2-(pyrimidin-2-yl)-1,2,4,5,6,7-hexahydro-3H-indazol-3-ones,” *Eur. J. Med. Chem.*, vol. 33, no. 5, pp. 349–361, Jun. 1998.

- [19] S. Kortagere, W. J. Welsh, J. M. Morrissey, T. Daly, I. Ejigiri, P. Sinnis, A. B. Vaidya, and L. W. Bergman, "Structure-based design of novel small-molecule inhibitors of *Plasmodium falciparum*," *J. Chem. Inf. Model.*, vol. 50, no. 5, pp. 840–9, May 2010.
- [20] J. N. Domínguez, J. E. Charris, M. Caparelli, and F. Riggione, "Synthesis and antimalarial activity of substituted pyrazole derivatives," *Arzneimittelforschung.*, vol. 52, no. 6, pp. 482–8, Jan. 2002.
- [21] A. A. Bekhit, A. Hymete, H. Asfaw, and A. E.-D. A. Bekhit, "Synthesis and biological evaluation of some pyrazole derivatives as anti-malarial agents," *Arch. Pharm. (Weinheim).*, vol. 345, no. 2, pp. 147–54, Feb. 2012.
- [22] L. Glans, A. Ehnbohm, C. de Kock, A. Martínez, J. Estrada, P. J. Smith, M. Haukka, R. a. Sánchez-Delgado, and E. Nordlander, "Ruthenium(II) arene complexes with chelating chloroquine analogue ligands: Synthesis, characterization and in vitro antimalarial activity," *Dalt. Trans.*, vol. 41, no. 9, p. 2764, 2012.
- [23] J. Quirante, D. Ruiz, A. Gonzalez, C. López, M. Cascante, R. Cortés, R. Messeguer, C. Calvis, L. Baldomà, A. Pascual, Y. Guérardel, B. Pradines, M. Font-Bardía, T. Calvet, and C. Biot, "Platinum(II) and palladium(II) complexes with (N,N') and (C,N,N') -ligands derived from pyrazole as anticancer and antimalarial agents: synthesis, characterization and in vitro activities," *J. Inorg. Biochem.*, vol. 105, no. 12, pp. 1720–8, Dec. 2011.
- [24] S. Boltina, M. Yankey, I. A. Guzei, L. C. Spencer, S. O. Ojwach, and J. Darkwa, "Novel O^N^N pyrazolyl-imine and imidazolyl-imine pincer palladium complexes as Heck coupling catalysts," *South African J. Chem.*, vol. 65, pp. 75–83.

- [25] T. V. Segapelo, I. a. Guzei, L. C. Spencer, W. E. V Zyl, and J. Darkwa, “(Pyrazolylmethyl)pyridine platinum(II) and gold(III) complexes: Synthesis, structures and evaluation as anticancer agents,” *Inorganica Chim. Acta*, vol. 362, no. 9, pp. 3314–3324, 2009.
- [26] F. K. Keter, S. Kanyanda, S. S. L. Lyantagaye, J. Darkwa, D. J. G. Rees, and M. Meyer, “In vitro evaluation of dichloro-bis(pyrazole)palladium(II) and dichloro-bis(pyrazole)platinum(II) complexes as anticancer agents.,” *Cancer Chemother. Pharmacol.*, vol. 63, no. 1, pp. 127–38, 2008.
- [27] P. Govender, L. C. Sudding, C. M. Clavel, P. J. Dyson, B. Therrien, and G. S. Smith, “The influence of RAPTA moieties on the antiproliferative activity of peripheral-functionalised poly[salicylaldiminato] metallodendrimers,” *Dalt. Trans.*, vol. 42, no. 4, pp. 1267–77, 2013.
- [28] P. Govender, N. C. Antonels, J. Mattsson, A. K. Renfrew, P. J. Dyson, J. R. Moss, B. Therrien, and G. S. Smith, “Anticancer activity of multinuclear arene ruthenium complexes coordinated to dendritic polypyridyl scaffolds,” *J. Organomet. Chem.*, vol. 694, no. 21, pp. 3470–3476, 2009.
- [29] P. Govender, F. Edafe, B. C. E. Makhubela, P. J. Dyson, B. Therrien, and G. S. Smith, “Neutral and cationic osmium(II)-arene metallodendrimers: Synthesis, characterisation and anticancer activity Metallodendrimers Special Issue,” *Inorganica Chim. Acta*, vol. 409, 2014.
- [30] P. Govindaswamy, B. Therrien, G. Süß-Fink, P. Štěpnička, and J. Ludvík, “Mono and dinuclear iridium, rhodium and ruthenium complexes containing chelating carboxylato pyrazine ligands: Synthesis, molecular structure and electrochemistry,” *J. Organomet.*

- Chem.*, vol. 692, no. 8, pp. 1661–1671, 2007.
- [31] T.-T. Thai, B. Therrien, and G. Süß-Fink, “Pentamethylcyclopentadienyl rhodium and iridium complexes containing oxinato ligands,” *Inorg. Chem. Commun.*, vol. 12, no. 8, pp. 806–807, 2009.
- [32] C. López, A. González, C. Moya, R. Bosque, X. Solans, and M. Font-Bardía, “Cyclopalladation of 3-methoxyimino-2-phenyl-3H-indoles,” *J. Organomet. Chem.*, vol. 693, no. 17, pp. 2877–2886, Aug. 2008.
- [33] S. Pérez, C. López, A. Caubet, X. Solans, M. Font-Bardía, M. Gich, and E. Molins, “Versatility in the mode of coordination $\{(N), (N,O)^-, (C,N)^- \text{ or } (C,N,O)2^-\}$ of $[(\eta^5-C_5H_5)Fe\{(\eta^5-C_5H_4)-CHN-(C_6H_4-2OH)\}]$ to palladium(II),” *J. Organomet. Chem.*, vol. 692, no. 12, pp. 2402–2414, May 2007.
- [34] P. R. R. Ranatunge-Bandarage, B. H. Robinson, and J. Simpson, “Ferrocenylamine complexes of platinum(II) including cycloplatinated derivatives,” *Organometallics*, vol. 13, no. 2, pp. 500–510, Feb. 1994.
- [35] Y. J. Wu, L. Ding, H. X. Wang, Y. H. Liu, H. Z. Yuan, and X. A. Mao, “Synthesis, characterization and structure of ferrocenylketimine complexes of platinum(II),” *J. Organomet. Chem.*, vol. 535, no. 1–2, pp. 49–58, May 1997.
- [36] A. D. Ryabov, I. M. Panyashkina, V. A. Polyakov, and A. Fischer, “Access to Central Carbon Chirality through Cycloplatination of 1-(2-Pyridinylthio)propanone by *cis*- $[PtCl_2(S-SOMe(p-tolyl))]$. The Crystal Structure of $(S_s S_c)$ - $[Pt\{py\{SCHC(O)Me\}_2\}Cl(SOMe(p-tolyl))]$,” *Organometallics*, vol. 21, no. 8, pp. 1633–1636, Apr. 2002.

- [37] S. Pérez, C. López, A. Caubet, X. Solans, and M. Font-Bardia, "Synthesis, characterisation and study of the reactivity of the first platinum(II) complex having a $[C(sp^2, ferrocene),N,N']$ - terdentate ligand," *New J. Chem.*, vol. 27, no. 6, p. 975, May 2003.
- [38] M. Crespo, M. Font-Bardia, J. Granell, M. Martínez, and X. Solans, "Cyclometallation on platinum(II) complexes; the role of the solvent and added base donor capability on the reaction mechanisms," *Dalton. Trans.*, no. 19, p. 3763, Sep. 2003.
- [39] J. Wiedermann, K. Mereiter, and K. Kirchner, "Palladium imine and amine complexes derived from 2-thiophenecarboxaldehyde as catalysts for the Suzuki cross-coupling of aryl bromides," *J. Mol. Catal. A Chem.*, vol. 257, no. 1–2, pp. 67–72, Sep. 2006.
- [40] J. H. Price, A. N. Williamson, R. F. Schramm, and B. B. Wayland, "Palladium(II) and platinum(II) alkyl sulfoxide complexes. Examples of sulfur-bonded, mixed sulfur- and oxygen-bonded, and totally oxygen-bonded complexes," *Inorg. Chem.*, vol. 11, no. 6, pp. 1280–1284, Jun. 1972.
- [41] M. M. Szafran, Zvi; Pike, Ronald M.; Singh, "Microscale Inorganic Chemistry: a Comprehensive Laboratory Experience by Szafran, Zvi; Pike, Ronald M; Singh, Mono M - AbeBooks," *Wiley*, 1991. [Online]. Available: <http://www.abebooks.com/book-search/isbn/0471619965/>. [Accessed: 15-Oct-2015].
- [42] P. M. M. and D. M. H. C. White, A. Yates, *Inorganic Syntheses*, vol. 29. Hoboken, NJ, USA: John Wiley & Sons, Inc., 1992.
- [43] J. Quirante, D. Ruiz, A. Gonzalez, C. López, M. Cascante, R. Cortés, R. Messeguer, C. Calvis, L. Baldomà, A. Pascual, Y. Guérardel, B. Pradines, M. Font-Bardía, T. Calvet,

and C. Biot, "Platinum(II) and palladium(II) complexes with (N,N') and (C,N,N') - ligands derived from pyrazole as anticancer and antimalarial agents: Synthesis, characterization and in vitro activities," *J. Inorg. Biochem.*, vol. 105, no. 12, pp. 1720–1728, 2011.



3.1 Introduction

In 1864, Hugo Schiff synthesized a class of flexible ligands that were subsequently named in honor of him [1]. The Schiff base ligands were successfully synthesized from an amine and a carbonyl compound by nucleophilic addition resulting in a hemiaminal functionality that is subsequently dehydrated *in situ* to produce an imine functionality (*vide supra*). These ligands possess an inherent characteristic structure that can be depicted as $RR_1C=NR_2$ ($R = R_1 = R_2 =$ alkyl, aryl, or hydrogen). The difference in the R substituted group separates these ligands into different subgroups of the same class. Aldimines ($R-CH=NR_2$) are a subgroup that have R as an alkyl or aryl and R_1 as a hydrogen atom. Compounds where both substituents ($R = R_1$) are alkyls or aryl groups are referred to as ketimines. Different subgroups of Schiff base ligands are shown in Figure 3.1.

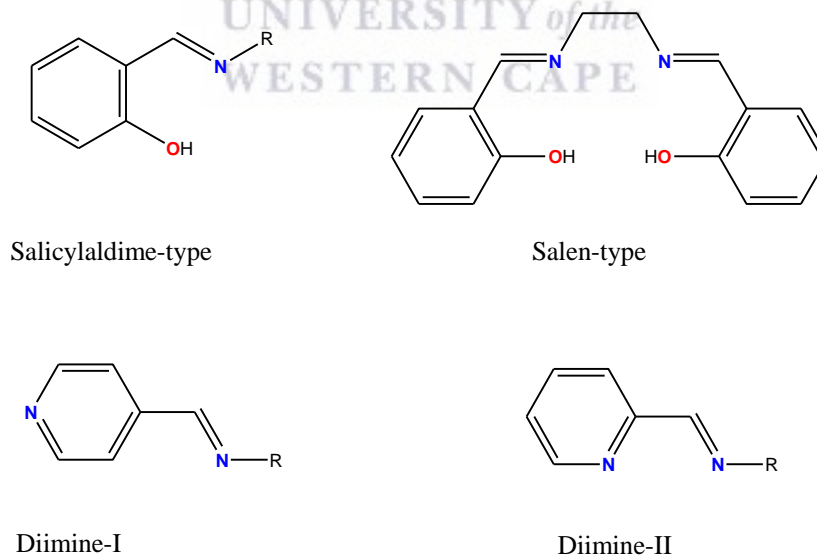


Figure 3.1: Different subclass of Schiff base ligands.

The type of subgroup that is of interest in this study is the salicylaldimine that have two hetero-donor sites that constitute of oxygen and nitrogen for chelation to the transition metals. Metal complexes anchored by Salen-type Schiff base ligands (Figure 3.1) have been extensively studied and employed as catalyst precursors and these include Pd^{II}(Salen), Pt^{II}(Salen), Ru^{II}(Salen), Co^{II}(Salen) and Zn^{II}(Salen) complexes and early metal complexes, Ti^{II}(Salen) and Zr^{II}(Salen), based on a chiral salen ligands just to mention a few that were varied according to the steric demand of the Salen ligand [2,3].

Recently, salicylaldimine/salen-metal complexes have also found a niche as metallomesogens; these include the Ni^{II}L₂, Cu^{II}L₂, VO^{II}L₂ and [La(L)₂(L-H)][NO₃]₂ (L = salicylaldimine ligand and L-H = zwitterions form of the salicylaldimine ligand) [4-6], extensively studied as biomimetic biological model compounds such as [(Mn^{II}(Salen), Cu^{II}(Diimine-II)Im and dinuclear diimine complexes [Cu₂(apy-pol)₂]²⁺, and [Cu₂(sal-pol)₂]²⁺, Im = Imidazole,) [7-9], and as metal complexes that are able to act as antimicrobial agents (Co^{II/III}, Cu^{II}, Ni^{II}, Zn^{II} metal precursors that are based on mercapto- and thiazole-derivative furally, thiophenyl, pyrrolyl, salicylyl, pyridinyl, and nicotinic-acid Schiff-base ligands) [10-14].

Furthermore, structural modifications of Schiff-bases in order to afford tridentate coordinating [N,O,S] ligands have inspired biomimetic studies of metal (Schiff-base) complexes that are capable of modelling the copper-containing enzymes. These biomimetic models include the Cu^I complex that is based on the tridentate (2-pyridylmethyl)imine and (2-pyridylmethyl)amine ligands and the oxo-bridged Cu^I complexes based on N₃S₃ thianisole ligands [(L^{ASM})Cu^I]⁺, [(L^{ESE})Cu^I]⁺, [(L^{EOE})Cu^I]⁺, (L^{ASM} = (2-(methylthio)-N,N-bis((pyridin-2-yl)methyl)benzenamine)), the same annotation reported in the literature for the tridentate ligands and corresponding copper complexes is herein used; L^{ESE} = 2-ethylthio-N,N-

bis((pyridin-2-yl)methyl)ethanamine) and $L^{EOE} =$ (2-ethoxy-*N,N*-bis((pyridin-2-yl)methyl)ethanamine)) [15-18]. Investigation of benzothiazolyl-, bis-thiazolyl and valinyl Schiff-base with Ni^{II}, Cu^{II}, Zn^{II} and Co^{III} metal complexes as candidates to model biological systems has recently been under the spotlight [19-22].

Sulphur containing heterocyclic compounds are playing a major role in the process of synthesizing new pharmaceuticals. One class of compounds lately studied are the heterocyclic thiophene compounds that have been shown to be effective pharmacological agents that possess biological activities such as anti-inflammatory, antifungal and antimicrobial. Another class of aromatic heterocyclic compounds that have recently received attention as pharmacological agents is the benzothiophene and its derivatives. Benzothiophene and related derivatives have been shown to be potent antibacterial, antifungal and anti-inflammatory agents [23-25]. Thiophene containing heterocyclics based on a polymer scaffold have also found a niche as chemical sensors [26-28], optoelectronic devices that are based on organic alkyl-substituted oligothiophenes and fused thiophenes that are employed as thin film transistors [29-30], novel drug candidates [31] and bio-diagnostics devices that are either based on an electrostatic polythiophene transducer and a fluorescent amino acid probe for DNA tagging or a fluorescent signal amplifier in order to detect nucleic acids [32,33].

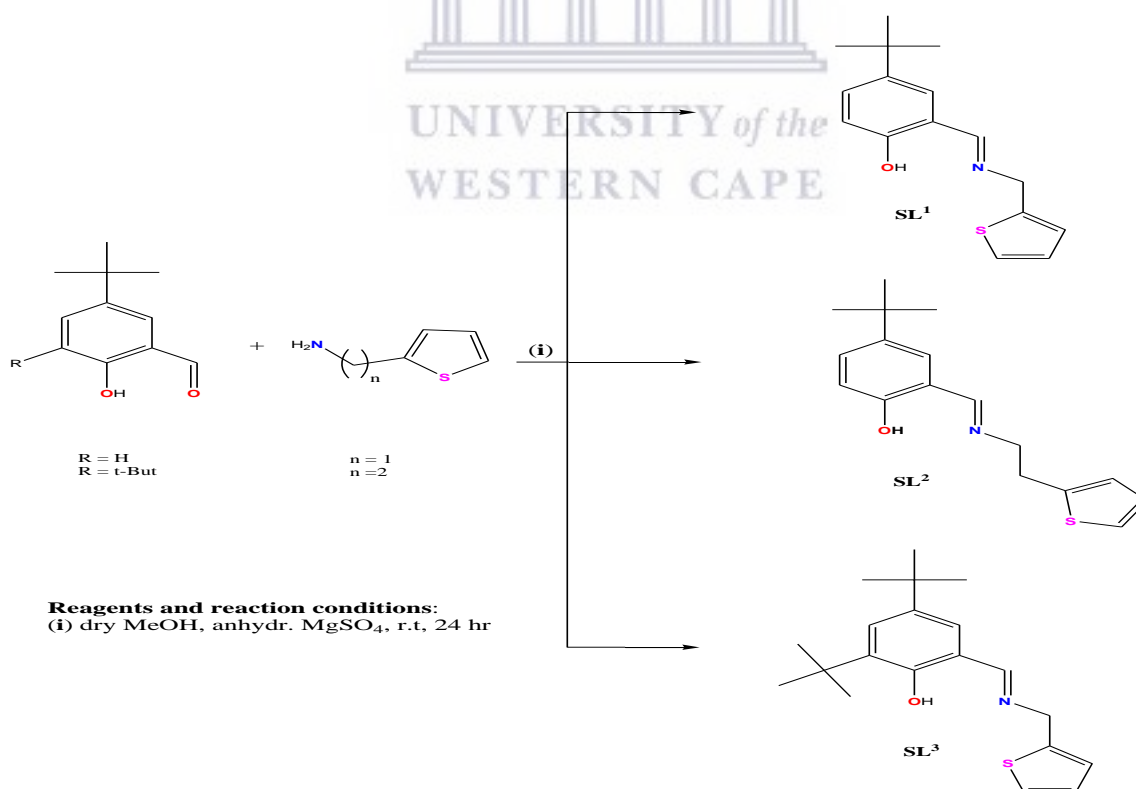
This chapter details the synthesis, characterization, and molecular structures of novel platinum-, ruthenium-, rhodium- and iridium salicylaldimine/ketimine ligands with a pendant thiophene arm. Spectroscopic (FT-IR, ¹H and ¹³C{¹H} NMR) techniques in conjunction with

analytical (C,H,O) techniques were employed in order to gain insight into the structural formulations of the ligands **SL**¹-**SL**⁵ and the corresponding metal complexes **C7**-**C11**.

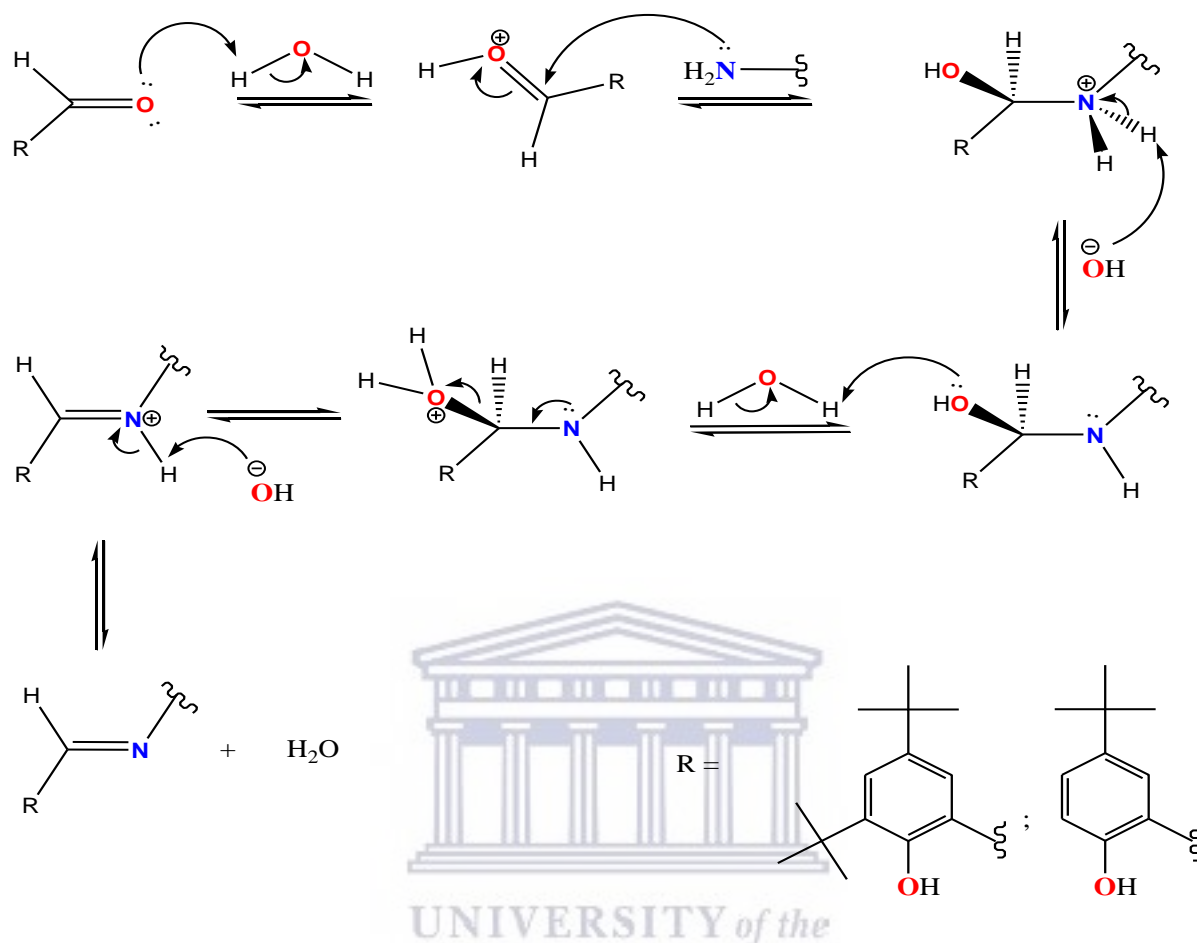
3.2 Results and Discussion

3.2.1 Synthesis and characterization of *N,O*-salicylaldimine ligands, **SL**¹-**SL**³.

The new *N,O*-salicylaldimine ligands **SL**¹-**SL**³ with a varied pendant thiophene arm were prepared by a modified literature method [34-37]. Substituted 3- or 3,5-*t*Bu-salicylaldehyde(s) was reacted with a desired heterocyclic amine (Scheme 3.1) using a Schiff base condensation reaction (Scheme 3.2, general reaction mechanism for the formation of a Schiff-base). The formation of the intended imine ($C=N_{imine}$) functional group with time was monitored by TLC and infrared spectroscopy.



Scheme 3.1: Synthesis of *N,O*-salicylaldimine ligands, **SL**¹-**SL**³.



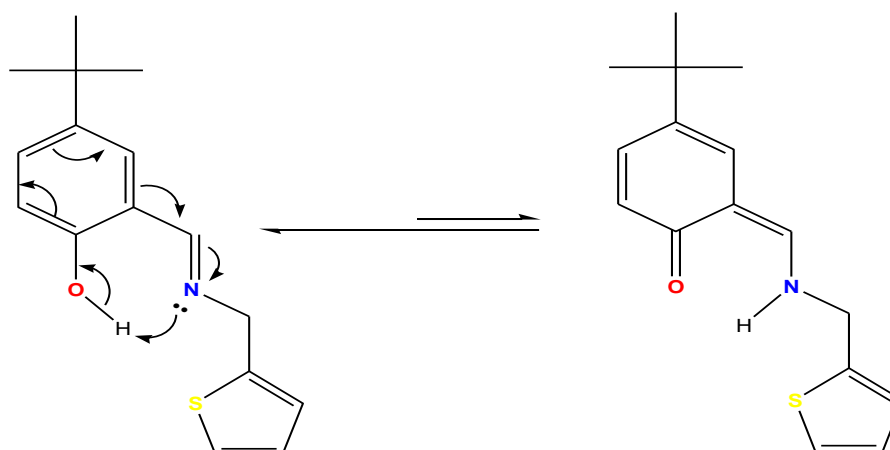
Scheme 3.2: Mechanistic outline of a general Schiff-base condensation reaction.

The salicylaldimine ligands **SL**¹-**SL**³ were separated from a methanolic solution after 12h at room temperature in the presence of anhydrous MgSO₄ that was employed to quench the by-product water (depicted in Scheme 3.2). The successful recovery of the prepared ligands was subsequently extracted using a liquid-liquid (water/dichloromethane) system in order to remove unreacted starting reagents. These ligands, **SL**¹-**SL**³, were isolated as yellow crystalline solids in good yields (Table 2.1). The ligands, **SL**¹-**SL**³, are all soluble in most organic solvents such as dichloromethane, methanol, toluene, diethyl ether and

dimethylsulfoxide. Spectroscopic (IR, ¹H, ¹³C{¹H} NMR) and analytical data (Elemental Analysis and Mass Spectrometry) techniques were employed in order to confirm the proposed structural formulations.

3.2.1.1 Infrared Spectroscopy of the N,O-salicylaldimine ligands, **SL¹-SL³**.

In order to successfully confirm the Schiff base condensation reaction, Infrared Spectroscopy was used to probe and monitor the key structural features that become evident in the formation of the salicylaldimine ligands. The spectra of these salicylaldimine ligands **SL¹-SL³** were recorded using KBr pellets. The stretching frequencies characteristic of a hydroxyl moiety were observed in the region 2900-3050 cm⁻¹ as broad “indicative” bands for all the ligands. The appearance of a strong stretching vibration at 1634, 1644, and 1637 cm⁻¹ (Table 2.2) for the ligands **SL¹**, **SL²** and **SL³**, respectively, were assigned to the imine (C=N_{imine}) stretching vibrations [38]. The possibility of tautomerism between the hydroxyimine and keto-amine structures as depicted in Scheme 3.3, was ruled out due to the absence of the stretching vibrations of the starting carbonyl (~1700 cm⁻¹) and amine (~3300 cm⁻¹) functionalities, respectively. These normally suggest the occurrence of tautomerism of the two in solution. The spectroscopic data obtained for the ligands **SL¹-SL³** was in accordance with the observation of similar NH⁺⋯O and OH⁺⋯N system that indicated the favourable formation of a hydroxyimine than the keto-imine as depicted in Scheme 3.3 [39].



Scheme 3.3: Possible tautomerism of the hydroxyimine (**SL¹**, left) to the keto-amine (right).

Table 3.1: Infrared data of the *N,O*-salicylaldimine ligands, **SL¹**-**SL³**.

Ligands	$\nu(\text{C}=\text{N})_{\text{imine}}^{\text{a}}$	$\nu(\text{C}=\text{C})_{\text{heterocyc}}^{\text{a}}$	$\nu(\text{OH})^{\text{a}}$	$\nu(\text{C}-\text{S}-\text{C})^{\text{a}}$	Yield (%)
SL¹	1634	1504	2955	1319	88
SL²	1644	1507	3050	1322	90
SL³	1637	1505	2980	1320	85

^a = stretching frequencies in cm^{-1}

The heterocyclic ring absorption bands (C–S–C) for the ligands were observed in the range 1319 -1321 cm^{-1} (Table 3.1) and these are in agreement with the reported literature values for ferrocenylimine and salicylaldimine ligands with a heterocyclic (thiophenyl and furyl) pendant arm [40-42]. The presence of a heterocyclic ring in the ligands was also supported by observed bands in the region 1504-1507 cm^{-1} , that are characteristic for a C=C stretching

vibrations of the heterocyclic frequency, especially thiophenyl. Similar observations have been reported for ferrocenylimine ligands with a pendant thiophenyl arm [41,42].

3.2.1.2 ^1H and ^{13}C { ^1H } NMR spectroscopy of *N,O*-salicylaldimine ligands, **SL¹**-**SL³**

All of the ^1H and ^{13}C { ^1H } NMR spectra of the synthesized *N,O*-salicylaldimine ligands, **SL¹**-**SL³**, were recorded in deuterated chloroform (CDCl_3).

The ^1H NMR spectra of all the ligands, **SL¹**-**SL³**, exhibited characteristic azomethine ($\text{HC}=\text{N}$) resonances. The appearance of the a singlet peak observed within the range of 8.43-8.45 ppm was thus attributed to the presence of an azomethine functionality. The formation of the azomethine ($\text{C}=\text{N}$) functionality resulted in imparted increase in the electron density between the C and N atoms, causing an up field shift in the resonance of the protons of the azomethine ($\text{HC}=\text{N}$) functionality relative to the proton of unreacted aldehyde that normally appear downfield at approximately 10 ppm. These chemical shift values are in good agreement with those reported for similar salicylaldimine, salen and salophen type Schiff-base ligands (Figure 3.1) [40]. The hydroxyl (HO-) protons were observed downfield in the range 12.99- 13.60 ppm for the ligands reported herein. This downfield appearance of the hydroxyl protons for these ligands **SL¹**-**SL³** (Table 3.2) can be attributed to the intramolecular hydrogen bonding ($\text{OH}\cdots\text{N}$), that has been observed to govern the appearance of a downfield hydroxyl signals in similar salicylaldimine ligands [43]. The chemical shifts of the methylene arm ($=\text{N-CH}_2$) for ligand **SL¹** and **SL³** appeared as singlets at 4.68 ppm and 4.81 ppm, respectively, compared to the 4.00 ppm signal of the heterocyclic amine starting

material, thus reflecting a downfield shift in the alkyl protons upon successful condensation reaction. The two triplets observed at 3.20 ppm and 3.71 ppm in **SL**² confirmed the presence of an ethylene arm (=N-CH₂CH₂) in the ligand [41,42] and the appearance of triplets indicated vicinal proton-proton coupling. The presence of the electron rich ethylene arm in ligand **SL**² influences the appearance of the signals upfield compared to the downfield appearance of the signals that correspond to the methylene arm for **SL**¹ and **SL**³. The analytical purity of these ligands was further confirmed by the absence of signals at 2.20 ppm and 9.90 ppm, which would represent unreacted -NH₂ and -CHO groups respectively.

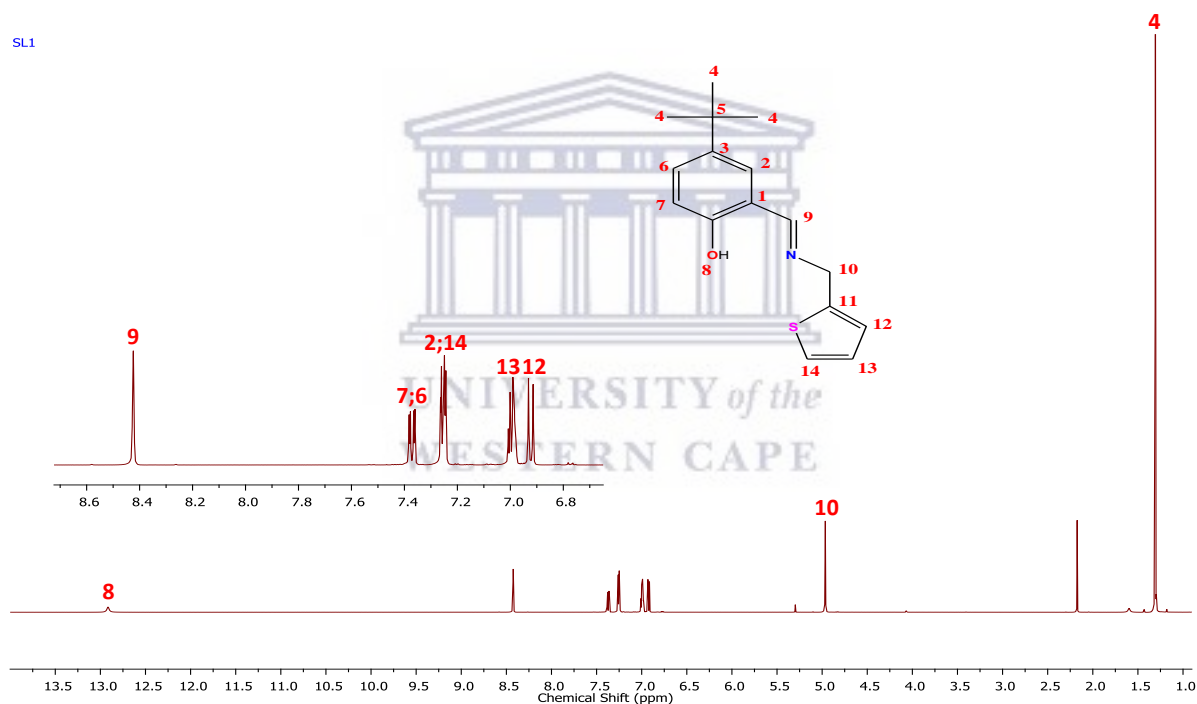


Figure 3.2: ¹H NMR of *N,O*-salicylaldimine ligand **SL**¹ with insert for ¹H NMR numbering scheme.

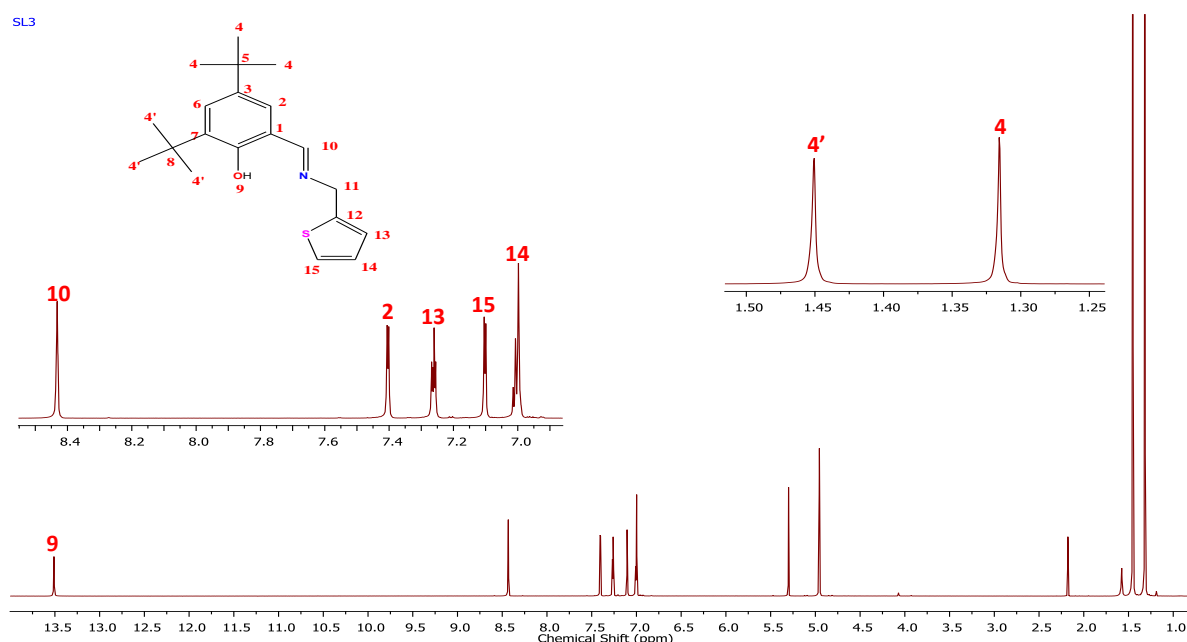


Figure 3.3: ¹H NMR of *N,O*-salicylaldimine ligand **SL³** with insert for ¹H NMR numbering scheme.

Table 3.2: ¹H NMR spectral data (δ in ppm) in $CDCl_3$ (unless noted otherwise).

Ligands	$\delta(C=NH)_{\text{imine}}$	$\delta(O-H)_{\text{heterocyc}}$
SL¹	8.42	12.91
SL²	8.30	13.08
SL³	8.43	13.51

In the ¹³C NMR analysis of the ligands, the characteristic signals for the iminic carbons appeared between 161.9 ppm and 163.3 ppm, which is within the range 161.8 – 165 ppm for similar salicylaldimine compounds [40,44]. The signals for the imine carbons also revealed an upfield shift compared to the unreacted aldehyde carbons, vividly confirming the presence of C=N bond. The carbon signals for the methylene arm in **SL¹** and **SL²** appeared at 57.4 ppm and 59.4 ppm, respectively. The two signals for the ethylene arm in **SL²** appeared at 63.1 ppm and further upfield at 31.5 ppm. The two carbon signals in **SL²** differ greatly because the

deshielding effect of the nitrogen atom becomes less pronounced as the length of the alkyl chain increases. These observations are consistent with those of similar compounds where the ethyl linker was reported to have a similar influence for ferrocenylimine and salicylaldimine ligands with an appended heterocyclic moiety [40,44,45].

Table 3.3: $^{13}\text{C}\{^1\text{H}\}$ NMR spectral data (δ in ppm) in CDCl_3 (unless noted otherwise).

Ligands	$\delta(\text{C}=\text{NH})_{\text{imine}}$	$\delta(\text{CO-H})_{\text{heterocyc}}$
SL¹	163.3	161.2
SL²	162.6	159.4
SL³	166.2	166.1

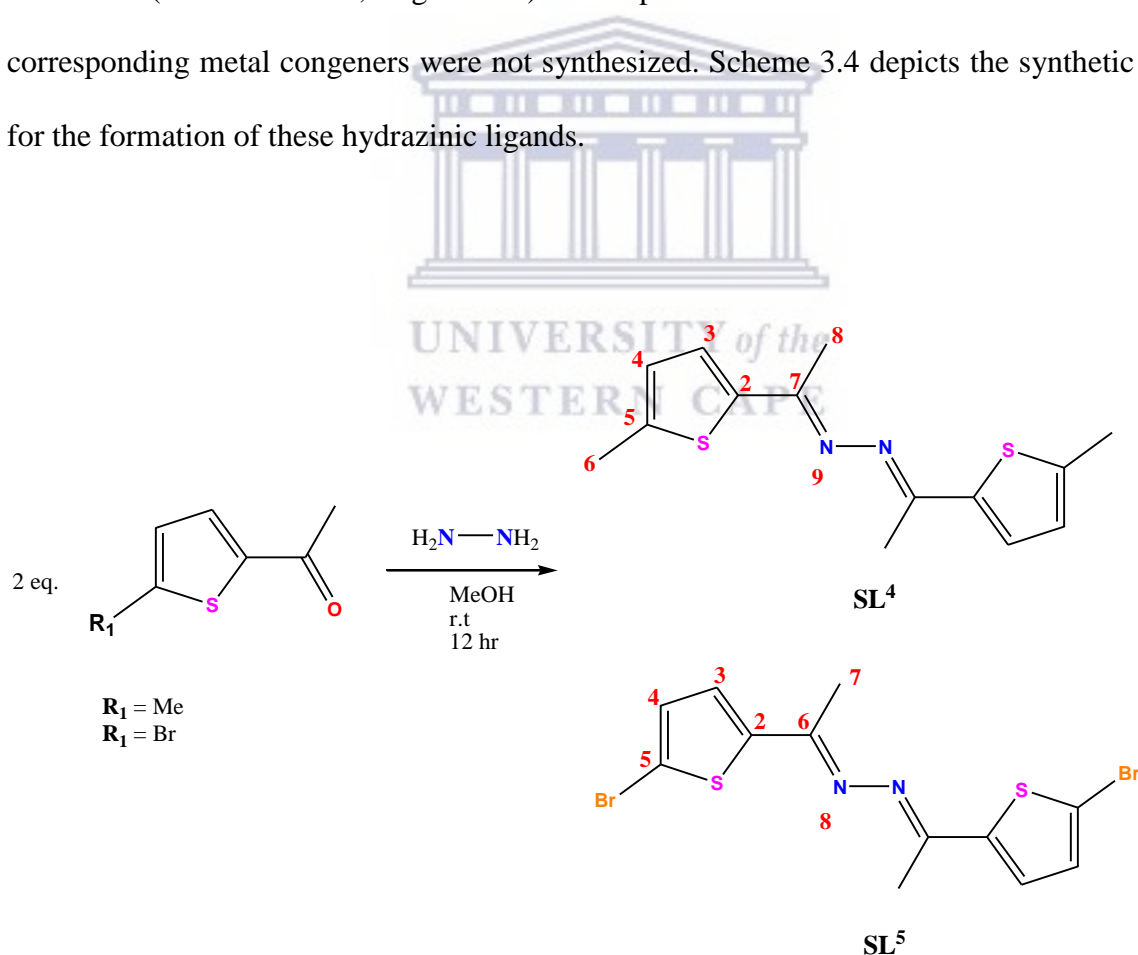
3.2.1.3 Elemental Analysis and Mass Spectroscopy of **SL¹** - **SL³**

The elemental analysis for all the *N,O*-salicylaldimine ligands were found to be consistent and within the acceptable limits. No solvent inclusion was observed and this was attributable to thorough recrystallization and drying of the ligands before microanalysis.

Electrospray ionisation mass spectrometry (ESI-MS) further confirmed the successful synthesis of the ligands as the molecular parent ions $[\text{M}]^+$ was observed for the respectively ligands.

3.2.1.4 Synthesis and Characterization of azine ligands, SL^4 and SL^5 .

The symmetric N,S- donor ligands were also synthesized following standardized Schiff base condensation reaction followed herein (*vide infra*) [41,42]. A suitable ketone was reacted with hydrazine hydrate in a methanolic solution to afford the azine derivatives SL^4 and SL^5 as yellow crystalline solids in good yields 88-90 %. The ligands are soluble in most common organic solvents such as chloroform, dichloromethane (DCM), dimethylsulphoxide, dimethylformamide (DMSO), etc. Although the ligands have been previously prepared, they have been independently prepared herein. To our knowledge, the respective molecular structures (section 3.2.4.1, Figure 3.6) are reported herein for the first time although corresponding metal congeners were not synthesized. Scheme 3.4 depicts the synthetic route for the formation of these hydrazinic ligands.

Scheme 3.4: General synthetic route for the hydrazinic/ketimines, SL^4 and SL^5 .

3.2.1.5 Infrared Spectroscopy of azine ligands SL^4 and SL^5 .

Absence of the stretching frequency corresponding to the aldehydic moiety ($\sim 1700\text{ cm}^{-1}$) and appearance of new strong stretching frequencies in the range $1649\text{-}1647\text{ cm}^{-1}$, attributed to the $\nu(C=N)_{\text{imine}}$, were indicative of a successful condensation reaction [41,42]. No discernible data from the infrared spectroscopy studies was obtained about the favoured geometry of the prepared ligands. The peaks at around 1019 cm^{-1} and 1058 cm^{-1} can be assigned to (N–N) of SL^4 and SL^5 , respectively. The structures of the compounds were confirmed by NMR spectroscopy and single crystal XRD. They are *trans*-/*anti*-(E) with respect to the imine functionality as confirmed by the X-ray studies.

Table 3.4: Infrared data of the N,O-salicylaldimine ligands, SL^4 and SL^5 .

Ligands	$\nu(C=N)_{\text{imine}}^a$	$\nu(C=C)_{\text{heterocyc}}^a$	$\nu(C-S-C)^a$	Yield (%)
SL^4	1646	1504	1319	88
SL^5	1640	1507	1322	90

^a = stretching frequencies reported in cm^{-1}

It was also observed that the substituents on the thiophene moiety influenced the observed stretching frequencies, as the electron-withdrawing group (Br, SL^5) had a blueshift (1322 cm^{-1}) influence compared to the electro-donating group (Me, SL^4) that had a redshift (1319 cm^{-1}).

3.2.1.6 ¹H and ¹³C NMR of azine ligands, **SL**⁴ and **SL**⁵

The ¹H and ¹³C{¹H} NMR spectra of the synthesized ketimine Schiff base ligands **SL**⁴ and **SL**⁵ were in agreement with the proposed structural formulations as shown in Scheme 3.4 above. Four signals (δ (ppm) H-6: 2.52, H-8: 3.21, H-4: 6.97, H-3: 7.33) and three signals (δ (ppm) H-7: 2.50, H-3: 7.09, H-4: 7.42) were observed in the ¹H NMR spectra of **SL**⁴ and **SL**⁵, respectively. Figure 3.4 depicts ¹H NMR spectrum of the bromo substituted hydrazinic (**SL**⁵) derivative. The proton signals were in agreement with the proposed structural formula of the ligand. The ¹³C NMR showed signals in the range 110-140 ppm that are characteristic of the heterocyclic carbons (C2-C5) and these resonances were within reported data for similar ligands such as diimine (Figure 3.1) and ferrocenylimine with an appended heterocyclic (thienyl or furyl) motifs [41]. The iminic C=N resonances were observed downfield with respect to the heterocyclic carbons (Table 3.5).

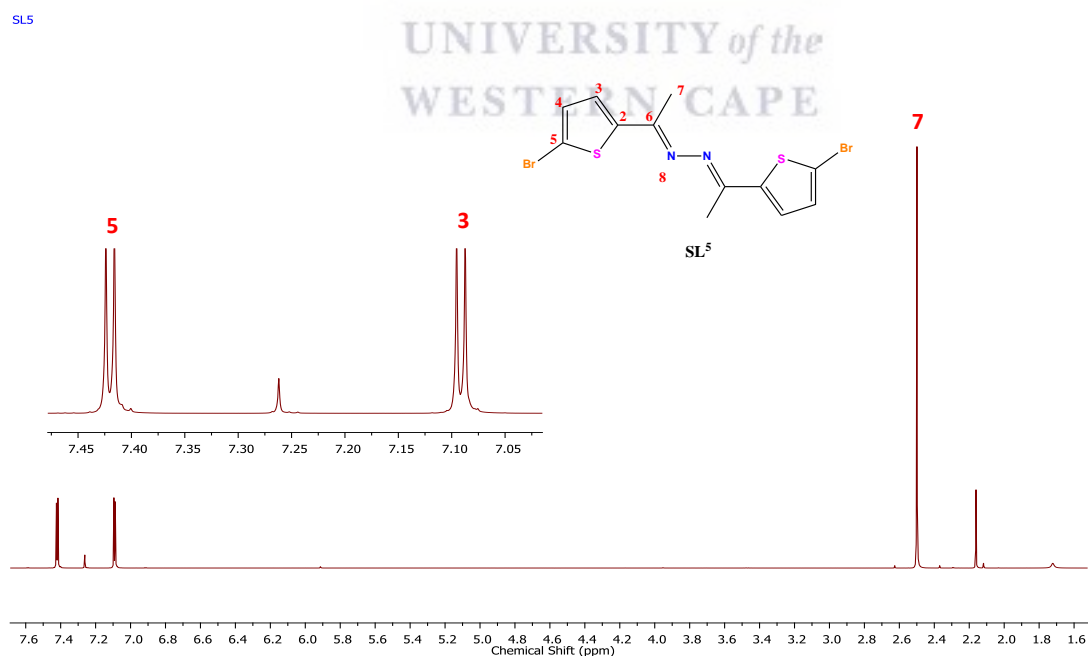


Figure 3.4: ¹H NMR spectra of ligand **SL**⁵ recorded in CDCl₃.

Table 3.5: ^1H and $^{13}\text{C}\{^1\text{H}\}$ NMR data for ligands, **SL⁴**-**SL⁵**.

Ligands	$\delta(\text{C}=\text{N})_{\text{imine}}$ [$^1\text{H}, ^{13}\text{C}$] ^a	$\delta(\text{C}=\text{C})_{\text{heterocyc}}$ [$^1\text{H}, ^{13}\text{C}$] ^a	Yield (%)
SL⁴	-,160.5	7.33&6.97, 110-140	88
SL⁵	-, 161.3	7.43&7.09, 110-140	90

3.3 Single X-ray crystallography

3.3.1 Crystal and Molecular structure of salicylaldimines, **SL¹** and **SL³**.

The single-crystal structures of the salicylaldimine **SL¹** and **SL³** corroborate the molecular composition of these Schiff bases. Summary of the crystallographic data and refinement residuals are given in Table 3.6 and the data for selected bond lengths and bond angles are summarized in Table 3.7. The complete data for the salicylaldimine ligands can be obtained from the compact disc (Appendix). Their molecular structures are depicted below in Figure 3.5.

The salicylaldimine ligands **SL¹** and **SL³** crystallize in the monoclinic space group *P21/c*. There was an observed distortion in the configuration of these ligands around the thienyl and ^tBu moieties. The C(6)-N(1)_{imine} bond distance of both ligands were reported to be within expected limits, 1.282(2) Å for **SL¹** and 1.280(2) Å for **SL³**, comparable to O,N,S-Schiff base ligands 1.275(2) Å that are reported in the literature [46,48]. The presence of the salicyl-OH

functionality in the two ligands was confirmed by the observed intramolecular hydrogen bond 0.9400(3) for SL^1 and 0.973(15) for SL^3 between the salicyl-OH and imine nitrogen [49]. The molecular packing of SL^1 and SL^3 only exhibited C–H $\cdots\pi$ interaction [50-57]. The salicylaldimine ligands consist of N,O-donor sets that are capable of chelating to metal centre through the imine nitrogen and the deprotonated phenolic oxygen atom (*vide infra*).

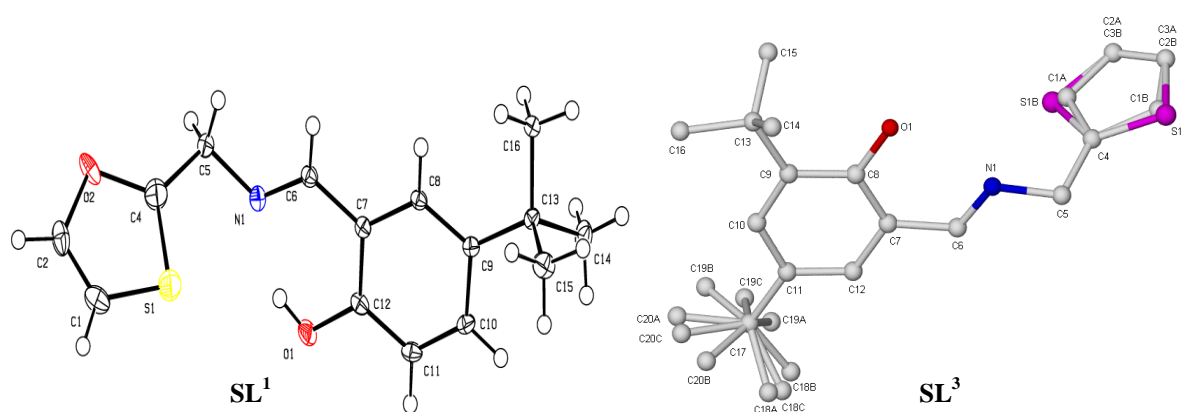


Figure 3.5: ORTEP representations of molecular structures of salicylaldimine ligands SL^1 (left) with hydrogen atoms included, and SL^3 (right) shown with 50% probability ellipsoids.

Table 3.6: Crystal data and structure refinement of ligand **SL¹** and **SL³**.

	SL¹	SL³
Formula	C ₁₆ H ₁₉ ClNOS	C ₂₀ H ₂₇ NOS
Formula weight	276.36	329.50
Crystal system, Space group	Monoclinic, <i>P21/c</i>	Monoclinic, <i>P21/c</i>
a (Å)	10.3061(3)	16.3063(8)
b (Å)	6.0431(2)	10.0545(9)
c (Å)	24.5788(6)	11.6245(11)
β (deg)	112.1940(4)	92.721(4)
V/Å ³	1422.87(7)	2542.7(2)
Z	4	4
D _c (g cm ⁻³)	1.29	1.660
μ (mm ⁻¹)	0.880	5.456
θ range for data collection (deg.)	1.2 to 28.4	1.9 to 28.4
no. of reflns meads	54904	12728
no. of reflns used (R _{int})	0.075	0.063
no. of params	575	575
Observed data R [<i>I</i> > 2σ(<i>I</i>)]	10402	11739
R ₁	0.0416	0.0311
wR ₂	0.0810	0.0640
R (all data)		
R ₁	0.04	0.03
wR ₂	0.0810	0.063
Min. Max. Resd. Dens. [e/Å ³]	-0.92, 0.46	-1.48, 1.01

Table 3.7: Selected bond lengths [\AA] and angles [$^\circ$] for salicylaldimine ligands SL^3 and SL^1

Interatomic distances	SL^1	SL^3
C6-N _{imine}	1.282(3)	1.280(2)(5)
C8-O1	1.356(13)	1.3596(18)
C4-S	1.703(3)	1.672(3)
C3-S	1.703(3)	1.643(3)
O(1)-H(1)...N1	0.9400(3)	0.973(15)
Angles		
N(1) _{imine} -C5-C4	110.3(2)	110.24(13)
N(1) _{imine} -C6-C7	121.2(2)	122.26(13)
C5-N(1) _{imine} -C6	117.89(19)	118.36(13)
C12[8]*-O1-H1A	109.5	106.1(11)
O1-C8-C7		119.35(13)
O1-C8-C9	118.98(19)	119.120.70(13)
O(1)-C(12)-C(11)	121.8(2)	
O(1)-C(12)-C(7)		

*= [$^\circ$] bond angle of SL^3



3.3.2 Crystal and Molecular structure of ketazine ligands, SL^4 and SL^5 .

Suitable crystals for SL^4 and SL^5 for single X-ray diffraction studies were grown from a concentrated methanolic solution under slow evaporation conditions. The molecular structure of the ligands unequivocally confirmed the success of the condensation reaction via the formation of the new azomethine bond. The bond distance N1-C6 in SL^4 is 1.2989(18)(2) \AA and 1.296(8) \AA for SL^5 , characteristic of the formation of an azomethine bond and within acceptable limits for reported Schiff-base ligands(C=N) bond distances of 1.296(10) \AA . SL^4 has a bite angle [N1-C6-C5] of 115.80(11) while SL^5 has a bite angle [N1-C6-C5] of

115.9(5), respectively, suggesting that the hybridization between C6-N1 (**SL**⁴) and C5-N1 (**SL**⁵) is sp^2 . The ligands **SL**⁴ and **SL**⁵ crystallizes in a *trans*-geometry with respect to the azomethine double bond (N1=C6), minimizing the repulsion between the two thiophenyl moieties and orientate in a fashion to accommodate metal chelation through the available N and S donor sites. The N-N1a bond distance of 1.4000(17) Å for **SL**⁴ and 1.393(6) Å for **SL**⁵ are comparable to the bond length of S-benzylidithiocarbamate 1.406 Å [58]. Table 3.8 summarizes selected parameters such as bond lengths, bond angles, cell volume, and density.

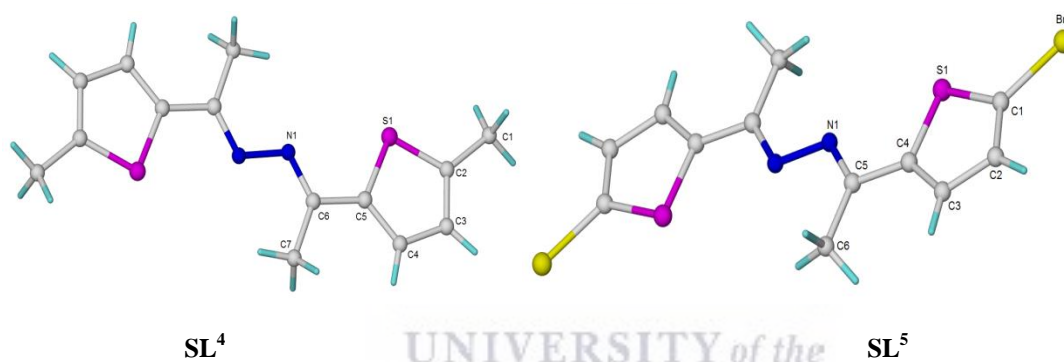


Figure 3.6: ORTEP representations of mononuclear ketimine ligands **SL**⁴(left) and **SL**⁵(right). Thermal ellipsoids are drawn at the 50 % probability level. Hydrogen atoms have been included.

Table 3.8: Crystal data and structure refinement of ligand **SL⁴** and **SL⁵**.

	SL⁴	SL⁵
Formula	C ₁₄ H ₁₆ CN ₂ S ₂	C ₁₂ H ₁₀ N ₂ S ₂
Formula weight	276.43	406.16
Crystal system, Space group	Monoclinic, <i>P21/n</i>	Monoclinic, <i>P21/n</i>
a (Å)	5.8357(5)	4.0317(7)
b (Å)	7.6207(7)	5.7627(10)
c (Å)	15.2026	29.848(5)
β (deg)	90.245	93.847(4)
V/Å ³	676.09(11)	691.9(2)
Z	2	2
D _c (g cm ⁻³)	1.358	1.950
μ (mm ⁻¹)	0.377	6.142
θ range for data collection (deg.)	2.7 to 28.4	2.7 to 28.4
no. of reflns meads	1695	1675
no. of reflns used (R _{int})	0.047	0.050
no. of params	84	83
Observed data R [I > 2σ(I)]	11459	8144
R ₁	0.0322	0.0531
wR ₂	0.0927	0.1204
R (all data)		
R ₁	0.03	0.05
wR ₂	0.0927	0.05
Min. Max. Resd. Dens. [e/Å ³]	-0.26, 0.31	-1.462, 0.90

Table 3.9: Selected bond lengths [Å] and angles [°] for ketamine ligand **SL**¹ and **SL**³.

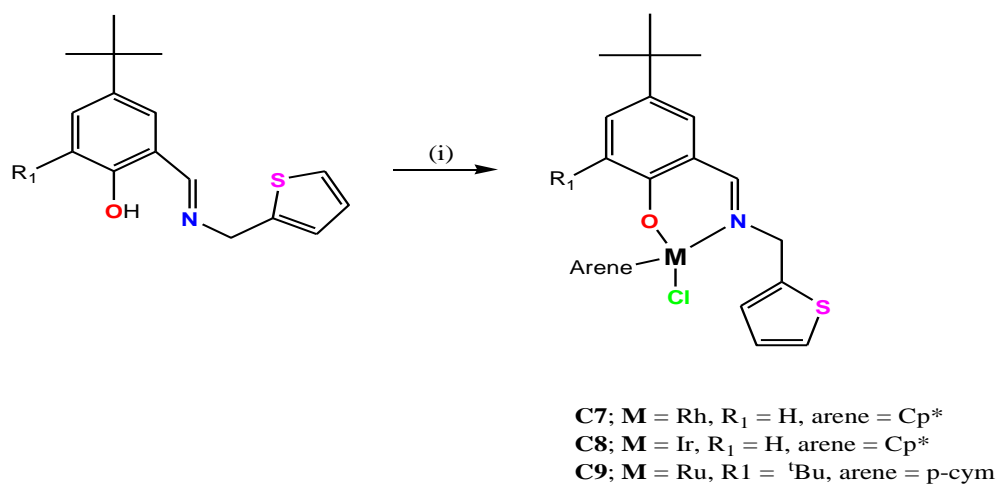
Interatomic distances	SL ⁴	SL ⁵
N _{imine} -C5[6]*	[1.2989(18)]	1.296(8)
S1-C1[2]*	[1.7197(14)]	1.720(5)
S1-C4[5]*	[1.7269(13)]	1.739(6)
N1-N1a	1.4000(17)	1.393(6)
Angles		
N1a-N _{imine} -C5	113.60(11)	113.5(5)
Nimine-C5[6]*-C4[5]*	[115.80(11)]	115.9(5)
N _{imine} -C5[6]*-C6[7]*	[126.53(13)]	126.1(5)

*= [°] bond angle of **SL**⁴

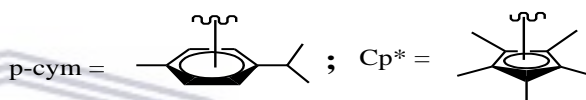
3.4 Synthesis and Characterization of *N,O*-salicylaldimine complexes, **C7-C11**.

Synthesis of the title complexes commenced with the synthesis of the suitable metal precursors such as **M**(II)Cl₂(COD) and *cis*-[**M**(II)Cl₂(DMSO)₂] (**M** = Pt) [59,61] and the dimeric metal precursors [**M**(II/III)(arene)(μ-Cl)₂Cl]₂, (**M** = Ru(II), Rh(III) and Ir(III); arene = *p*-cymene for Ru(II) and cyclopentadienyl for Rh(III) and Ir(III)) following methodologies reported in the literature [62,64]. The appropriate metal precursors were then subsequently reacted with the parent ligands **SL**¹-**SL**³, independently, in the presence of the weak base triethylamine (Et₃N). The weak base was initially allowed to deprotonate the parent ligands before the addition of an appropriate metal precursor. The strategic preparation of complexes **C7-C9** involved the dimer, [**M**(II/III)(arene)(μ-Cl)₂Cl]₂, splitting reaction in a presence of a weak base using a 1:2 (metal precursor: ligand) molar ratios.

The complexes synthesized herein are reported for the first time according to our knowledge.

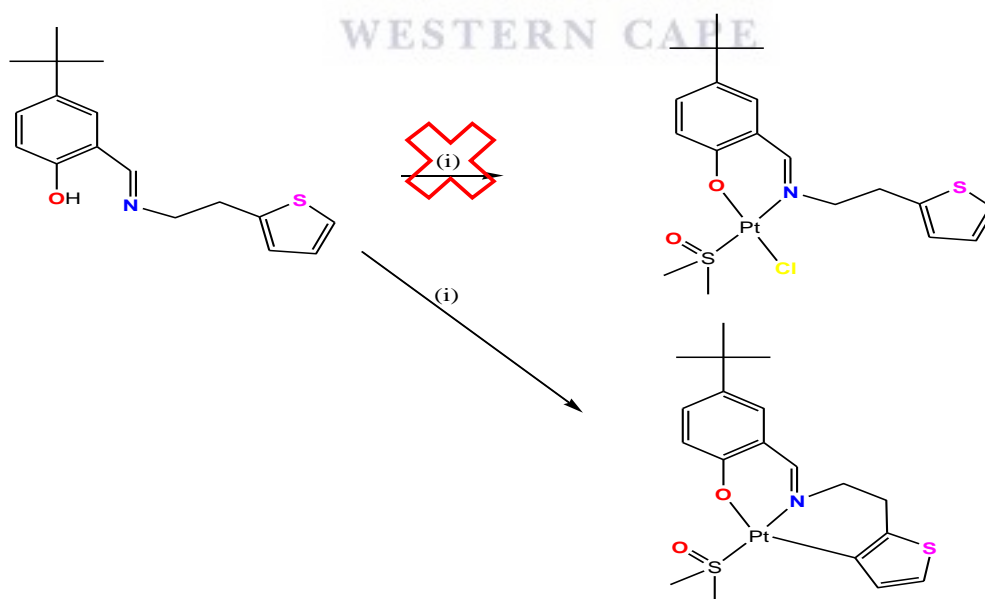


Arenes



Reagents and reaction conditions: (i) dry MeOH, [M(arene)(*u*-Cl₂)Cl]₂, rt, overnight

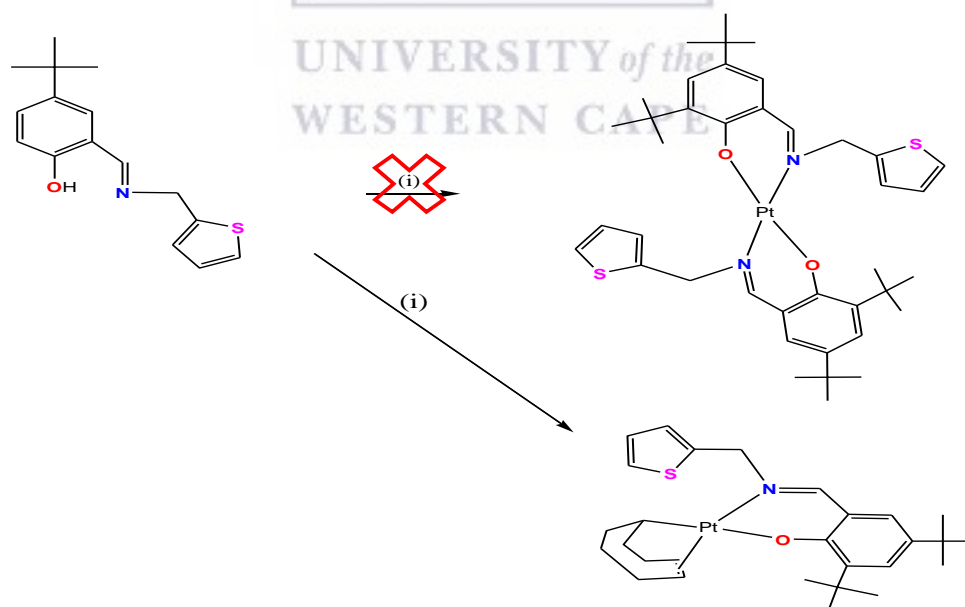
Scheme 3.5: General synthesis of half-sandwich/arene salicylaldimine complexes, **C7-C9**.



Reagents and reaction conditions: (i) PtCl₂(dmsO)₂, dry MeOH, 2 mol. eq. Et₃N, rt, overnight

Scheme 3.6: Synthesis of the unexpected platinacycle **C10**.

Synthesis of the complex **C10** was undertaken as depicted in Scheme 3.6. As observed with complex **C11**, the reaction conditions employed to synthesize the Pt^{II} metal complexes did not favour the intended bis-chelation mode. The reaction conditions instead favoured the C-H activation of the heterocyclic moiety to form a thioplatin species, with the DMSO ligand still attached to the metal ion (*vide supra*, Scheme 3.6) in the case of complex **C10**. The isolation of complex **C11** instead of the envisioned bis-chelated one was attributed to the steric demand of tBu substituent at 5-position of the ligand **SL**³. Both complex, **C10** and **C11**, were isolated as a yellow crystalline solids, that are soluble in common organic solvents such as DCM and $CHCl_3$. The 1H and ^{13}C $\{^1H\}$ NMR confirmed the formation metallacycle and crystals suitable for X-ray studies were grown from slow diffusion hexane into a concentrated DCM solution of the metal complex.



Reagents and reaction conditions: (i) $PtCl_2(COD)$, dry MeOH, 2 mol. eq. Et_3N , rt, overnight

Scheme 3.7: Synthesis of salicylaldimine Pt^{II} -*H*(COD) complex, **C11**.

The proposed structural formulations for the platinum complexes were found to form different complexes depending on the starting metal precursor, Pt(II)Cl₂(COD) or [Pt(II)Cl₂(DMSO)₂], used. The formation of the proposed bis-chelate complex **C10** was found not to be favoured under the reaction conditions used (Scheme 3.7). The use of 2 molar equivalence of triethylamine as a base to deprotonate the ligand **SL**³ (*vide infra*, Scheme 3.8) resulted in the formation of a Pt^{II}-(COD) complex where the fluxional chloride atom has been abstracted. The formation of the Pt^{II}-(COD) complex as the favoured complex was confirmed by ¹H and ¹³C {¹H} NMR.

3.4.1 Infrared Spectroscopy, **C7-C11**.

The vibration of the complexes in solution when irradiated by the infrared radiation was studied in order to gain insight into the behaviour of the title complexes and to confirm coordination by monitoring the stretching frequency of the key functional groups that are proposed to be involved in the chelation to the metal centres. The chelation/coordination of the ligands to the Pt^{II}, Ru^{II}, Rh^{III} and Ir^{III} metalions was confirmed by a pronounced shift in the stretching frequencies of the imine (C=N_{imine}) moiety of the free ligands (from 1644cm⁻¹-1634 cm⁻¹) to lower stretching vibrations in the range 1630-1623 cm⁻¹. The absence of the hydroxyl functionality, (OH)_{hydroxyl}, stretching vibration at about 2950 cm⁻¹ confirmed the deprotonation of the ligands and the formation of the σ-bond with the metal ions (*vide infra*, Scheme 3.8). The stretching frequencies of the heterocyclic (C-S-C) moiety were observed in the region 1319-1340 cm⁻¹. The presence of a M-C bond for complex **C10** through the ortho activation of the heterocyclic ring was also evident as the stretching frequencies of the thiophenyl moiety were blueshifted (1340 cm⁻¹) compared complex **C7-C9** and **C11** that

chelated only through the N,O-donor sites. The appearance of a new band in the range 499–478 cm⁻¹ confirms the coordination via a nitrogen atom to the metal atoms.

Table 3.10: Infrared data of the *N,O*-salicylaldimine ligands, **C7-C11**.

Complexes	$\nu(\text{C}=\text{N})_{\text{imine}}^{\text{a}}$	$\nu(\text{OH})^{\text{a}}$	$\nu(\text{C}-\text{S}-\text{C})^{\text{a}}$	Yield (%)
C7	1624	-	1319	88
C8	1627	-	1322	90
C9	1623	-	1320	85
C10	1630	-	1340	76
C11	1627	-	1324	72

^a = stretching frequencies reported in cm⁻¹.

3.4.2 ¹H and ¹³C {H} NMR, **C7-C11**.

The ¹H NMR spectra of the salicylaldiminato complexes **C7-C11** all exhibited a distinctive upfield singlet in the range 1.25-1.30 ppm, which was assigned to the ^tBu substituent at 3-position. An upfield shifts for all the iminic proton complexes was also observed, from ~8.4 ppm for the uncoordination ligand to ~7.7 ppm for the complexes. In the ¹H NMR spectra of complexes [Cp**Rh*^{III}Cl(**SL**¹)] (**C7**), [Cp**Ir*^{III}Cl(**SL**¹)] (**C8**) and [(*p*-cym)*Ru*^{II}Cl(**SL**³)] (**C9**), the methylene (-CH₂-) linker, adjacent to the iminic functionality, experienced diastereotopic splitting due to the induced chirality by the bidentate chelating ligand (Figure 3.7, 3.8 and 3,9). The methyl protons of the cyclopentadienyl ring (Cp*CH₃) for complex **C7** and **C8** were observed upfield as a singlet that intergrates for 15-protons, respectively, in the region 1.5 - 1.2 ppm. Complex **C9** displayed two distinct doubles that were assigned to the methyl protons of the isopropenyl substituents of the ring that appeared in the region 1.07-1.20 ppm and the methyl protons of the ring appeared as a singlet at 2.25 ppm, respectively. Four

distinct doublets were observed in the region 5.0-5.6 ppm that were attributed to the presence of the *p*-cyme ring. For complex **C9** and **C11**, an additional singlet appeared at ~1.20 ppm and it was attributed to the presence of an additional ^tBu at 5-position of the ligand and singlet corresponding to this signal was observed downfield shifted compared to the free ligand (1.55 ppm), indicative of the participation of the phenoxy O- atom in the coordination to the metal ion. For complex **C10**, the disappearance of the characteristic peak of the heterocyclic *H*-3 proton was indicative of a C-H activation of the thiophene moiety. The observations were in agreement with the data reported in the literature for thiophenylcyclo ruthenate, Pd(II) and Pt(II) metallacycles [65-77].

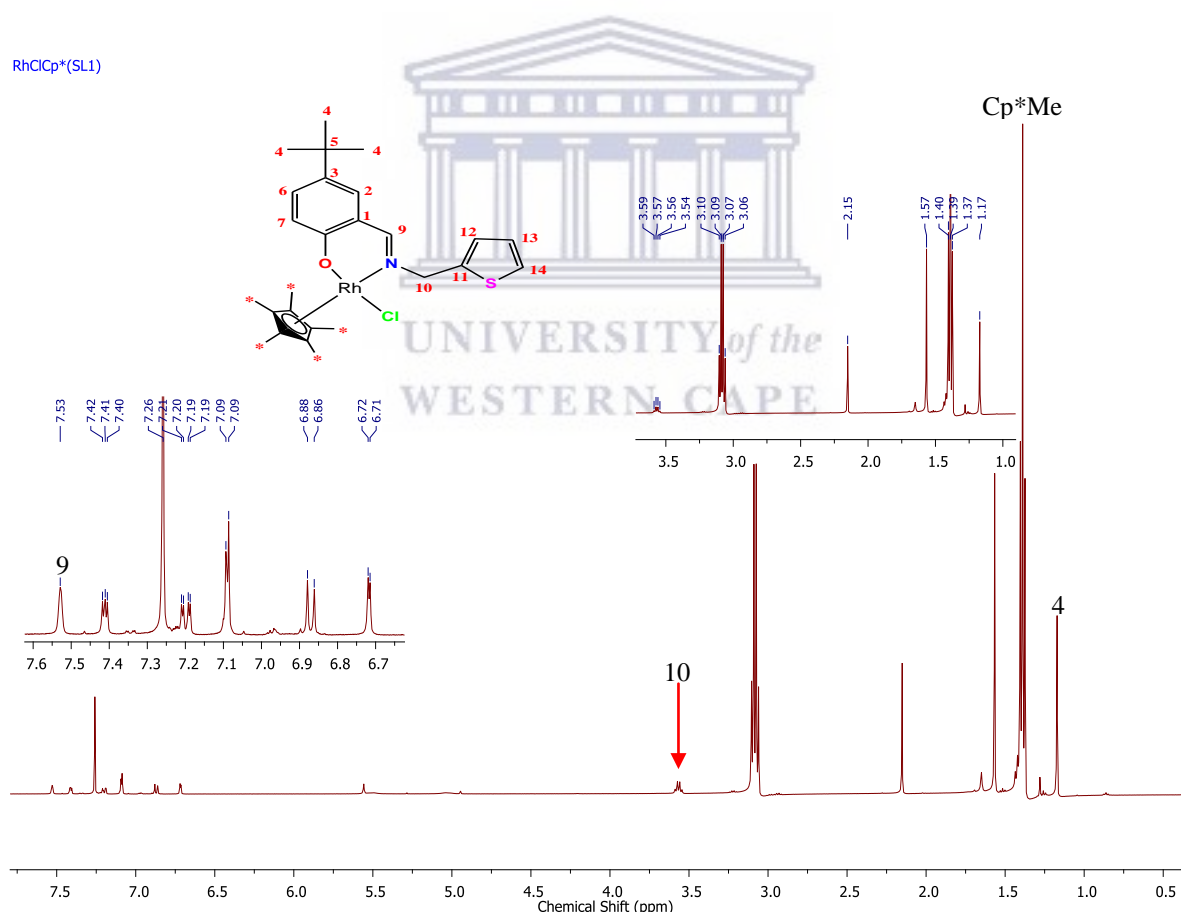


Figure 3.7: ¹H NMR spectrum of the salicylaldiminato-rhodium(III) complex **C7**, recorded in CDCl₃.

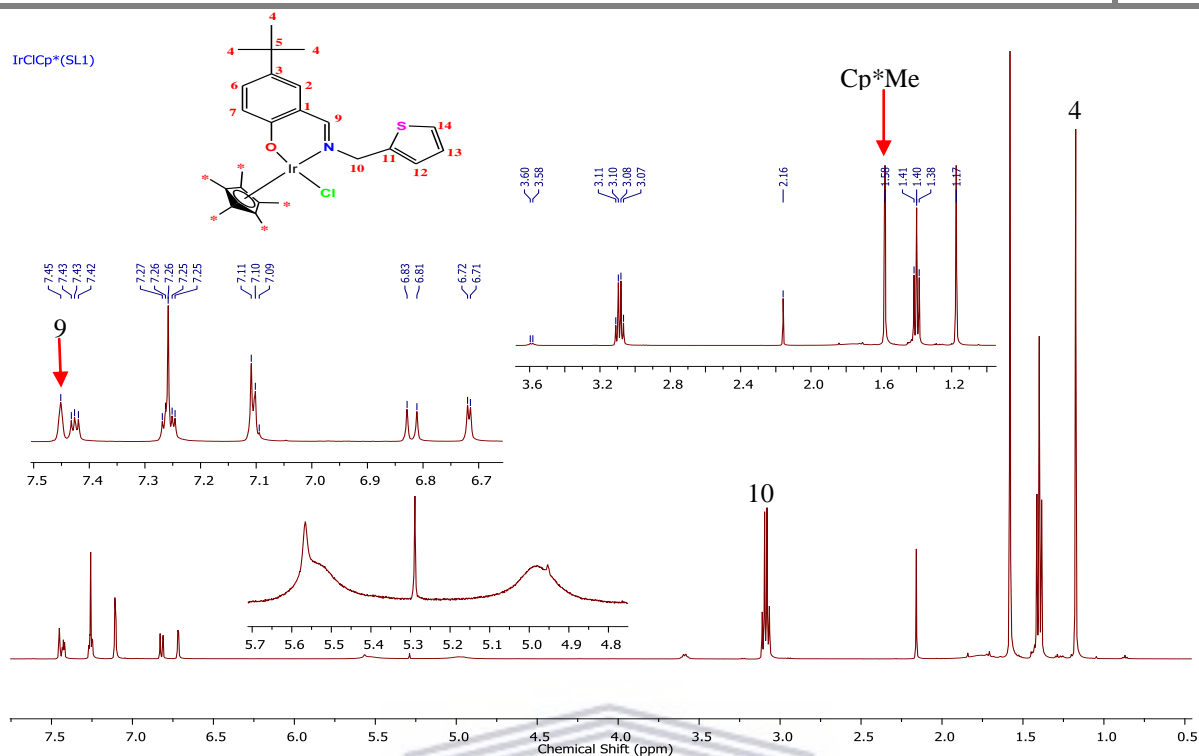


Figure 3.8: 1H NMR spectrum of the salicylaldiminato-iridium(III) complex **C8**, recorded in $CDCl_3$.

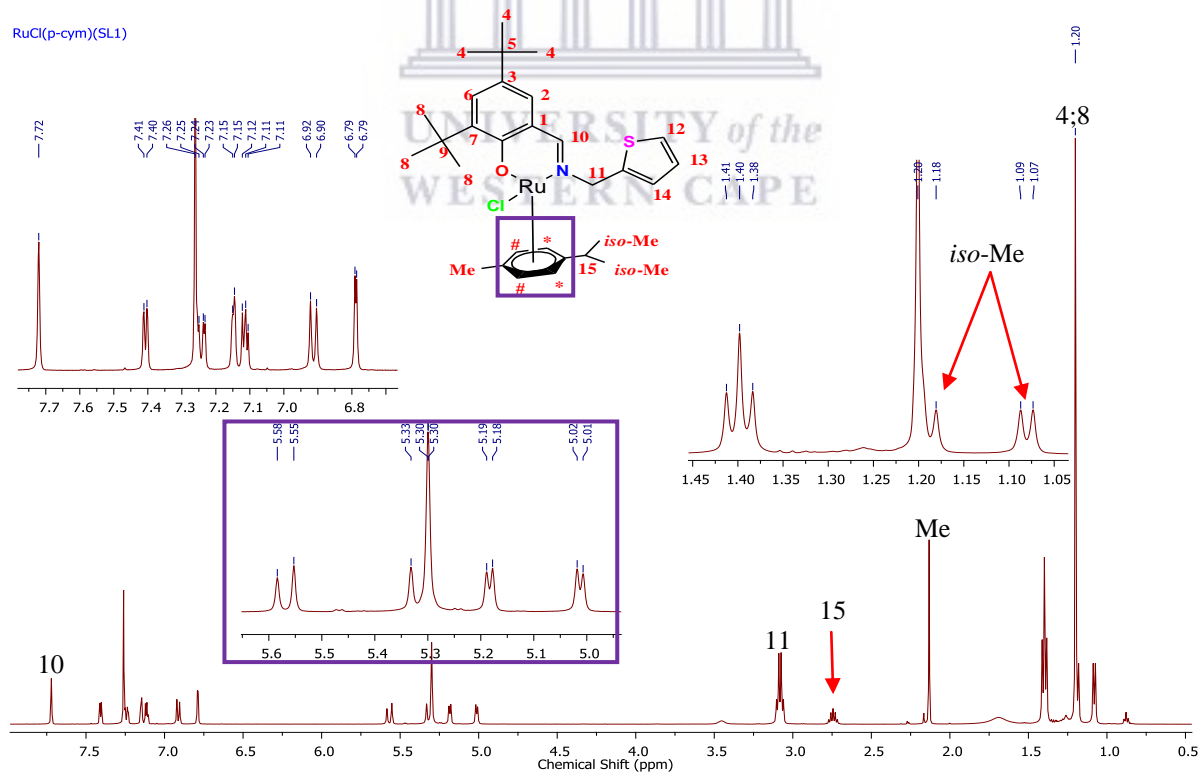
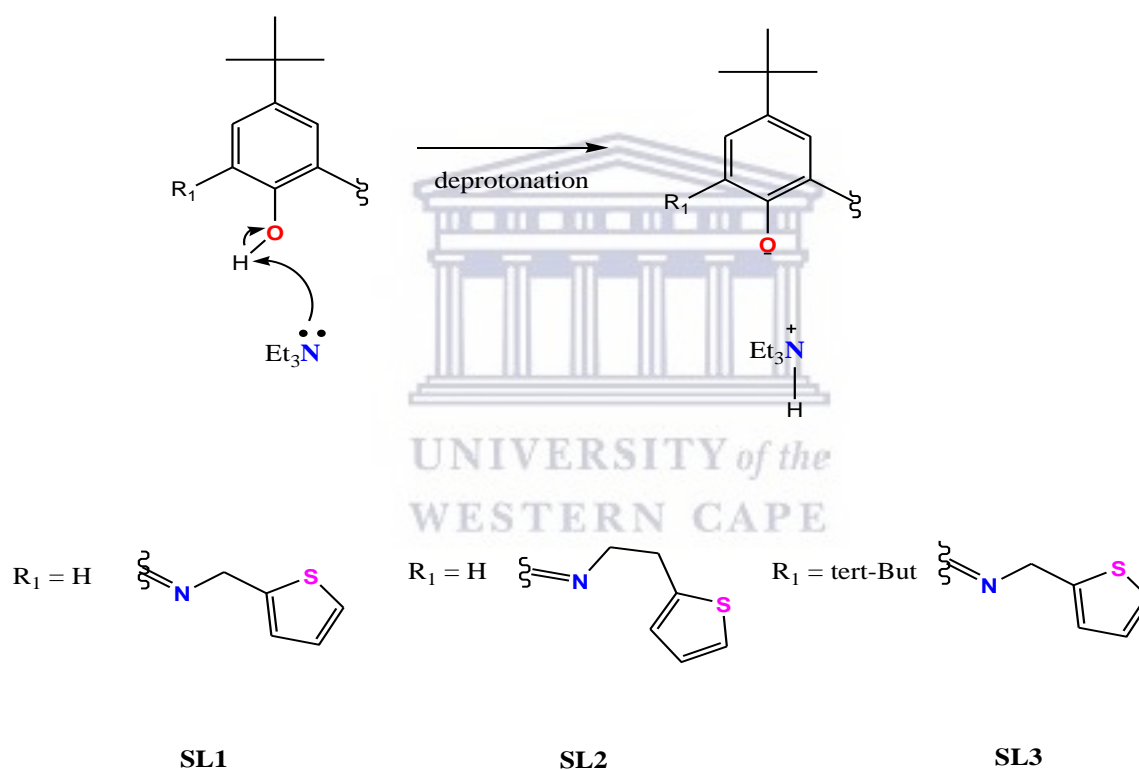


Figure 3.9: 1H NMR spectrum of the salicylaldiminato-ruthenium(II) complex **C9**, recorded in $CDCl_3$.

In the ^{13}C { 1H } NMR spectra of the salicylaldimine complexes **C7-C11**, the aromatic carbons were observed in the region 112-140 ppm. The observed chemical shifts of the imine protons and the aromatic protons was attributed to the influence modulated by the chelation of the imine nitrogen and phenolic oxygen to metal ions. The appearance of a downfield signal at 200 ppm for complex **C10** further confirmed the formation of a M-C σ -bond between the platinum ion and the C-3 of the heterocyclic moiety as observed with a series of thiophene-based ruthenacycles [65].



Scheme 3.8: Deprotonation mechanism of the phenolic proton for the salicylaldimine ligands, **SL¹-SL³**.

3.4.3 Elemental Analysis and Mass Spectroscopy, C7 - C11

The title complexes were subjected to micro-analysis and mass spectroscopy studies in order to gain insight about the percentage composition of the complexes and molecular, base peaks, respectively.

The chelation of the ligands to the metal precursors proceeds via deprotonation of the parent ligands leading to the formation of the by-product Et₃NH⁺Cl⁻ (*vide supra*, Scheme 3.8) as a by-product that is observable in the ¹H NMR. The ESI mass spectrometry data was consistent with the NMR spectroscopy data observed. The mass-to charge (m/z) data is in agreement with a loss of chloride ion {[M - Cl]}⁺, confirming the likelihood of salicylaldiminato complexes to lose a chloride atom as reported in the literature.

3.5 Single-Crystal X-ray diffraction

3.5.1 Crystal and molecular structures of complex C7 and C8

Suitable single x-ray crystals for the complexes [Cp*Rh^{III}Cl(SL¹)] (C7) and [Cp*Ir^{III}Cl(SL¹)] (C8) were achieved by slow evaporation of hexane into a concentrated solution of the complexes in DCM. The data collection and processing parameters for each the salicylaldimine complexes is summarized below (see Table 3.10) and selected bond angles and lengths are listed in Table 3.11. The pseudotetrahedral or “piano-stool” configuration around the neutral mononuclear [Cp*Rh^{III}Cl(SL¹)] (C7) and [Cp*Ir^{III}Cl(SL¹)] (C8) metal centres was confirmed by single-crystal x-ray diffraction studies. The metal complexes [Cp*Rh^{III}Cl(SL¹)] (C7) and [Cp*Ir^{III}Cl(SL¹)] (C8) crystallizes in monoclinic crystal system with *P21* space group. The coordination of the salicylaldiminato ligand SL¹ was shown to be bidentate, chelating through the deprotonated phenolic oxygen and the imine nitrogen

moieties (Figure 3.7). The molecular structure of the complexes further confirmed the stereogenic nature of the two neutral mononuclear complexes **C7** and **C8**. The Rh(1)–N(1) and Ir(1)–N(1) bond lengths are 2.078(5) Å for complex **C7** and 2.090(5) Å for complex **C8**, shorter than the reported complexes [(η⁵-C₅Me₅)RhCl(*S*-1-phenylethylsalicylaldimine)] [2.136(3) Å] and [(η⁵-C₅Me₅)IrCl(*S*-1-phenylethylsalicylaldimine)] [2.121(3) Å] [78]. The M–Cl bond lengths are 2.4062(17) Å (in **C7**) and 2.400(8) Å (in **C8**), which are closely comparable to those reported for poly-pyridyl rhodium complex cation [(η⁵-C₅Me₅)RhCl(4'-phenyl-2,2':6',2''-terpyridine)]⁺ [2.3984(1) Å] [79]. The M–C_{arene} bond distance for [Cp**Rh*^{III}Cl(**SL**¹)] (**C7**) 2.154(5) Å and [Cp**Ir*^{III}Cl(**SL**¹)] (**C8**) 2.1540(6) Å is comparable to the neutral ruthenium complexes [Cp**Ru*^{II}Cl(**SL**)] (**SL** = salicylaldimine) [2.154(15)] Å [80]. The bond distances of these salicylaldimine [Cp**Rh*^{III}Cl(**SL**¹)] (**C7**) and [Cp**Ir*^{III}Cl(**SL**¹)] (**C8**) complexes were in agreement with geometric parameters reported in the literature for similar salicylaldimineRh^{III} and Ir^{III} analogues [81-83].

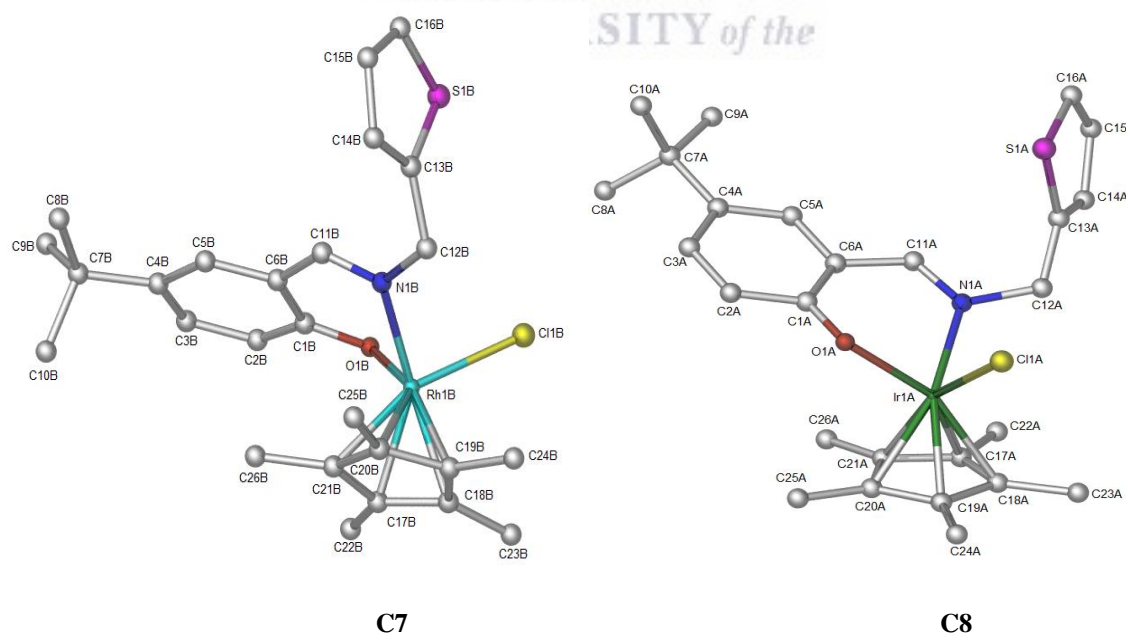


Figure 3.10: ORTEP representations of mononuclear ligand **C7**(left) and **C8** (right). Thermal ellipsoids are drawn at the 50 % probability level. Hydrogen atoms have been omitted for clarity.

Table 3.11: Data collection and selected parameters for the salicylaldimine complexes **C7** and **C8**

	C7	C8
Formula	C ₂₆ H ₃₃ ClNORh S	C ₂₆ H ₃₃ ClIrNOS
Formula weight	545.96	635.27
Crystal system, Space group	Monoclinic, <i>P21</i>	Monoclinic, <i>P21</i>
a (Å)	12.3089(14)	12.2823(6)
b (Å)	12.3391(12)	12.3773(6)
c (Å)	17.0088(19)	17.0339(8)
β (deg)	101.423(2)	100.9090(10)
V/Å ³	2532.1(5)	2542.7(2)
Z	4	4
D _c (g cm ⁻³)	1.432	1.660
μ (mm ⁻¹)	0.880	5.456
θ range for data collection (deg.)	1.2 to 28.4	1.9 to 28.4
no. of reflns meads	54904	12728
no. of reflns used (R _{int})	0.075	0.063
no. of params	575	575
Observed dataR [I > 2σ(I)]	10402	11739
R ₁	0.0416	0.0311
wR ₂	0.0810	0.0640
R (all data)		
R ₁	0.04	0.03
wR ₂	0.0810	0.063
Min. Max. Resd. Dens. [e/Å ³]	-0.92, 0.46	-1.48, 1.01

Table 3.12: Selected bond lengths [Å] and angles [°] for salicylaldimine complexes **C7** and **C8**.

Interatomic distances	C7	C8
M-N _{imine}	2.078(5)	2.090(5)
M-O	2.082(4)	2.083(5)
M-Cl	2.4062(17)	2.400(2)
M-C _{arene}	2.154(5)	2.1500(6)
Angles		
Cl-M-N _{imine}	89.62(14)	87.19(16)
Cl-M-O	88.30(11)	87.11(15)
O-M-N _{imine}	83.89(17)	84.1(2)

3.5.2 Crystal and molecular structure studies of complex **C10** and **C11**.

Suitable crystals for the two complexes were also obtained by slow diffusion of hexane into concentrated solution of DCM of the complexes. The complexes adopt a distorted square-planarity configuration. These Pt(II)-metal complexes Pt(**C10**) and Pt(**C11**) also crystallizes in monoclinic crystal system with *P21* space group. Selected bond distances and angles in complexes **C10** and **C11** are given in Table 3.12 and Table 3.13, respectively. The bond distances for Pt-N in **C10** and **C11** are within range for those observed in related reported complexes [84-91] although in **C10** the Pt-N bond distance (2.039(2) and 2.040(2) Å for **C11**, respectively, shorter than other reported platinum analogues 2.1662(15) Å and the Pt-C bond distance from the thiophenyl moiety of **C10** was 2.002(3) Å and it is observed to be within limits although a bit longer than the Pt-C bond distance [Pt₂(CH₃)₄(μ-S(CH₃)₂)₂] 1.9719(18) Å [92-94]. It is also worth noting that the Pt-N bond distance of 2.039(2) is

almost identical to the one found in Au-N, 2.035(4) Å, in [Au{C₆H₄(PPh₂=N(C₆H₅))₂}(PPh₃)] [95]. The Pt-O bond distance for the two metal complexes was 2.081(2) Å for **C10** and 2.0808(18) for **C11**, a bit shorter than the Pt (II) NHC complexes [Pt(C[^]C*)(O[^]O)] 2.116(16) Å but longer than 2.050(11) Å for the same series of cyclometallating ligands (C[^]C*) and β-diketonato auxiliary ligand (O[^]O). The distances Pt–X₁ and Pt–X₂ to the centroids of the C=C double bond character of the COD ligand are 2.1465(3) Å and 2.047(3) Å, respectively. This has been shown to be an indication that reflects the higher *trans* influence of O versus N (longer Pt–X₁ distance) [96].

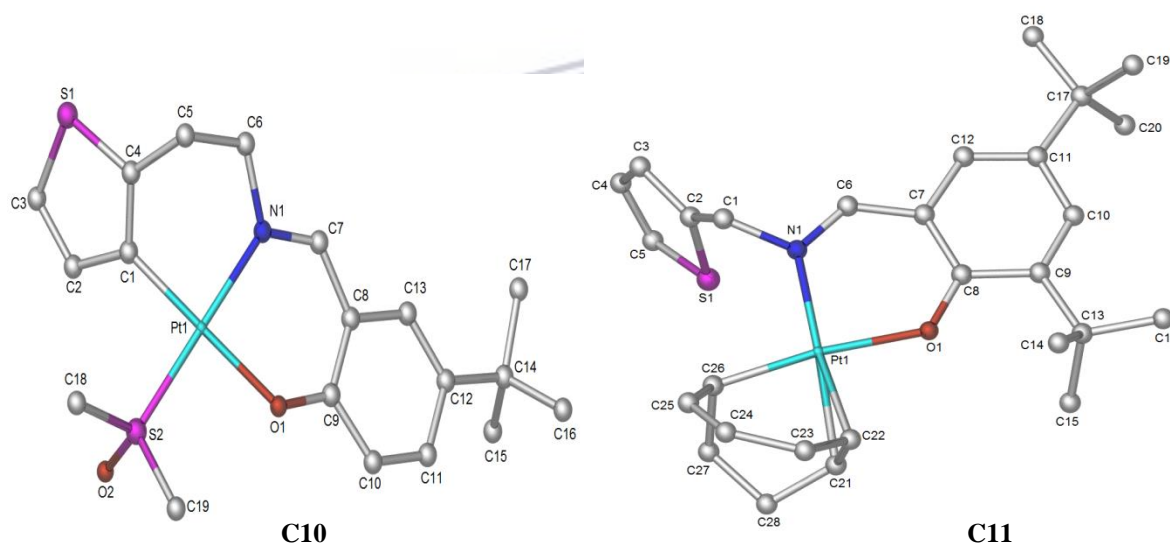


Figure 3.11: ORTEP representations of mononuclear ligand **C10** (left) and **C11** (right). Thermal ellipsoids are drawn at the 50 % probability level. Hydrogen atoms have been omitted for clarity.

Table 3.13: Data collection and selected parameters for the salicylaldimine complexes **C10** and **C11**

	C10	C11
Formula	C ₁₉ H ₂₅ NO ₂ PtS ₂	C ₂₈ H ₃₇ NOPtS
Formula weight	558.62	630.74
Crystal system, Space group	Monoclinic, P21/c	Monoclinic, P21/n
a (Å)	14.1436(8)	12.3077(12)
b (Å)	11.1982(6)	10.7551(11)
c (Å)	13.5302(7)	19.317(2)
β (deg)	112.4690(10)	95.585(2)
V/Å ³	1980.27(19)	2544.9(4)
Z	4	4
D _c (g cm ⁻³)	1.874	1.646
μ (mm ⁻¹)	7.309	5.616
θ range for data collection (deg.)	1.6 to 28.3	1.9 to 28.4
no. of reflns meads	4930	6386
no. of reflns used (R _{int})	0.057	0.058
no. of params	231	295
Observed data R [I > 2σ(I)]	4352	5559
R ₁	0.0198	0.0198
wR ₂	0.0455	0.0459
R (all data)		
R ₁	0.02	0.02
wR ₂	0.0455	0.0459
Min. Max. Resd. Dens. [e/Å ³]	-0.96, 1.18	-1.61, 0.72

Table 3.14: Selected bond lengths [Å] and angles [°] for salicylaldimine complexes **C10** and **C11**

Interatomic distances	C10	C11
M-N _{imine}	2.039(2)	2.040(2)
M-O	2.081(2)	2.0808(18)
M-C	2.002(3)	
M-S ₂	2.2091(8)	
M-X ₁ ^a		2.1465(3)
M-X ₂ ^a		2.047(3)
Angles		
X ₂ -M-N _{imine}	89.70(11)	96.53(10)
X ₁ -M-O	89.44(9)	90.31(9)
O-M-N _{imine}	89.93(6)	90.40(8)
S-M-O	91.11(9)	
X ₁ -M-X ₂		85.65(11)

^a = centroid distance between the C=C of 1,5-cyclooctadiene

3.6 Summary and Conclusion

A series of new salicylaldimine-2-((E)-((thiophen-2-yl)methylimino)methyl)-4-tert-butylphenol (**SL¹**), 2-((E)-(2-(thiophen-2-yl)ethylimino)methyl)-4-tert-butylphenol (**SL²**), -2-((E)-((thiophen-2-yl)methylimino)methyl)-4,6-di-tert-butylphenol (**SL³**) and azine ligands 1,2-bis(1-(5-methylthiophen-2-yl)ethylidene)hydrazine (**SL⁴**) and 1,2-bis(1-(5-bromothiophen-2-yl)ethylidene)hydrazine (**SL⁵**) have been successfully synthesized and characterized by a range of spectroscopic (¹H, ¹³C{¹H} NMR, Infrared, Mass Spectrometry) and analytical (C,N,O,S) techniques. Their structural formulations were further confirmed by

single crystal X-ray diffraction studies. The ligands were obtained as yellow crystalline solids in good yields. Corresponding novel salicylaldiminato [Cp*Rh^{III}Cl(SL¹)] (**C7**), [Cp*Ir^{III}Cl(SL²)] (**C8**), [Cp*Ru^{II}Cl(SL³)] (**C9**), [H(COD)Pt^{II}(SL³)] (**C11**) complexes and the terdentate C,N,O-[dmsopT^{II}(SL²)] (**C10**) platinacycle complex were also synthesized and thoroughly characterized using a combination of spectroscopic and analytical techniques. The proposed structural formulations and coordination modes, through the imine nitrogen and phenolic oxygen atoms, were further unequivocally affirmed by single crystal X-ray diffraction studies. The ortho activation in order to afford M-C complex **C10** was studied by FT-IR, ¹H, ¹³C{¹H} NMR and confirmed by single crystal X-ray. The complexes were obtained as air stable yellow-orange solids, in good yields.

3.7 Experimental

3.7.1 Chemistry

3.7.1.1 Materials and Methods

All reactions were carried out under nitrogen atmosphere using a dual vacuum/nitrogen line and standard Schlenk line techniques unless stated otherwise. All commercial chemicals, used herein, were purchased from Sigma Aldrich and used as received. The palladium and platinum metal precursors, MCl₂(COD) and *cis*-[M(II)Cl₂(DMSO)₂] (M = Pt) [59-61], [M(III)(η⁵-C₁₀H₁₅)(μ-Cl)₂Cl]₂ (M = Rh and Ir) [97] were prepared according to the established protocols reported in the literature. The Solvents were dried and purified by heating at reflux under nitrogen in the presence of a suitable drying agent. Dichloromethane was dried over phosphorus pentoxide while hexane was refluxed and distilled from calcium



hydride (CaH). Diethyl ether was dried over sodium wire and benzophenone under nitrogen while methanol and ethanol were dried from magnesium wire. Reaction progress and product mixtures were monitored by IR spectroscopy. Anhydrous magnesium sulphate (MgSO₄) was used for drying the organic layer in the aqueous extraction. NMR spectra were recorded on a Varian Inova 500 MHz (Lund University, Sweden) and 500 MHz Bruker (University of the Western Cape, South Africa) spectrometer using the solvent resonance as an internal standard for ¹H NMR and ¹³C NMR shifts. Infrared spectra were recorded on a Nicolet Avatar 360 FT-IR spectrometer (Lund University, Sweden).

3.8 Synthesis

3.8.1 General Synthesis of salicylaldimine ligands, **SL¹** - **SL³**.

A solution of 3-tert-butyl-2-hydroxybenzaldehyde/3,5-di-tert-butyl-2-hydroxybenzaldehyde (1 mmol) in methanol (5 ml) was stirred at room temperature and a solution of 2-thiophenemethylamine/2-thiopheneethylamine (1.1 mmol) in methanol (5 ml) was added to the solution dropwise. The colour of the reaction changed immediately to yellow and a precipitate formed. The reaction was monitored by TLC and was allowed to continue at room temperature for 12 hr. The precipitate was collected and washed with cold methanol and hexane. The solids were dried over CaCl₂ to obtain yellow crystalline solids after 24 hr.

3.8.1.1 2-((*E*)-((thiophen-2-yl)methylimino)methyl)-4-tert-butylphenol, **SL¹**

IR data (KBr, cm⁻¹) **SL¹**: 2955 ν(CO-H), 1634 ν(C=N), 1504 ν(C=C).

¹H NMR data (CDCl₃, ppm): 7.28 (1H, s), 7.13 (1H, d, *J* = 5.11 Hz), 6.99 (1H, s), 6.83–6.90 (2H, m), 6.66 (1H, s), 4.08 (2H, t, *J* = 6.40 Hz), 3.37 (1H, t, *J* = 6.37 Hz), 2.17 (3H, s). ¹³C

NMR (CDCl₃, ppm): 163.3 (C=N), 161.2 (C-OH), 158.2 (C-8), 142.1 (C-3), 140.3 (C-11), 127.3 (C-13), 126.9 (C-6), 126.2 (C-12), 125.6 (C-2), 119.1 (C-7), 55.3 (C-10), 41.4 (C-5), 33.1(C-4). Anal.Calc. ForC₁₆H₁₉NOS: C, 70.29; H, 7.00; N, 5.12; S, 11.73%. Found: C, 70.55; H, 7.08; N, 5.42; S, 11.65%. ESI-MS, *m/z*: 273{[M] + H}

3.8.1.2 2-((*E*)-(2-(thiophen-2-yl)ethylimino)methyl)-4-*tert*-butylphenol, **SL²**

IR data (KBr, cm⁻¹) **SL²**: 3050 ν (CO-H), 1644 ν (C=N), 1507 ν (C=C).

¹H NMR data (CDCl₃, ppm): 7.28 (1H, s), 7.13 (1H, d, *J* = 5.11 Hz), 6.99 (1H, s), 6.83–6.90 (2H, m), 6.66 (1H, s), 4.08 (2H, t, *J* = 6.40 Hz), 3.37 (2H, t, *J* = 6.37 Hz), 2.17 (3H, s). ¹³C

NMR (CDCl₃, ppm): 159.4 (C=N), 159.4 (C-OH), 157.8 (C-8), 143.2 (C-3), 127.3 (C-13), 126.9 (C-6), 126.2 (C-12), 125.6 (C-2), 119.1 (C-7), 65.1 (C-10), 38.4 (C-11), 33.1 (C-4).

Anal.Calc.For C₁₇H₂₁NOSC, 71.04; H, 7.36; N, 4.87; S, 11.16%. Found: C, 71.11; H, 7.30; N, 5.17; S, 11.08%. ESI-MS, *m/z*: 287{[M] + H}

UNIVERSITY of the
WESTERN CAPE

3.8.1.3 2-((*E*)-((thiophen-2-yl)methylimino)methyl)-4,6-*di-tert*-butylphenol, **SL³**

IR data (KBr, cm⁻¹) **SL³**: 2980 ν (CO-H), 1637 ν (C=N), 1505 ν (C=C).

¹H NMR data (CDCl₃, ppm): 7.28 (2H, s), 7.13 (1H, d, *J* = 5.11 Hz), 6.99 (1H, s), 6.83–6.90 (2H, m), 6.66 (1H, s), 4.08 (2H, t, *J* = 6.40 Hz), 3.37 (2H, t, *J* = 6.37 Hz), 2.17 (3H, s).

¹³CNMR (CDCl₃, ppm): 166.2 (C=N), 159.9 (C-OH), 155.2 (C-9), 141.1 (C-3), 139.3 (C-12), 137.1 (C-7), 126.8 (C-14), 126.6 (C-13), 126.2 (C-6), 123.3 (C-2). 55.3 (C-10), 42.1 (C-5), 34.2 (C-4), 33.9 (C-4'), 30.8 (C-8). Anal.Calc. For C₂₀H₂₇NOS: C, 72.90; H, 8.26; N, 4.25; S, 9.73%. Found: C, 72.83; H, 8.31; N, 4.55; S, 9.69%. ESI-MS, *m/z*: 330.47{[M] + H}

3.8.2 General synthesis of azine ligands, **SL⁴** and **SL⁵**.

3.8.2.1 1,2-bis(1-(5-methylthiophen-2-yl)ethylidene)hydrazine, **SL⁴**

IR data (KBr, cm^{-1}) **SL⁴**: 1646 $\nu(\text{C}=\text{N})$, 1504 $\nu(\text{C}=\text{C})$, 1319 $\nu(\text{C}-\text{S}-\text{C})$.

^1H NMR data (CDCl_3 , ppm): 7.28 (2H, s), 7.13 (2H, d, $J = 5.11$ Hz), 6.99 (2H, s), 6.83–6.90 (4H, m), 6.66 (2H, s), 4.08 (4H, t, $J = 6.40$ Hz), 3.37 (4H, t, $J = 6.37$ Hz), 2.17 (6H, s). ^{13}C NMR (CDCl_3 , ppm): 160.5 (C=N), 127.2 (C-3), 126.7 (C-4), 139.0 (C-5), 140.6 (C-2), 16.6 (C-6), 14.9 (C-8). Anal.Calc. For $\text{C}_{14}\text{H}_{16}\text{N}_2\text{S}_2$: C, 60.83; H, 5.83; N, 10.13%. Found: C, 60.84; H, 5.85; N, 10.43%. ESI-MS, m/z : 276{[M] + H}

3.8.2.2 1,2-bis(1-(5-bromothiophen-2-yl)ethylidene)hydrazine, **SL⁵**

IR data (KBr, cm^{-1}) **SL⁵**: 1640 $\nu(\text{C}=\text{N})$, 1507 $\nu(\text{C}=\text{N})$, 1322 $\nu(\text{C}-\text{S}-\text{C})$.

^1H NMR data (CDCl_3 , ppm): 7.28 (2H, s), 7.13 (2H, d, $J = 5.11$ Hz), 6.99 (2H, s), 6.83–6.90 (4H, m), 6.66 (2H, s), 4.08 (4H, t, $J = 6.40$ Hz), 3.37 (4H, t, $J = 6.37$ Hz), 2.17 (6H, s). ^{13}C NMR (CDCl_3 , ppm): 161.3 (C=N), 150.2 (C-5), 129.6 (C-3), 139.3 (C-2), 131.2 (C-4), 14.9 (C-7). Anal.Calc. For $\text{C}_{12}\text{H}_{10}\text{Br}_2\text{N}_2\text{S}_2$: C, 35.49; H, 2.48; N, 6.90%. Found: C, 35.53; H, 2.52; N, 7.20%. ESI-MS, m/z : 406{[M] + H}

3.8.3 General synthesis of $[\text{Cp}^*\text{Rh}^{\text{III}}\text{Cl}(\text{SL}^1)]$ (C7), $[\text{Cp}^*\text{Ir}^{\text{III}}\text{Cl}(\text{SL}^1)]$ (C8) and $[\text{Cp}^*\text{Ru}^{\text{II}}\text{Cl}(\text{SL}^2)]$ (C9) complexes

A methanolic solution (10mL) of the ligand (2 mmol, **SL¹** and 2 mmol **SL²**) and a methanolic (5 mL) solution of the base triethylamine (Et_3N , 2 mmol **SL¹** and 2 mmol **SL²**) were stirred at room temperature (rt) for 30 minutes in order to deprotonate the ligand. After that, 15 mL methanolic solution of the dimeric metal precursor (1 mmol) at rt, was added dropwise. There

was an immediate colour change and an orange-red precipitate formed. The reaction solution was kept at rt 12 hr. The precipitates was subsequently collected by filtration and washed with cold methanol several times and dried in a vacuum desiccator over anhydrous CaCl₂.

IR data (KBr, cm⁻¹) **C7**: 1624 ν(C=N), 1324 ν(C-S-C).

¹H NMR (500 MHz, CDCl₃) δ: 8.41 (s, 1H), 7.53 (s, 1H), 7.43 – 7.39 (m, 1H), 7.26 (s, 4H), 7.20 (dd, *J* = 8.8, 2.6 Hz, 1H), 7.09 (d, *J* = 3.7 Hz, 2H), 6.87 (d, *J* = 8.8 Hz, 1H), 6.72 (d, *J* = 2.5 Hz, 1H), 5.56 (s, 1H), 5.28 (s, 1H), 4.95 (s, 1H), 3.57 (q, *J* = 7.2 Hz, 2H), 3.08 (q, *J* = 7.3 Hz, 46H), 2.15 (s, 5H), 1.65 (s, 2H), 1.57 (s, 14H), 1.40 (dt, *J* = 14.7, 7.3 Hz, 70H), 1.17 (s, 9H). Anal. calc. for C₂₆H₃₃ClNORhS: C, 57.20; H, 6.09; N, 2.57; S, 5.87%. Found: C, 57.16; H, 6.01; N, 2.51; S, 5.80%. ESI-MS, *m/z*: 510.55{[M]⁺ - Cl}

IR data (KBr, cm⁻¹) **C8**: 1627 ν(C=N), 1322 ν(C-S-C).

¹H NMR (500 MHz, CDCl₃) δ: 7.45 (s, 1H), 7.44 – 7.41 (m, 1H), 7.28 – 7.24 (m, 3H), 7.12 – 7.09 (m, 2H), 6.82 (d, *J* = 8.8 Hz, 1H), 6.72 (d, *J* = 2.6 Hz, 1H), 5.57 (s, 1H), 5.29 (s, 1H), 3.59 (d, *J* = 7.3 Hz, 1H), 3.09 (q, *J* = 7.3 Hz, 9H), 2.16 (s, 1H), 1.58 (s, 16H), 1.41 (q, *J* = 7.2 Hz, 13H), 1.17 (s, 9H). Anal. calc. for C₂₆H₃₃ClNOIrS: C, 49.16; H, 5.24; N, 2.20; S, 5.05%. Found: C, 49.10; H, 5.20; N, 2.15; S, 4.98%. ESI-MS, *m/z*: 599.86{[M]⁺ - Cl}

IR data (KBr, cm⁻¹) **C9**: 1623 ν(C=N), 1320 ν(C-S-C).

¹H NMR (500 MHz, CDCl₃) δ 7.72 (s, 1H), 7.40 (dd, *J* = 5.1, 1.1 Hz, 1H), 7.26 (s, 1H), 7.24 (d, *J* = 2.6 Hz, 1H), 7.23 (d, *J* = 2.6 Hz, 1H), 7.14 (d, *J* = 2.7 Hz, 1H), 7.11 (dd, *J* = 5.0, 3.5 Hz, 1H), 6.90 (d, *J* = 8.9 Hz, 1H), 6.78 (d, *J* = 2.6 Hz, 1H), 5.56 (d, *J* = 15.6 Hz, 1H), 5.31 (d, *J* = 15.1 Hz, 3H), 5.18 (d, *J* = 5.7 Hz, 1H), 5.01 (d, *J* = 5.7 Hz, 1H), 3.09 (q, *J* = 7.2 Hz, 6H),

2.73 (hept, $J = 6.9$ Hz, 1H), 2.16 (s, 1H), 2.12 (s, 3H), 1.39 (t, $J = 7.2$ Hz, 9H), 1.22 – 1.13 (m, 13H), 1.07 (d, $J = 6.8$ Hz, 3H). Anal.calc. for $C_{26}H_{33}ClNORuS$: C, 60.13; H, 6.73; N, 2.34; S, 5.35%. Found: C, 59.06; H, 6.66; N, 2.29; S, 5.29%. ESI-MS, m/z : 563.82{[M]⁺- Cl}

3.8.3.1 Synthesis of platinacycle, (C10)

IR data (KBr, cm^{-1}) **C10**: 1630 ν (C=N), 1340 ν (C-S-C).

¹H NMR (500 MHz, $CDCl_3$) δ 11.74 (s, 7H), 7.81 (s, 1H), 7.32 (dd, $J = 8.9, 2.4$ Hz, 1H), 7.26 (s, 6H), 7.21 (d, $J = 4.1$ Hz, 1H), 7.12 – 7.06 (m, 2H), 6.94 – 6.91 (m, 1H), 6.88 (d, $J = 8.9$ Hz, 1H), 6.34 (s, 2H), 5.83 (d, $J = 36.8$ Hz, 3H), 5.62 (s, 1H), 5.11 (d, $J = 11.5$ Hz, 4H), 4.02 (s, 1H), 3.60 (q, $J = 7.2$ Hz, 3H), 3.11 (q, $J = 7.3$ Hz, 7H), 2.76 (d, $J = 19.4$ Hz, 2H), 2.49 – 2.35 (m, 2H), 1.93 (d, $J = 18.4$ Hz, 6H), 1.43 (dt, $J = 26.2, 7.3$ Hz, 10H), 1.26 (s, 12H). Anal.calc. for $C_{26}H_{33}ClNORuS$: C, 40.85; H, 4.51; N, 2.51; S, 11.48%. Found: C, 40.81; H, 4.46; N, 2.50; S, 11.40%. ESI-MS, m/z : 558.14 {[M] + H}

3.8.3.2 Synthesis of [Pt^{II}SL³(HCOD)] **C11**

IR data (KBr, cm^{-1}) **C11**: 1627 ν (C=N), 1324 ν (C-S-C).

¹H NMR (500 MHz, $CDCl_3$) δ 13.05 (s, 2H), 10.87 (s, 1H), 9.90 (s, 1H), 8.30 (s, 4H), 8.21 (s, 1H), 7.59 (dd, $J = 8.7, 2.4$ Hz, 1H), 7.53 – 7.47 (m, 5H), 7.35 (dd, $J = 8.6, 2.4$ Hz, 4H), 7.26 (s, 3H), 7.20 (d, $J = 2.4$ Hz, 4H), 7.15 (dt, $J = 5.6, 3.6$ Hz, 6H), 6.99 – 6.87 (m, 13H), 6.85 (d, $J = 2.6$ Hz, 4H), 6.80 (d, $J = 8.9$ Hz, 2H), 5.30 (s, 1H), 3.87 (t, $J = 6.8$ Hz, 8H), 3.82 – 3.75 (m, 4H), 3.42 – 3.36 (m, 13H), 3.27 – 3.18 (m, 10H), 2.98 (dd, $J = 11.4, 6.1$ Hz, 4H), 1.59 (s, 5H), 1.28 (dt, $J = 14.5, 11.7$ Hz, 78H). Anal.calc. for $C_{26}H_{33}ClNORuS$: C, 53.23; H, 6.06; N, 2.22; S, 5.08%. Found: C, 53.15; H, 4.98; N, 2.25; S, 5.00%. ESI-MS, m/z : 630.78 {[M] + H}

3.9 References

- [1] H. Schiff, "Mittheilungen aus dem Universitätslaboratorium in Pisa: Eine neue Reihe organischer Basen," *Ann. der Chemie und Pharm.*, vol. 131, no. 1, pp. 118–119, 1864.
- [2] P. G. Cozzi, "Metal-Salen Schiff base complexes in catalysis: practical aspects," *Chem. Soc. Rev.*, vol. 33, no. 7, pp. 410–21, Sep. 2004.
- [3] C. M. Che and J. S. Huang, "Metal complexes of chiral binaphthyl Schiff-base ligands and their application in stereoselective organic transformations," *Coord. Chem. Rev.*, vol. 242, no. 1–2, pp. 97–113, 2003.
- [4] K. Binnemans, D. W. Bruce, S. R. Collinson, R. V. Deun, Y. G. Galyametdinov, and F. Martin, "Towards magnetic liquid crystals," *Philos. Trans. R. Soc. A Math. Phys. Eng. Sci.*, vol. 357, no. 1762, pp. 3063–3077, Nov. 1999.
- [5] N. Hoshino, "Liquid crystal properties of metal-salicylaldimine complexes. Chemical modifications towards lower symmetry," *Coord. Chem. Rev.*, vol. 174, pp. 77–108, 1998.
- [6] R. W. Date, E. F. Iglesias, K. E. Rowe, J. M. Elliott, and D. W. Bruce, "Metallomesogens by ligand design Based on the presentation given at Dalton Discussion No. 5, 10–12th April 2003, Noordwijkerhout, The Netherlands," *Dalt. Trans.*, no. 10, p. 1914, May 2003.
- [7] T. C. O. Mac Leod, V. P. Barros, A. L. Faria, M. A. Schiavon, I. V. P. Yoshida, M. E. C. Queiroz, and M. D. Assis, "Jacobsen catalyst as a P450 biomimetic model for the oxidation of an antiepileptic drug," *J. Mol. Catal. A Chem.*, vol. 273, no. 1–2, pp. 259–264, Aug. 2007.
- [8] A. M. D. C. Ferreira, M. L. P. Dos Santos, E. M. Pereira, M. O. Damasceno, and W.

- A. Alves, "Mimics of copper proteins: structural and functional aspects," *An. Acad. Bras. Cienc.*, vol. 72, no. 1, pp. 51–58, Mar. 2000.
- [9] E.-G. Jäger, J. Knautd, M. Rudolph, and M. Rost, "Activation of Molecular Oxygen by Biomimetic Schiff Base Complexes of Manganese, Iron, and Cobalt," *Chem. Ber.*, vol. 129, no. 9, pp. 1041–1047, Sep. 1996.
- [10] S. K. Z H Chohan, "Synthesis, Characterization and Biological Properties of Tridentate NNO, NNS and NNN Donor Thiazole-Derived Furanyl, Thiophenyl and Pyrrolyl Schiff Bases and Their Co(II), Cu(II), Ni(II) and Zn(II) Metal Chelates.," *Met Based Drugs*, vol. 1, no. 7, pp. 17–22, 2000.
- [11] C. T. S. Zahid H Chohan, Abdul Rau, Sobia Noreen, Andrea Scozzafava, "Antibacterial cobalt(II), nickel(II) and zinc(II) complexes of nicotinic acid-derived Schiff-bases.," *J Enzym. Inhib Med Chem*, vol. 2, no. 17, pp. 101–6, 2002.
- [12] C. T. S. Zahid H Chohan, Humayun Pervez, Abdul Rauf, Khalid M Khan, "Antibacterial cobalt (II), copper (II), nickel (II) and zinc (II) complexes of mercaptothiadiazole--derived furanyl, thienyl, pyrrolyl, salicylyl and pyridinyl Schiff bases.," *J Enzym. Inhib Med Chem*, vol. 21, no. 2, pp. 193–201, 2002.
- [13] C. T. S. Z H Chohan, M F Jaffery, "Antibacterial Co(II), Cu(II), Ni(II) and Zn(II) complexes of thiadiazole derived furanyl, thiophenyl and pyrrolyl Schiff bases.," *Met Based Drugs*, vol. 2, no. 2, pp. 95–101, 2001.
- [14] C. T. S. Z H Chohan, M F Jaffery, "Antibacterial Co(II), Cu(II), Ni(II) and Zn(II) Complexes of Thiadiazoles Schiff Bases.," *Met Based Drugs*, vol. 1, no. 7, pp. 95–101, 2001.
- [15] S. A. Turner, Z. D. Remillard, D. T. Gijima, E. Gao, R. D. Pike, and C. Goh,

- “Syntheses and structures of closely related copper(I) complexes of tridentate (2-pyridylmethyl)imine and (2-pyridylmethyl)amine ligands and their use in mediating atom transfer radical polymerizations.” *Inorg. Chem.*, vol. 51, no. 20, pp. 10762–73, Oct. 2012.
- [16] Y. Lee, D.-H. Lee, G. Y. Park, H. R. Lucas, A. A. Narducci Sarjeant, M. T. Kieber-Emmons, M. A. Vance, A. E. Milligan, E. I. Solomon, and K. D. Karlin, “Sulfur donor atom effects on copper(I)/O(2) chemistry with thioanisole containing tetradentate N(3)S ligand leading to μ -1,2-peroxo-dicopper(II) species.” *Inorg. Chem.*, vol. 49, no. 19, pp. 8873–85, Oct. 2010.
- [17] B. K. Santra, P. A. N. Reddy, M. Nethaji, and A. R. Chakravarty, “Structural model for the CuB site of dopamine β -hydroxylase and peptidylglycine α -hydroxylating monooxygenase: crystal structure of a copper(ii) complex showing N3OS coordination and axial sulfur ligation,” *J. Chem. Soc. Dalt. Trans.*, no. 24, pp. 3553–3555, Dec. 2001.
- [18] B. K. Santra, P. A. N. Reddy, M. Nethaji, and A. R. Chakravarty, “Structural Model for the Cu B Site of Dopamine β -Hydroxylase: Crystal Structure of a Copper(II) Complex Showing N 3 OS Coordination with an Axial Sulfur Ligation,” *Inorg. Chem.*, vol. 41, no. 5, pp. 1328–1332, Mar. 2002.
- [19] S. Chandra, S. Gautam, H. K. Rajor, and R. Bhatia, “Syntheses, spectroscopic characterization, thermal study, molecular modeling, and biological evaluation of novel Schiff’s base benzil bis(5-amino-1,3,4-thiadiazole-2-thiol) with Ni(II), and Cu(II) metal complexes.” *Spectrochim. Acta. A. Mol. Biomol. Spectrosc.*, vol. 137, pp. 749–60, Feb. 2015.

- [20] R. Alizadeh, M. Afzal, and F. Arjmand, "In vitro DNA binding, pBR322 plasmid cleavage and molecular modeling study of chiral benzothiazole Schiff-base-valine Cu(II) and Zn(II) complexes to evaluate their enantiomeric biological disposition for molecular target DNA.," *Spectrochim. Acta. A. Mol. Biomol. Spectrosc.*, vol. 131, pp. 625–35, Oct. 2014.
- [21] A. Balaban Gündüzalp, N. Özbek, and N. Karacan, "Synthesis, characterization, and antibacterial activity of the ligands including thiophene/furan ring systems and their Cu(II), Zn(II) complexes," *Med. Chem. Res.*, vol. 21, no. 11, pp. 3435–3444, Nov. 2011.
- [22] M. C. Heffern, J. W. Kurutz, and T. J. Meade, "Spectroscopic elucidation of the inhibitory mechanism of Cys2His2 zinc finger transcription factors by cobalt(III) Schiff base complexes.," *Chemistry*, vol. 19, no. 50, pp. 17043–53, Dec. 2013.
- [23] A. M. Isloor, B. Kalluraya, and K. Sridhar Pai, "Synthesis, characterization and biological activities of some new benzo[b]thiophene derivatives.," *Eur. J. Med. Chem.*, vol. 45, no. 2, pp. 825–30, Feb. 2010.
- [24] E. Pinto, M.-J. R. P. Queiroz, L. A. Vale-Silva, J. F. Oliveira, A. Begouin, J.-M. Begouin, and G. Kirsch, "Antifungal activity of synthetic di(hetero)arylamines based on the benzo[b]thiophene moiety.," *Bioorg. Med. Chem.*, vol. 16, no. 17, pp. 8172–7, Sep. 2008.
- [25] M. A. Gouda, M. A. Berghot, G. E. Abd El-Ghani, and A. M. Khalil, "Synthesis and antimicrobial activities of some new thiazole and pyrazole derivatives based on 4,5,6,7-tetrahydrobenzothiophene moiety.," *Eur. J. Med. Chem.*, vol. 45, no. 4, pp. 1338–45, Apr. 2010.

- [26] D. T. McQuade, A. E. Pullen, and T. M. Swager, "Conjugated Polymer-Based Chemical Sensors," *Chem. Rev.*, vol. 100, no. 7, pp. 2537–2574, Jul. 2000.
- [27] M. Sebastian, M. Hissler, C. Fave, J. Rault-Berthelot, C. Odin, and R. Réau, "Phosphole-modified poly(thiophene): unique postfunctionalizable conjugated polymers that sense elemental chalcogenides.," *Angew. Chem. Int. Ed. Engl.*, vol. 45, no. 37, pp. 6152–5, Sep. 2006.
- [28] D. M. Vriezema, J. Hoogboom, K. Velonia, K. Takazawa, P. C. M. Christianen, J. C. Maan, A. E. Rowan, and R. J. M. Nolte, "Vesicles and polymerized vesicles from thiophene-containing rod-coil block copolymers.," *Angew. Chem. Int. Ed. Engl.*, vol. 42, no. 7, pp. 772–6, Feb. 2003.
- [29] M. Halik, H. Klauk, U. Zschieschang, G. Schmid, S. Ponomarenko, S. Kirchmeyer, and W. Weber, "Relationship Between Molecular Structure and Electrical Performance of Oligothiophene Organic Thin Film Transistors," *Adv. Mater.*, vol. 15, no. 11, pp. 917–922, Jun. 2003.
- [30] Y. M. Sun, Y. Q. Ma, Y. Q. Liu, Y. Y. Lin, Z. Y. Wang, Y. Wang, C. A. Di, K. Xiao, X. M. Chen, W. F. Qiu, B. Zhang, G. Yu, W. P. Hu, and D. B. Zhu, "High-Performance and Stable Organic Thin-Film Transistors Based on Fused Thiophenes," *Adv. Funct. Mater.*, vol. 16, no. 3, pp. 426–432, Feb. 2006.
- [31] C. Wu, E. R. Decker, N. Blok, H. Bui, T. J. You, J. Wang, A. R. Bourgoyne, V. Knowles, K. L. Berens, G. W. Holland, T. A. Brock, and R. A. F. Dixon, "Discovery, modeling, and human pharmacokinetics of *N*-(2-acetyl-4,6-dimethylphenyl)-3-(3,4-dimethylisoxazol-5-ylsulfamoyl)thiophene-2-carboxamide (TBC3711), a second generation, ETA selective, and orally bioavailable endothelin antagonist.," *J. Med.*

- Chem.*, vol. 47, no. 8, pp. 1969–86, Apr. 2004.
- [32] K. Doré, S. Dubus, H.-A. Ho, I. Lévesque, M. Brunette, G. Corbeil, M. Boissinot, G. Boivin, M. G. Bergeron, D. Boudreau, and M. Leclerc, “Fluorescent polymeric transducer for the rapid, simple, and specific detection of nucleic acids at the zeptomole level,” *J. Am. Chem. Soc.*, vol. 126, no. 13, pp. 4240–4, Apr. 2004.
- [33] K. Doré, M. Leclerc, and D. Boudreau, “Investigation of a fluorescence signal amplification mechanism used for the direct molecular detection of nucleic acids,” *J. Fluoresc.*, vol. 16, no. 2, pp. 259–65, Mar. 2006.
- [34] A. B. Powell, J. R. Brown, K. V Vasudevan, and A. H. Cowley, “Facile syntheses of thiophene-substituted 1,4-diazabutadiene (alpha-diimine) ligands and their conversion to phosphonium triiodide salts,” *Dalton Trans.*, no. 14, pp. 2521–7, Apr. 2009.
- [35] T. Janosik and J. Bergman, “Chapter 5.1: Five-Membered Ring Systems: Thiophenes and Se/Te Analogues,” in *Progress in Heterocyclic Chemistry*, vol. 21, 2009, pp. 115–144.
- [36] Y.-F. Tzeng, C.-Y. Wu, W.-S. Hwang, and C.-H. Hung, “Reactions of N-(2-thienylmethylidene)-2-thienylmethylamine derivatives with diiron nonacarbonyl: Characterization and structures of cyclometallated diiron complexes $\text{Fe}^2(\text{CO})^6(\text{R}-\text{C}^4\text{HS}-\text{CH}^2\text{NCH}^2-\text{C}^4\text{H}^3\text{S})$ and linear tetrairon clusters $\text{Fe}^4(\text{CO})^{10}(\text{R}-\text{C}^4\text{HS}-\text{CH}=\text{NCH}^2-\text{C}^4\text{H}^3\text{S})^2$,” *J. Organomet. Chem.*, vol. 687, no. 1, pp. 16–26, Dec. 2003.
- [37] W. Hwang, “Reactions of cyclometalated carbonyliron complex derived from thienyl Schiff base,” *J. Organomet. Chem.*, vol. 613, no. 2, pp. 231–235, Nov. 2000.
- [38] S. Kundu, S. Biswas, A. S. Mondal, P. Roy, and T. K. Mondal, “Template synthesis of square-planar Ni(II) complexes with new thiophene appended Schiff base ligands:

- Characterization, X-ray structure and DFT calculation,” *J. Mol. Struct.*, vol. 1100, pp. 27–33, Nov. 2015.
- [39] H. H. Freedman, “Intramolecular H-Bonds. I. A Spectroscopic Study of the Hydrogen Bond between Hydroxyl and Nitrogen,” *J. Am. Chem. Soc.*, vol. 83, no. 13, pp. 2900–2905, Jul. 1961.
- [40] W. M. Motswainyana and M. O. Onani, “New phenylene bridged binuclear bis (imino-quinolyl) palladium (II) complexes: Synthesis, characterization and Heck reactions,” *Inorg. Chem. Commun.*, vol. 24, pp. 221–224, 2012.
- [41] W. M. Motswainyana, S. O. Ojwach, M. O. Onani, E. I. Iwuoha, and J. Darkwa, “Novel hemi-labile pyridyl-imine palladium complexes: Synthesis, molecular structures and reactions with ethylene,” *Polyhedron*, vol. 30, no. 15, pp. 2574–2580, Sep. 2011.
- [42] C. López, S. Pérez, X. Solans, M. Font-Bardía, A. Roig, and E. Molins, “Heterodimetallic Palladium(II) Complexes with Bidentate (N,S) or Terdentate (C,N,S) - Ferrocenyl Ligands. The Effect of the Ligand Donor Atoms on the Regioselectivity of the Allylic Alkylation of Cinnamyl Acetate,” *Organometallics*, vol. 26, no. 3, pp. 571–576, Jan. 2007.
- [43] X. R. Bu, C. R. Jackson, D. Van Derveer, X. Z. You, Q. J. Meng, and R. X. Wang, “New copper(II) complexes incorporating unsymmetrical tetradentate ligands with cis-N₂O₂ chromophores: synthesis, molecular structure, substituent effect and thermal stability,” *Polyhedron*, vol. 16, no. 17, pp. 2991–3001, Jan. 1997.
- [44] W. Zhang, W.-H. Sun, B. Wu, S. Zhang, H. Ma, Y. Li, J. Chen, and P. Hao, “Synthesis of palladium complexes containing 2-methoxycarbonyl-6-iminopyridine ligand and

- their catalytic behaviors in reaction of ethylene and norbornene,” *J. Organomet. Chem.*, vol. 691, no. 22, pp. 4759–4767, Nov. 2006.
- [45] D. Pou, A. E. Platero-Prats, S. Pérez, C. López, X. Solans, M. Font-Bardía, P. W. N. M. van Leeuwen, G. P. F. van Strijdonck, and Z. Freixa, “Schiff bases containing ferrocenyl and thienyl units and their utility in the palladium catalyzed allylic alkylation of cinnamyl acetate,” *J. Organomet. Chem.*, vol. 692, no. 22, pp. 5017–5025, Oct. 2007.
- [46] C. G. Hamaker and D. P. Halbach, “Synthesis, structure, and characterization of some ruthenium arene complexes of N-(arylmethylene)-2-(methylthio)anilines and 2-(methylthio)aniline,” *Inorganica Chim. Acta*, vol. 359, no. 3, pp. 846–852, Feb. 2006.
- [47] D. P. Halbach and C. G. Hamaker, “Synthesis, characterization, and X-ray structural analysis of some half-sandwich ruthenium(II) arene complexes with new N,S-donor Schiff base ligands,” *J. Organomet. Chem.*, vol. 691, no. 15, pp. 3349–3361, Jul. 2006.
- [48] M. Kalita, T. Bhattacharjee, P. Gogoi, P. Barman, R. D. Kalita, B. Sarma, and S. Karmakar, “Synthesis, characterization, crystal structure and bioactivities of a new potential tridentate (ONS) Schiff base ligand N-[2-(benzylthio) phenyl] salicylaldimine and its Ni(II), Cu(II) and Co(II) complexes,” *Polyhedron*, vol. 60, pp. 47–53, Aug. 2013.
- [49] H. H. Monfared, O. Pournalimardan, and C. Janiak, “Synthesis and Spectral Characterization of Hydrazone Schiff Bases Derived from 2,4-Dinitrophenylhydrazine. Crystal Structure of Salicylaldehyde-2,4-Dinitrophenylhydrazone,” *Zeitschrift für Naturforsch. B*, vol. 62, no. 5, Jan. 2007.
- [50] X.-J. Yang, F. Drepper, B. Wu, W.-H. Sun, W. Haehnel, and C. Janiak, “From model

- compounds to protein binding: syntheses, characterizations and fluorescence studies of [RuII(bipy)(terpy)L]²⁺ complexes (bipy = 2,2'-bipyridine; terpy = 2,2':6',2''-terpyridine; L = imidazole, pyrazole and derivatives, cytochrome c).” *Dalton Trans.*, no. 2, pp. 256–67, Jan. 2005.
- [51] M. Nishio, “CH/π hydrogen bonds in crystals,” *CrystEngComm*, vol. 6, no. 27, p. 130, May 2004.
- [52] M. Nishio, Y. Umezawa, K. Honda, S. Tsuboyama, and H. Suezawa, “CH/π hydrogen bonds in organic and organometallic chemistry,” *CrystEngComm*, vol. 11, no. 9, p. 1757, Aug. 2009.
- [53] and Y. U. Minoru Hirota, Motohiro Nishio, *Wiley: The CH/π Interaction: Evidence, Nature, and Consequences - Motohiro Nishio, Minoru Hirota, Yoji Umezawa*. 1998.
- [54] Y. Umezawa, S. Tsuboyama, H. Takahashi, J. Uzawa, and M. Nishio, “interaction in the conformation of organic compounds. A database study,” *Tetrahedron*, vol. 55, no. 33, pp. 10047–10056, Aug. 1999.
- [55] Y. Umezawa, S. Tsuboyama, K. Honda, J. Uzawa, and M. Nishio, “CH/π Interaction in the Crystal Structure of Organic Compounds. A Database Study.” *Bull. Chem. Soc. Jpn.*, vol. 71, no. 5, pp. 1207–1213, Feb. 1998.
- [56] C. Janiak, S. Temizdemir, S. Dechert, W. Deck, F. Girgsdies, J. Heinze, M. J. Kolm, T. G. Scharmann, and O. M. Zipffel, “Binary [Hydrotris(indazol- 1- yl)borato]metal Complexes, M(Tp^{4B0})₂^[1] with M = Fe, Co, Ni, Cu, and Zn: Electronic Properties and Solvent- Dependent Framework Structures through C–H···π Interactions,” *Eur. J. Inorg. Chem.*, vol. 2000, no. 6, pp. 1229–1241, Jun. 2000.
- [57] T. Dorn, A.-C. Chamayou, and C. Janiak, “Hydrophilic interior between hydrophobic

- regions in inverse bilayer structures of cation-1,1'-binaphthalene-2,2'-diyl phosphate salts," *New J. Chem.*, vol. 30, no. 2, pp. 156–167, Feb. 2006.
- [58] M. K. Bin Break, M. I. M. Tahir, K. A. Crouse, and T.-J. Khoo, "Synthesis, Characterization, and Bioactivity of Schiff Bases and Their Cd(2+), Zn(2+), Cu(2+), and Ni(2+) Complexes Derived from Chloroacetophenone Isomers with S-Benzylidithiocarbamate and the X-Ray Crystal Structure of S-Benzyl-β-N-(4-chlorophenyl)methylenedithiocarbamate," *Bioinorg. Chem. Appl.*, vol. 2013, p. 1-13, Jan. 2013.
- [59] J. Wiedermann, K. Mereiter, and K. Kirchner, "Palladium imine and amine complexes derived from 2-thiophenecarboxaldehyde as catalysts for the Suzuki cross-coupling of aryl bromides," *J. Mol. Catal. A Chem.*, vol. 257, no. 1–2, pp. 67–72, Sep. 2006.
- [60] J. H. Price, A. N. Williamson, R. F. Schramm, and B. B. Wayland, "Palladium(II) and platinum(II) alkyl sulfoxide complexes. Examples of sulfur-bonded, mixed sulfur- and oxygen-bonded, and totally oxygen-bonded complexes," *Inorg. Chem.*, vol. 11, no. 6, pp. 1280–1284, Jun. 1972.
- [61] M. M. Szafran, Zvi; Pike, Ronald M.; Singh, "Microscale Inorganic Chemistry: a Comprehensive Laboratory Experience by Szafran, Zvi; Pike, Ronald M; Singh, Mono M - AbeBooks," *Wiley*, 1991. [Online]. Available: <http://www.abebooks.com/book-search/isbn/0471619965/>. [Accessed: 15-Oct-2015].
- [62] Z.-Q. Feng, X.-L. Yang, and Y.-F. Ye, "Pd(II) and Zn(II) based complexes with Schiff base ligands: synthesis, characterization, luminescence, and antibacterial and catalytic activities.," *Scientific World Journal.*, vol. 2013, p. 956840, Jan. 2013.
- [63] M. A. Bennett and A. K. Smith, "Arene ruthenium(II) complexes formed by

- dehydrogenation of cyclohexadienes with ruthenium(III) trichloride,” *J. Chem. Soc. Dalton Trans.*, no. 2, p. 233, Jan. 1974.
- [64] M. A. Bennett, T. W. Matheson, G. B. Robertson, A. K. Smith, and P. A. Tucker, “Highly fluxional arene cyclooctatetraene complexes of zerovalent iron, ruthenium, and osmium. Single-crystal x-ray study of (cyclooctatetraene)(hexamethylbenzene)ruthenium(0), $Ru(\eta^6\text{HMB})(1\text{-}4\text{-}\eta^4\text{-COT})$,” *Inorg. Chem.*, vol. 19, no. 4, pp. 1014–1021, Apr. 1980.
- [65] L. Cuesta, I. Maluenda, T. Soler, R. Navarro, and E. P. Urriolabeitia, “Novel thiophene-based cycloruthenated compounds: synthesis, characterization, and reactivity,” *Inorg. Chem.*, vol. 50, no. 1, pp. 37–45, Jan. 2011.
- [66] A. Caires, “Recent Advances Involving Palladium (II) Complexes for the Cancer Therapy,” *Anticancer. Agents Med. Chem.*, vol. 7, no. 5, pp. 484–491, Sep. 2007.
- [67] H. P. Dijkstra, M. D. Meijer, J. Patel, R. Kreiter, G. P. M. van Klink, M. Lutz, A. L. Spek, A. J. Canty, and G. van Koten, “Design and Performance of Rigid Nanosize Multimetallic Cartwheel Pincer Compounds as Lewis-Acid Catalysts,” *Organometallics*, vol. 20, no. 14, pp. 3159–3168, Jul. 2001.
- [68] S. P. Fricker, “Cysteine proteases as targets for metal-based drugs,” *Metallomics*, vol. 2, no. 6, pp. 366–77, Jun. 2010.
- [69] M. R. Crimmin, D. A. Colby, J. A. Ellman, and R. G. Bergman, “Synthesis and coordination chemistry of tri-substituted benzamidrazones,” *Dalton Trans.*, vol. 40, no. 2, pp. 514–22, Jan. 2011.
- [70] G. Gasser, I. Ott, and N. Metzler-Nolte, “Organometallic anticancer compounds,” *J. Med. Chem.*, vol. 54, no. 1, pp. 3–25, Jan. 2011.

- [71] P. Chellan, K. M. Land, A. Shokar, A. Au, S. H. An, D. Taylor, P. J. Smith, K. Chibale, and G. S. Smith, "Di- and Trinuclear Ruthenium-, Rhodium-, and Iridium-Functionalized Pyridyl Aromatic Ethers: A New Class of Antiparasitic Agents," *Organometallics*, vol. 32, no. 17, pp. 4793–4804, Sep. 2013.
- [72] J. J. Yan, A. L.-F. Chow, C.-H. Leung, R. W.-Y. Sun, D.-L. Ma, and C.-M. Che, "Cyclometalated gold(III) complexes with N-heterocyclic carbene ligands as topoisomerase I poisons.," *Chem. Commun. (Camb)*, vol. 46, no. 22, pp. 3893–5, Jun. 2010.
- [73] S.-K. Leung, K. Y. Kwok, K. Y. Zhang, and K. K.-W. Lo, "Design of luminescent biotinylation reagents derived from cyclometalated iridium(III) and rhodium(III) bis(pyridylbenzaldehyde) complexes.," *Inorg. Chem.*, vol. 49, no. 11, pp. 4984–95, Jun. 2010.
- [74] P.-K. Lee, H.-W. Liu, S.-M. Yiu, M.-W. Louie, and K. K.-W. Lo, "Luminescent cyclometallated iridium(III) bis(quinolylbenzaldehyde) diimine complexes--synthesis, photophysics, electrochemistry, protein cross-linking properties, cytotoxicity and cellular uptake.," *Dalton Trans.*, vol. 40, no. 10, pp. 2180–9, Mar. 2011.
- [75] W. Kandioller, C. G. Hartinger, A. A. Nazarov, C. Bartel, M. Skocic, M. A. Jakupec, V. B. Arion, and B. K. Keppler, "Maltol-derived ruthenium-cymene complexes with tumor inhibiting properties: the impact of ligand-metal bond stability on anticancer activity in vitro.," *Chemistry*, vol. 15, no. 45, pp. 12283–91, Nov. 2009.
- [76] J.-P. Djukic, J.-B. Sortais, L. Barloy, and M. Pfeffer, "Cycloruthenated Compounds - Synthesis and Applications," *Eur. J. Inorg. Chem.*, vol. 2009, no. 7, pp. 817–853, Mar. 2009.

- [77] R. Cortés, M. Crespo, L. Davin, R. Martín, J. Quirante, D. Ruiz, R. Messeguer, C. Calvis, L. Baldomà, J. Badia, M. Font-Bardía, T. Calvet, and M. Cascante, "Seven-membered cycloplatinated complexes as a new family of anticancer agents. X-ray characterization and preliminary biological studies.," *Eur. J. Med. Chem.*, vol. 54, pp. 557–66, Aug. 2012.
- [78] H. Brunner, A. Köllnberger, T. Burgemeister, and M. Zabel, "Optically active transition metal complexes," *Polyhedron*, vol. 19, no. 12, pp. 1519–1526, Jun. 2000.
- [79] H. Aneetha, P. . Zacharias, B. Srinivas, G. . Lee, and Y. Wang, "Synthesis and characterization of Cp* Rh (III) and Ir (III) polypyridyl complexes:," *Polyhedron*, vol. 18, no. 1–2, pp. 299–307, Dec. 1998.
- [80] N. Goswami, R. Alberto, C. L. Barnes, and S. Jurisson, "Rhodium(III) Complexes with Acyclic Tetrathioether Ligands. Effects of Backbone Chain Length on the Conformation of the Rh(III) Complex," *Inorg. Chem.*, vol. 35, no. 26, pp. 7546–7555, 1996.
- [81] A. R. Burgoyne, B. C. E. Makhubela, M. Meyer, and G. S. Smith, "Trinuclear Half-Sandwich Ru II , Rh III and Ir III Polyester Organometallic Complexes: Synthesis and in vitro Evaluation as Antitumor Agents," *Eur. J. Inorg. Chem.*, vol. 2015, no. 8, pp. 1433–1444, Mar. 2015.
- [82] P. Govindaswamy, B. Therrien, G. Süß-Fink, P. Štěpnička, and J. Ludvík, "Mono and dinuclear iridium, rhodium and ruthenium complexes containing chelating carboxylato pyrazine ligands: Synthesis, molecular structure and electrochemistry," *J. Organomet. Chem.*, vol. 692, no. 8, pp. 1661–1671, 2007.
- [83] T.-T. Thai, B. Therrien, and G. Süß-Fink, "Pentamethylcyclopentadienyl rhodium and

- iridium complexes containing oxinato ligands,” *Inorg. Chem. Commun.*, vol. 12, no. 8, pp. 806–807, 2009.
- [84] C. M. Anderson, M. A. Weinstein, J. Morris, N. Kfoury, L. Duman, T. A. Balema, A. Kreider-Mueller, P. Scheetz, S. Ferrara, M. Chierchia, and J. M. Tanski, “Biscyclometalated platinum complexes with thiophene ligands,” *J. Organomet. Chem.*, vol. 723, pp. 188–197, Jan. 2013.
- [85] C. Anderson, M. Crespo, J. Morris, and J. M. Tanski, “Reactivity of cyclometallated platinum complexes with chiral ligands,” *J. Organomet. Chem.*, vol. 691, no. 26, pp. 5635–5641, Dec. 2006.
- [86] C. Anderson and M. Crespo, “Cyclometallated platinum complexes with heterocyclic ligands,” *J. Organomet. Chem.*, vol. 689, no. 9, pp. 1496–1502, May 2004.
- [87] M. Crespo, M. Font-Bardía, and X. Solans, “Synthesis, reactivity and crystal structures of platinum (II) and platinum (IV) cyclometallated compounds derived from 2- and 4-biphenylimines,” *J. Organomet. Chem.*, vol. 691, no. 3, pp. 444–454, Jan. 2006.
- [88] C. Anderson, M. Crespo, and F. D. Rochon, “Stereoselective oxidative addition of methyl iodide to chiral cyclometallated platinum(II) compounds derived from (R)-(+)-1-(1-naphthylethylamine). Crystal structure of [PtMe{3-(R)-(C₁₀H₇)CHMeNCHC₄H₂S}PPh₃},” *J. Organomet. Chem.*, vol. 631, no. 1–2, pp. 164–174, Aug. 2001.
- [89] M. Crespo, M. Font-Bardía, and X. Solans, “A comparative study of metallating agents in the synthesis of [C,N,N’]-cycloplatinated compounds derived from biphenylimines,” *J. Organomet. Chem.*, vol. 691, no. 9, pp. 1897–1906, Apr. 2006.
- [90] A. Capapé, M. Crespo, J. Granell, M. Font-Bardía, and X. Solans, “Synthesis and

- reactivity of cyclometallated platinum (II) compounds containing [C,N,N'] terdentate ligands: Crystal structures of [PtCl{(CH₃)₂N(CH₂)₃NCH(4-ClC₆H₃)}], [PtCl{(CH₃)₂N(CH₂)₃NCH(2-ClC₆H₃)}] and [PtCl{(CH₃)₂N(CH₂)₃NCH(3-(CH₃)C₆H₃)}],” *J. Organomet. Chem.*, vol. 690, no. 19, pp. 4309–4318, Oct. 2005.
- [91] P. Jolliet, M. Gianini, A. von Zelewsky, G. Bernardinelli, and H. Stoeckli-Evans, “Cyclometalated Complexes of Palladium(II) and Platinum(II): cis -Configured Homoleptic and Heteroleptic Compounds with Aromatic C₆N Ligands,” *Inorg. Chem.*, vol. 35, no. 17, pp. 4883–4888, Jan. 1996.
- [92] A. Zamora, S. A. Pérez, V. Rodríguez, C. Janiak, G. S. Yellol, and J. Ruiz, “Dual Antitumor and Antiangiogenic Activity of Organoplatinum(II) Complexes,” *J. Med. Chem.*, vol. 58, no. 3, pp. 1320–1336, Feb. 2015.
- [93] N. Cutillas, A. Martínez, G. S. Yellol, V. Rodríguez, A. Zamora, M. Pedreño, A. Donaire, C. Janiak, and J. Ruiz, “Anticancer C,N-cycloplatinated(II) complexes containing fluorinated phosphine ligands: synthesis, structural characterization, and biological activity,” *Inorg. Chem.*, vol. 52, no. 23, pp. 13529–35, Dec. 2013.
- [94] J. Ruiz, J. Lorenzo, C. Vicente, G. López, J. María López-de-Luzuriaga, M. Monge, F. X. Avilés, D. Bautista, V. Moreno, and A. Laguna, “New palladium(II) and platinum(II) complexes with 9-aminoacridine: structures, luminiscence, theoretical calculations, and antitumor activity,” *Inorg. Chem.*, vol. 47, no. 15, pp. 6990–7001, Aug. 2008.
- [95] D. Aguilar, M. Contel, R. Navarro, and E. P. Urriolabeitia, “Organogold(III) iminophosphorane complexes as efficient catalysts in the addition of 2-methylfuran and electron – rich arenes to methyl vinyl ketone.” American Chemical Society, 02-

Aug-2007.

- [96] M. Frik, J. Fernández-Gallardo, O. Gonzalo, V. Mangas-Sanjuan, M. González-Alvarez, A. Serrano del Valle, C. Hu, I. González-Alvarez, M. Bermejo, I. Marzo, and M. Contel, "Cyclometalated Iminophosphorane Gold(III) and Platinum(II) Complexes. A Highly Permeable Cationic Platinum(II) Compound with Promising Anticancer Properties.," *J. Med. Chem.*, vol. 58, no. 15, pp. 5825–41, Aug. 2015.
- [97] P. M. M. and D. M. H. C. White, A. Yates, *Inorganic Syntheses*, vol. 29. Hoboken, NJ, USA: John Wiley & Sons, Inc., 1992.



4.1 Introduction

Despite the enormous advancement in modern 21st-century medicine, malaria still remains one of the greatest problems facing developing nations, especially in the tropical and subtropical regions. It afflicts more than 500 million people, with a mortality rate of more than 800 000 per annum [1-4]. The drug chloroquine (CQ) was for several decades the preferred chemotherapeutic agent in the treatment of uncomplicated malaria [5-7]. This quinoline derivative belongs to the class of 4-aminoquinolines, which have been extensively explored as therapeutic agents for malaria treatment. Other compounds possessing a quinoline moiety that have been explored as antimalarial drugs include, *inter alia*, amodiaquine, piperaquine, and pyronaridine. These drugs have been shown to support the build-up of hemozoin, which is lethal to the parasite, by complexing with hemozoin and interrupting a biomineralization process [8,9]. The parasite employs this biomineralization as a defence mechanism in order to detoxify hemozoin into crystalline malaria pigment, hemozoin, which is harmless to the parasite [10-14].

The battle against malaria is still intensified by the constant development of resistance to current treatments; hence there is a consistent need for the development of hybrid antimalarial compounds [15,16] that ideally should possess novel structures, unique modes of action, or both, in order to successfully restore the potency of known organic compounds currently in use. Within the efforts to restore activity, one strategy that has gained considerable interest involves the incorporation/coordination of a transition metal to known organic skeletons with antimalarial activity, in order to enhance or restore the activity [6,16].

Such metal complexes remain a relatively unexplored area of modern medicinal chemistry, and they have shown to offer a rich source of effective therapeutic drugs against the malaria parasite. Sánchez-Delgado *et al.* reported the incorporation of a metal fragment into an organic drug, CQ, of known biological importance. This was demonstrated by the advent of the first antimalarial organometallic complex [RhCl(COD)CQ] (*vide supra*, Chapter 1) [16].

One of the major achievements in the efforts aimed at restoring the activity of the parent chloroquine drug was the incorporation of a ferrocenyl moiety into the side chain of chloroquine. This strategy led to the discovery of ferroquine (FQ) that has exhibited enhanced activity when evaluated against CQ-susceptible and CQ-resistant strains of *P. falciparum* [17-21]. Ferroquine is the single most active compound of a growing family of organometallic conjugates and it has entered Phase IIb clinical trials. Significant progress into the parasite genomics and the identification of a few biomolecular targets has been made and this offers new leads [22] that may further aid the development of anti-malarial drugs, including metal-based drugs.

This chapter presents data from the evaluation of chloroquine analogous ligands **L¹-L³** with their generic metal complexes **C1-C6** as antiplasmodium agents against a CQ-sensitive **NF54** strain of *P. falciparum* and as agents capable of inhibiting the formation of the synthetic β -hematin.

4.2 *In vitro* antiplasmodial activity of chloroquine analogues and corresponding complexes

4.2.1 Antiplasmodial activity of ligand L¹-L³ against the chloroquine sensitive strain of plasmodium falciparum

The structures of the ligands L¹-L³ (Figure 4.1) were confirmed by spectroscopic and analytical techniques. The antimalarial activities of the three chloroquine analogues and corresponding metal complexes were assessed on *in vitro* cultures of the NF54 chloroquine-sensitive strain (CQS) of *P. falciparum*. Ligand L³ was included in the antimalarial study as a comparison to L¹, even though a corresponding metal complex had not been synthesized. In the assays, chloroquine (CQ) and artesunate were employed as reference standard drugs for the treatment of malaria.

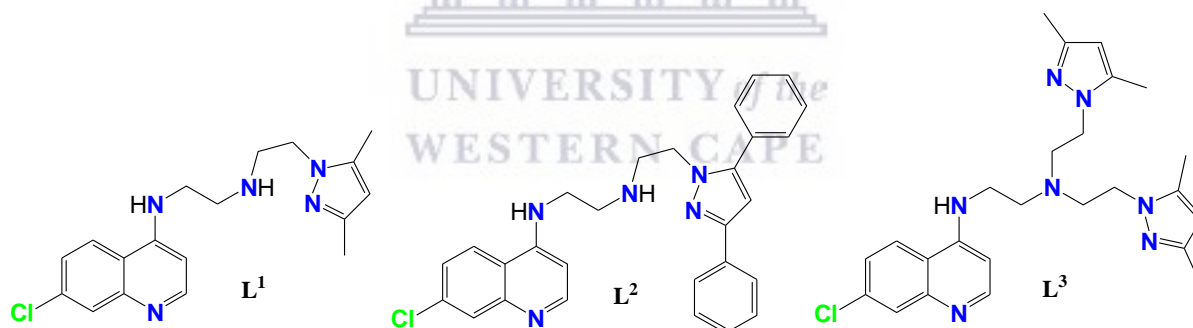


Figure 4.1: Ligands evaluated for their antiplasmodial activity against the CQS NF54 of plasmodium falciparum.

The antimalarial activities of the CQ analogue ligands L¹, L² and L³ are summarized in Table 1. Ligands L¹ and L³ exhibited similar activity against *P. falciparum* with IC₅₀-values of 19 nM and 21 nM, respectively, approximately twice as high as for chloroquine phosphate. Ligand L² exhibited moderate activity, with an IC₅₀ of 43 nM, i.e. half as potent as L¹ or L³.

Table 4.1: *In vitro* anti-plasmodial activities of L¹-L³ and 1-6, against NF54

Compound	<i>P. falciparum</i>	
	(IC ₅₀ , ng/ml ± SD) NF54	(IC ₅₀ , nM ± SD) NF54
L ¹	6.6 ± 1.3	19.3 ± 3.9
L ²	19.7 ± 1.8	42.3 ± 4.0
L ³	9.6 ± 0.7	20.6 ± 1.4
CQ	4.80 ± 0.82	9.31 ± 1.6
Artesunate	2.52 ± 0.37	6.55 ± 1.0

Comparison of L¹ with L² revealed that the steric bulkiness around the heterocyclic pyrazolyl moiety does not influence activity as envisioned. L¹ was the most active in these ligand series, half as active as the structurally similar reference drug CQ, indicating that the one pendant pyrazole arm might be sufficient for activity that might be comparable or even better than CQ. The ligands reported herein exhibited better antimalarial activity compared to the organometallic silicon containing CQ (61.40-459.54 nM) and ferrocenyl-salicylaldimine hydrazone (3940-32830 nM) analogues, exhibiting activity that is far more superior to most compounds against the same CQ-sensitive NF54 strain with comparable activity to that of ferroquine (0.033 μM or 33 nM) respectively [23-25]. The performance of these ligands as active antimalarial candidates has paved a way into possible modifications around the pyrazolyl moiety that might augment the inherent activity these of ligands even further.

4.2.2 Antiplasmodial activity of complex **C1-C6** against the chloroquine sensitive strain of *plasmodium falciparum*, **NF54**.

Complexes **C1-C3** demonstrated relatively good antiplasmodial activities, although the activities of **C1** and **C2** were not significantly different from **L¹**. This suggests that the coordination site of the ligand might be the pharmacophore of the molecule, hence the complexation did not augment the activity of the ligand significantly. Antimalarial activity CQ analogue complexes **C1-C6** are summarized in Table 4.2.

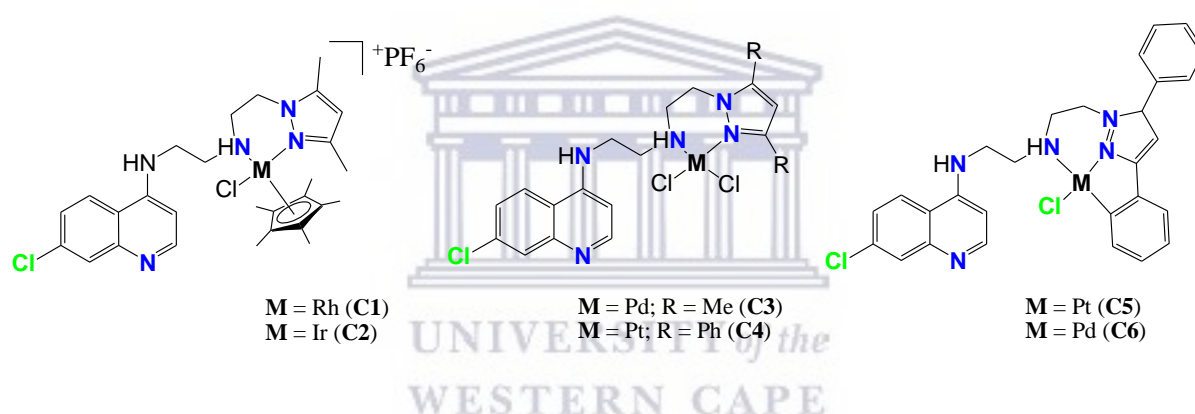


Figure 4.2: Complexes evaluated for their antiplasmodial activity against the CQS **NF54** of *plasmodium falciparum*

Complex **C3** is a coordination palladium complex of ligand **L¹**. As stated (*vide supra*), coordination of the palladium ion by **L¹** through the amine (*NH*) and the pyrazolyl (*N=C*) nitrogen atoms did not improve the antimalarial activity of the parent ligand **L¹**, as the antimalarial activity of the metal complex **C3** (48 nM) was observed to be lower compared to the free ligand **L¹** (19 nM). The antimalarial activity of **C5** was found to be moderate with IC₅₀-value less than 170 nM while complex **C4** and **C6** displayed weak activities against the **NF54** *P. falciparum* strain. It should be noted that the cyclometallated complex **C5** was more

potent compared to the corresponding dichlorido complex **C4**. The chloroquine metallacycles **C5** and **C6** also exhibited better activity compared to those pyrazolyl metallacycles that were synthesized and evaluated as antimalarials by Quirante *et. al.* [26]. The latter compounds were obtained after the orthometallation of the 3-phenyl ring of the pyrazole moiety without the appended quinoline moiety. The improved antimalarial activity reported herein can be attributed to the presence of the quinoline moiety, that has been shown to be crucial for antimalarial activity (*vide supra*, Chapter 1), that is inherent to the ligands and the generic metal complexes. The platinacycle **C5** performed better compared to the palladacycle **C6**; this observation might be due to the increased and faster rate of hydrolysis of the latter compared to the former as reported in the literature [26], thus rendering the platinacycle analogue more active due to the slower hydrolysis rate of the Pt-Cl bond, and a resultant relative stability of the platinacycle as compared to the palladacycle. In general, the new pyrazole-containing derivatives and their corresponding metal complexes display good (**C1-C3**), moderate (**C5**) to weak (**C4** and **C6**) inhibitory effects relative to the standard drugs chloroquine and artesunate. The ligands (**L¹-L³**) exhibited superior activity compared to their corresponding metal compounds.

Stability tests on **C1** and **C2** in DMSO-*d*₆ were conducted in order to gauge if whether the complexes were stable under the experimental conditions. The NMR stability tests of **C1** and **C2** revealed that complexes were stable under the experimental conditions even after 24 hr as no uncoordinated parent ligand **L¹** was observed in the NMR spectra of the complexes. .

Table 4.2: *In vitro* anti-plasmodial activities of C1-C6, against CQ-susceptible strain NF54

Compound	<i>P. falciparum</i> (IC ₅₀ , ng/ml ± SD) NF54	<i>P. falciparum</i> (IC ₅₀ , nM ± SD) NF54
C1	13.5 ±4.3	17.7 ±5.7
C2	15.2 ±2.4	20.0 ±3.1
C3	25.4 ±4.0	48.7 ±7.8
C4	312 ±39.4	401 ±51
C5	117 ±35.6	168 ±51
C6	219 ±56.9	360 ±93
CQ	4.80 ±0.82	9.31 ±1.6
Artesunate	2.52 ±0.37	6.55 ±1.0

4.2.3 Heme Aggregation Inhibition Assays

The malaria parasite, *P. falciparum*, is most active in its blood (erythrocytic) stage as it degrades large amounts of the hosts's hemoglobin in order to nourish and grow. This active phase of the parasite's life cycle that mainly involves the digestion of the proteins from haemoglobin occurs in an acidic, pH in the range 4.5-4.9, compartment termed the digestive vacuole [27,28]. The consumption and degradation of 70-95 % of haemoglobin [29,30] by the parasite for biosynthetic requirements is a highly ordered process involving several proteases [31,33]. This process results in the formation of the non-toxic (to the parasite) by-product, heme. The larger amounts of generated non-toxic free heme (heme b, ferriprotoporphyrin-IX or Fe(II)PPIX) from hemoglobin is autoxidized into toxic ferric form (hematin, hemin or aquaferriprotoporphyrin-IX or H₂O-Fe(III)PPIX) that results in the inhibition of vacuolar

proteases and damaged parasite membranes as was seen with chloroquine, artemisinin and amodiaquine that exhibited enhanced peroxidase activity of heme [34,38]. Thus it is vital for the parasite's survival to get rid of the toxic heme through a biomineralization (detoxification mechanism) process, converting heme into a highly insoluble microcrystalline malaria pigment hemazoin that is non-toxic to the parasite. Antimalarial drugs, such as artemisin and chloroquine, have been observed to block this detoxification mechanism by complexing with the heme and this has been demonstrated to be the likely mode of action for these antimalarial drugs [39,40].

Chloroquine and 4-aminoquinoline compounds have been shown to interrupt the detoxification of the toxic heme to the nontoxic hemazoin by binding with the Fe(III)-PPIX, thus encouraging the build-up of the cytotoxic Fe(III)-PPIX by-product (*vide supra*, Chapter 1) [41,42]. This antiplasmodial activity was studied through the structure-activity relationships of 4-aminoquinolines and the effects of alkylating heme with artemisinin. It has also been shown that in some instances the chloroquine and related 4-aminoquinoline target hemazoin as the mode of action as thiourea, thiazolidinedione and thioparabanic acid derivatives of 4-aminoquinoline exhibited antimalarial activity with potent β -hematin inhibition formation as well as the proposed noncovalent binding sites of these quinoline derivatives [43,44].

4.2.3.1 Heme Aggregation Inhibition Assays of the ligands, **L¹-L³**.

The ability of the ligands, **L¹-L³**, to act as heme aggregation agents was investigated because the ligands exhibited good activity against the CQS **NF54** of *p. falciparum*. The results are tabulated (*vide supra*, table 4.3) and represented graphically below.

Table 4.3: β -haematin inhibition activity of ligands L¹-L³.

Compounds	IC ₅₀ (value \pm SD)
L ¹	65.91 \pm 1.5
L ²	60.30 \pm 1.2
L ³	92.22 \pm 3.2
CQ	78.5 \pm 2.2
AQ	76.8 \pm 1.3

SD – Standard deviation

CQ – Chloroquine

AQ – Amidoquine

The ligands were assessed using a reported literature procedure employing Nonidet P-40 (NP-40) detergent mediated assay [45]. The detergent, NP-40, was used in the interactive study of the ligands in order to imitate the neutral lipids found in digestive vacuole of the parasite and therefore probe the ability of the ligands L¹-L³ and corresponding complexes C1-C6 to inhibit β -hematin formation [46,47]. Methods used to measure the amount of β -hematin inhibited have been reported in the literature; titration calorimeter and spectrophotometric titration, and the latter has been found to be a preferred replacement in the absence of the former and yields comparable association constants to the former technique [27,48,49].

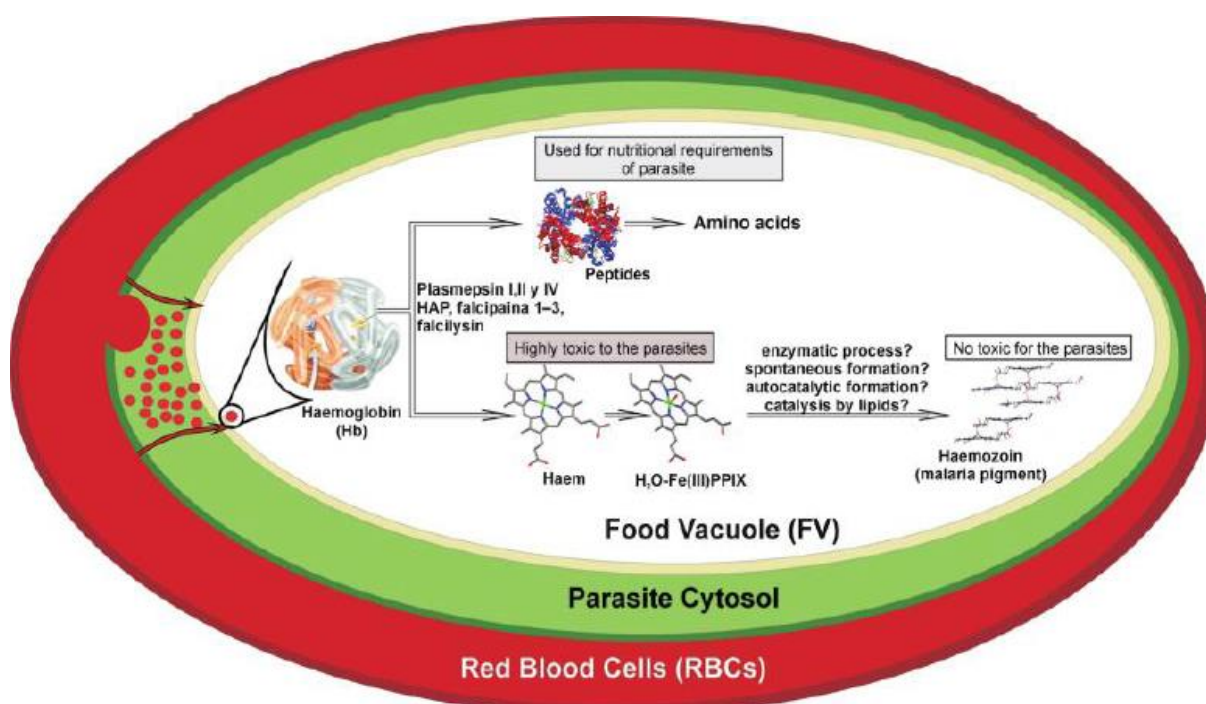


Figure 4.3: Process of haemoglobin degradation and heme detoxification by intraerythrocytic malaria parasite, picture taken from ref [6].

The ligands **L¹** and **L²** were found to act as better β -hematin inhibition agents, with lower IC₅₀ values comparable to the standard drugs chloroquine diphosphate (CQDP) and amidoquine (AQ). Ligand **L²**, with two phenyl rings on the pyrazole moiety, performed slightly better than **L¹**, with methyl substituents on the pyrazole moiety. This suggests that the two phenyl rings on the pyrazole moiety of **L²** might be interacting better with heme than **L¹**, by interfering with the parasite's inherent behaviour to detoxify and thus resulting in the blockage/ sequestration of toxic heme that leads to the death of the parasite [50,51].

4.2.3.2 Heme Aggregation Inhibition Assays of the metal complexes, C1-C6.

The metal complexes **C1-C6** were also probed for their ability to act as the synthetic β -hematin inhibition agents. The efficacy of the prepared metal complexes in the heme

aggregation inhibition assay (HAIA) was conducted in a buffer medium as reported in the literature using the titration colometric methods [45,49]. The β -hematin inhibitory activity of the complexes **C1-C6** were conducted in an acetate buffer at the pH 4.7. The obtained IC₅₀ values of the complexes were comparable to the standard drug CQDP. The correlation between the dependence of the antimalarial activity to the β -hematin inhibitory activity was studied. No observable trend could be extrapolated for this series of metal complexes unlike similar reported metal-CQ complexes, such as the half-sandwich ruthenium(II), [Au(CQ)(PPh₃)]PF₆ and ruthenium(II) chloroquine complexes, where a correlation was established between the anti-malarial activity, hemin and β -hematin inhibition [7,52,53].

Table 4.4: β -haematin inhibition activity of complexes **C1-C6**.

Compounds	IC ₅₀ (value \pm SD)
C1	62.1 \pm 1.4
C2	86.5 \pm 1.7
C3	>100
C4	83.5 \pm 2.1
C5	85 \pm 1.1
C6	82 \pm 1.4
CQ	78 \pm 2.1
AQ	76.2.0

SD – Standard deviation
 CQ – Chloroquine
 AQ – Amidoquine

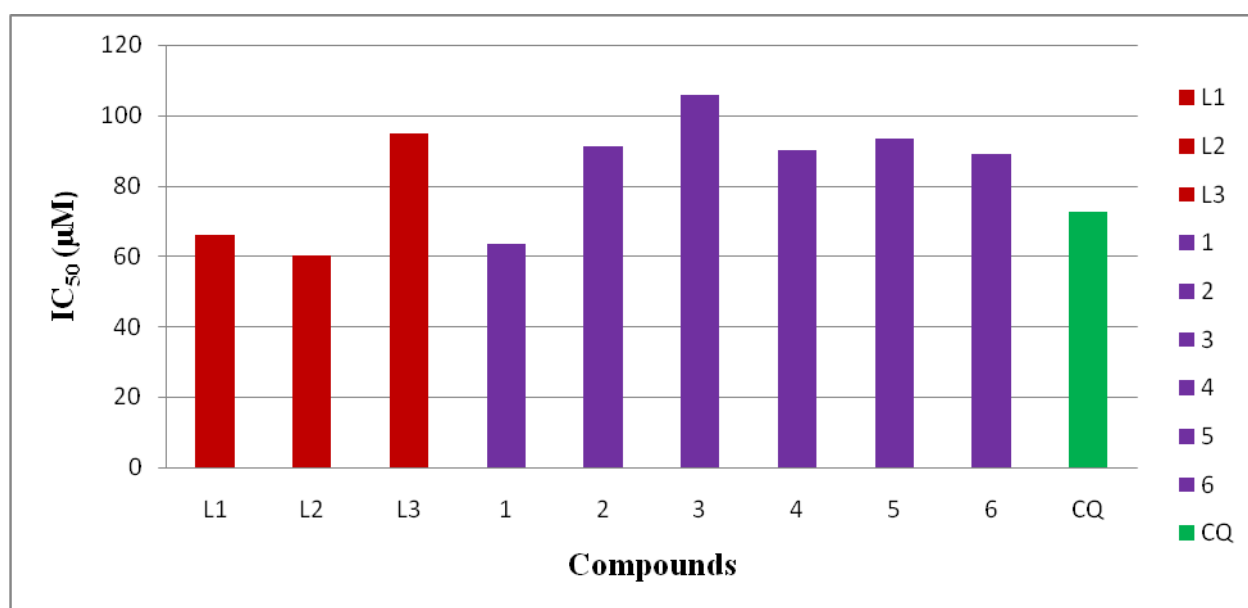


Figure 4.4: Graphical representation of the IC₅₀ values for the ligands L¹-L³ and corresponding complexes C1-C6.

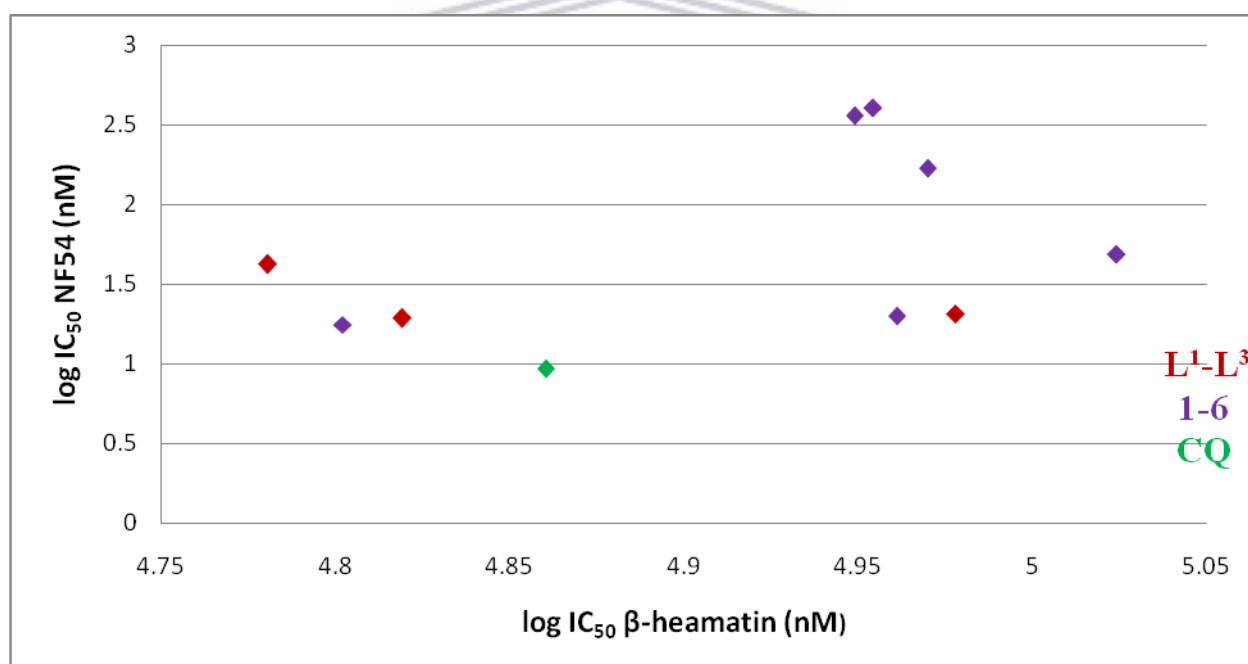


Figure 4.5: Correlation of drug inhibition of β-haematin inhibition induced by haemozoin at pH 4.7 and inhibition of parasite growth using the CQ-sensitive *P. falciparum* strain NF54. Values are given for ligands (L¹-L³), metal complexes (C1-C6), and chloroquine (CQ).

The results obtained showed that there was no distinguishable correlation between the antimalarial activity and the β-haematin inhibition activity of the ligands L¹-L³ and metal

complexes C1-C6 *in vitro*. The antiplasmodial activity exerted by the compounds against the CQ-sensitive NF54 strain of *P. falciparum* did not automate the ligands and complexes to exert enhanced activity as β -haematin inhibition agents. As it can be ascertained from the plot above (Figure 4.5), no correlation was observed between β -haematin inhibition activity and the potency of this series of compounds compared to the CQ-sensitive NF54 strain of *P. falciparum* although Dorn *et. al.* and Vippagunta *et. al.* have demonstrated good correlation between hematin polymerisation inhibition and parasite growth inhibition for quinoline-containing blood schizonticides [54,55]. It is known that for a compound to act as a better β -haematin inhibition agent, its compounds physiological properties must allow for sufficient accumulation in high concentration in the digestive vacuole of the parasite [56-59]. These suggest that physiological properties of the prepared compounds play a role in the antimalarial and β -haematin inhibition activity, respectively. Thus changes in structural formulation might affect the cellular accumulation of CQ analogues in the DV of the parasite resulting in impeded activity [60-62]. A study into the accumulation of the prepared CQ analogues and corresponding metal complexes, can aid with the correlation of the antimalarial activity and β -haematin inhibition establishment [63].

4.3 Computational studies

4.3.1 Molecular Docking of chloroquine analogues, L¹-L³.

The dimeric enzyme from *Plasmodium falciparum* dihydrofolate reductase–thymidylate synthase (PfDHFR-TS) has been identified as the crucial target of antimalarial drugs [64,65]. Antimalarial drugs such as pyrimethamine and the pro drug proguanil has been shown to

inhibit dihydrofolate reductase enzyme although rapid parasite immunity has been documented [66]. Thus it was in the interest of the present study to evaluate the ligands **L**¹-**L**³ as folate antagonists that might offer different modes of action and overcome the emergence of resistance to known folate antagonists.

Figure 4.6-4.8 show the conformations of the docked ligands (**L**¹, **L**² and **L**³) with dihydrofolate reductase-thymidylate synthase (PDB ID - 1J3I) present in *P. falciparum*. The active site of the protein was assessed through the information available in the literature, as the crystal structure of PfDHFR-TS revealed the favourable conformation for the potent inhibitor WR99210 over the pyrimethamine [64-66]. All ligands were docked into the active site pocket of the protein and the resulting docked conformations were selected on the basis of the interaction energy parameters and scoring functions of the binding energy efficiency. The assessed scores of the molecular docking are summarized in Table 4.5. All ligands showed the Root Mean Square Deviation (RMSD) values (<2 Å), indicating the reliability of the docked complexes. The **L**¹ interacted with Ile14, Ala16, Leu40, Phe58, Ile112, Ile 164 and Tyr170 (Figure 4.6). Similarly, **L**² showed interaction with Ala16, Val45, Leu46, Phe58, Ile112 and Pro113 (figure 4.7). Furthermore, **L**³ interacted with highest number of residues (Ile14, Ala16, Leu46, Cys50, Met55, Phe58, Met104, Ser111, Ile112, Pro113, Phe116, Leu119, Ile 164 and Tyr170) as illustrated in Figure 4.8, showed highest binding efficiency towards dihydrofolate reductase-thymidylate synthase with binding energy of -7.13 kcal/mol, which is in accordance with the experimental results.

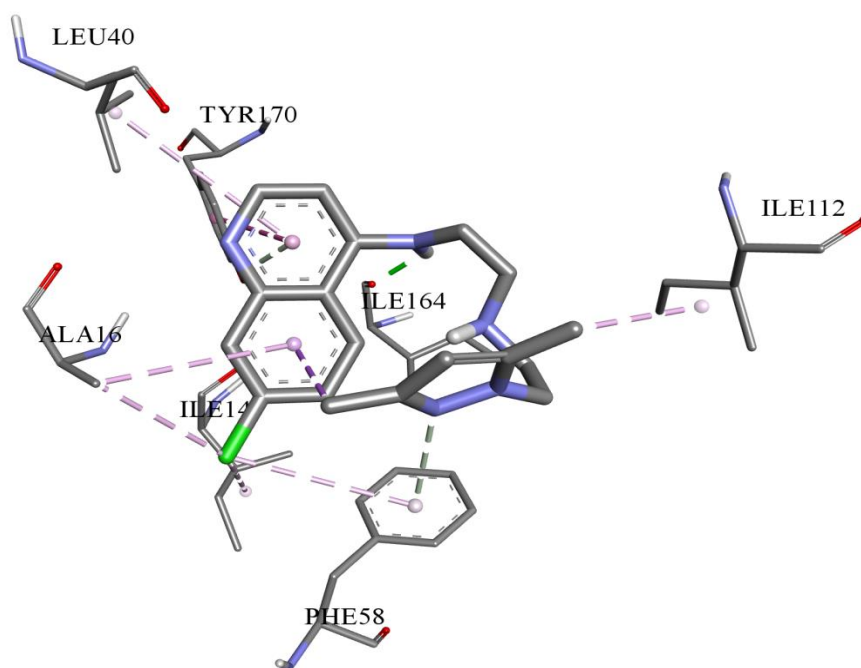


Figure 4.6: Docked conformation of **L¹** with *P. falciparum* dihydrofolate reductase-thymidylate synthase (The dotted line shows the hydrogen bonds between the **L¹** and protein residues).

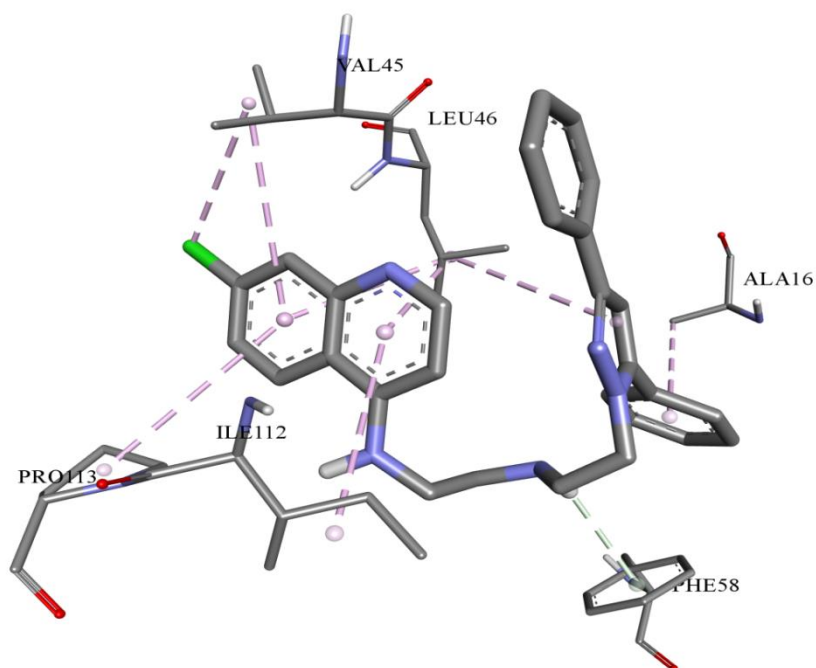


Figure 4.7: **L²** bound into the *P. falciparum* dihydrofolate reductase-thymidylate synthase. The dotted lines show the hydrogen bonds.

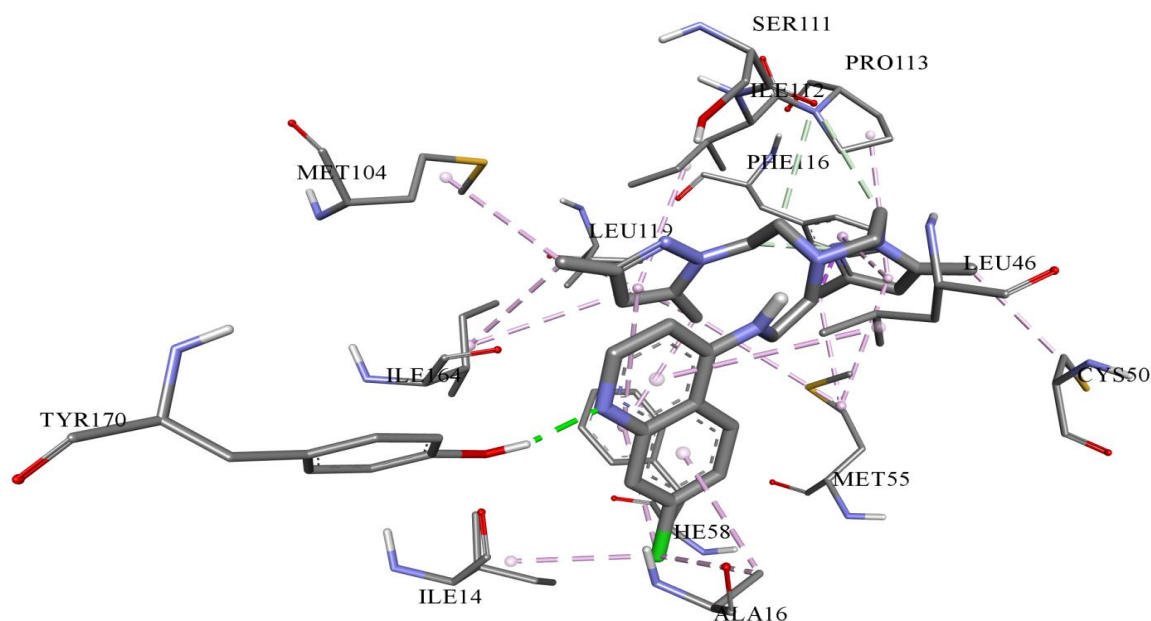


Figure 4.8: Docked conformation of dihydrofolate reductase-thymidylate synthase with L³.

Table 4.5: List parameters generated from molecular docking showing the interaction behaviours of protein and ligands.

S. No	Ligand name	Selected Docked Pose	DrugScoreX scoring results	Free energy of Binding (kcal/mol)	Ligand Efficiency	vdW + Hbond + desolv Energy (kcal/mol)	Intermolecular energy (kcal/mol)	Total internal (kcal/mol)	Torsional energy (kcal/mol)
1.	L ¹	42	-100	-6.49	-0.27	-8.83	-8.58	-2.47	2.09
2.	L ²	29	-142	-8.61	-0.25	-11.52	-11.29	-2.05	2.68
3.	L ³	41	-137	-7.13	-0.22	-10.36	-10.11	-2.26	2.98

4.4 Summary and Conclusions:

In the present work, a class of new chloroquine analogues was prepared and fully characterized. The syntheses of these new series of 4-aminoquinoline derivatives were achieved by varying the pendant pyrazoles in efforts to gain insight into new leads for hybrids that might have pharmacological activity against the lethal *plasmodium falciparum* parasite.

The 4-aminoquinoline ligands L¹-L³ exhibited substantial activity with L¹ and L² having the highest activity. The highest activity showed by the corresponding complexes was seen for complex C1 against the chloroquine sensitive strain (CQS) of *P. falciparum*. The activity of the compounds can be arranged as follows, L¹~L³<L², C1~C2<C3 and C5~C6<C4. The promising feature about some of the compounds synthesized was that L¹-L³ and complex C1-C3 displayed activity against the CQS that was below 50nM. The ligands L¹-L³ and complexes C1-C6 have been shown to interact with haem. These chloroquine analogues and their corresponding metal-based antimalarial candidates have shown to inhibit β-haematin formation to a comparable extent than chloroquine diphosphate (CQDP) and other known metal-based anti-malarial agents reported in the literature. Molecular docking also provided some insight into the interaction of the ligands with the active site of the parasite.

4.5 Experimental

4.5.1 Determination of *in vitro* antiplasmodial activity

The test samples were tested in triplicate on one or two separate occasions against chloroquine sensitive (CQS) strain of *Plasmodium falciparum* (NF54). Continuous *in vitro* cultures of asexual erythrocyte stages of *P. falciparum* were maintained using a modified method of Trager and Jensen [67]. Quantitative assessment of antiplasmodial activity *in vitro* was determined via the parasite lactate dehydrogenase assay using a modified method described by Makler [68]. The test samples were prepared to a 20 mg/ml stock solution in 100% DMSO. Samples were tested as a suspension if not completely dissolved. Stock solutions were stored at -20°C. Further dilutions were prepared on the day of the experiment. Chloroquine (CQ) and artesunate were used as the reference drugs in all experiments. A full

dose-response was performed for all compounds to determine the concentration inhibiting 50% of parasite growth (IC₅₀-value). Test samples were tested at a starting concentration of 1000 ng/ml, which was then serially diluted 2-fold in complete medium to give 10 concentrations; with the lowest concentration being 2 ng/ml. The same dilution technique was used for all samples. The highest concentration of solvent to which the parasites were exposed to had no measurable effect on the parasite viability (data not shown). The IC₅₀-values were obtained using a non-linear dose-response curve fitting analysis via Graph Pad Prism v.4.0 software.

4.5.2 Heme Aggregation Inhibition Assay

The colorimetric method used to quantify the formation of β-haematin was a template of the method described by Wright *et. al.* [45]. Test compounds were prepared as a 10mM stock solution in 100% DMSO. Test samples were tested at a starting concentration of 500μM and the lowest drug concentration being 5 μM. The stock solution was serially diluted to give 12 concentrations in a 96 well flat-bottom assay plate. NP-40 detergent was then added to mediate the formation of β-haematin (30.55 μM, final concentration). A 25 mM stock solution of haematin was prepared by dissolving haemin (16.3 mg) in dimethyl sulfoxide (1 ml). A 177.76 μl aliquot of haematin stock was suspended in 20 ml of a 2 M acetate buffer, pH 4.7. The haematin suspension was then added to the plate to give a final haematin concentration of 100 μM. The plate was then incubated for 16 hours at 37°C. The well-established method developed by Ncokazi and Egan, using the pyridineferrochrome was employed.[49] 32 μl of a solution of 50% pyridine 20% acetone, 20% water, and 10% 2M HEPES buffer (pH 7.4) was added to each well. To this, 60 μl acetone was then added to each

well and mixed. The absorbance of the resulting complex was measured at 405 nm on a SpectraMax 340PC plate reader. The IC₅₀ values were obtained using a non-linear dose-response curve fitting analysis via Graph Pad Prism v.5.0 software.

4.6 Computational Studies

4.6.1 Molecular Docking

The docking studies were performed against the active site of dihydrofolate reductase-thymidylate synthase (PDB ID - 1J3I) of *P. falciparum* by using the AutoDock 4[69] package, in order to evaluate the binding mechanism of **L**¹, **L**² and **L**³ with the respective protein. The AutoDock uses the combination of a free energy based empirical force field along with Lamarckian Genetic algorithm for the prediction of the bound conformations [69]. The grid dimensions of 41 x 71 x 49 Å beside the XYZ directions was assigned in accordance with active site of the protein [64] by using the AutoGrid module with grid spacing of 0.392 Å. The Lamarckian genetic algorithm was used with the default parameters. Around 100 conformations were generated which were clustered according to the RMSD tolerance of 2.0 Å. The obtained conformations were rescored using the DrugScoreX server [70] and the best conformation was selected on the basis of consensus of the obtained parameters. The docked complexes were optimized and validation using modules present in the “Receptor-Ligand Interactions” section of Discover Studio 4.0 [71]. Furthermore, docked complexes were minimized using CHARMM [72] force field.

4.7 References:

- [1] “WHO | Fact Sheet: World Malaria Report 2015.”
- [2] S. I. Hay, C. A. Guerra, A. J. Tatem, A. M. Noor, and R. W. Snow, “The global distribution and population at risk of malaria: past, present, and future.,” *Lancet. Infect. Dis.*, vol. 4, no. 6, pp. 327–36, Jun. 2004.
- [3] P. Cravo, R. Culleton, A. Afonso, I. Ferreira, and V. do Rosario, “Mechanisms of Drug Resistance in Malaria: Current and New Challenges,” *Antiinfect. Agents Med. Chem.*, vol. 5, no. 1, pp. 63–73, Jan. 2006.
- [4] R. G. A. Feachem, A. A. Phillips, J. Hwang, C. Cotter, B. Wielgosz, B. M. Greenwood, O. Sabot, M. H. Rodriguez, R. R. Abeyasinghe, T. A. Ghebreyesus, and R. W. Snow, “Shrinking the malaria map: progress and prospects.,” *Lancet (London, England)*, vol. 376, no. 9752, pp. 1566–78, Nov. 2010.
- [5] P. A. Winstanley and A. M. Breckenridge, “Currently important antimalarial drugs.,” *Ann. Trop. Med. Parasitol.*, vol. 81, no. 5, pp. 619–27, Oct. 1987.
- [6] M. Navarro, W. Castro, and C. Biot, “Bioorganometallic compounds with antimalarial targets: Inhibiting hemozoin formation,” *Organometallics*, vol. 31, no. 16, pp. 5715–5727, 2012.
- [7] L. Glans, A. Ehnbohm, C. de Kock, A. Martínez, J. Estrada, P. J. Smith, M. Haukka, R. A. Sánchez-Delgado, and E. Nordlander, “Ruthenium(II) arene complexes with chelating chloroquine analogue ligands: synthesis, characterization and in vitro antimalarial activity.,” *Dalton Trans.*, vol. 41, no. 9, pp. 2764–73, Mar. 2012.

- [8] S. Bawa, S. Kumar, S. Drabu, and R. Kumar, "Structural modifications of quinoline-based antimalarial agents: Recent developments.," *J. Pharm. Bioallied Sci.*, vol. 2, no. 2, pp. 64–71, Apr. 2010.
- [9] A. C. C. Aguiar, R. M. de Santos, F. J. B. Figueiredo, W. A. Cortopassi, A. S. Pimentel, T. C. C. França, M. R. Meneghetti, and A. U. Krettli, "Antimalarial activity and mechanisms of action of two novel 4-aminoquinolines against chloroquine-resistant parasites," *PLoS One*, vol. 7, no. 5, pp. 1–9, 2012.
- [10] L. M. B. Ursos and P. D. Roepe, "Chloroquine resistance in the malarial parasite, *Plasmodium falciparum*," *Med. Res. Rev.*, vol. 22, no. 5, pp. 465–91, Sep. 2002.
- [11] T. J. Egan and H. M. Marques, "The role of haem in the activity of chloroquine and related antimalarial drugs," *Coord. Chem. Rev.*, vol. 190–192, pp. 493–517, Sep. 1999.
- [12] C. R. Chong and D. J. Sullivan, "Inhibition of heme crystal growth by antimalarials and other compounds: implications for drug discovery," *Biochem. Pharmacol.*, vol. 66, no. 11, pp. 2201–2212, Dec. 2003.
- [13] A. Leed, K. DuBay, L. M. B. Ursos, D. Sears, A. C. de Dios, and P. D. Roepe, "Solution Structures of Antimalarial Drug–Heme Complexes †," *Biochemistry*, vol. 41, no. 32, pp. 10245–10255, Aug. 2002.
- [14] K. A. de Villiers and T. J. Egan, "Recent advances in the discovery of haem-targeting drugs for malaria and schistosomiasis.," *Molecules*, vol. 14, no. 8, pp. 2868–87, Jan. 2009.
- [15] R. A. Sánchez-Delgado and A. Anzellotti, "Metal complexes as chemotherapeutic agents against tropical diseases: trypanosomiasis, malaria and leishmaniasis.," *Mini*

- Rev. Med. Chem.*, vol. 4, no. 1, pp. 23–30, Jan. 2004.
- [16] R. a Sánchez-Delgado, M. Navarro, H. Pérez, and J. a Urbina, “Toward a novel metal-based chemotherapy against tropical diseases. 2. Synthesis and antimalarial activity in vitro and in vivo of new ruthenium- and rhodium-chloroquine complexes.,” *J. Med. Chem.*, vol. 39, no. 5, pp. 1095–1099, 1996.
- [17] C. Biot, G. Glorian, L. A. Maciejewski, and J. S. Brocard, “Synthesis and antimalarial activity in vitro and in vivo of a new ferrocene-chloroquine analogue.,” *J. Med. Chem.*, vol. 40, no. 23, pp. 3715–8, Nov. 1997.
- [18] C. Biot, W. Daher, N. Chavain, T. Fandeur, J. Khalife, D. Dive, and E. De Clercq, “Design and synthesis of hydroxyferroquine derivatives with antimalarial and antiviral activities.,” *J. Med. Chem.*, vol. 49, no. 9, pp. 2845–9, May 2006.
- [19] L. Delhaes, C. Biot, L. Berry, L. . Maciejewski, D. Camus, J. . Brocard, and D. Dive, “Novel ferrocenic artemisinin derivatives: synthesis, in vitro antimalarial activity and affinity of binding with ferroprotoporphyrin IX,” *Bioorg. Med. Chem.*, vol. 8, no. 12, pp. 2739–2745, Dec. 2000.
- [20] C. Biot, W. Daher, C. M. Ndiaye, P. Melnyk, B. Pradines, N. Chavain, A. Pellet, L. Fraisse, L. Pelinski, C. Jarry, J. Brocard, J. Khalife, I. Forfar-Bares, and D. Dive, “Probing the role of the covalent linkage of ferrocene into a chloroquine template.,” *J. Med. Chem.*, vol. 49, no. 15, pp. 4707–14, Jul. 2006.
- [21] C. Biot, F. Nosten, L. Fraisse, D. Ter-Minassian, J. Khalife, and D. Dive, “The antimalarial ferroquine: from bench to clinic.,” *Parasite*, vol. 18, no. 3, pp. 207–14, Aug. 2011.

- [22] M. Navarro, C. Gabbiani, L. Messori, and D. Gambino, "Metal-based drugs for malaria, trypanosomiasis and leishmaniasis: recent achievements and perspectives.," *Drug Discov. Today*, vol. 15, no. 23–24, pp. 1070–8, Dec. 2010.
- [23] Y. Li, C. De Kock, P. J. Smith, H. Guzgay, D. T. Hendricks, K. Naran, V. Mizrahi, D. F. Warner, K. Chibale, and G. S. Smith, "Synthesis, characterization, and pharmacological evaluation of silicon-containing aminoquinoline organometallic complexes as antiplasmodial, antitumor, and antimycobacterial agents," *Organometallics*, vol. 32, no. 1, pp. 141–150, 2013.
- [24] N. Baartzes, T. Stringer, P. Chellan, J. M. Combrinck, P. J. Smith, A. T. Hutton, and G. S. Smith, "Synthesis, characterization, antiplasmodial evaluation and electrochemical studies of water-soluble heterobimetallic ferrocenyl complexes," *Inorganica Chim. Acta*, vol. 446, pp. 111–115, Mar. 2016.
- [25] T. Stringer, H. Guzgay, J. M. Combrinck, M. Hopper, D. T. Hendricks, P. J. Smith, K. M. Land, T. J. Egan, and G. S. Smith, "Synthesis, characterization and pharmacological evaluation of ferrocenyl azines and their rhodium(I) complexes," *J. Organomet. Chem.*, vol. 788, pp. 1–8, Jul. 2015.
- [26] J. Quirante, D. Ruiz, A. Gonzalez, C. López, M. Cascante, R. Cortés, R. Messeguer, C. Calvis, L. Baldomà, A. Pascual, Y. Guérardel, B. Pradines, M. Font-Bardía, T. Calvet, and C. Biot, "Platinum(II) and palladium(II) complexes with (N,N') and (C,N,N') - ligands derived from pyrazole as anticancer and antimalarial agents: Synthesis, characterization and in vitro activities," *J. Inorg. Biochem.*, vol. 105, no. 12, pp. 1720–1728, 2011.
- [27] R. Hayward, K. J. Saliba, and K. Kirk, "The pH of the digestive vacuole of

- Plasmodium falciparum is not associated with chloroquine resistance.” *J. Cell Sci.*, vol. 119, no. Pt 6, pp. 1016–25, Mar. 2006.
- [28] D. G. Spiller, P. G. Bray, R. H. Hughes, S. A. Ward, and M. R. H. White, “The pH of the Plasmodium falciparum digestive vacuole: holy grail or dead-end trail?,” *Trends Parasitol.*, vol. 18, no. 10, pp. 441–4, Oct. 2002.
- [29] T. J. Egan, “Discovering Antimalarials,” *Chem. Biol.*, vol. 9, no. 8, pp. 852–853, 2002.
- [30] B. Gligorijevic, T. Bennett, R. McAllister, J. S. Urbach, and P. D. Roepe, “Spinning disk confocal microscopy of live, intraerythrocytic malarial parasites. 2. Altered vacuolar volume regulation in drug resistant malaria.”, *Biochemistry*, vol. 45, no. 41, pp. 12411–23, Oct. 2006.
- [31] K. K. Eggleston, K. L. Duffin, and D. E. Goldberg, “Identification and characterization of falcilysin, a metallopeptidase involved in hemoglobin catabolism within the malaria parasite Plasmodium falciparum.”, *J. Biol. Chem.*, vol. 274, no. 45, pp. 32411–7, Nov. 1999.
- [32] R. Banerjee, J. Liu, W. Beatty, L. Pelosof, M. Klemba, and D. E. Goldberg, “Four plasmepsins are active in the Plasmodium falciparum food vacuole, including a protease with an active-site histidine.”, *Proc. Natl. Acad. Sci. U. S. A.*, vol. 99, no. 2, pp. 990–5, Jan. 2002.
- [33] P. J. Rosenthal, P. S. Sijwali, A. Singh, and B. R. Shenai, “Cysteine proteases of malaria parasites: targets for chemotherapy.”, *Curr. Pharm. Des.*, vol. 8, no. 18, pp. 1659–72, Jan. 2002.
- [34] P. A. Berman and P. A. Adams, “Artemisinin Enhances Heme-Catalysed Oxidation of

- Lipid Membranes,” *Free Radic. Biol. Med.*, vol. 22, no. 7, pp. 1283–1288, Jan. 1997.
- [35] J. Zhang, M. Krugliak, and H. Ginsburg, “The fate of ferriprotophyrin IX in malaria infected erythrocytes in conjunction with the mode of action of antimalarial drugs,” *Mol. Biochem. Parasitol.*, vol. 99, no. 1, pp. 129–141, Mar. 1999.
- [36] H. Ginsburg, O. Famin, J. Zhang, and M. Krugliak, “Inhibition of glutathione-dependent degradation of heme by chloroquine and amodiaquine as a possible basis for their antimalarial mode of action,” *Biochem. Pharmacol.*, vol. 56, no. 10, pp. 1305–1313, Nov. 1998.
- [37] O. Famin and H. Ginsburg, “Differential effects of 4-aminoquinoline-containing antimalarial drugs on hemoglobin digestion in *Plasmodium falciparum*-infected erythrocytes,” *Biochem. Pharmacol.*, vol. 63, no. 3, pp. 393–398, Feb. 2002.
- [38] E. Deharo, D. Barkan, M. Krugliak, J. Golenser, and H. Ginsburg, “Potentiation of the antimalarial action of chloroquine in rodent malaria by drugs known to reduce cellular glutathione levels,” *Biochem. Pharmacol.*, vol. 66, no. 5, pp. 809–817, Sep. 2003.
- [39] S. R. Meshnick, “Artemisinin: mechanisms of action, resistance and toxicity,” *Int. J. Parasitol.*, vol. 32, no. 13, pp. 1655–1660, Dec. 2002.
- [40] G. P. Saad H. Abdalla, “Malaria: A Hematological Perspective (Tropical Medicine: Science and Practice: Vol. 4),” *Imperial College Press: London*, 2004. [Online]. Available: <http://www.amazon.co.uk/Malaria-Hematological-Perspective-Tropical-Medicine/dp/1860943578>. [Accessed: 16-Feb-2016].
- [41] C. H. Kaschula, T. J. Egan, R. Hunter, N. Basilico, S. Parapini, D. Taramelli, E. Pasini, and D. Monti, “Structure–Activity Relationships in 4-Aminoquinoline

- Antiplasmodials. The Role of the Group at the 7-Position,” *J. Med. Chem.*, vol. 45, no. 16, pp. 3531–3539, Aug. 2002.
- [42] A. Robert, Y. Coppel, and B. Meunier, “Alkylation of heme by the antimalarial drug artemisinin,” *Chem. Commun.*, no. 5, pp. 414–415, Feb. 2002.
- [43] N. Sunduru, K. Srivastava, S. Rajakumar, S. K. Puri, J. K. Saxena, and P. M. S. Chauhan, “Synthesis of novel thiourea, thiazolidinedione and thioparabanic acid derivatives of 4-aminoquinoline as potent antimalarials,” *Bioorg. Med. Chem. Lett.*, vol. 19, no. 9, pp. 2570–3, May 2009.
- [44] R. Buller, M. L. Peterson, Ö. Almarsson, and L. Leiserowitz, “Quinoline Binding Site on Malaria Pigment Crystal: A Rational Pathway for Antimalaria Drug Design,” *Cryst. Growth Des.*, vol. 2, no. 6, pp. 553–562, Nov. 2002.
- [45] R. D. Sandlin, M. D. Carter, P. J. Lee, J. M. Auschwitz, S. E. Leed, J. D. Johnson, and D. W. Wright, “Use of the NP-40 detergent-mediated assay in discovery of inhibitors of beta-hematin crystallization,” *Antimicrob. Agents Chemother.*, vol. 55, no. 7, pp. 3363–9, Jul. 2011.
- [46] A. N. Hoang, R. D. Sandlin, A. Omar, T. J. Egan, and D. W. Wright, “The neutral lipid composition present in the digestive vacuole of Plasmodium falciparum concentrates heme and mediates β -hematin formation with an unusually low activation energy,” *Biochemistry*, vol. 49, no. 47, pp. 10107–16, Nov. 2010.
- [47] A. N. Hoang, K. K. Ncokazi, K. A. de Villiers, D. W. Wright, and T. J. Egan, “Crystallization of synthetic haemozoin (beta-haematin) nucleated at the surface of lipid particles,” *Dalton Trans.*, vol. 39, no. 5, pp. 1235–44, Feb. 2010.

- [48] T. J. Egan, "Haemozoin formation," *Mol. Biochem. Parasitol.*, vol. 157, no. 2, pp. 127–36, Feb. 2008.
- [49] K. K. Ncokazi and T. J. Egan, "A colorimetric high-throughput beta-hematin inhibition screening assay for use in the search for antimalarial compounds," *Anal. Biochem.*, vol. 338, no. 2, pp. 306–19, Mar. 2005.
- [50] P. Olliaro, "Mode of action and mechanisms of resistance for antimalarial drugs," *Pharmacol. Ther.*, vol. 89, no. 2, pp. 207–219, Feb. 2001.
- [51] L. Tilley, P. Loria, and M. Foley, "Chloroquine and Other Quinoline Antimalarials," pp. 87–121, 2001.
- [52] M. Navarro, W. Castro, A. Martínez, and R. A. Sánchez Delgado, "The mechanism of antimalarial action of [Au(CQ)PPh₃]PF₆: structural effects and increased drug lipophilicity enhance heme aggregation inhibition at lipid/water interfaces," *J. Inorg. Biochem.*, vol. 105, no. 2, pp. 276–82, Feb. 2011.
- [53] C. S. K. Rajapakse, A. Martínez, B. Naoulou, A. A. Jarzecki, L. Suárez, C. Deregnacourt, V. Sinou, J. Schrével, E. Musi, G. Ambrosini, G. K. Schwartz, and R. A. Sánchez-Delgado, "Synthesis, characterization, and in vitro antimalarial and antitumor activity of new ruthenium(II) complexes of chloroquine," *Inorg. Chem.*, vol. 48, no. 3, pp. 1122–31, Feb. 2009.
- [54] A. Dorn, S. R. Vippagunta, H. Matile, C. Jaquet, J. L. Vennerstrom, and R. G. Ridley, "An Assessment of Drug-Haematin Binding as a Mechanism for Inhibition of Haematin Polymerisation by Quinoline Antimalarials," *Biochem. Pharmacol.*, vol. 55, no. 6, pp. 727–736, Mar. 1998.

- [55] S. R. Vippagunta, A. Dorn, H. Matile, A. K. Bhattacharjee, J. M. Karle, W. Y. Ellis, R. G. Ridley, and J. L. Vennerstrom, "Structural Specificity of Chloroquine–Hematin Binding Related to Inhibition of Hematin Polymerization and Parasite Growth," *J. Med. Chem.*, vol. 42, no. 22, pp. 4630–4639, Nov. 1999.
- [56] K. J. Saliba, P. I. Folb, and P. J. Smith, "Role for the plasmodium falciparum digestive vacuole in chloroquine resistance.," *Biochem. Pharmacol.*, vol. 56, no. 3, pp. 313–20, Aug. 1998.
- [57] R. Hayward, K. J. Saliba, and K. Kirk, "The pH of the digestive vacuole of Plasmodium falciparum is not associated with chloroquine resistance.," *J. Cell Sci.*, vol. 119, no. Pt 6, pp. 1016–25, Mar. 2006.
- [58] K. Kirk and K. J. Saliba, "Chloroquine resistance and the pH of the malaria parasite's digestive vacuole.," *Drug Resist. Updat.*, vol. 4, no. 6, pp. 335–7, Dec. 2001.
- [59] Y. Kuhn, P. Rohrbach, and M. Lanzer, "Quantitative pH measurements in Plasmodium falciparum-infected erythrocytes using pHluorin.," *Cell. Microbiol.*, vol. 9, no. 4, pp. 1004–13, Apr. 2007.
- [60] S. R. Hawley, P. G. Bray, M. Mungthin, J. D. Atkinson, P. M. O'Neill, and S. A. Ward, "Relationship between antimalarial drug activity, accumulation, and inhibition of heme polymerization in Plasmodium falciparum in vitro.," *Antimicrob. Agents Chemother.*, vol. 42, no. 3, pp. 682–6, Mar. 1998.
- [61] A. V Pandey, B. L. Tekwani, R. L. Singh, and V. S. Chauhan, "Artemisinin, an endoperoxide antimalarial, disrupts the hemoglobin catabolism and heme detoxification systems in malarial parasite.," *J. Biol. Chem.*, vol. 274, no. 27, pp.

- 19383–8, Jul. 1999.
- [62] D. J. Sullivan, H. Matile, R. G. Ridley, and D. E. Goldberg, “A common mechanism for blockade of heme polymerization by antimalarial quinolines,” *J. Biol. Chem.*, vol. 273, no. 47, pp. 31103–7, Nov. 1998.
- [63] P. M. O’Neill, D. J. Willock, S. R. Hawley, P. G. Bray, R. C. Storr, S. A. Ward, and B. K. Park, “Synthesis, antimalarial activity, and molecular modeling of tebuquine analogues,” *J. Med. Chem.*, vol. 40, no. 4, pp. 437–48, Feb. 1997.
- [64] J. Yuvaniyama, P. Chitnumsub, S. Kamchonwongpaisan, J. Vanichtanankul, W. Sirawaraporn, P. Taylor, M. D. Walkinshaw, and Y. Yuthavong, “Insights into antifolate resistance from malarial DHFR-TS structures,” *Nat. Struct. Biol.*, vol. 10, no. 5, pp. 357–65, May 2003.
- [65] Y. Yuthavong, J. Yuvaniyama, P. Chitnumsub, J. Vanichtanankul, S. Chusacultanachai, B. Tarnchompoo, T. Vilaiwan, and S. Kamchonwongpaisan, “Malarial (*Plasmodium falciparum*) dihydrofolate reductase-thymidylate synthase: structural basis for antifolate resistance and development of effective inhibitors,” *Parasitology*, vol. 130, no. Pt 3, pp. 249–59, Mar. 2005.
- [66] S. J. Foote, D. Galatis, and A. F. Cowman, “Amino acids in the dihydrofolate reductase-thymidylate synthase gene of *Plasmodium falciparum* involved in cycloguanil resistance differ from those involved in pyrimethamine resistance,” *Proc. Natl. Acad. Sci. U. S. A.*, vol. 87, no. 8, pp. 3014–7, Apr. 1990.
- [67] W. Trager and J. B. Jensen, “Human malaria parasites in continuous culture,” *Science*, vol. 193, no. 4254, pp. 673–5, Aug. 1976.

- [68] M. T. Makler, J. M. Ries, J. A. Williams, J. E. Bancroft, R. C. Piper, B. L. Gibbins, and D. J. Hinrichs, "Parasite lactate dehydrogenase as an assay for Plasmodium falciparum drug sensitivity.," *Am. J. Trop. Med. Hyg.*, vol. 48, no. 6, pp. 739–41, Jun. 1993.
- [69] G. M. Morris, R. Huey, W. Lindstrom, M. F. Sanner, R. K. Belew, D. S. Goodsell, and A. J. Olson, "AutoDock4 and AutoDockTools4: Automated docking with selective receptor flexibility.," *J. Comput. Chem.*, vol. 30, no. 16, pp. 2785–91, Dec. 2009.
- [70] G. Neudert and G. Klebe, "DSX: a knowledge-based scoring function for the assessment of protein-ligand complexes.," *J. Chem. Inf. Model.*, vol. 51, no. 10, pp. 2731–45, Oct. 2011.
- [71] "BIOVIA Discovery Studio | Predictive Modeling & Science Simulation Software App." [Online]. Available: <http://accelrys.com/products/collaborative-science/biovia-discovery-studio/>. [Accessed: 28-Mar-2016].
- [72] K. Vanommeslaeghe, E. Hatcher, C. Acharya, S. Kundu, S. Zhong, J. Shim, E. Darian, O. Guvench, P. Lopes, I. Vorobyov, and A. D. Mackerell, "CHARMM general force field: A force field for drug-like molecules compatible with the CHARMM all-atom additive biological force fields.," *J. Comput. Chem.*, vol. 31, no. 4, pp. 671–90, Mar. 2010.

5.1 Introduction

To date Malaria may be a threat to a large population of mankind; however, it has been able to have some cure and even possible inoculation. So many other dreaded diseases exist which kill far above malaria. Other diseases such as TB, HIV/AIDS and cancer are more or less a death sentence. As the lifestyles of the general populace, both from the developed and developing countries, continue to deteriorate the number of people suffering from cancer is expected to increase to 20 million in the next coming two decades. This global expected increase in cancer incidences is envisioned to be accompanied by the emergence of new cancer incidences that will burden the prophylaxis and care of patients throughout the world. Therefore, all efforts aimed at addressing changes that will arise from "complicated" cancer incidences will be needed in order to address this global scourge [1].

Cisplatin, (cis-diamminedichloroplatinum, *cis*-[Pt(NH₃)₂(Cl)₂], Figure 5.1, (i)), the first successful member of the category of platinum-containing anticancer drugs was initially identified for its ability to exert anti-bacterial activity, was later discovered to be active against cancer. The platinum complex exhibited activity when evaluated as an anticancer agent against testicular, ovarian, bladder, head and neck cancers and other solid tumours [2]. The activity was associated with the ability of these complexes to bring "destructive" changes to the DNA through the formation of an adduct between the Pt-DNA as the results of the absorption of the drug [3,4]. Extensive study into the use of *cis*-platin however limited its therapeutic use as severe side effects, which include nephrotoxicity, nausea, and vomiting were among ailments identified [5]. The search for clinically beneficial platinum analogues resulted in the discovery and achievement of oxaliplatin Figure 5.1, (ii)), amongst the arrays

of investigated complexes and a very small number of clinically approved platinum drugs, an excellent candidate that emerged superior in the treatment of colon cancer [6].

Organometallic complexes offer great potential for design as anticancer drugs. They can act as inert scaffolds and specifically inhibit enzymes such as kinases, or as pro-drugs which undergo activation by various mechanisms [7].

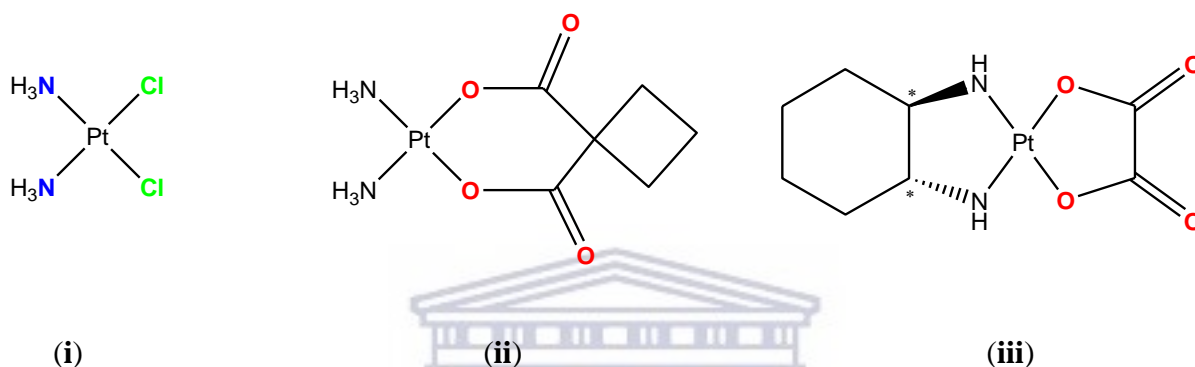


Figure 5.1: Structure of the prominent anticancer platinum derivatives, cis-platin (i), carboplatin (ii), and oxaliplatin (iii).

Platinum (II) salicylaldiminato complexes with a pendant heterocyclic thiophene moiety, thioplatin, have been shown to have antitumor activity that is corresponding to cisplatin without the accompanying grave side effects associated with the latter [8-10]. The associable activity of thioplatin can be attributed to the inherent lipophilic nature, leading to thioplatins accumulating readily in *cis*-platin-resistant cells [11].

5.1.1 Biochemical mechanism of *cis*-platin action

With the successful advances made in the chemotherapy of cancer with *cis*-platin and other platinum based metal drugs, one of the teething problems that researchers have been trying to

clearly understand is the biochemical interaction of the *cis*-platin with the DNA. It is now accepted that *cis*-platin exerts its cytotoxicity by binding with the DNA and forming DNA-adducts, that have been characterized, resulting in cell death (see Figures 5.3(a) and (b)) [12-20].

5.1.2 Binding modes of bioinorganics to DNA structure

Literature has shown that only a limited number of metal containing drug candidates are able to interact with the DNA as their target. These include bulky intercalating complexes of [Ru(bpy)(2)dppz]²⁺ (bpy = 2,2'-bipyridine and dppz = dipyrrophenazine) [21] that were luminescent upon binding to duplex DNA, cobalt polypyridyl coordination compounds [Co(L₃)]³⁺ (L=1,10-phenanthroline (phen), and bpy) [22] that have been shown to interact with 6-mercaptapurine and calf thymus DNA, mononuclear Ni(II) and Cu(II) complexes [(NiL(1Me-Im)] (1), [(CuL(1Me-Im)] (2) and [(NiL(PPh₃)] (3) (1Me-Im = 1-methylimidazole and PPh₃ = triphenylphosphine) that were investigated for their binding ability to DNA [23]. Some copper complexes [(tom^{Me}){Cu(OAc)}₂] (Cu₂(OAc)₂), (tom^{Me} = 2,7-Bis(N,N-di((6-methylpyridin-2-yl)methyl)-aminomethyl)-1,8-bis(methoxymethoxy)naphthalene) were shown to target the neighboring phosphates of the DNA backbone by molecular recognition [20]. On the other hand, salicylaldiminato-Ni(II), Cu(II) and Zn(II) complexes exerted their activity through DNA-binding affinity and were shown to be effective intercalating agents with DNA [24]. Rare-earth metal compounds of [LnL₂(NO₃)₂].NO₃ [Ln=La(1), Sm(2), Dy(3), Eu(4), where the ligand L is the 6-hydroxy chromone-3-carbaldehyde-(2'-hydroxy) benzoyl hydrazone, have also been shown to bind calf thymus DNA presumably via the intercalation mechanism with Eu(III) exhibiting the

strongest binding affinity [25,26]. It has been shown that coordination compounds are able to interact with DNA via two main interactive modes; the irreversible (covalent or coordination binding) and reversible (intermolecular association) mode due to the complexity of DNA strand that offers many potential binding sites.

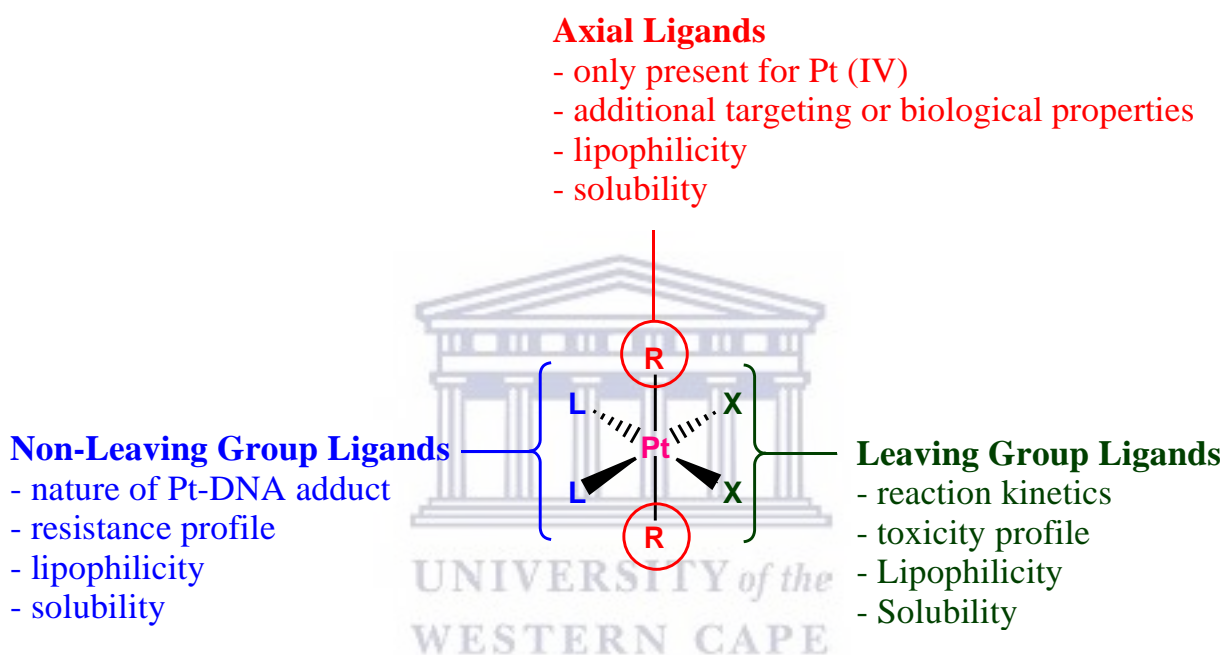


Figure 5.2: Different components of platinum anticancer agents. Additional factors that can be varied are the stereochemistry and the respective number of non-leaving group and leaving group ligands, picture modified from ref [27].

5.1.2.1 Covalent binding

The size of the coordination compounds dictates the manner in which the compounds interact and bind to DNA or nucleotide sequence [28]. One of the requirements of the chemotherapeutic agents necessary in order to act effectively as an antineoplastic agent is the propensity of the coordination compounds to produce activated, aquated form(s). Cisplatin has been shown to readily undergo stepwise hydrolysis in aqueous solution by nucleophilic

substitution of chloride with water, producing the activated molecules cis - $[PtCl(H_2O)(NH_3)_2]^+$ and cis - $[Pt(H_2O)_2(NH_3)_2]^{2+}$. The cationic monoaqua complex cis - $[PtCl(NH_3)_2(H_2O)]^+$ is the most reactive hydrolysed species and is believed to readily bond with the purine bases of the DNA [29-37].

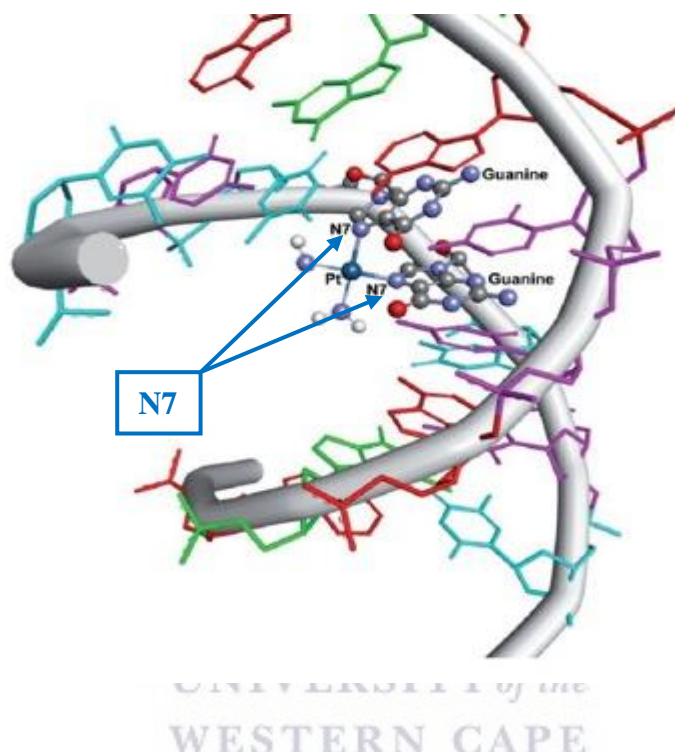


Figure 5.3(a): Representation of the *cis*-Pt-DNA adduct formed with the N-7 of the guanine base, picture take from ref [28].

Studies into binding affinity of *cis*-platin to DNA, shows the preferential binding of *cis*-platin to the N7 position of the purine DNA bases. This binding of *cis*-platin to the purine DNA bases results in the formation of an intrastrand cross-links *cis*-Pt-DNA adduct between two adjacent guanine-guanine [*cis*-Pt(NH₃)₂d(pGpG), 1,2-GG] (Figure 5.2(b)). The nitrogen atom N7 of the purines are known to be electron-rich and as such they are the accesible site for an electrophilic attack by the platinum metal centre in the DNA as they are exposed in the major groove of the double helix strand excluding the hydrogen bonding base pair interaction. The

Pt-DNA adduct formed is perceived as the most important lesion in the platinum-induced DNA kink [37-41].

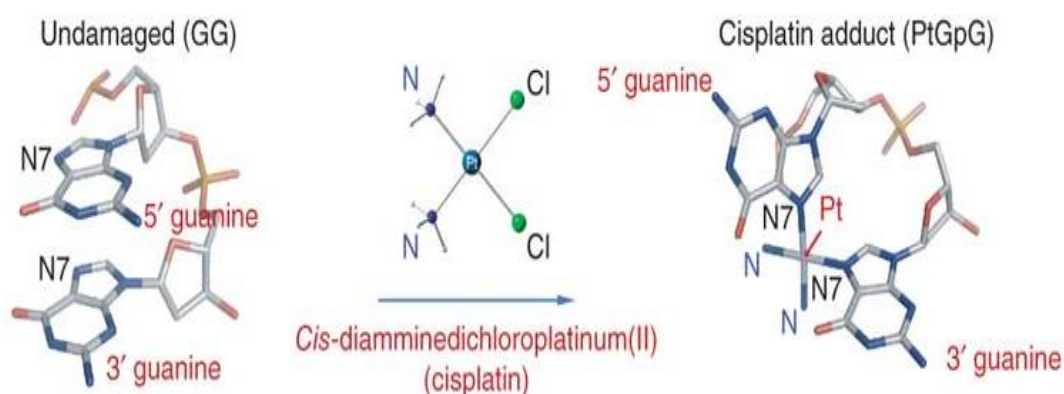


Figure 5.4(b): Reaction of $cis\text{-PtCl}_2(\text{NH}_3)_2$ with purine DNA bases to form $[cis\text{-Pt}(\text{NH}_3)_2\text{d}(\text{pGpG}), 1,2\text{-GG}]$ adduct, picture taken from ref [42].

5.2 Other bioinorganic compounds as anticancer agents

5.2.1 Ruthenium

The therapeutic properties of ruthenium were later discovered in the 1970s as a result of a search for alternative metal-based drug candidates that might possess lesser side effects and be active against a range of cancerous cells with an improved selectivity than their platinum counterparts. The first organoruthenium complex reported was the antitumor agent that is the half-sandwich 1- β -hydroxyethyl-2-methyl-5-nitro-imidazole (metronidazole) (Figure 5.5) which was discovered to be an effective chemotherapeutic agent *in vitro*. The metronidazole complex was more active than the free ligand [43].

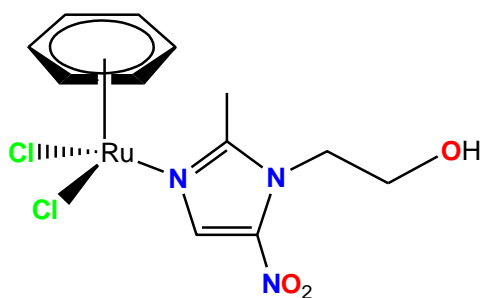


Figure 5.5: The first reported half-sandwich Ru^{II} -based antitumor agent [43].

Clark *et. al.* reported the successful synthesis of $[Ru(NH_3)_5(\text{purine})]^{3+}$ complex that was discovered to inhibit DNA and protein synthesis in human nasopharyngeal carcinoma cells *in vitro* [44,45]. The scope of the Ru^{II} complexes was later expanded by the development of Ru^{II} complexes that had dimethylsulfoxide (DMSO) and chloride ligands, orientated in a *cis*- and *trans*- $[RuCl_2(\text{dmsO})_4]$ configuration, by Mestroni *et. al.* These ruthenium complexes exhibited anticancer activities as they were shown to target and interact with DNA both *in vitro* and *in vivo* [46].

The continued effort aimed at synthesizing novel Ru^{II} -based drug candidates led to two of the Ru^{II} -based anticancer drugs: NAMI-A [47-49] and KP1019 [50-53] (Figure 5.6), entering clinical trials.

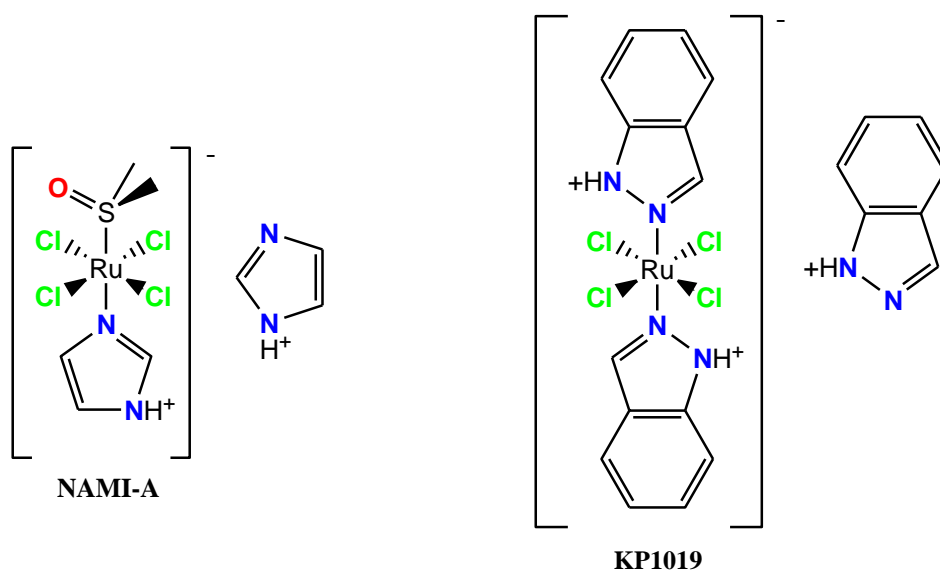


Figure 5.6: Chemical structures of the Ru^{II} -based drug candidates in clinical trials: NAMI-A and KP1019.

It has thus been shown that Ru^{II} and Os^{II} arene complexes exhibit appreciable cytotoxic activity against human ovarian cancerous cells possessing potent activity comparable to *cis*-platin and carboplatin as their structure-activity relationship has been established [30-42]. The chemistry of Ru^{II} -based anticancer agents has been broadly investigated equally to Ru^{III} complexes [43-62]. Half-sandwich complexes based on the ruthenium-arene and ruthenium-cyclopentadienyl have been the most extensively studied organoruthenium compounds [62]. Ruthenium^{II} complexes, just like other d^6 metal centres (Os^{II} , Ir^{III} or Rh^{III}), are known to form three binding configurations with the ligands coordinated around the metal centre (Figure 5.7).

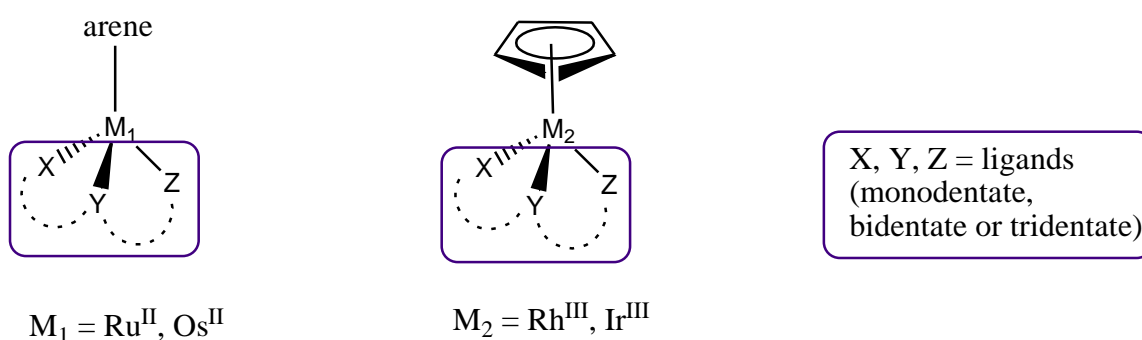


Figure 5.7: A general representation of Ru^{II} , Os^{II} -, Rh^{III} - and Ir^{III} -based 1 half-sandwich ‘piano-stool’ complexes.

The nature of the ligand on the complexes that are shown above governs the coordination mode, as such the ligand can bind in a monodentate (Z), bidentate (X-Y) or tridentate (X-Y-Z) fashion, resulting in neutral or charged complexes (isolated as salts). The inherent reactivity (labile or inert) character of the metal complexes is regulated by the different types of coordinating ligands (X, Y, Z and arene/Cp). The π -donor ability of the arene/Cp ligands on the metal centres have been shown to stabilize and protect the metal centres from oxidation [47].

5.2.2 Rhodium and Iridium

Organometallic rhodium(III) and iridium(III) complexes have found their niche as chemotherapeutic agents in the treatment of cancerous cell lines, and they have been discovered to be stabilized by the negatively charged pentamethylcyclopentadienyl ligand (Cp*) ring moiety, possessing bidentate ligand with nitrogen, oxygen and/or carbon donor atoms such as $N^{\wedge}N^-$, $N^{\wedge}O^-$, $O^{\wedge}O$, or even the C-H activated $C^{\wedge}N$ -chelating ligand, Z = Cl or py) have shown appreciable cytotoxic activity against different human cancer cell lines

although only a small number of literature articles have thus far reported on their anticancer activity [63-75].

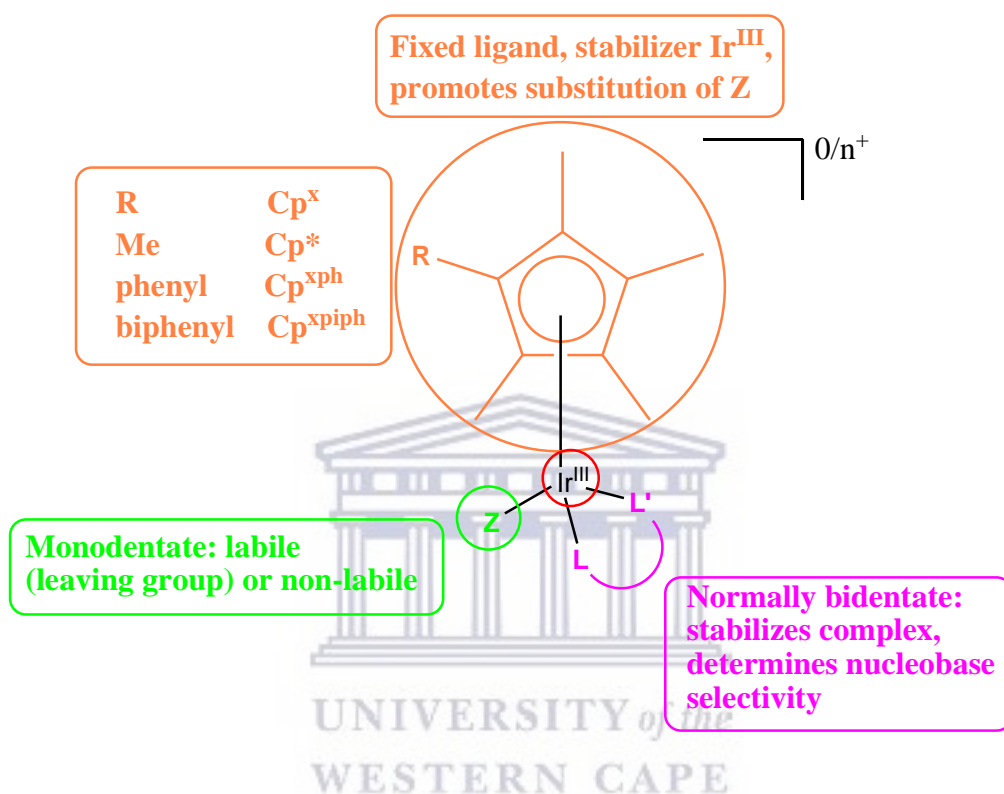


Figure 5.8: General structure of half-sandwich Ir^{III} cyclopentadienyl complexes. The ligands tune the chemical and biological activity. Picture taken and modified from ref [74].

5.3 Results and Discussion

5.3.1 *In vitro* screening of *N,O*-salicylaldimine ligands and corresponding complexes.

5.3.1.1 *In vitro* anticancer activity of *N,O*-salicylaldimine ligands, SL^1 - SL^3 .

The *in vitro* preliminary cytotoxic activity of the synthesized salicylaldimine ligands SL^1 - SL^3 (Figure 5.2) as agents able to circumvent the proliferation of cancerous cells was evaluated against four different human cancer cell lines, namely, breast adenocarcinoma (MCF-7), human hepatocellular liver carcinoma (HepG2), non-cancer Human Fibroblast (KMST-6), non-tumorigenic epithelial cell line (MCF-12) together with the antineoplastic standard reference drug, cis-platin. The *in vitro* IC_{50} values for the salicylaldimine ligands are listed below in Table 5.1.

The highest activity for the ligands evaluated was observed for SL^1 , with IC_{50} value of $17 \pm 0.9 \mu M$ with the transformed/malignant cells (MCF-7) and $35 \pm 1.3 \mu M$ for the healthy untransformed/non-malignant cells (MCF-12). Ligand SL^1 was found to exhibit the lowest cytotoxicity against the non-malignant MCF-12 cells, a necessary prerequisite for a compound to be considered as a viable anticancer agent due to its selective nature (Table 5.1, $SI = 0.48$). This is the only ligand that performed better than its corresponding metal complexes (*vide infra*). Ligand SL^2 , with the ethylene ($-CH_2CH_2-$) linker showed cytotoxicities that were the least promising of the ligand series with an IC_{50} value of $38.59 \mu M$ against the malignant MCF-7 cells although it was more active in comparison to the reference drug cis-platin ($IC_{50} = 100 \pm 2.0 \mu M$). Ligand SL^1 was more cytotoxic than SL^3 ($33.43 \pm 1.1 \mu M$), although structurally similar except that ligand SL^3 has a di-substituted ^tBu

in position 3- and 5- on the salicylaldimine moiety, indicating preferential selectivity for the malignant MCF-7 cell line by **SL¹** than the latter ligand.

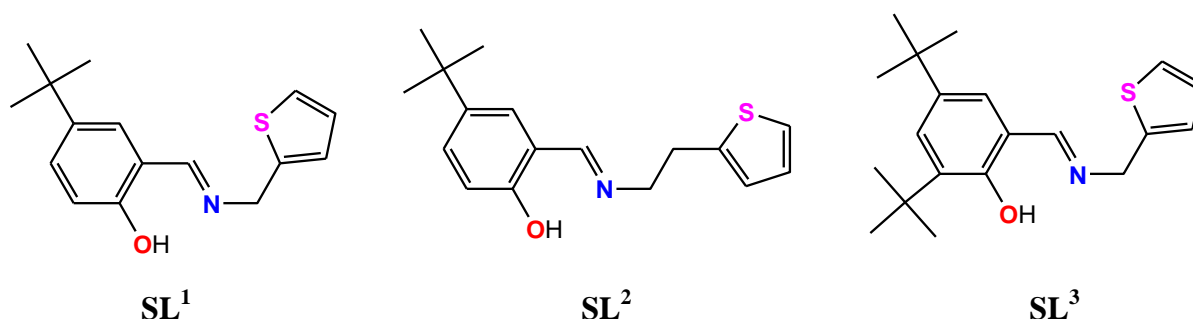


Figure 5.9: Ligands, **SL¹-SL³**, evaluated against different human cancer cell lines.

Table 5.1: IC₅₀ (μm) values of the salicylaldimine ligands **SL¹-SL³** and the reference drug *cis*-platin against the different human tumor cell lines^b.

Cancer cell lines ^c		SL¹	SL²	SL³	Cis-platin
MCF-7		17 ± 1.1	38.59 ± 1.2	33.43 ± 1.2	100 ± 2.1
HepG2		60.16 ± 1.8	83.5 ± 1.4	N.D	>100
KMST-6	(IC ₅₀ ^a ± SD ^b)	99.53 ± 2.1	N.D ^d	N.D	>100
MCF-12		35.78 ± 1.3	N.D	N.D	>100
MCF-12/MCF-7	SELECTIVITY INDEX (SI)	2.1	-	-	N.D
MCF-12/HepG2		0.54	-	-	N.D

^aIC₅₀ corresponds to the concentration required to inhibit 50% of the cell growth when the cells are exposed to the compounds during 24h. Each value is the average of three independent experiments.

^bStandard deviation.

^cBreast adenocarcinoma (MCF-7), HepG2 (Human hepatocellular liver carcinoma), KMST-6 (Non Cancer Human Fibroblast), MCF-12 (non-tumorigenic epithelial cell line). ^dNot determined (precisely).

5.3.1.2 *In vitro* anticancer activity of *N,O*-salicylaldimine complexes, **C7-C10**.

The coordination/organometallic complexes, **C7-C10** (Figure 5.10), were screened for *in vitro* cytotoxicity against human breast carcinoma (MCF-7), Human hepatocellular liver carcinoma (HepG2), non-tumorigenic epithelial cell line (MCF-12) cell lines with varied concentrations of the synthesized complexes in 24 hr employing the well-established colorimetric 3-(4,5-dimethyl-2-thiazolyl)-2,5-diphenyl-2H-tetrazolium bromide (MTT) bio-assay, respectively.

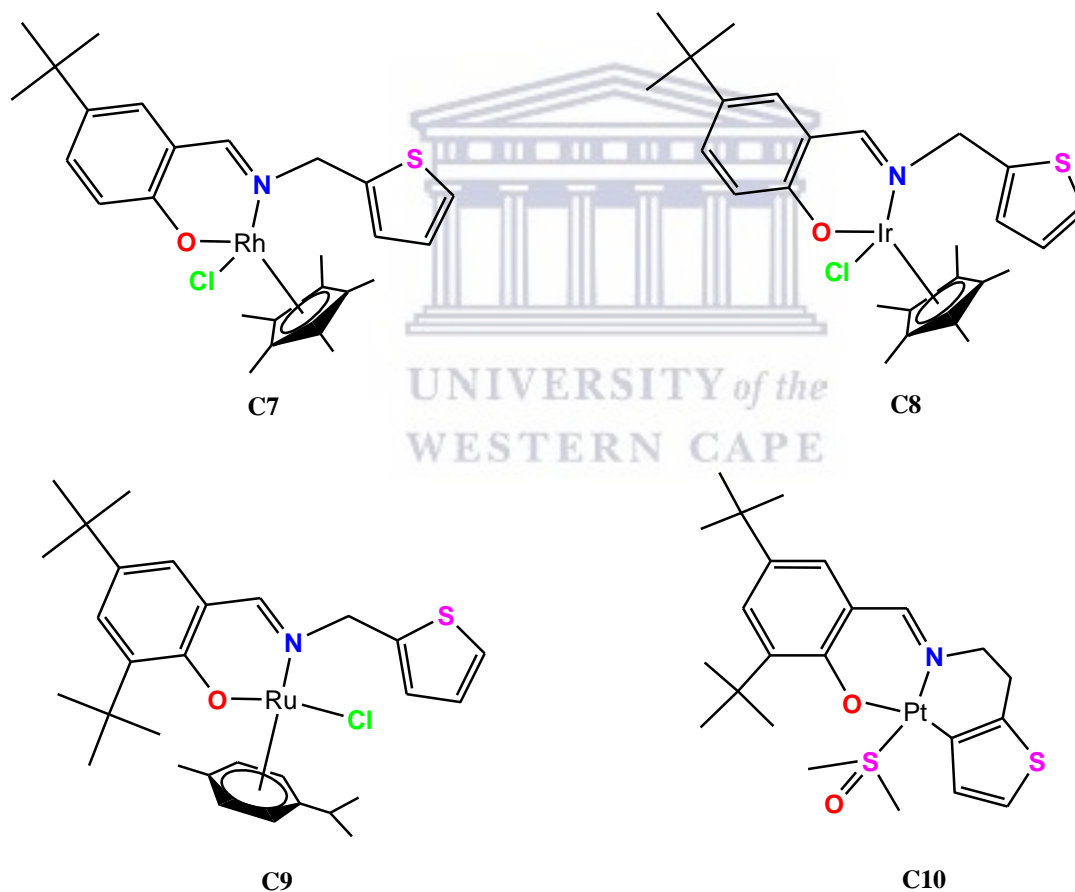


Figure 5.10: *N,O*-salicylaldimine complexes, **C7-C10**, evaluated against different human cancer cell lines.

The MTT bio-assay employed in this study has been shown to quantify the amount of MTT dye that has been reduced by the mitochondrial dehydrogenase as live cells incorporate and bind to the dye. All the compounds were soluble in dms0 and medium used herein. The effective dms0 percentage used for probing cytotoxicity profiles of all of the complexes was less than 1%. The corresponding IC₅₀ values for the studies are listed below (Table 5.2). The standard anticancer drug *cis*-platin was also evaluated under the same experimental condition in order to fully compare the cytotoxicities.

Table 5.2: IC₅₀ (μm) values of the complexes **C7-C10** against the different human tumor cell lines^b

Complexes	IC ₅₀ (μM ± SD) ^a			SELECTIVITY INDEX (SI)	
	MCF-7	HepG2	MCF-12	MCF-12/MCF-7	MCF-12/HepG2
C7	24.4 ± 1.2	N.D	53.59 ± 1.5	2.19	-
C8	43.75 ± 1.7	89.68 ± 1.1	24.53 ± 1.3	0.56	0.27
C9	63.01 ± 2.2	N.D	N.D	-	-
C10	21.25 ± 1.9	N.D	55.47 ± 2.2	2.61	-
<i>cis</i>-platin	100 ± 2.1	>100	>100 ± 2.4	N.D	N.D

^aIC₅₀ corresponds to the concentration required to inhibit 50% of the cell growth when the cells are exposed to the compounds during 24 h. Each value is the average of three independent experiments.

^bBreast adenocarcinoma (MCF-7), HepG2 (Human hepatocellular liver carcinoma), MCF-12 (non-tumorigenic epithelial cell line).

^dNot determined (precisely).

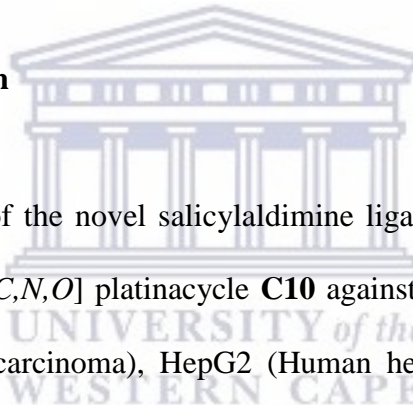
The IC₅₀ values tabulated above indicate that the platinacycle complex **C10** was the most active against MCF-7 cancer cell line. A tetracycle, and metallacycles have been shown to have promising antitumor activity when evaluated against different cancer cell lines [75-85]. The presence of a metal-carbon σ-bond appears to increase the stability of the complexes, and therefore giving the cyclometallated complexes an advantage of being target specific as they are evaluated for their pharmacological abilities [86]. Complex **C10** is a square planar

complex and as it has been indicated in the literature, square planar complexes exert their activity via binding to the DNA intercalation and as such the complex **C10** may also exert its chemotherapeutic effect through DNA intercalation as well [87].

Comparison between complex **C7** and **C8**, two different metal complexes Rh^{III}(**C7**) and Ir^{III}(**C8**) anchored by the same ligand **SL**¹ in the same oxidation state, showed that complex **C7** ($24.4 \pm 1.2 \mu\text{M}$) possessed potent activity than its counterpart **C8** ($43.74 \pm 1.9 \mu\text{M}$) when screened against the invasive breast cancer cell line MCF-7. The activity of complex **C8** was almost half of complex **C7**. The difference in the metal centres of these complexes thus lead us to conclude that rhodium complexes of similar fashion can be viable candidates as antitumor agents as they are herein observed to retain activity, suggesting that structural modifications of this series of ligands and corresponding metal complexes might augment the cytotoxic profile. The opposite was observed for the non-tumorigenic epithelial cell line MCF-12, complex **C8** exhibited enhanced cytotoxicity profile ($24.53 \mu\text{M} \pm 1.3$) than **C7** ($53.59 \pm 1.5 \mu\text{M}$). The selective index for complex **C7** and **C10**, calculated as the ratio of IC₅₀ (non-malignant cells, MCF-12)/IC₅₀ (malignant cells, MCF-7), were found to be higher than ca. 2, compared to 0.5 for complex **C8**. The greater (greater than 2) the SI value is, the more selective the complex is. Since the SI (0.56) value of complex **C8** is lower than 2, the pure complex is regarded as toxic [88,89]. The similarities in the cytotoxicity profiles of **C7** and **C10** suggests that the complexes might exert their antiproliferative activity in the estrogen receptor of MCF-7 cells by having the same target sites [88-90]. The same extrapolation was made with the non-malignant MCF-12 cells, suggesting that the **C7** and **C10** might share the same target sites. The effect of the metal centre was also investigated as **C7** was a Rh(III) and **C8** was a Ir(III) metal complex bound by the same ligand (**SL**¹). The Rh(III) metal centre proved to retain comparable activity to the ligand **SL**¹ while the Ir(III)

complex (C8) exhibited a decrease in the cytotoxic activity in comparison with that of the free ligand. These observations were in agreement with reported Rh(III) complexes [Cp*RhIII(Cl)(N^N)] (N^N = bipyridyl, phenanthroline) evaluated against MCF-7 and human ovarian cancer cells A2780 [91]. The complexes reported herein were observed to be potent anticancer agents (IC₅₀ values below 50 μM), far more antiproliferative than some of the Rh(III) complexes reported in the literature (between 50-100 μM or even inactive) [91]. The activity of the salicylaldimine complexes can thus be arranged in the order of increasing activity C10>C7>C8>C9 (MCF-7) and C8>C7>C10 (MCF-12).

5.4 Summary and Conclusion



The cytotoxicity assessment of the novel salicylaldimine ligands (SL¹-SL³) and complexes (C7-C9) with the terdentate [C,N,O] platinumacycle C10 against a panel of human cancer cell lines MCF-7 (human breast carcinoma), HepG2 (Human hepatocellular liver carcinoma), KMST-6 (Non Cancer Human Fibroblast), MCF-12 revealed that the complexes exhibit a comparable antiproliferative activity to *cis*-platin in the two human cancerous and two normal cell lines, with complex C10 showing cytotoxic activity that is five times that of the standard drug *cis*-platin. The activity of the complexes against the cancerous MCF-7 cell line can be arranged as follows C10>C7>C8>C9 as the complexes behaved better across all tested concentrations compared to the standard drug. The preliminary studies indicated that the synthesized complexes possess the potential of becoming better antitumor agents compared to the reference standard drug *cis*-platin.

5.5 Experimental

5.5.1 Materials

5.5.2 Commercial Kits/ Molecular Probes

3-(4, 5-Dimethylthiazol-2-yl)-2, 5-Diphenyltetrazolium bromide (MTT dye) Sigma Aldrich

Table 5.3: Tissue culture media used in the study and the suppliers.

Chemicals	Suppliers
Phosphate Buffer Saline (PBS) without CaCl ₂ , MgCl	GIBCO® Life Technologies
Foeta Bovineserum (FBS)	Biochrom
Penicillin-streptomycin	Lonza
Dulbecco's Modified Eagles's Medium (DMEM)	GIBCO® Life Technologies
Trypsin	
DMEM/F12	
Bovine insulin	Roche
Human Epidermal Groth Factor (HEGF)	SAFC Biosciences
Hydrocortisone	Sigma-Aldrich

5.5.3 General Solutions and Buffers

70% Ethanol: 700 ml of ethanol in 300 ml of distilled water.

5.5.4 Tissue Culture

All the cells (Table 5.4) used in this study were maintained in a 37°C incubator with 5% CO₂ saturation. HepG2, MCF-7, and KMST6 cells were maintained in DMEM media containing 10% FBS, 10% penicillin-streptomycin, while MCF-12A cells were maintained in, DMEM/F12 supplemented with 10% (v/v) FBS, 10% PENSTREP, 20ng/ml LONG® human epidermal growth factor (EGF: SAFC Biosciences), 0.01 mg/ml bovine insulin and 500 ng/ml hydrocortisone.

Table 5.4: Cell lines used in this study

CELL LINE	SPECIES ORIGIN	GROWTH MEDIUM
HepG2 (Human hepatocellular liver carcinoma)	Human	DMEM
MCF-7 (Breast adenocarcinoma)	Human	DMEM
KMST-6 (Non Cancer Human Fibroblast)	Human	DMEM
MCF-12 (non-tumorigenic epithelial cell line)	Human	DMEM/F-12

5.5.5 Thawing of cells

An amount of 5ml of DMEM media was placed at 4°C to cool. A vial of frozen cultured cells indicated in Table 5.4 was removed from the -150°C freezer and thawed in a 37°C water bath. The cells were transferred to a 15ml tube which contained the pre-cooled 5ml of DMEM media and centrifuged at 3000 g for 3 minutes. The supernatant was decanted and the pellet detached. The cells were then resuspended in 5ml media. The latter was put into a 25cm² tissue culture flask. The flask was incubated at 37°C at 5% CO₂ until confluence was reached.

5.5.6 Trypsinization of cells

The cells were trypsinized once confluency was reached. The DMEM media in the flask was discarded and cells were washed with phosphate buffered saline (PBS). The PBS was discarded and cells were trypsinized with the addition of 1 x trypsin and allowed to trypsinize at 37 °C for 2–3 minutes. DMEM media was added to the flask to stop trypsinization. The cells were collected by centrifugation at 3,000g.

5.5.7 Cell count

Cell counts were performed using the countessTM automated cell counter (Invitrogen). The countessTM automated cell counter is a bench top automated cell counter that performs cell counts and cell viability measurements using trypan blue stain. The countessTM automated cell counter uses disposable cell counting chamber slides that contain two enclosed chambers to chambers to hold the samples to allow for measurement of two different samples or perform replicates of the same sample. The cell counting occurs in the central location of the counting chamber and the volume counted is 0.4 μ L, the same as counting four (1 mm x 1 mm) squares in a standard hemocytometer.

5.5.8 Seeding of cells

Once cells were thawed and incubated in a 25 cm³ tissue culture flask, cells were incubated at 37°C until confluency was reached. Cells were then trypsinized and centrifuged to remove the supernatant and resuspended in 5ml of DMEM media. Cells were counted with the use of

the countessTM automated cell counter (Invitrogen) and seeded at the following densities: 5ml of 2.4×10^4 cells/ml in 25cm² flasks, 100 μ l of 1.0×10^4 cells/ml/well in 96-well plates. When 96 well plates were used, 100 μ l of cells were seeded respectively. Cells were incubated at 37°C until ready for testing.

5.5.9 Freezing of cells

For long term storage the cells were trypsinized and centrifuged. The cell pellet was re-suspended in DMEM media containing 10% DMSO. The latter was aliquoted into 2ml cryovials and stored at -150°C.



5.6 BIOASSAYS

5.6.1 Evaluation of cytotoxicity using MTT Assay

Cell proliferation was determined using the MTT assay following the methods described by Mosmann, 1983; Eguchi, *et al.*, (1997) and Freimoser, *et al.*, (1999) with minor modifications (Eguchi, *et al.*, 1997; Freimoser, *et al.*, 1999; Mosmann, 1983). The MTT assay is a method that is technically convenient, it doesn't involve washing steps and it is easy to apply in most experimental designs. Cells were trypsinized and cell counts of 2.4×10^4 were prepared in 50ml cell culture tubes. From this 100 μ l was withdrawn and seeded in each well of 96 well plates and were let to grow to the required confluence. Then culture medium was removed and replaced with 100 μ l of fresh medium without or with various concentrations of the test compounds. Triplicate wells were established for each concentration and the cells were incubated for 4 hours at 37°C in a humidified CO₂ incubator. Tetrazolium salt 3-[4,5-

dimethylthiazol-2-yl]-2,5-diphenyltetrazolium bromide (MTT) was dissolved in PBS (pH 7.2) to obtain a concentration of 0.5mg/ml and 10 µl of MTT solution was added to each well. The plates were incubated for 4 hours at 37°C in a humidified CO₂ incubator. At the end of the incubation period media was removed from each well and replaced with 100 µl DMSO. The plates were shaken on a rotating shaker for 10 minutes before taking readings at 560 nm using a microplate reader. Results of cellular viability were tabulated as mean absorbance of each compound expressed as a percentage of the untreated control and plotted against compound concentration. IC₅₀ values were tabulated from the graphs as compound concentrations that reduced the absorbance at 560 nm by 50% of the untreated control wells. To exclude background readings, three wells were seeded with untreated cells in which MTT was not added. Assays were done in triplicate to ensure reproducibility.

The percentage inhibitions of cell proliferation were calculated using the following formula:

$$\% \text{ inhibition} = 100(\%) - \left\{ \frac{(A_p - A_{cm})}{(A_{cc} - A_{cm})} \times 100\% \right\}$$

where A_{cm}=mean background absorbance of wells without cells (control of the medium); A_{cc}=mean absorbance in wells containing untreated cells (control of the cells); and A_p=absorbance value of the well containing cells treated with the tested compound at the concentration of interest.

Dose– response curves were plotted from %IC (Inhibition of cell proliferation values versus concentration of test compounds mM/ml) x-axis, log scale. Concentrations that inhibit cells proliferation by 50% (IC₅₀) were calculated by locating the x-axis values corresponding to 50% inhibition of cell proliferation Y – axis.

5.7 References

- [1] A. S. Abu-Surrah and M. Kettunen, "Platinum group antitumor chemistry: design and development of new anticancer drugs complementary to cisplatin.," *Curr. Med. Chem.*, vol. 13, pp. 1337–1357, 2006.
- [2] G. Momekov and D. Momekova, "Recent developments in antitumour platinum coordination compounds," *Expert Opin. Ther. Pat.*, Oct. 2006.
- [3] D. Wang and S. J. Lippard, "Cellular processing of platinum anticancer drugs.," *Nat. Rev. Drug Discov.*, vol. 4, no. 4, pp. 307–20, Apr. 2005.
- [4] W. H. Ang, M. Myint, and S. J. Lippard, "Transcription inhibition by platinum-DNA cross-links in live mammalian cells.," *J. Am. Chem. Soc.*, vol. 132, no. 21, pp. 7429–35, Jun. 2010.
- [5] F. K. Keter, S. Kanyanda, S. S. L. Lyantagaye, J. Darkwa, D. J. G. Rees, and M. Meyer, "In vitro evaluation of dichloro-bis(pyrazole)palladium(II) and dichloro-bis(pyrazole)platinum(II) complexes as anticancer agents.," *Cancer Chemother. Pharmacol.*, vol. 63, no. 1, pp. 127–38, 2008.
- [6] M. A. Jakupec, M. Galanski, V. B. Arion, C. G. Hartinger, and B. K. Keppler, "Antitumour metal compounds: more than theme and variations.," *Dalton Trans.*, no. 2, pp. 183–94, Jan. 2008.
- [7] A. M. Pizarro, A. Habtemariam, and P. J. Sadler, "Activation Mechanisms for Organometallic Anticancer Complexes," in *Medicinal organometallic chemistry*, vol. 32, G. Jaouen and N. Metzler-Nolte, Eds. Springer Berlin Heidelberg, 2010, pp. 21–56.
- [8] X. Wang And and Z. Guo, "The role of sulfur in platinum anticancer chemotherapy.," *Anticancer. Agents Med. Chem.*, vol. 7, no. 1, pp. 19–34, Jan. 2007.

- [9] H. P. Lipp and J. T. Hartmann, “[Platinum compounds: metabolism, toxicity and supportive strategies].,” *Praxis (Bern. 1994).*, vol. 94, no. 6, pp. 187–98, Feb. 2005.
- [10] J. T. Hartmann and H.-P. Lipp, “Toxicity of platinum compounds.,” *Expert Opin. Pharmacother.*, vol. 4, no. 6, pp. 889–901, Jun. 2003.
- [11] E. Amtmann, M. Zöller, H. Wesch, and G. Schilling, “Antitumoral activity of a sulphur-containing platinum complex with an acidic pH optimum,” *Cancer Chemother. Pharmacol.*, vol. 47, pp. 461–466, 2001.
- [12] S. G. K.R., B. B. Mathew, C. N. Sudhamani, and H. S. B. Naik, “Mechanism of DNA Binding and Cleavage,” *Biomed. Biotechnol.*, vol. 2, no. 1, pp. 1–9, Jan. 2014.
- [13] L. J. Boerner and J. M. Zaleski, “Metal complex-DNA interactions: from transcription inhibition to photoactivated cleavage.,” *Curr. Opin. Chem. Biol.*, vol. 9, no. 2, pp. 135–44, Apr. 2005.
- [14] A. M. Pizarro and P. J. Sadler, “Unusual DNA binding modes for metal anticancer complexes.,” *Biochimie*, vol. 91, no. 10, pp. 1198–211, Oct. 2009.
- [15] B. Lippert, Ed., *Cisplatin*. Zürich: Verlag Helvetica Chimica Acta, 1999.
- [16] V. M. Gonzalez, M. A. Fuertes, C. Alonso, and J. M. Perez, “Is Cisplatin-Induced Cell Death Always Produced by Apoptosis?,” *Mol. Pharmacol.*, vol. 59, no. 4, pp. 657–663, Apr. 2001.
- [17] V. Brabec and O. Nováková, “DNA binding mode of ruthenium complexes and relationship to tumor cell toxicity.,” *Drug Resist. Updat.*, vol. 9, no. 3, pp. 111–22, Jun. 2006.
- [18] V. Cepeda, M. A. Fuertes, J. Castilla, C. Alonso, C. Quevedo, and J. M. Pérez, “Biochemical mechanisms of cisplatin cytotoxicity.,” *Anticancer. Agents Med. Chem.*, vol. 7, no. 1, pp. 3–18, Jan. 2007.

- [19] M. A. Fuertes, J. Castilla, C. Alonso, and J. M. Pérez, “Cisplatin biochemical mechanism of action: from cytotoxicity to induction of cell death through interconnections between apoptotic and necrotic pathways.,” *Curr. Med. Chem.*, vol. 10, no. 3, pp. 257–66, Feb. 2003.
- [20] T. Jany, A. Moreth, C. Gruschka, A. Sischka, A. Spiering, M. Dieding, Y. Wang, S. H. Samo, A. Stammeler, H. Bögge, G. Fischer von Mollard, D. Anselmetti, and T. Glaser, “Rational design of a cytotoxic dinuclear Cu_2 complex that binds by molecular recognition at two neighboring phosphates of the DNA backbone.,” *Inorg. Chem.*, vol. 54, no. 6, pp. 2679–90, Mar. 2015.
- [21] H. Song, J. T. Kaiser, and J. K. Barton, “Crystal structure of Δ -[Ru(bpy)₂dppz]²⁺ bound to mismatched DNA reveals side-by-side metalloinsertion and intercalation.,” *Nat. Chem.*, vol. 4, no. 8, pp. 615–20, Aug. 2012.
- [22] C. Zhou, X. Du, and H. Li, “Studies of interactions among cobalt(III) polypyridyl complexes, 6-mercaptopurine and DNA.,” *Bioelectrochemistry*, vol. 70, no. 2, pp. 446–51, May 2007.
- [23] S. Saha, S. Jana, S. Gupta, A. Ghosh, and H. P. Nayek, “Syntheses, structures and biological activities of square planar Ni(II), Cu(II) complexes,” *Polyhedron*, vol. 107, pp. 183–189, Mar. 2016.
- [24] G. Barone, A. Terenzi, A. Lauria, A. M. Almerico, J. M. Leal, N. Busto, and B. García, “DNA-binding of nickel(II), copper(II) and zinc(II) complexes: Structure–affinity relationships,” *Coord. Chem. Rev.*, vol. 257, no. 19–20, pp. 2848–2862, Oct. 2013.
- [25] B. Wang, Z.-Y. Yang, and T. Li, “Synthesis, characterization, and DNA-binding properties of the Ln(III) complexes with 6-hydroxy chromone-3-carbaldehyde-(2'-

- hydroxy) benzoyl hydrazone.," *Bioorg. Med. Chem.*, vol. 14, no. 17, pp. 6012–21, Sep. 2006.
- [26] B.-D. Wang and Z.-Y. Yang, "Synthesis, characterization, DNA-binding properties of the Ln(III) complexes with 6-hydroxy chromone-3-carbaldehyde-(4'-hydroxy) benzoyl hydrazone.," *J. Fluoresc.*, vol. 18, no. 2, pp. 547–53, Mar. 2008.
- [27] J. J. Wilson and S. J. Lippard, "Synthetic methods for the preparation of platinum anticancer complexes.," *Chem. Rev.*, vol. 114, no. 8, pp. 4470–95, Apr. 2014.
- [28] J. C. García-Ramos, R. Galindo-Murillo, F. Cortés-Guzmán, and L. Ruiz-Azuara, "Metal-Based Drug-DNA Interactions," *J. Mex. Chem. Soc.*, vol. 57, no. 3, pp. 245–259.
- [29] E. R. Jamieson and S. J. Lippard, "Structure, Recognition, and Processing of Cisplatin-DNA Adducts.," *Chem. Rev.*, vol. 99, no. 9, pp. 2467–98, Sep. 1999.
- [30] S. J. Berners-Price and T. G. Appleton, "The Chemistry of Cisplatin in Aqueous Solution," pp. 3–35, 2000.
- [31] J. Kozelka, F. Legendre, F. Reeder, and J.-C. Chottard, "Kinetic aspects of interactions between DNA and platinum complexes," *Coord. Chem. Rev.*, vol. 190–192, pp. 61–82, Sep. 1999.
- [32] M. S. Davies, S. J. Berners-Price, and T. W. Hambley, "Slowing of Cisplatin Aquation in the Presence of DNA but Not in the Presence of Phosphate: Improved Understanding of Sequence Selectivity and the Roles of Monoaquated and Diaquated Species in the Binding of Cisplatin to DNA," *Inorg. Chem.*, vol. 39, no. 25, pp. 5603–5613, Dec. 2000.
- [33] F. Legendre, V. Bas, J. Kozelka, and J. C. Chottard, "A complete kinetic study of GG versus AG plantination suggests that the doubly aquated derivatives of cisplatin are the

- actual DNA binding species.,” *Chemistry*, vol. 6, no. 11, pp. 2002–10, Jun. 2000.
- [34] M. S. Davies, S. J. Berners-Price, and T. W. Hambley, “Rates of Platination of AG and GA Containing Double-Stranded Oligonucleotides: Insights into Why Cisplatin Binds to GG and AG but Not GA Sequences in DNA,” *J. Am. Chem. Soc.*, vol. 120, no. 44, pp. 11380–11390, Nov. 1998.
- [35] S. J. Berners-Price, T. A. Frenkiel, U. Frey, J. D. Ranford, and P. J. Sadler, “Hydrolysis products of cisplatin: pK_a determinations via $[1H, 15N]$ NMR spectroscopy,” *J. Chem. Soc. Chem. Commun.*, no. 10, p. 789, Jan. 1992.
- [36] B. Lippert, *Cisplatin: Chemistry and Biochemistry of a Leading Anticancer Drug*. John Wiley & Sons, 1999.
- [37] J. P. Caradonna, S. J. Lippard, M. J. Gait, and M. Singh, “The antitumor drug cis-dichlorodiammineplatinum forms an intrastrand d(GpG) crosslink upon reaction with $[d(ApGpGpCpCpT)]_2$,” *J. Am. Chem. Soc.*, vol. 104, no. 21, pp. 5793–5795, Oct. 1982.
- [38] A. M. Fichtinger-Schepman, A. T. van Oosterom, P. H. Lohman, and F. Berends, “cis-Diamminedichloroplatinum(II)-induced DNA adducts in peripheral leukocytes from seven cancer patients: quantitative immunochemical detection of the adduct induction and removal after a single dose of cis-diamminedichloroplatinum(II).” *Cancer Res.*, vol. 47, no. 11, pp. 3000–4, Jun. 1987.
- [39] A. M. J. Fichtinger-Schepman, J. L. Van der Veer, J. H. J. Den Hartog, P. H. M. Lohman, and J. Reedijk, “Adducts of the antitumor drug cis-diamminedichloroplatinum(II) with DNA: formation, identification, and quantitation,” *Biochemistry*, vol. 24, no. 3, pp. 707–713, Jan. 1985.
- [40] J. Filipinski, K. W. Kohn, and W. M. Bonner, “The nature of inactivating lesions

- produced by platinum(II) complexes in phage lambda DNA.,” *Chem. Biol. Interact.*, vol. 32, no. 3, pp. 321–30, Nov. 1980.
- [41] A. Eastman, “Reevaluation of interaction of cis-dichloro(ethylenediamine)platinum(II) with DNA,” *Biochemistry*, vol. 25, no. 13, pp. 3912–3915, Jul. 1986.
- [42] A. Ummat, O. Rechkoblit, R. Jain, J. Roy Choudhury, R. E. Johnson, T. D. Silverstein, A. Buku, S. Lone, L. Prakash, S. Prakash, and A. K. Aggarwal, “Structural basis for cisplatin DNA damage tolerance by human polymerase η during cancer chemotherapy.,” *Nat. Struct. Mol. Biol.*, vol. 19, no. 6, pp. 628–32, Jun. 2012.
- [43] L. D. Dale, J. H. Tocher, T. M. Dyson, D. I. Edwards, and D. A. Tocher, “Studies on DNA damage and induction of SOS repair by novel multifunctional bioreducible compounds. II. A metronidazole adduct of a ruthenium-arene compound.,” *Anticancer Drug Des.*, vol. 7, no. 1, pp. 3–14, Feb. 1992.
- [44] M. Clarke, “Oncological implications of the chemistry of ruthenium,” *Met. Ions Biol. Syst.*, vol. 11, pp. 231–283, 1980.
- [45] A. Kelman, M. Clarke, S. Edmonds, and H. Peresie, “Biological activity of ruthenium purine complexes,” *J Clin Hematol Oncol*, 1977.
- [46] E. Baulieu, D. T. Forman, M. Ingelman-Sundberg, L. Jaenicke, J. A. Kellen, Y. Nagai, G. F. Springer, L. Träger, L. Will-Shahab, and J. L. Wittliff, Eds., *Ruthenium and Other Non-Platinum Metal Complexes in Cancer Chemotherapy*, vol. 10. Berlin, Heidelberg: Springer Berlin Heidelberg, 1989.
- [47] P. J. Dyson and G. Sava, “Metal-based antitumour drugs in the post genomic era.,” *Dalton Trans.*, no. 16, pp. 1929–33, Apr. 2006.
- [48] E. Alessio, G. Mestroni, A. Bergamo, and G. Sava, “Ruthenium antimetastatic agents.,” *Curr. Top. Med. Chem.*, vol. 4, no. 15, pp. 1525–35, Jan. 2004.

- [49] I. Bratsos, S. Jedner, T. Gianferrara, and E. Alessio, "Ruthenium Anticancer Compounds: Challenges and Expectations," *Chim. Int. J. Chem.*, vol. 61, no. 11, pp. 692–697, Nov. 2007.
- [50] M. Galanski, V. B. Arion, M. A. Jakupec, and B. K. Keppler, "Recent developments in the field of tumor-inhibiting metal complexes.," *Curr. Pharm. Des.*, vol. 9, no. 25, pp. 2078–89, Jan. 2003.
- [51] C. G. Hartinger, S. Zorbas-Seifried, M. A. Jakupec, B. Kynast, H. Zorbas, and B. K. Keppler, "From bench to bedside--preclinical and early clinical development of the anticancer agent indazolium trans-[tetrachlorobis(1H-indazole)ruthenate(III)] (KP1019 or FFC14A).," *J. Inorg. Biochem.*, vol. 100, no. 5–6, pp. 891–904, May 2006.
- [52] F. Lentz, A. Drescher, A. Lindauer, M. Henke, R. A. Hilger, C. G. Hartinger, M. E. Scheulen, C. Dittrich, B. K. Keppler, and U. Jaehde, "Pharmacokinetics of a novel anticancer ruthenium complex (KP1019, FFC14A) in a phase I dose-escalation study.," *Anticancer. Drugs*, vol. 20, no. 2, pp. 97–103, Feb. 2009.
- [53] C. G. Hartinger, M. A. Jakupec, S. Zorbas-Seifried, M. Groessl, A. Egger, W. Berger, H. Zorbas, P. J. Dyson, and B. K. Keppler, "KP1019, a new redox-active anticancer agent--preclinical development and results of a clinical phase I study in tumor patients.," *Chem. Biodivers.*, vol. 5, no. 10, pp. 2140–2155, Oct. 2008.
- [54] A. F. A. Peacock and P. J. Sadler, "Medicinal organometallic chemistry: designing metal arene complexes as anticancer agents.," *Chem. Asian J.*, vol. 3, no. 11, pp. 1890–9, Nov. 2008.
- [55] S. J. Dougan, M. Melchart, A. Habtemariam, S. Parsons, and P. J. Sadler, "Phenylazo-pyridine and phenylazo-pyrazole chlorido ruthenium(II) arene complexes: arene loss, aquation, and cancer cell cytotoxicity.," *Inorg. Chem.*, vol. 45, no. 26, pp. 10882–

- 10894, Dec. 2006.
- [56] F. Wang, A. Habtemariam, E. P. L. van der Geer, R. Fernández, M. Melchart, R. J. Deeth, R. Aird, S. Guichard, F. P. A. Fabbiani, P. Lozano-Casal, I. D. H. Oswald, D. I. Jodrell, S. Parsons, and P. J. Sadler, “Controlling ligand substitution reactions of organometallic complexes: tuning cancer cell cytotoxicity.,” *Proc. Natl. Acad. Sci. U. S. A.*, vol. 102, no. 51, pp. 18269–18274, Dec. 2005.
- [57] R. E. Morris, R. E. Aird, P. del Socorro Murdoch, H. Chen, J. Cummings, N. D. Hughes, S. Parsons, A. Parkin, G. Boyd, D. I. Jodrell, and P. J. Sadler, “Inhibition of Cancer Cell Growth by Ruthenium(II) Arene Complexes,” *J. Med. Chem.*, vol. 44, no. 22, pp. 3616–3621, Oct. 2001.
- [58] R. E. Aird, J. Cummings, A. A. Ritchie, M. Muir, R. E. Morris, H. Chen, P. J. Sadler, and D. I. Jodrell, “In vitro and in vivo activity and cross resistance profiles of novel ruthenium (II) organometallic arene complexes in human ovarian cancer.,” *Br. J. Cancer*, vol. 86, no. 10, pp. 1652–7, May 2002.
- [59] A. L. Noffke, A. Habtemariam, A. M. Pizarro, and P. J. Sadler, “Designing organometallic compounds for catalysis and therapy.,” *Chem. Commun. (Camb)*, vol. 48, no. 43, pp. 5219–5246, May 2012.
- [60] G. Süss-Fink, “Arene ruthenium complexes as anticancer agents.,” *Dalton Trans.*, vol. 39, no. 7, pp. 1673–88, Feb. 2010.
- [61] W. H. Ang, A. Casini, G. Sava, and P. J. Dyson, “Organometallic ruthenium-based antitumor compounds with novel modes of action,” *J. Organomet. Chem.*, vol. 696, no. 5, pp. 989–998, Mar. 2011.
- [62] A. A. Nazarov, C. G. Hartinger, and P. J. Dyson, “Opening the lid on piano-stool complexes: An account of ruthenium(II)–arene complexes with medicinal

- applications,” *J. Organomet. Chem.*, vol. 751, pp. 251–260, Feb. 2014.
- [63] Z. Liu, L. Salassa, A. Habtemariam, A. M. Pizarro, G. J. Clarkson, and P. J. Sadler, “Contrasting Reactivity and Cancer Cell Cytotoxicity of Isoelectronic Organometallic Iridium(III) Complexes,” *Inorg. Chem.*, vol. 50, no. 12, pp. 5777–5783, Jun. 2011.
- [64] Z. Liu, A. Habtemariam, A. M. Pizarro, S. A. Fletcher, A. Kisova, O. Vrana, L. Salassa, P. C. A. Bruijninx, G. J. Clarkson, V. Brabec, and P. J. Sadler, “Organometallic half-sandwich iridium anticancer complexes,” *J. Med. Chem.*, vol. 54, no. 8, pp. 3011–26, Apr. 2011.
- [65] Z. Liu, A. Habtemariam, A. M. Pizarro, G. J. Clarkson, and P. J. Sadler, “Organometallic Iridium(III) Cyclopentadienyl Anticancer Complexes Containing C,N-Chelating Ligands,” *Organometallics*, vol. 30, no. 17, pp. 4702–4710, Sep. 2011.
- [66] M. Schmidlehner, L. S. Flocke, A. Roller, M. Hejl, M. A. Jakupec, W. Kandioller, and B. K. Keppler, “Cytotoxicity and preliminary mode of action studies of novel 2-aryl-4-thiopyrone-based organometallics,” *Dalton Trans.*, vol. 45, no. 2, pp. 724–33, Dec. 2015.
- [67] F. Hackenberg, L. Oehninger, H. Alborzinia, S. Can, I. Kitanovic, Y. Geldmacher, M. Kokoschka, S. Wöfl, I. Ott, and W. S. Sheldrick, “Highly cytotoxic substitutionally inert rhodium(III) tris(chelate) complexes: DNA binding modes and biological impact on human cancer cells,” *J. Inorg. Biochem.*, vol. 105, no. 7, pp. 991–9, Jul. 2011.
- [68] S. Wirth, C. J. Rohbogner, M. Cieslak, J. Kazmierczak-Baranska, S. Donevski, B. Nawrot, and I.-P. Lorenz, “Rhodium(III) and iridium(III) complexes with 1,2-naphthoquinone-1-oximate as a bidentate ligand: synthesis, structure, and biological activity,” *J. Biol. Inorg. Chem.*, vol. 15, no. 3, pp. 429–40, Mar. 2010.
- [69] C. G. Hartinger, “Trapping Unstable Benzoquinone Analogues by Coordination to a

- [(η^5 -C₅Me₅)Ir] Fragment and the Anticancer Activity of the Resulting Complexes,” *Angew. Chemie Int. Ed.*, vol. 49, no. 45, pp. 8304–8305, Nov. 2010.
- [70] S. Wirth, F. Barth, and I.-P. Lorenz, “1,4-Bis(4-nitrosophenyl)piperazine: novel bridging ligand in dinuclear complexes of rhodium(III) and iridium(III).,” *Dalton Trans.*, vol. 41, no. 7, pp. 2176–86, Feb. 2012.
- [71] A. J. Millett, A. Habtemariam, I. Romero-Canelón, G. J. Clarkson, and P. J. Sadler, “Contrasting Anticancer Activity of Half-Sandwich Iridium(III) Complexes Bearing Functionally Diverse 2-Phenylpyridine Ligands.,” *Organometallics*, vol. 34, no. 11, pp. 2683–2694, Jun. 2015.
- [72] U. Sliwińska, F. P. Pruchnik, I. Pelińska, S. Ułaszewski, A. Wilczok, and A. Zajdel, “Synthesis, structure and antitumor activity of [RhCl₃(N-N)(DMSO)] polypyridyl complexes.,” *J. Inorg. Biochem.*, vol. 102, no. 10, pp. 1947–51, Oct. 2008.
- [73] H. Amouri, J. Moussa, A. K. Renfrew, P. J. Dyson, M. N. Rager, and L.-M. Chamoreau, “Discovery, structure, and anticancer activity of an iridium complex of diselenobenzoquinone.,” *Angew. Chem. Int. Ed. Engl.*, vol. 49, no. 41, pp. 7530–3, Oct. 2010.
- [74] Z. Liu and P. J. Sadler, “Organoiridium complexes: anticancer agents and catalysts.,” *Acc. Chem. Res.*, vol. 47, no. 4, pp. 1174–85, Apr. 2014.
- [75] G. Gasser, I. Ott, and N. Metzler-Nolte, “Organometallic anticancer compounds.,” *J. Med. Chem.*, vol. 54, no. 1, pp. 3–25, 2011.
- [76] R. Cortés, M. Crespo, L. Davin, R. Martín, J. Quirante, D. Ruiz, R. Messeguer, C. Calvis, L. Baldomà, J. Badia, M. Font-Bardía, T. Calvet, and M. Cascante, “Seven-membered cycloplatinated complexes as a new family of anticancer agents. X-ray characterization and preliminary biological studies.,” *Eur. J. Med. Chem.*, vol. 54, pp.

- 557–66, Aug. 2012.
- [77] A. C. F. Caires, “Recent advances involving palladium (II) complexes for the cancer therapy.,” *Anticancer. Agents Med. Chem.*, vol. 7, no. 5, pp. 484–91, Sep. 2007.
- [78] M. R. Crimmin, D. A. Colby, J. A. Ellman, and R. G. Bergman, “Synthesis and coordination chemistry of tri-substituted benzamidrazones.,” *Dalton Trans.*, vol. 40, no. 2, pp. 514–22, Jan. 2011.
- [79] J.-P. Djukic, J.-B. Sortais, L. Barloy, and M. Pfeffer, “Cycloruthenated Compounds - Synthesis and Applications,” *Eur. J. Inorg. Chem.*, vol. 2009, no. 7, pp. 817–853, Mar. 2009.
- [80] S. P. Fricker, R. M. Mosi, B. R. Cameron, I. Baird, Y. Zhu, V. Anastassov, J. Cox, P. S. Doyle, E. Hansell, G. Lau, J. Langille, M. Olsen, L. Qin, R. Skerlj, R. S. Y. Wong, Z. Santucci, and J. H. McKerrow, “Metal compounds for the treatment of parasitic diseases.,” *J. Inorg. Biochem.*, vol. 102, no. 10, pp. 1839–45, Oct. 2008.
- [81] W. Kandioller, C. G. Hartinger, A. A. Nazarov, C. Bartel, M. Skocic, M. A. Jakupec, V. B. Arion, and B. K. Keppler, “Maltol-derived ruthenium-cymene complexes with tumor inhibiting properties: the impact of ligand-metal bond stability on anticancer activity in vitro.,” *Chemistry*, vol. 15, no. 45, pp. 12283–91, Nov. 2009.
- [82] P.-K. Lee, H.-W. Liu, S.-M. Yiu, M.-W. Louie, and K. K.-W. Lo, “Luminescent cyclometallated iridium(III) bis(quinolylbenzaldehyde) diimine complexes--synthesis, photophysics, electrochemistry, protein cross-linking properties, cytotoxicity and cellular uptake.,” *Dalton Trans.*, vol. 40, no. 10, pp. 2180–9, Mar. 2011.
- [83] S.-K. Leung, K. Y. Kwok, K. Y. Zhang, and K. K.-W. Lo, “Design of luminescent biotinylation reagents derived from cyclometalated iridium(III) and rhodium(III) bis(pyridylbenzaldehyde) complexes.,” *Inorg. Chem.*, vol. 49, no. 11, pp. 4984–95,

- Jun. 2010.
- [84] R. W.-Y. Sun, D.-L. Ma, E. L.-M. Wong, and C.-M. Che, "Some uses of transition metal complexes as anti-cancer and anti-HIV agents.," *Dalton Trans.*, no. 43, pp. 4884–92, Nov. 2007.
- [85] J. J. Yan, A. L.-F. Chow, C.-H. Leung, R. W.-Y. Sun, D.-L. Ma, and C.-M. Che, "Cyclometalated gold(III) complexes with N-heterocyclic carbene ligands as topoisomerase I poisons.," *Chem. Commun. (Camb)*, vol. 46, no. 22, pp. 3893–5, Jun. 2010.
- [86] G. L. Edwards, D. S. . Black, G. B. Deacon, and L. P. Wakelin, "Effect of charge and surface area on the cytotoxicity of cationic metallointercalation reagents," *Can. J. Chem.*, vol. 83, no. 6–7, pp. 969–979, Jun. 2005.
- [87] J. Quirante, D. Ruiz, A. Gonzalez, C. López, M. Cascante, R. Cortés, R. Messeguer, C. Calvis, L. Baldomà, A. Pascual, Y. Guérardel, B. Pradines, M. Font-Bardía, T. Calvet, and C. Biot, "Platinum(II) and palladium(II) complexes with (N,N') and (C,N,N') - ligands derived from pyrazole as anticancer and antimalarial agents: Synthesis, characterization and in vitro activities," *J. Inorg. Biochem.*, vol. 105, no. 12, pp. 1720–1728, 2011.
- [88] A. Koch, P. Tamez, J. Pezzuto, and D. Soejarto, "Evaluation of plants used for antimalarial treatment by the Maasai of Kenya.," *J. Ethnopharmacol.*, vol. 101, no. 1–3, pp. 95–9, Oct. 2005.
- [89] R. B. Badisa, S. F. Darling-Reed, P. Joseph, J. S. Cooperwood, L. M. Latinwo, and C. B. Goodman, "Selective cytotoxic activities of two novel synthetic drugs on human breast carcinoma MCF-7 cells.," *Anticancer Res.*, vol. 29, no. 8, pp. 2993–6, Aug. 2009.

- [90] K. Likhitwitayawuid, C. K. Angerhofer, H. Chai, J. M. Pezzuto, G. A. Cordell, and N. Ruangrunsi, "Cytotoxic and antimalarial alkaloids from the bulbs of *Crinum amabile*," *J. Nat. Prod.*, vol. 56, no. 8, pp. 1331–1338, Aug. 1993.
- [91] J. J. Soldevila-Barreda, A. Habtemariam, I. Romero-Canelón, and P. J. Sadler, "Half-sandwich rhodium(III) transfer hydrogenation catalysts: Reduction of NAD(+) and pyruvate, and antiproliferative activity," *J. Inorg. Biochem.*, vol. 153, pp. 322–333, Dec. 2015.



6.1 Conclusions

6.1.1 Synthesis

Novel chloroquine analogues N-(2-(2-(3,5-dimethyl-1H-pyrazol-1-yl)ethylamino)ethyl)-7-chloroquinolin-4-amine (**L**¹), N-(2-(2-(3,5-diphenyl-1H-pyrazol-1-yl)ethylamino)ethyl)-7-chloroquinolin-4-amine (**L**²) and N-(2-(bis(2-(3,5-dimethyl-1H-pyrazol-1-yl)ethyl)amino)ethyl)-7-chloroquinolin-4-amine (**L**³) that are appended with a pyrazolyl arm that are varied by steric hindrance around the pyrazole moiety have been successfully synthesized and fully characterized by spectroscopic (FT-IR, homonuclear ¹H, COSY and ¹³C{¹H}, heteronuclear 2-dimensional HSQC and HMBC) and analytical techniques. These chloroquine analogues possessed an inherent secondary chelation site that is availed by the incorporation of the “softer” coordinative pyrazole moiety in addition to the quinoline basic nitrogen atom.

Corresponding coordination ([Cp*^{III}Rh^{III}Cl(**L**¹)] (**C1**), [Cp*^{III}Ir^{III}Cl(**L**¹)] (**C2**), [Pd^{II}Cl₂(**L**¹)] (**C3**), [Pd^{II}Cl₂(**L**²)] (**C4**) and organometallic metal complexes [Pd^{II}Cl(**L**²-H)] (**C5**) and [Pt^{II}Cl(**L**²-H)] (**C6**) based on **L**² have also been synthesized and fully characterized using the aforementioned spectroscopic and analytical techniques.

Three new salicylaldimine 2-((E)-((thiophen-2-yl)methylimino)methyl)-4-tert-butylphenol (**SL**¹), 2-((E)-2-(thiophen-2-yl)ethylimino)methyl)-4-tert-butylphenol (**SL**²), 2-((E)-((thiophen-2-yl)methylimino)methyl)-4,6-di-tert-butylphenol (**SL**³) with a pendant thiophene arm and two new hydrazinic 1,2-bis(1-(5-methylthiophen-2-yl)ethylidene)hydrazine (**SL**⁴), 1,2-bis(1-(5-bromothiophen-2-yl)ethylidene)hydrazine (**SL**⁵) ligands have been also synthesized and fully characterized using the aforementioned spectroscopic and analytical techniques. The molecular structures of **SL**¹, **SL**², **SL**⁴ and **SL**⁵ have been confirmed by

single crystal X-ray diffraction studies and their respective geometrical orientation confirmed.

Novel salicylaldiminato $[\text{Cp}^*\text{Rh}^{\text{III}}\text{Cl}(\text{SL}^1)]$ (**C7**), $[\text{Cp}^*\text{Ir}^{\text{III}}\text{Cl}(\text{SL}^1)]$ (**C8**), $[\text{Cp}^*\text{Ru}^{\text{II}}\text{Cl}(\text{SL}^3)]$ (**C9**), $[(\text{dmsO})\text{Pt}^{\text{II}}(\text{SL}^1)]$ (**C10**) and $[(\text{HCOD})\text{Pt}^{\text{II}}(\text{SL}^3)]$ (**C11**) complexes have also been successfully synthesized and characterized using a range of aforementioned spectroscopic and analytical techniques. The molecular structures of complex **C7**, **C8**, **C10** and **C11** have been confirmed by single crystal X-ray diffraction studies.

6.1.2 *In vitro* antiplasmodial activity

The chloroquine analogues L^1 - L^3 and the generic metal complexes **C1-C6** were evaluated for their antiplasmodial activity against the CQ-sensitive NF54 strain.

The ligands L^1 - L^3 were found to exhibit good antiplasmodial activity (below 50 nM) with L^1 exhibiting the best activity out of this series, with IC_{50} of 19 nM, half as active as the reference drug chloroquine diphosphate.

The corresponding metal complexes **C1-C6** were found to exhibit activity that ranged from good (**C1-C3**) through moderate (**C5**) and weak (**C4** and **C6**). The best activity displayed by complex **C1-C3** were found to be below 50 nM with **C1** exhibiting the best activity with IC_{50} of 17 nM.

The new chloroquine analogues and corresponding complexes were also screened for their ability to inhibit β -hematin. The ligands L^1 and L^2 exhibited potent inhibitory activity relative to the standard drugs chloroquine and amodiaquine. The metal complexes displayed activity

that was comparable to the standard drugs chloroquine and amodiaquine with complex **C1** showing the best β -hematin inhibitory effect out of all this series of metal complexes.

6.1.3 Molecular docking

The ligands **L¹-L³** were docked on the active site of *Plasmodium falciparum* dihydrofolate reductase–thymidylate synthase (PfDHFR-TS). The ligands were found to be viable candidates as antifolate antagonist in the active site of the PfDHFR-TS enzyme with **L³** showing the highest binding efficiency and high binding energy (-7.13 kcal/mol) as it interacted with the highest protein residues. The binding score were better than reported antifolate antagonist and comparable to the potent inhibitor WR99210.

6.1.4 In vitro anticancer studies

The salicylaldimine **SL¹-SL³** and corresponding metal complexes **C7-C10** were screened for their anticancer activity against a range of cancer cell lines such as breast adenocarcinoma (MCF-7), HepG2 (Human hepatocellular liver carcinoma), KMST-6 (Non Cancer Human Fibroblast), MCF-12. The salicylaldiminato ligands and corresponding metal complexes exhibited potent anticancer activity against MCF-7 compared to *cis*-platin (100 μ M) with the best ligand activity for **SL¹** 17 μ M and 21 μ M, 24 μ M for **C10** and **C7**, respectively. Cyclometallation of ligand **SL²** proved to be beneficial in the anticancer activity of the complex, affirming previous reports on metallacycles. The best IC₅₀ obtained for all the compounds was for **SL¹** and **C10** on all tested cancer cell lines.

6.2 Recommendations and future outlooks

The data obtained and presented herein, with literature support, permit us to propose making these structural modifications (Figure 6.1) that might enhance the activity of the herein reported chloroquine analogues and generic complexes.

The best activity demonstrated by the chloroquine analogues reported herein will be selected and tested against different CQ-resistant strains such as Dd2 and K1. The ligands will also be screened for their anticancer activity against different cancer cell lines (MCF-7), HepG2 (Human hepatocellular liver carcinoma), KMST-6 (Non Cancer Human Fibroblast), MCF-12, A2780 and A2780*cisR* (Human ovarian cancer). The physiochemical characteristics *viz* lipophilicity and basicity of the compounds will also be investigated.

The quinoline moiety has been shown to be essential for antiplasmodial (as it complexes with Fe(III)-PPIX) and β -hematin inhibition activity. The structural modifications envisioned include retaining the quinoline motif in order to retain the antimalarial and β -hematin inhibition activity.

The ferrocenyl moiety will also be introduced in order to help the compounds overcome Plasmodium chloroquine resistance transporter (*PfCRT*) and increase the lipophilicity of the compounds.

A secondary chelation site will also be introduced to enable incorporation of a secondary metal centre. This site will also act as a weak base that can assist drug accumulation inside the digestive vacuole (DV) of the parasite.

The incorporation of each fragment (Figure 6.1) to assemble the desired ferroquine analogues, will be studied in order to gauge the effect brought about by each fragment and

the impact they have on the pharmacological activity against different CQ-sensitive and CQ-resistant strains of *P. falciparum*.

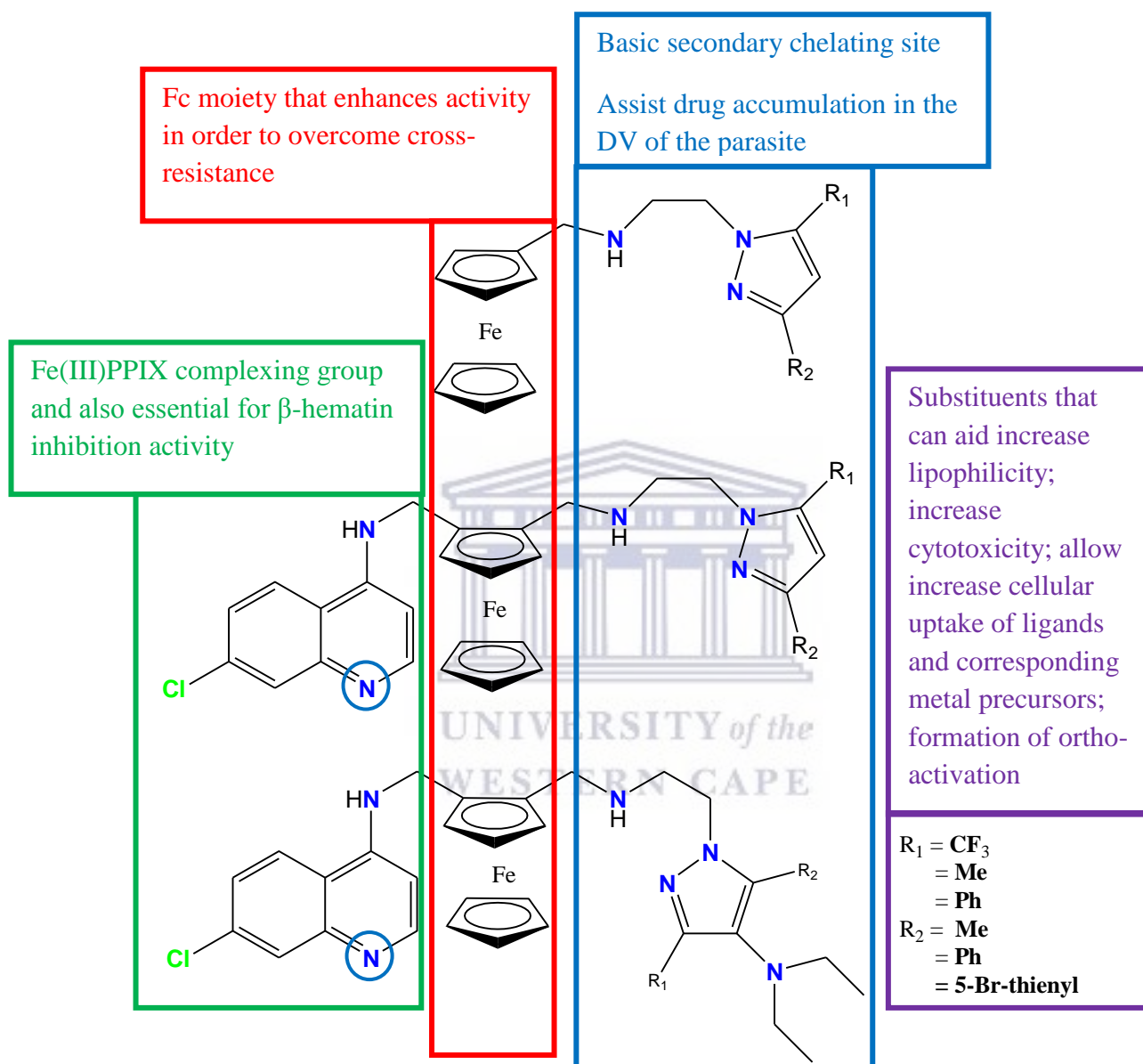


Figure 6.1: Proposed structural modifications for a new series of ferroquine analogues as antimalarial agents.

We also envision to expand the study of the salicylaldiminato-metallo-drugs (Cu^{II} , Ni^{II} , Zn^{II} , Cr^{II} , VO^{IV} , Os^{II}) and to investigate the preferred binding mode of these metallo-drugs to DNA

and probe which nucleotide pairs are able to form preferred chelation complexes. DNA-binding (absorption and fluorescent) studies of the salicylaldiminato-Pt(II), Ru(II), Rh(III) and Ir(III) complexes will be investigated in order to ascertain the binding modes of the complexes with purine DNA bases. It is also within future plans to investigate the selectivity of the metallodrugs as they target nucleotides. Future endeavours will also focus on factors that affect the binding affinity of the metallodrugs to DNA such as the pH changes, halide variation and halide concentration.

Techniques such as the ^1H NMR and X-ray crystallography will be employed in order to investigate the metal complexes-Drug interactions and to probe the preferred DNA site in conjunction with High Pressure Liquid Chromatography (HPLC) that will aid resolve any mixture of products that might form.

